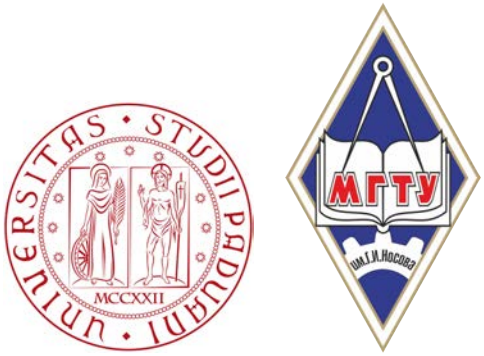

Università degli Studi di Padova

Dipartimento di Ingegneria Industriale-DII

Corso di Laurea Magistrale in Ingegneria dei Materiali

DEVELOPMENT OF INNOVATIVE HIGH CHROMIUM CAST IRONS WITH IMPROVED WEAR RESISTANCE CHARACTERISTICS

Relatore: Prof. Manuele Dabalà

Correlatore: Prof. Marina Potapova

Laureando:

Mattia Franceschi

Matricola N. 1154313

Anno accademico 2018/2019

ABSTRACT

The thesis work presented in the following pages is the result of a period of research conducted at the Nosov Magnitogorsk Technical State University, located in Magnitogorsk in Russia, where is located one of the biggest metallurgical plant in the world, during the Erasmus$^+$ period between September 2018 and February 2019. This thesis deals with issues concerning metallurgy, in particular it focuses on some types of ferrous alloys, which are *White Cast Iron with High Chromium Content*. The most important fields of use of this type of cast iron are molds, pumps, components to be used in mining and grinding mills, since this cast irons have high hardness and wear resistance because there is no presence of graphite between the microstructural constituents and thanks to high presence of carbides.

The main objective, for which the research was done on this type of material, is top try to develop new improvement for the techniques of production and for the performances and properties of these cast irons, at microscopic and macroscopic level. From the point of view of the characteristics of the alloys the focus has been of two: the first was the hardness (HRC) and the second was a tribological property, which is the wear resistance, expressed through the wear resistance coefficient K_i. These two properties have been chosen because are very important for the industrial fields and for the type of products cited before. On this properties the effect of the alloying element, typically present on white cast irons, was studied and two mathematical models was built in order to predict the values of the the properties fixing a certain content of the alloying elements and finding the best combination of them. More specifically, what was done was trying to get new compositions of white cast iron with a high content of chromium, also alloyed with manganese, nickel and titanium, which are the typical alloying elements for these materials, which are able to maximize the properties of HRC and/or wear resistance coefficient K_i.

The models have been built starting from experimental data of hardness and wear resistance, measured on alloys with known composition and with the content of each element in each one represent the lower or the upper limit of the range of concentration, which are the typical used in practice. The starting composition have been fixed from the theory used for building models. The models were built

using the theory of the factorial experiment with two levels factors. Once the model was built, as first, have been validated using statistical instruments, after from the practical point of view. The practical validation started comparing the values of the properties of the firsts alloys used for the models. After that *the Steep Ascent Method* has been used to find the compositions which are able to optimize the two properties inside the range of composition explored. The samples of these compositions have been produced by melting operations in the laboratory, also in order to validate the models again. In both cases it has been observed that the constructed mathematical models are able to predict well the real characteristics of the alloys. Subsequently, economic analysis has been carried out and to assess which of the alloys was the best compromise in terms of high hardness, high wear resistance and low cost through material selection strategies.

In the second and last part of the work, a study was conducted on samples of white cast iron, high chromium content with the addition of some additional alloy elements to the previous ones, such as aluminum, in the form of tubes. The pipes were made by pouring the material into silica glass tubes through the use of a vacuum pump, ensuring very high cooling and solidification speeds. This was done to verify the result of an attempt to develop a new method to produce thin-walled pipes and the effect of ultra-high cooling rates. From the analysis point of view, characterization tests were carried out, which revealed an anisotropic structure and a very fragile material.

SOMMARIO

Il lavoro di tesi presentato nelle pagine seguenti è il risultato di un periodo di ricerca condotto presso la Nosov Magnitogorsk Technical State University, situata a Magnitogorsk in Russia, dove si trova uno dei più grandi impianti metallurgici del mondo, durante l'Erasmus$^+$ nel periodo tra settembre 2018 e febbraio 2019. Questa tesi tratta questioni riguardanti la metallurgia, in particolare si concentra su alcuni tipi di leghe ferrose, che sono *le Ghise Bianche ad Alto Contenuto di Cromo*. L'obiettivo principale, per il quale è stata effettuata la ricerca su questo tipo di materiale, è quello di provare a sviluppare nuovi miglioramenti per le tecniche di produzione e per le prestazioni e le proprietà di queste ghise, a livello microscopico e macroscopico. Dal punto di vista delle caratteristiche delle leghe, l'attenzione è stata focalizzata su due: la prima è stata la durezza (HRC) e la seconda è una proprietà tribologica, che è la resistenza all'usura, espressa attraverso il coefficiente di resistenza all'usura K_i. Queste due proprietà sono state scelte perché sono molto importanti per particolari impegati nei settori industriali precedentemente citati. Su queste proprietà è stato studiato l'effetto degli elementi alliganti, tipicamente presenti nelle ghise bianche (C, Mn, Cr, Ni, Ti) e sono stati costruiti due modelli matematici per predire i valori di queste proprietà una volta fissato un determinata combinazione degli elementi di lega e trovare la migliore combinazione di essi. Più specificamente, ciò che è stato fatto è stato cercare di ottenere nuove composizioni di ghisa bianca con un alto contenuto di cromo, anche in lega con manganese, nichel e titanio, che sono i tipici elementi di lega per materiali, che sono in grado di massimizzare le proprietà di HRC e/o coefficiente di resistenza all'usura K_i.

I modelli sono stati costruiti a partire da dati sperimentali di durezza e K_i, misurati su leghe con composizione nota e il contenuto di un certo elemento in ognuno rappresenta il limite inferiore o superiore dell'intervallo di concentrazione, che sono i tipicamente utilizzati nella pratica, in varie combinazioni stabilite dalla teoria che porta alla costruzione dei modelli. I modelli sono stati costruiti utilizzando la teoria degli esperimenti fattoriali con fattori a due livelli, sono stati dapprima convalidati utilizzando strumenti statistici e poi dal punto di vista pratico. La validazione pratica è iniziata a confronto tra i valori delle proprietà misurati nelle prime leghe utilizzate per i modelli e quelli predetti dal modello. Una volta fatto

questo, è stato usato lo *Steep Ascent Method* per trovare le composizioni che sono in grado di ottimizzare le due proprietà all'interno degli intervalli di composizione esplorati. I campioni di queste composizioni sono stati prodotti nel corso di fusioni in laboratorio, anche per convalidare nuovamente i modelli. In entrambi i casi è stato osservato che i modelli matematici costruiti sono in grado di prevedere bene le caratteristiche reali delle leghe. Successivamente sono state condotte analisi economiche anche per valutare quale delle leghe è il miglior compromesso in termini di elevata durezza, elevata resistenza all'usura e basso costo attraverso strategie di selezione dei materiali.

Nella seconda e ultima parte del lavoro, è stato condotto uno studio su campioni di ghisa bianca, ad alto contenuto di cromo con l'aggiunta di alcuni elementi in lega supplementari ai primi, come l'alluminio, sottoforma di tubi. I tubi sono stati realizzati colando il materiale in tubi in vetro di silice attraverso l'utilizzo di una pompa da vuoto, garantendo altissime velocità di raffreddamento e solidificazione. Ciò è stato fatto per verificare il risultato di un tentativo di sviluppare un nuovo metodo per produrre tubi a pareti sottili e l'effetto di altissime velocità di raffreddamento sul materiale. Dal punto di vista dell'analisi, sono stati effettuati test di caratterizzazione, che hanno rivelato una struttura anisotropa e un materiale molto fragile.

Contents

List of Figures

List of Tables

INTRODUCTION

Actuality of work

Metal materials are one of the most important classes of materials and are certainly among the most used in the industrial sector for the construction of structures, components and objects in many sectors, particularly in the mining and forming and pump industries. It is important to try to encourage the development of metals to improve their performance, make the products made with them better and increase the competitiveness of these materials. In those years people are trying to develop the modern machine-building industry and in particular this improvement and development is associated with the quality of the instrumentation used. The question of increasing the efficiency of the component used in industrial environment, in spite of numerous studies and long-term researches, have not yet been concluded and this is an important problem of great scientific, technical and practical importance in Russian Federation.

It is important to consider that numerous scientific researches show that the cast objects and the properties of the cast material have not lower performances respect to the forged tool, and in some cases they overcome them. There is a group of promising material for the production of a cast tool for mining equipment and hot-deforming dies under force loading and under the effect of high temperature, this is the category of the white cast irons, from the point of view the structure's singularities they are able to provide a high level of mechanical properties as hardness, strength and several performance properties like wear resistance, heat resistance; all of these are distributed in a very wide range.

The main reasons why the use of foundry products are not diffused are related to the presence of a rough cast structure and carbide non-homogeneity of the castings and, as a consequence, anisotropy of the properties. This has a very negative effect on the performance of the tool and objects. Due to metallurgical processing of the molten material, it is possible to improve the structural features and performance properties of cast products obtained from an already known as cast irons or steel. Much and more attention should be paid to the choice of the method for preparing the initial batch of liquid metal, the search for ideal conditions for the solidification and crystallization phase in the mold, the removal

of the hereditary connection which is present into the structure and composition of the charge materials with the properties and structures of the melts. There is an effective method of thermal treatment, this is a high-temperature treatment of the cast iron melt and it allows to eliminate the signs and features of heredity of the structure, to reduce the size of the crystalline phase, the sizes and number of shrinkage defects and to obtain a huge complex of high and special mechanical and operational properties of the cast object. This type of treatment, which will be explained later, is certainly one of the most advanced metal working techniques. Another way to improve the performance of the components is certainly also to find new combinations of alloying elements and treatments, taking into consideration also the economic aspects in order to reach the maximum performances supporting the minimum expense. In particular, the thesis work will be mainly devoted to the research of the effects of alloying elements on the mechanical characteristics of white cast irons, in particular from the point of view of hardness and wear resistance. Once this is done, the objective is to try to find the composition that maximizes the two characteristics of the metal, which are of fundamental interest for the above-mentioned areas of work. In all this, the economic aspect is obviously taken into consideration, because it is a parameter which is not negligible in the materials engineering and in the development of components.

Objective:

Choice and motivation of the set-up parameters of the chemical composition of cast irons for pump, mining equipment and dies. In order to reach this aim, the following activities have been performed:

1. Definition of the characteristics of micro and macrostructure that are formed after the solidification of the metal taking into account the cooling speed into the mold.

2. The research of a correlation between the preparation conditions of the molten metal, the rate of cooling of the alloys in the mold, the chemical composition, the content of the alloying element and finally the primary cast structure that is possible to obtain.

3. Establish the best chemical composition and combination of elements in order to improve the properties of materials and the value of the best cooling and solidification rate.

4. Investigations on extremely rapid cooled cast iron in form of tubes.

Scientific novelty of the work:

1. The effect of alloyed elements on properties;

2. their ability to influence the characteristics of the material;

3. optimal chemical composition of white cast iron with high wear resistance and hardness;

4. effect of high cooling rate.

Practical significance of the work:

1. The final properties of the micro- and macrostructure of the solidified alloy allow us to justify the quantitative parameters that have been found for the alloying.

2. The values of mechanical hardness of HRC and ex-exploitation properties (coefficient of wear resistance K_i) of the cast iron in the cast state after solidification performed at different rates could be used as reference data for the building of mathematical model.

3. The effect of various chemical alloying elements on the overall set of properties of cast irons that have been obtained allows us to determine their specific chemical compositions to reach certain properties.

4. The effect of cooling rate on the microstructure, properties of the material.

Basic provisions to be protected:

1. The mathematical and statistical analysis for the realization of a mathematical model for the optimization of the composition;

2. the obtained mathematical model;

3. results of practical investigation on the effect of alloying element on the properties of material, in particular on hardness and wear resistance;

4. new optimized composition of white cast iron.

Reliable results have been obtained thanks to the use of modern and precise instruments to carry out measurements and tests during the research. The fusion processes have been carried out according to the regulations.

Chapter 1

STATE OF THE QUESTION, THEORETICAL RECALLS AND OBJECTIVE OF THE STUDY

This research work focuses on the behavioral analysis of a very important class of alloys, which belongs to the family of metals, in particular the white cast irons are investigated. This category of metals is very interesting because different versions are the main materials used for the production of pumps and molds for the most varied industrial sectors and components for the mining sector. However, very often the conditions in which they are working are extremely burdensome and are responsible for the damage of the parts and/or the malfunctioning of the component, up to cause a disservice. It is therefore very important to study the conditions in which the metals operate and understand the problems concerning the components. All this allows us first to narrow down the field of investigation and understand what are the points on which to focus and then to understand what are the factors that influence the behavior of the metal, the methods to process the metal and finally the gimmicks thanks to which it is possible increase their performance. In this first chapter it is essentially divided into two parts and both are a fundamental part to understand all the subsequent work. The first observations provide an overview of the main situations in which the two alloys are mainly used, mining and foundry, explaining in particular the problems related to them. The last sections focus on some references to the theory concerning the new frontiers of metal processing treatments, necessary to improve their characteristics and increase their performance. What has been introduced in the initial overview and what derives from the theory will then is the basis and the starting point for the realization of the researches and in-depth analyzes.

1.1 Analysis of dies

1.1.1 Analysis of working conditions of dies for hot deformation

From what is reported in the regulations [1], a mold is a support tool for treatment, and one of the faces or the perimeter coincides with the whole or with a part of the worked piece. The idea is to group materials for the production of hot working molds [4]: that is based on the chemical composition and structure and for properties and use. It is important to analyze the majority of the critical issues about the material used for this type of tools:

1. High temperature increase of the molds during their use. The temperature of the surface layers (on a thickness of 0.6±1.0 mm thickness) of the molds and high-speed presses can even reach 650−750 °C during the printing of heat-resistant materials and other deformable materials [5]. The core of the material, on the other hand, is at significantly lower temperatures, which are around 400−500°C. Sometimes, in some special hot-forging processes, the skin of the molds in contact with the workpiece can even reach a level of 900−1000 °C for a few millimeters of thickness [6].

2. One of the most relevant problems in this area is certainly the cyclicity of the load of forces and temperature, and therefore phenomena of thermal and mechanical fatigue. All this leads to a considerable softening of the material with the formation of a granular type of perlite, and in some cases to the emergence of an increased hardness layer and a softened area located behind it. The magnitude of this hardness drop, the nucleation rate and the rate at which the cracks develop depend greatly on the nature of the structural constituents and the diffusion processes that occur in the volumes of material in contact with the piece that is formed [5, 7].

3. Another important question of note is the high specific pressure on the instrument. It depends on the type of material that is poured and which solidifies inside, from the heating temperature, from the shape of the object to be formed, from the type of lubricant, from the degree of decalcification, from the wear of the mold, etc. [8, 10]. It is possible to distinguish those types of damage: worn sections due to abrasion, adhesion and oxidation; plastic deformation; cracks of thermal origin (thermo-mechanical), which extend on the surface of the piece; finally, cracks due to the mechanical fatigue formed where the effort is most concentrated [11, 13].

What is required from a material used for die is divided in two main classes: operational and technological. The operating requirements are about the fact that

the material must have high mechanical properties in the temperature range of die heating.

1. The die must have high heat resistance, this can allows the necessary resistance to plastic deformation on the working surface of the die during the increasing of temperature; this kind of resistance is expressed with two values of temperature. The first one is about the yield strength of the material and it indicates the temperature at which σ_y remain at least 900÷1000 MPa, because the specific pressure during hot forming reaches values in the range 800÷900 MPa. The second temperature that represents the heat resistance is relative to the hardness, and it the one after which the metal presents the value of the HRC hardness higher than 45 or 50 for the material with the higher resistance to heat.

2. The hardness is of course one of the reference parameters used to characterize a metal, it indicates the resistance to the plastic deformation when the material is subject to a stress. Hardness is a function on a wide complex of elements, such chemical composition, macro and microstructure, treatments and the value can vary in wide intervals of values.

3. It is necessary to take in account also the resistance to thermal fatigue, and higher is the resistance to the high temperature of the alloy and higher will be the value viscosity (ρ=kg/m^3) and the coefficient of thermal expansion (α=1/°C) [14, 17].

4. Yield point (σ_y) of the metal, which must not be overcome by the pressure.

5. The material have to present an high resistance to wear during the operations. This strength is indicated by the Coefficient for High Wear Resistance K_i , it is a function of the chemical composition, structure, thermal treatment (the heat treatment of the molten alloy is included), working condition that determine the kind of wear and at the end the configuration of the workpiece.

6. It is very important that cast irons and steels have very high sensibility to the quenching treatment in order to obtain the correct microstructure but mostly homogeneous in the overall section.

7. Materials need to present very low sensibility to tempering embrittlement, because if this phenomenon manifests itself in the range of temperature 650÷700 °C it causes a lower viscosity and it may cause nucleation and propagation of cracks that can bring the material to the failure [18].

8. Another critical aspect is the hydrogen released during the operation due to the oxidation of the material and that could be absorbed into material from the surface, it diffuses and cause hydrogen embrittlement [19].

Technological aspects for materials,which are used for the production of dies, are:

1. Processing of pressure and cutting;
2. resistance against decarburization and oxidation;
3. deformability;
4. sensitivity to cracking during heat treatment;
5. hardening and hardenability;
6. sensitivity to overheating and burns.

1.1.2 Application of a die

In these years there have been an important development and improvement of techniques of tool making, which are methods of plastic deformation as forging and deep drawing. Casting is also an interesting way of production, the realization of dies by casting with subsequent mechanical and thermal processing for the required properties allows to avoid forging and reduces the use of cutting tools, especially for dies with complex shapes. Furthermore, since cast iron is a material mainly used in foundry it is possible to exploit the important characteristics that make this material interesting. There is also an another advantage, labor fees are reduced, the amount of metal scrap is reduced, and the entire production time is reduced. Some studies,[11], show that the die cast and the properties of the cast material have similar performance of the products obtained for plastic deformation and machining, and in some cases they are better. The main differences between a mold obtained by casting and foundry processes and one obtained from the deformation concern two aspects: viscosity and wear resistance. For example, in fact, in general cast material has better wear resistance than a deformed one and the viscosity of foundry products is $25-30\%$ lower than the same material worked by forging [16]. One of the main advantages deriving from the fact that structure and properties in materials subject to foundry processes are isotropic; in pieces machined with plastic deformation processes these are very dependent on the direction of the metal flow and the product is therefore anisotropic. The reasons why machined and forged mold are preferred and usually used is related to the fact that there is a lack of knowledge about relationship between final structure and processing and the way to obtain favorable structure, the correct composition of the material

and the type of thermal treatment applicable. Firstly, the use of molds is limited due to the obtainment of a heterogeneous crude solidification structure, especially with regard to carbides. What worries mainly about the heterogeneity of the structure is the fact that it can lead to the appearance of a significant number of defects, reduction of sustainable loads and embrittlement, which obviously have a negative impact on the operation of the instrument. On the other hand, instead, in forging, the metal is hardened, the grain is refined and fibrous. Some studies [4] show that there is the possibility of improving the structure and performance of cast matrices obtained from already known types of steel and cast iron, thanks to metallurgical processes and optimization of heat treatments [20, 24]. This should allow for the proper functioning of the forging molds but at the same preserving the advantages of the foundry product. It is essential in this field to choose correctly the way to obtain the liquid metal, to pay attention in the search for the optimal conditions for its solidification and, consequently, to obtain an optimal structure without evidence of hereditary structure. The characteristics of the liquid metal are mainly determined by the loaded starting material, melting unit, melting and processing methods (deoxidation, refining and modification).

1.2 Analysis of the situation for mining equipment and pumps

Crushers, ball mills, screens, spiral classifiers, hydrocyclones, floats, sand and ground pumps and other equipment are components that are often used in non-ferrous and ferrous metallurgical processing plants, mines and chemical raw materials and building materials industry. As is clear from previous studies [65], due to the severe operating conditions of the equipment, the life of many of these devices is limited, for example the life of the components of a ball mill is 3-6 months, while for impellers, sand pits and pumps that work in the ground, 150-400 h [65]. From the observation of the components it is possible to see that these parts are mainly subjected to abrasive wear and there is also a wear component linked to impact stresses. A role of particular importance is therefore played by the nature of the abrasive particles in contact with the material of the part and the presence of a medium, that can be liquid or gaseous. From the analysis of the samples it follows that for most of the cases mentioned above, the wear mechanism is abrasive or with a sliding or impact. Furthermore, it is possible to observe that the parts of the continuous flow part in the ground pumps, the impellers and the wheels are the part generally subject to the most intense wear. The intensity of wear in general is mainly related to:

1. chemical-mineralogical composition of the particles with which the metal

comes into contact;

2. presence and type (liquid or gas) of the medium between metal and particles
3. the speed of movement of the particles and their granulometry;
4. the geometry of the component.

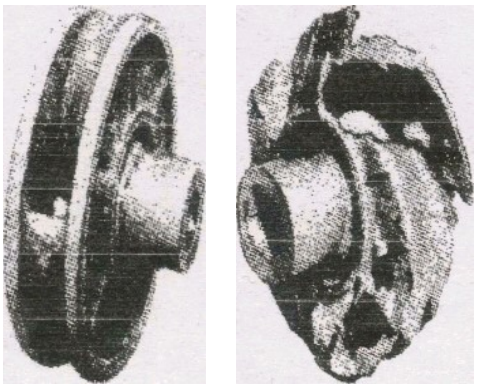

(a) *Impellers before wear* (b) *Impellers after wear*

Figure 1.1: Pumps

The appearance of local wear is characterized by the presence of depressions or cavities that lead to a sharp drop in the wear resistance of the entire casting and, consequently, to the failure of the component and to a malfunction. The wear resistance of this type of instrumentation is strongly linked to the chemical composition of the metal, to the macro and to the microstructure of the metal, as well as to the operating conditions. It is important to underline that, depending on the conditions in which the device operates, it is necessary to choose the material appropriately and adjust its properties in an appropriate manner to guarantee maximum performance. It is not true, in fact, that the same material with the same characteristics behaves well in different environments. According to some study it is possible to say that:

- The wear mechanism is divided into local and general. The local mechanism is related to some specific parts of the pump and is strongly linked to impacts. The general component involves the whole surface of the pump, this type of wear causes the information and the rapid development of through holes in the parts and a change in the length of the components, which is the main reason for the reduced life of these machines. The general wear, which

extends over the entire surface of the component, although it is the main cause of a great loss of metal, affects less the duration of these parts.

- The impact of the environment in which the pump works is extremely significant on the life time of the pump. When working on sandy or gravel soils, the output elements of the blades, the rear disc and the bottom of the design section are subject to more intense wear. On shallow sandy soils, wear is more uniform, and on sandy and gravelly soils, wear is clearly irregular. On small sandy soils, all signs of wear can be characterized as total abrasive wear. On sandy and gravelly soils, wear can be characterized as a mix of abrasive and local abrasive wear, while the total wear of the abrasive increases with the increase in the area concerned.

Currently, for the production of working parts of pumps operating under abrasive wear conditions, both special steels and white cast iron are used. Some experiments and practical data have shown, for example, that in abrasive and abrasive wear conditions with impact, the wear resistance of high-alloyed cast irons can also be significantly higher than that of steels, even exceeding a factor of 8. For example, for the construction of pumps for the enrichment plants it is more appropriate to use high-alloyed white cast iron with respect to the steels.

Alloy	Chemical composition										HRC
	C	Cr	Si	Mn	Ni	S	P	Mo	V	Ti	
Climex Alaia 42	3-3.6	12-18	0.3-0.6	0.8-0.9	-	0.06	0.1	2.75-3.25	-	-	60-62
15-3LC	2.4-3	12-18	0.3-0.6	0.5-0.9	-	0.06	0.1	3.0-3.5	-	-	60-62
ICHKH12M	2.6-3	11.5-18	0.7	0.5-1	-	0.06	0.1	1.4-1.6	-	-	58-60
ICX12G3M	2.5-3.2	12-15	0.4-0.7	3.4-3.9	-	0.06	0.1	0.5-0.8	-	-	45-50
ICH16MT	2.8-3.2	15-17	1.0	1.0	-	0.08	0.08	1.0-1.5	-	0.5-1.0	58-62
ICH28N2	2.7-3.0	28-30	0.7-1.4	0.5-0.8	14.5-3.0	0.08	0.1	-	-	-	47-55
ICH28N2M2	2.63-3.0	28-30	0.4-0.8	0.4-1	1.5-30	0.05	0.1	1.8-2.2	-	-	60-67
Vanadium	1.5-4.8	<7	<7	5.0-17	8	-	-	<7	2-15	<3.0	58-63
High chrome	3.4-3.8	29-31	0.8	1	0.3-0.6	0.8-1	-	-	0.2-0.4	0.2-0.3	50-54

Table 1.1: Composition of cast iron for pumps

1.3 The influence of technological factors on the structure and properties of foundry tool

An important strategy that can be applied in order to increase the properties of the cast metal until reaching the performance of the cast materials is to obtain the optimal phase structure of the metal and the product by introduction of alloying element e following the best condition for solidification and crystallization [25, 31]. The melting of the metal is performed at high temperatures and is accompanied by several and complex physio-chemical processes like the interaction between the molten metal, slags , atmosphere inside the furnace and furnace refractory lining. The choice of the method for the obtaining of the metal bath and the type of melting unit are function of the chemical composition and properties of iron, production volume, the mass of castings, the required quality and the technical and economic issues regarding the process. The metals with high content of alloying element are liquefied in electric arc furnaces with basic lining and induction crucible furnaces. The electric arc process has a lot of advantages: the use of ordinary batch, the small oxidation and loss of alloying elements, the possibility to carry out desulphurization and dephosphorization and high quality. On the other end there is low resistance of the refractory line when working with interruptions and these reduces productivity. The disadvantages of the induction process are: it is necessary to use pure raw materials, low temperature of slags, their high viscosity and low activity, this make the processes of dephosphorization less effective, and also desulphurization and deoxidation. At the same time, the high viscosity of slags and their low liquid mobility is very useful because in this way it protect the metal from the penetration of gases which are present in the atmosphere as hydrogen (H_2) and nitrogen (N_2). Other advantages include: high productivity, low burning of alloying elements; rapid heating and good mixing, which helps to make homogeneous the temperature throughout the entire volume of the bath and this provide also a greater homogeneity of the chemical composition of the metal; there is not also an increase of the carbon content of the metal, which can come from the electrodes made of graphite, which makes it possible to remelt high-alloy waste without addition of low-carbon billet [32, 33].

The main factors determining the results of the solidification of the melt and the properties of the product are the cooling rate and the pouring temperature. When technological regimes of metal melting are developed, the value of the optimum process temperature is one of the most important parameter that is necessary to control. The casting temperature of the metal should be should be at least 80 °C above the liquidus temperature. The melt overheating temperature depends mainly on the design of the castings: thinner is wall thickness, the greater is the melt size, the higher must be the melt temperature. The cooling speed is a

parameter that strongly influences the characteristics of the primary structure in molten iron. By determining the entity of the supercooling at which crystallization starts, the cooling speed of the metal changes the crystallization parameters - the rate of formation of the center and the linear growth rate of the crystals. The cooling speed of the casting is a function of the low thickness of the casting, of the type of casting piece, of the casting temperature and is not the same on the surface and in the core of the casting in the particularly massive product. The knowledge of the nature of the changes in these properties allows to control the final structure of the casting of the alloys and to predict their properties. Experiments, carried out in order to determine the influence of the main technological factors of cast ferrous alloys, have demonstrated that the upgrade of their properties during fast heat removal is due to the formation of a more dispersed and homogeneous structure. In the case of steel for example, fast cooling can allows to obtain pieces with higher the level of properties than deformed material with similar chemical composition [27].

The production of large castings requires the use of special methods: controlled cooling during solidification and various melting methods. This makes possible to obtain products with a structure as similar as possible to the structure of a deformed material. Melting technology has great importance in obtaining high quality cast iron and, more generally, metal product, it should ensure metal cleaning from non-metallic inclusions and unwanted impurities. For this, it is necessary to have pure raw materials, to carry out a special treatment of the molten liquid (refining and modification). The increase in contamination of the grain boundaries of the metal leads to a reduction in plasticity and viscosity [29, 34]. In the manufacture of cast iron in any unit, one of the tasks is to obtain a given mass of liquid alloy of a certain chemical composition, in order to obtain this the procedure includes metal refining, deoxidization and alloying, which is also a way to improve the material.

1.3.1 Alloying and micro-alloying of metals

It is known that one of the main ways used to improve the performance of metals is the alloying. The alloying elements influence the structure and properties of steels, cast irons, and in general for all the alloys and this is the result of complex physical-chemical processes that take place in the liquid, in the solidification process and finally in the solid state. The complex bond with several elements is exploited to obtain more functional structures and operating properties of the alloy, in this case ferrous, definitely higher [35, 38]. The main alloying elements that are used for cast irons and steels are manganese, chromium, nickel, titanium, molybdenum, vanadium, silicon and tungsten, sometimes in some steels, those that are called high speed steels (HSS), also have cobalt [31, 35, 37]. Depend-

ing on the operating conditions of the component that is wanted to be obtained, different properties are required, and in particular different values of them, these required characteristics can be obtained by mixing different components and in different quantities. For the realization of steels e cast irons alloying it is necessary to follow some principles in order to realize dies and tool for all the operations:

1. The choice of the alloy elements and the specific composition, also in terms of quantity of the elements, of the individual materials must be chosen in such a way as to obtain the maximum possible values of the properties that are mainly required for this specific application, while at the same time achieving maintain other characteristics at a satisfactory level in order not to induce other problems.

2. Any introduction of a certain alloying element and/or a certain amount of it within the metal alloy is justified only when it leads to an effective and significant increase in performance, durability and reliability of the instruments.

3. There are no universally used irons. The search for new and specific rational fields of application of well-known brands should be based on a preliminary prediction of the service life and reliability of the instruments.

4. Despite the differences in the structure and properties of carbide tool and cast iron for carbide curing, the values of the main characteristics, as resistance to wear, hardness, strength, toughness, etc., can be defined and maximized.

In the theory of the alloy, proposed by Professor Yu. A. Geller [5] some concepts have been presented:

1. the hardness and heat resistance of steels for tools and irons are greater, the more the amount of reinforcing particles grows, in particular the stability against the coagulation process which would lead to larger and smaller particles and therefore less reinforcement.

2. The higher the temperature at which tempering is carried out to obtain the maximum secondary hardness, and the heat resistance of alloys for making tools and molds is higher.

3. Tungsten carbides (WC) and molybdenum carbide (Mo_2C), vanadium (VC), chromium ($Cr_{23}C_6$), and other intermetallic compounds are the main reinforcing steps of tool steels and cast iron and other metal alloys.

4. The carbides are arranged in decreasing order as the ability to harden the steels and the heat resistant alloys: $Cr_{23}C_6$, Mo_2C and VC.

5. Carbides for their quality, ie for the property level (resistance against coagulation, hardness, shear modulus, specific gravity, misalignment between crystalline lattices and martensite lattice, while maintaining a coherent or semi-uniform border) consistent with each other, etc.) are arranged in ascending order: $Cr_{23}C_6$, Mo_2C and VC.

6. The extent of the reinforcement that are able to offer the carbides gradually becomes more and more significant as the solubility of the carbon and the alloying elements in the austenite grows and consequently in the martensite that can be obtained thanks to the treatment of hardening.

7. With increase in the tempering temperature and approximating the structure of steel and alloys to the equilibrium state, carbides MC, $M_{23}C_6$ and intermetallic compounds like M_6, M_7 maintain their crystal lattice.

8. The properties of carbides depend on their chemical composition and are determined by the ratio of the concentrations of alloying components and carbon in martensite, from which they are released during tempering.

9. The limiting tempering temperature (PTO): the heating at which it is possible to obtain the greatest hardness of the tool in time, depends strongly on the temperature of the polymorphic transformation of iron-based alloys [2, 6].

10. A noticeable decrease in the hardness during heating of dispersion-hardened of steels and alloys is associated with coagulation of hardening particles and with development recrystallization of martensite.

The law of influence of the chemical composition of the alloys on the melting diagram and the ultimate solubility in the iron are as follows:

1. the degree of isomorphism of the crystal lattice of the alloying element with the one of the iron determines which of them stabilize.

2. The extent of the γ-region is influenced by the value of the atomic radius of the element [4, 9];

3. The solubility in iron, as in other metals, of the alloying elements is dependent on the difference in the atomic diameters, the ability of the elements to form stable carbides, nitrides and other phases and compounds, that give boundary for the region of the solid solutions and the isostructural nature of the alloying element and the determined variation of the iron. According to the rule of Hume-Rotery, their content should not exceed $\pm$ 15% [9, 14].

In order to have higher performances during the operation considering an economical consumption and use of expensive alloying elements, great attention is dedicated to micro-alloying. The effect of the micro-alloying additions appears substantially in the solid state when the interstitial or substitution solutions form, there is an influence on degree of dispersion of secondary grains and nonmetallic inclusions, on the dispersion of grain boundaries, the fine structure and neutralization of influence of harmful impurities. This allows to perform the technological process by providing fine initial austenite grain, minimum grain growth at process of deformation and shaping and heat treatment [39, 40]. Usually, in order to increase the durability of the mold, it is realized a modification of the existing solution and the creation of new kinds of alloy in order to obtain the required properties for an object as high index of the impact-strength, heat resistance, toughness, coefficient for wear resistance and other mechanical properties [7, 31, 35, 36]. However, it is important to observe that the new developed grades steel and irons are complex and high alloyed, this is equivalent to saying that the cost of the product is very high. Therefore, it would be useful to observe the growth of the quality of the mold and an in-depth study on the improvement of metal properties for tools already known and normally used in industry.

1.3.2 Refining and deoxation of the liquid ferrous metal

The refining is the process in which is carried out the removal of harmful and unwanted impurities from metal bath. It is known that refining of metal is one of the most important, and often the only one, way to obtain high-quality metal. This process can be carried out both inside the furnace and outside the furnace, in a ladle, and also in special other units. Refining can be carried out by adding oxidizers and reducing agents and purging inert gases in the liquid metal. When a liquid metal is obtained in electric arc furnaces, it is easier to ensure conditions for more complete deoxidizing of the metal and removal of inclusions, in order to achieve a higher purity in the content of sulfur and phosphorus. Smelting, as a rule, is carried out by remelting the alloyed wastes with both blowing oxygen and without blowing. Refining is carried out under carbide or white slag, which is usually not dicahrged and deoxidized with coke powder and ferro-silicon. For the melting of steel in induction furnaces, a relatively pure charge for sulfur and phosphorus is required. A better metal refinement from dangerous impurities, nonmetallic inclusions and gases is possible through special methods of melting: vacuum induction melting, vacuum arc, electroslag, electron beam and plasma arc remelting [4, 25, 41]. The processes of melting and casting are accompanied by chemical reactions related to the interaction of the components of liquid with oxygen. The melting process of the ferrous metal should be completed by the process of its deoxidation. The oxygen content of the liquid metal before deoxidation is a

function on the carbon content and bath temperature, as it is possible to see for example in the Vacher-Hamilton diagram.

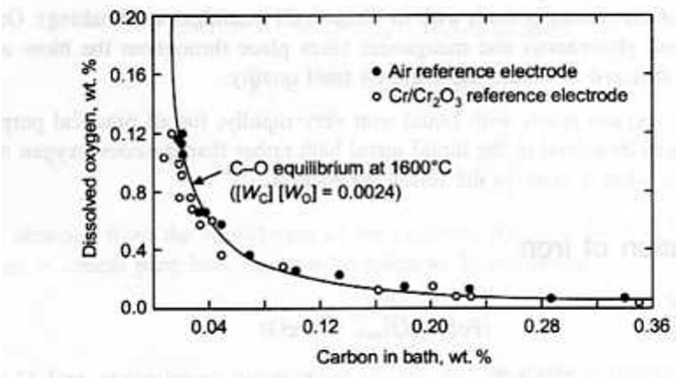

Figure 1.2: Vacher-Hamilton diagram

The most common way to remove oxygen from the metal is to add deoxidizing agents. It is used in the smelting of steel in all steelmaking aggregates and these are elements that bind oxygen to sufficiently strong oxides. More or less complete removal of the formed oxide inclusions - the products of deoxidation - occurs as a result of their introduction in the liquid-floating up or outflow of metal flows and transition to slag or solid interface surfaces. There is also second method of ferrous metal deoxidization which is is the diffusion deoxidation, it occurs as a result of the development of diffusion processes between the metal and a slag which has a content FeO lower than 1%. Such a slag can be a reducing agent with respect to the metal and it can make the oxygen content very low. At the end, the third way to remove oxygen is to realize a treatment with vacuum, in fact in vacuum the equilibrium oxygen content decreases with carbon. It is known that of all the technological parameters of melting processes, the processes of oxygen removal, which determine the nature and the type of nonmetallic inclusions, have the greatest influence on properties. The deoxidizing agents, which are at the same time modifiers, have a great influence on the microstructure and on the properties of the material. The most important deoxidizer are aluminum and silicon due to their high chemical affinity for acid. Also used are manganese, titanium, vanadium, calcium and rare earth. They have different melting temperature and different ability in the removal of oxygen:

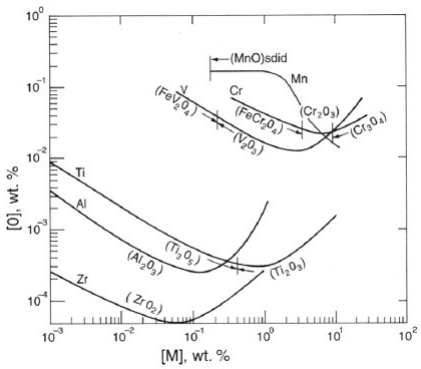

Figure 1.3: Effect of the deoxidising agent

It is possible to carry out a simple deoxidation with only one type of deoxidizer or a complex deoxidation adding different types of them as Si-Mn, Ca-Si, Ca-Si-Al, etc. The dissolved oxygen content is lower in complex deoxidation as compared to simple deoxidation. The deoxidation product, if liquid, agglomerates easily into larger sizes and consequently floats up faster, making the iron cleaner. This is what happens in many complex deoxidation such as in the example presented above. Properties of inclusions remaining in solidified metal can be made better by complex deoxidation, thus yielding a metal of superior quality. The mechanism of the dissolution of deoxidizers in the bath depends on their melting point: if it is lower than that of steel, it may become molten, with the crust of solid steel intact as an extreme case. If the melting point of the agent is at temperature above than that of liquid, such in the case of ferro-tungsten, then the crust of steel will remelt, exposing the alloy to the melt and leading to its dissolution by simultaneous heat and mass transfer The typical reaction of deoxidation is:

$$x[M] + y[O] \rightleftharpoons (M_xO_y) \tag{1.1}$$

$$K = \frac{(M_xO_y)}{[M]^x \times [O]^y} \tag{1.2}$$

$$logK = \frac{A}{T} + B \tag{1.3}$$

In dilute solution the activity of dissolved elements can be considered equal to their concentration. All the chemical reactions between the dissolved oxygen and deoxidizers take place both on the surface of oxidizers and on the surface of oxide formed. there is also a difference in the effect of the deoxidizing agent linked to the mode of introduction of it: in fact, there is a more marked effect if the agent is introduced through a cored wire with respect to when the agent is immersed. It is possible to see it in the following diagram for aluminum:

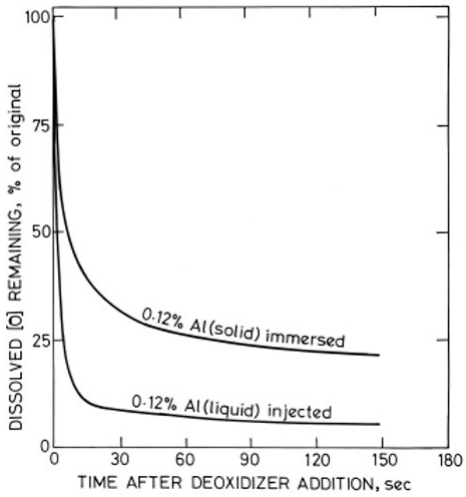

Figure 1.4: Difference between cored wire system and immersion system for aluminum

The solubility of the additive in the solid phase should be small, with the formation of a refractory eutectic with the base of the alloy (iron) being desirable. The modifiers of the second kind not only crush the dimensions of the crystalline grain, but also change the crystal growth forms. They prevent the development of lamellar crystals, giving them a rounded shape. It has been experimentally established that it is expedient to use alkali and alkaline-earth metals as modifiers of the second kind. Wide application is found for the out-of-furnace treatment of liquid steel by a compound containing calcium (Ca or Ca-Si). In this case, the effect of calcium on the structure and properties of the metal in very strong, because it has a very high chemical activity: it can allows deoxidation and desulphurization, modification of macro - and microstructure. Its most important effect is to make non-metallic inclusions globular. Calcium, in fact, has a very high capacity to remove inclusions of alumina which are very dangerous and harmful, due to the fact that their shape is generally very sharp and elongated which causes high stress intensifying factors. When studying the effect of modification on the structure and properties of die-cast metals, the following positive points can be singled out:

- making the cast structure finer due to changes in the crystallization parameters, increase of cooling rate, reduction of the transcrystallization zone;
- Increase the homogeneity of the distribution in the casting of carbon, sulfur, phosphorus, to avoid the weakening effect by segregation phenomena;
- improving the performance of castings due to change and improvements in the cast structure. The modification of the metal is similar in nature to the

increase in the rate of cooling during crystallization. Due to the inevitability of fluctuations in such parameters as oxidation, gas saturation, metal contamination, its physio-chemical properties, melt temperature, and its dwell time in a ladle, in practice there is a serious problem of reliable reproducibility of the results of modification even under conditions of a single melting point shop.

1.4 Heredity of the structure

When choosing a method for the production of high alloy cast steel, particular attention should be paid to the elimination of the consolidated hereditary relationship between the structure and composition of the materials loaded with the properties of the melted funds and the structures and jets formed by them. . The inheritance is the ability of the spindle to reproduce and transfer characteristics in metal products, in particular the chemical and structural organization of the raw materials and the almost unchanged chemical composition of the alloy [45]. The phenomenon of structural inheritance in alloys can be like a set of regularities that explains the sequence and the mechanism of the development, transfer and manifestation of structural information in the system of "Charge - metallic melt - part" (solid-liquid-solid)) [46]. For cast iron alloys, the main phases in which certain information is placed "metallogenetic" are the melting and crystallization processes. In these processes there is a certain relationship between the liquid and solid states of the metal, and each of them carries some inherited characteristics of another state. This creates the prerequisites for the effective use of the manifestation of metallurgical and structural inheritance in the production of cast products [10]. Through appropriate treatments, of which the technological parameters are fixed, in which the corresponding external influences on the liquid metal are modified and which intentionally solidifies the characteristics of the jet structure and causes increases and reduction of inheritance it is possible to obtain the necessary properties physical and mechanical properties of the desired casting products [9]. After the melting of all the components of the steel and the obtaining of a macroscopically homogeneous fluid, the transition from various types of short-range order continues: the components of the charge are organized obtaining a more homogeneous atomic structure. A change in external conditions, such as temperature, leads to a change in the structure of short-range order: the interatomic distances, the geometry of the arrangement of atoms and the size of the clusters. It is known that the greater the degree of equilibrium of the melt and the uniform distribution of the atoms of the alloy components in it, the weaker the hereditary effect of the charge materials and the more stable the quality of the castings. The main way to obtain metals without traces of structural inheritance

is to heat the melt.

1.5 High-temperature treatment of liquid metal

This method has a very significant effect, it has been developed in Russia with high success and it is a way to threat the molten iron, it should be called as high-temperature and BTOR is the acronym in Russian language. This method leads to to the refining and homogenization of the metal bath, and as consequence it increases the complex of operative characteristics and the quality of castings. The high temperature treatment of the melt uses the thermal action, the metal is heated to a certain temperature, higher than the liquidus temperature, there is an exposure for a certain period of time, cooling in the furnace to the casting temperature and holding the metal near the casting temperature to homogenize and to reach the perfect condition for the casting[47, 49]. In the production of cast iron in an electric arc or induction furnaces, it is possible to adjust the composition and temperature in the liquid state by choosing optimal conditions of heat treatment time. During the casting of metal in the furnace into the metal bath is normally supplied the same weight batch and melted, and after it is important to rapidly raise the temperature for the discharge. In the same way, with the heat treatment it is necessary to put scraps in metal bath in order to avoid high wear of the lining. During the processing of the molten metal occurs the loss of the most alloying elements, which must be compensated by the introduction of them into the charge. The most susceptible elements are carbon, aluminum, chromium and vanadium, because they are the most exposed to the carbon monoxide.

The time at which the material is maintained at a certain temperature is determined by study on the changes on the structure, of physical properties of liquid alloys, under the thermal action and relationship between the structure formation and molten state.

By studying the time dependencies of properties as surface tension, viscosity, magnetic susceptibility, etc., it was found that after heating and melting the sample to a target temperature the change in the properties during the isothermal hold follows a pattern with damped oscillations [47]. The state of the multi-component industrial melts, a after a complete crystal-liquid phase transition, is not generally a state of equilibrium. For each melt, there are temperatures at which there are intensive changes in structure, these are so-called critical ones, heating to these critical temperature promotes a transition of the system to equilibrium condition or to a state close to the equilibrium. The higher is the degree of equilibrium of the liquid and also the uniformity of distribution of the atoms in the alloying components, weaker is the effect of heredity from the starting materials and higher is quality of castings.

Elimination of heredity happens in the liquid when it is heated to a predetermined temperature passes through the phase transition dynamics [45, 46, 52], without a chemical reaction, so there are not generation of molecules. The values of the critical temperatures are established in laboratory studying the temperature dependencies of the properties of the melt. These values, as the relaxation time, do not depend on the studied volume but they determined by the kinetic processes that occurs at microscopic level. With the growth of the melt superheat, but not above the optimum value that is different for each material, the crystallization interval shrinks due to the lowering of the liquidus temperature, the density jump increases almost twice during the isolation of the primary austenite crystals, the density of the solidified sample increases. The thermal influence on the melt reduces the effect of unwanted impurities and produces alloys with the desired structure, chemical composition and controls the content of gas and nonmetallic inclusions, this allows to obtain casting with a finer grains and improved deformability and strength of the metal [45, 53, 55].

A change in the structure of the cast metal due to enrichment of equilibrium in the melt has effects on its operational characteristics: for example the ductility of steels can increase in a range of 20-40%, in particular at temperatures for hot deformation. There is also 30% increase in the elastic behaviour of the steels and thermal conductivity increases by 10% [45].

It can be said that the thermal treatment is a method that allows to control the degree of dispersion of the particles in the metallic melt and homogeneity of the bath [47, 56]. It was discovered that the metal after the remelt retains certain features of the structure of the starting raw materials. As regards the morphological characteristics of the structure, the repeated remelting of the steel with a different initial structure causes its regular changes depending on the inherited hereditary characteristics of the charge and the time-temperature conditions of the crystallization. The possibility of creating certain positive metallogenic (hereditary) features during the crystallization in the original structure creates the prerequisites for not only preserving them, but also increasing significantly during subsequent re-melting. An important role in the manifestations of the metallogenetic heredity belongs to the totality of the defective and atomic-crystalline structure, since the probability of inheritance increases with the decrease in the element of heredity. Theoretical basis is the notion of liquid metals as microinhomogeneous systems consisting of two zones, completely disordered with increased energy and ordered (cluster) - crystal-like groupings of atoms, with reduced energy. Both zones continuously exchange atoms with each other and exist separately for 10- 12 seconds [57, 59]. The genetic relationship of solid and liquid metallic material is satisfactorily explained from the standpoint of fluid models that are based on the concept of a quasi-polycrystalline description. *Quasicrystallism* is the modeling of the liquid

structure based on actual interparticle interactions, exhibiting, in the absence of thermal motion, a pronounced crystal structure.

Proof of the effective use of the concept: quasicrystallism is a model which can describe the structure of the reals liquids and all the properties of the metallic melts:

- the melt consists of micro-regions of clusters, the arrangement of the atoms in clusters has a certain short-range order.
- Due to the intensive thermal motion of particles clusters do not have clear boundaries and for this reason the lifetime of cluster equilibrium limited and depends on the composition, on the types of chemical bonds and temperature. It is possible to find the existence of clusters of two or more types of order.

The non equivalence of energy inter-atomic interactions causes different types of clusters with different structure and composition and also having different stability over time. The most stable clusters, with the longest life, are formed by the most strongly interacting components, these are iron and oxygen. The reasons for microinhgomogeneity is the disparity of inter-atomic bonds. When there is a change in the physical properties of the melts, due to overheating above the liquidus temperature, is often observed an abnormal trend on the curves. These anomalies are expressed in the inflections and discontinuities of the curves, in the appearance of hysteresis. When the melt is heated to the temperature of the anomaly, irreversible destruction of the cluster begins. The higher is the temperature of anomaly, the smaller is the size of the anomaly. It can be thought that, when temperature of the anomaly is low, it disintegrates completely the micro-cladding envelope. If the temperature of the anomaly is low, then carbide-like clusters of the Me-C type can remain in the melt. Before crystallization in the melt, equilibrium micro-groups can exist on the basis of Me-Al and Me-C bonds [47]. Crystallization of the melt from the supercooled state of the package is completed, there is a change the cluster packing changes from chaotically disordered to dense in connection with cluster growth. Before a spontaneous transition of a part of the freely ordered atoms into a crystalline lattice, a skeleton is formed from clusters that touch each other, the space between them is filled with freely ordered atoms. The contact of clusters with one another induces the formation of an embryo, so immediately spontaneous crystallization of the remaining part of free-ordered atoms occurs immediately [51]. When the metal is subjected to a subsequent cooling liquid metal, the previously destroyed micro groups are not formed again. Thus, the high temperature treatment allows the melt to reach a state of equilibrium, which leads to an increase in the degree of dispersion of the dendritic structure, the reduction of its chemical and physical heterogeneity, the elimination of an undesirable heredity, the reduction of

the size and the number of the defects. The improvement of the theoretical and technological bases for the production of metal with finer grain structure makes it possible to effectively control the heredity of the materials and to realize cast product with better and more useful cast micro and macrostructure and required mechanical and operational properties. Conclusions

- It has been determined that the use of casting die ferrous alloys is limited due to the coarse grain structure, primary carbide and cast structure and high heterogeneity, all of these element causes high anisotropy.
- Despite of the large amount of work devoted to the ironmaking and steelmaking process factors, this process is not well known.
- There is an insufficient amount of information to establish a relationship between this treatment and the various rates of cooling of alloys during crystallization and the structure of the steel in the solid state.

1.6 White cast iron for wear resistance

The actual working conditions of equipment and tools regarding abrasive wear can be associated with various external load patterns. All these situations can be classified according to the type of impact of an abrasive particle on the friction surface: sliding and rolling friction, the impact of a metal with an abrasive and specific phenomena that occur when the flow of abrasive particles transported by air or liquid manifests itself at the work surface. Among the factors that have a major influence on component wear, there is the hardness of the abrasive and the size and shape of the particles. With increasing particle size and roughness on their surface, the intensity of wear increases. Furthermore, the wear conditions of a current of abrasive particles in a liquid or gas are also influenced by the abrasive concentration in the current, the impact velocity of the particles and the angle of inclination between the velocity vector and the surface of the part. The intensity of wear depends significantly on the movement speed of the abrasive particles, which determines their kinetic energy when they meet the wear surface. Aggressive and abrasive wear can occur under conditions of high impact, rubbing and rolling on an abrasive. The abrasive wear is therefore influenced by the nature, the geometric shape, the hardness, the fragility, the thickness of the layer of abrasive particles, the impact energy, the physical and mechanical properties, the structure of the material of the part. The abrasive wear is then characterized by a particular formation of reliefs on the wear surface in the form of alternate holes, formed as a result of local plastic deformation and bridges between them. With the repeated interaction of the abrasive with the surface of the piece, the diameter of

the holes is expanded and their depth increases, the surface is repeatedly deformed, riveted and the particles are detached from it. Such a mechanism of destruction is characteristic of viscous structures. When impact abrasion wear of solid and brittle structures, surface destruction occurs due to the fragile chipping of metal enclosed between the holes formed during impact. The presence in the structure of alloys of hard and brittle phases (carbides, carbonitrides, nitrides, borides, etc.) facilitates nucleation, development and fusion of microcracks and therefore the rate of material removal. The wear resistance of metals and alloys will be determined by a set of properties, the main of which are hardness, strength and shear strength. When methods are chosen to increase the resistance of parts to impact, particular attention should be paid to the tendency of the fragile chipping surface layer and its ability to deform.

1.6.1 The influence of the chemical composition of the cast iron on its wear resistance

The typical carbon (C) content in wear-resistant white cast irons is between 1.7% and 3.6%. Carbon is the main regulator of the amount of carbides present inside the metal matrix. One of the main reasons that can explain why the carbon concentration range is so wide is certainly linked to the need to obtain specific amounts and types of carbides in the structure. The impact of carbon on wear resistance and durability is remarkable, in particular a maximum of K_i is reached when the concentration of carbon is in the range $2.8 \div 3.6\%$, while the hardness always increases with the increase of the carbon content. The fact that a decrease in strength and wear resistance with higher carbon content is observed is associated with the release of hypereutectic primary carbides as $(Fe,Cr)_{23}C_6$ which have a greater effect on wear resistance and resistance respect to hardness [65].

Chromium (Cr) is the most important alloy element in white wear-resistant cast iron, it actually reduces the carbon solubility in the α -and γ iron, it increases the stability of the austenite solid solution and the amount of eutectic component. In cast iron, chromium has a very high solubility [65] and even with a small chromium content, a carbide phase is formed. Chromium can partially replace iron atoms in orthorhombic carbide iron $(Fe,Cr)_3$ C or form chromium carbides in which some of the chromium atoms are substituted by iron: trigonal $(Cr,Fe)_7C_3$ and cubic $(Cr,Fe)_{23}C_6$ [65]. When the chromium content is $12 \div 24\%$, the carbides M_7C_3 are formed, they contribute to the increase in hardness, mechanical strength and wear resistance of the alloy. However, as a result of increasing the chromium content, it reduces the wear resistance of the alloy, since in the iron there can be large needle-shaped and fragile hypereutectic carbides M_7C.

In the white cast irons, silicon (Si) can be considered as an alloying element

which is distributed during crystallization between austenite and molten eutectic. Its content can generally be between 0.3% and 2.0%. Silicon increases the temperature of eutectic crystallization, extends the eutectic transformation interval, prevents supercooling and reduces the effect of cooling speed. This leads to a decrease in all properties [65].It also promotes the formation of graphite, and opposes the obtainment of a white cast iron.

Manganese (Mn) is able to stabilize the austenite (γ-Fe), with an increase in the manganese content the carbon is redistributed between the austenite and the melt with eutectic composition, and its concentration in austenite increases significantly. At the same time, the amount of carbides is significantly reduced and the percentage of residual austenite increases. This allows a reduction of wear resistance, mechanical strength and hardness. On the other hand, wear-resistant manganese alloy cast irons are characterized by high levels of ductility and toughness, which are advantageous when operating in severe conditions in terms of wear and abrasive impact. Moreover, the wear resistance of white cast irons with significant manganese presence can also increase due to the structural and phase transformation of austenite [65].

With a nickel (Ni) content of 2.0%, it is observed that K_i, σ_B and HRC decrease, all that is associated with an increase in the amount of residual austenite in the iron structure. This reduces the hardness, increases the ductility and toughness of the alloys, which can be useful for wear-resistant parts subjected to shock loads.

Molybdenum (Mo) is generally present with a content comprised in the range 0.3÷5.0% in wear-resistant cast-iron. It is part of those elements that strongly delay the decomposition of austenite in the perlitic region, which increases the hardenability and production of martensite. With the increase of the molybdenum's concentration it can be seen that wear resistance and hardness increase, especially at Mo$>$ 0.8%, and mechanical strength reaches its maximum in the range 1.3-1.8% Mo and while outside it does not change with the increase of its concentration. Molybdenum is distributed between the three phases: carbides Mo_2C, M_7C_3 and in solid solution. In cast iron with Mo up to 1.5%, half of it is bound are linked to Mo_2C carbide, about a quarter is in austenite, the rest is combined. Only a small part of molybdenum (0.2%) is in solid solution. Given its distribution, there is no significant effect on the transformation of perlite, so molybdenum additions of 3.0% or more are required in high-chromium cast irons. One of the most critical issues related to molybdenum is related to the fact that it is very expensive and scarce, so what is more convenient is to use it in combination with Ti, V, Cu, B. This strategy allows to reduce the molybdenum content to 0.3÷1.0% depending on the concentrations of other elements [65]. The addition in the chrome white cast iron with vanadium (V) and titanium (Ti) allows to note a significant increase of their K_i, σ_B and HRC, all this for the formation of carbides VC and TiC with

a very high microhardness (H_{50}> 30000 MPa). These are the hardest carbides of all those known in white cast irons [65]. Vanadium and chromium-vanadium cast irons have special carbides in the structure that, in combination with austenite, are formed during the double Eutectic crystallization A + VC and A +(Fe, Cr)$_7$C$_3$ and triple Eutectic A + (Fe, Cr)$_7$C$_3$+VC. These cast irons have a high wear resistance and are used for parts that operate in harsh environments (dry friction, abrasive materials, high static and dynamic loads). Wear-resistant non-stick cast irons have not yet found great space in practice: vanadium has a very high cost per unit mass and its availability is limited, titanium, on the other hand, causes difficulties during fusion and since the active titanium cast irons are with respect to atmospheric gases, refractory linings and form materials. However, the results available on the use of chrome cast iron with vanadium and titanium make it possible to state that this combination of alligator elements is very valid [65].

The amount of vanadium in the cast iron can reach a level of 6.0÷7.0%, while the titanium of the order 1.0÷1.5%. A 2.0% vanadium causes an increase in abrasive wear resistance. Titanium has a very powerful effect with a peak that is around when its concentration is between 0.3% and 0.7%. The decrease in the properties of Ti alloys>0.6% is associated with the saturation of the gas, the decrease in density and the increase in the porosity of the casting.

Copper (Cu) has practically no solubility in cementite and carbides and it has a negligible effect on the primary structure of white cast iron with high wear resistance. Its most important ability is certainly to regulate the solid state transformations. In the chrome-molybdenum and chromium-manganese cast irons, in fact, copper is often introduced to increase the hardenability. The solubility of copper in iron is limited, so its content does not exceed 1.0÷1.5% normally. Maximum performance is achieved with a copper content in cast iron in the range 0.4% ÷ 0.6%. There is a decrease in wear resistance when the concentration of Cu is higher than 0.6%, this fact can be traced back to the fact that the areas enriched with copper have a low resistance to the action of the abrasive particles[65].

Boron (B), antimony (Sb) and calcium (Ca), on the other hand, are generally added as micro-alloying element and modifiers inside the white cast iron with high wear resistance. Boron has a strong effect on the hardenability of the metal, contributes to the formation of martensite, thus increasing both the micro-hardness and the overall hardness, also favors the formation of hexaborides in the matrix, which allow to increase resistance to wear. It is also capable to decrease the melting temperature of the alloy, without causing an increase in the viscosity of the melt. With a concentration of boron equal to 0.008%÷0.015% the mechanical strength and the hardness of the cast iron have a minimum increase up to a content of 0.01% and therefore drastically decrease. Such a drop in K_i, σ_B, HRC is associated with an increase in the brittleness of the alloy due to the release of a large number of

borides and carbides of complex composition. This facilitates the dispersion of microvolumes under wear from abrasive particles [65].

Antimony has an effect similar to that of boron. When the antimony content is between 0.01-0.015%, there is a maximum resistance of the cast iron. It has a strong modifying effect on white cast iron and its influence is very strong on the crystallization of austenite and on the solidification of the eutectic component. The antimony modifies the binary phase diagram Fe-C and in particular shifts the eutectic point to a lower carbon content and this allows to have a eutectic content in the final solid. With the introduction of an optimal antimony content, there is an increase in the crystallization rate of cementite in low-alloy cast iron and austenite, the carbide phase [65].

Finally, it has a modifying effect that is able to prevent dendritic crystallization of austenite, increase the number of eutectics, and reduce the cementite fields without structures. Calcium also has a strong effect on the cleanliness and quality of the metallic bath, it is, as already explained, a strong fluxing agent but at the same time also desulfurizing, has a strong effect in removing phosphorus and allows to remove non-metallic inclusions . Excellent calcium additions contribute to improving the wear resistance of white cast irons, however, excessive content reduces it. Some studies show a significant increase of all properties to Ca>0.007%, however, when it exceeds 0.015% there is a strong reduction of K_i [65].

Alloy	Country	Chemical composition,%					
		C	Si	Mn	Cr	Ni	Mo
Nihard-2	USA	2.7-3.6	0.4-0.7	0.4-0.7	1.5-2.6	3-5	-
Nihard-1	USA	3.13	0.41	0.54	1.68	3.5	-
Nihard-4	USA	3.14	1.31	0.27	7.34	5.33	-
IC290H12M	RUSSIA	2.7-3.2	0.4-0.9	0.4-0.8	12-15	-	1.4-1.6
IC300H16MT	RUSSIA	2,8-3,2	<1	<1	15-17	-	1.0-1.5
IC210H12G5	RUSSIA	1.9-2.3	0.4-1	4.6-5.6	11-14	-	-
ZA	UK	2.4-3	<1	0.5-1.5	14-17	<1	<2,5
ZV	UK	3-3.6	<1	0.5-1.5	14-17	<1	1-3
IC28N2	RUSSIA	2.7-3	0.7-1.4	0.5-0.8	28-30	1.5-3	-
IC170H30GZ	RUSSIA	1.7-2	0.5-0.9	2.8-3.5	29-326-	1-1,5	
V5700	GERMANY	2.3-2.9	0.5-1.5	0.5-1.5	24-28	1.2	1
HIC	USA	2.3-3	0.2-1.5	<1.5	24-28	<1.2	0.6
3D	UK	2.4-2.8	<1	0.5-1.5	22-28	<1	-

Table 1.2: Wear resistant cast iron

1.6.2 The influence of the microstructure of the cast iron on its wear resistance

In alloys with a concentration of chromium of Cr 3.5÷5% with Fe_3C carbides with microhardness of 8000÷10000 MPa despite having high hardness at macroscopic level, 60÷68 units after heat treatment of hardening are characterized by low resistance to abrasion due to the absence of M_7C_3 carbides and $M_{23}C_6$. Alloys which, on the other hand, have a chromium content in the 12÷24% range, as has been previously introduced, more complex carbides whose microhardness is 12000÷15000 MPa. At the macroscopic level, the resulting hardness is slightly lower, 55÷68 HRC units, but they are considerably more durable[65]. Furthermore, it is possible to observe that cast iron with a carbon content slightly above 2% has a low resistance to wear due to the low carbide content. The high resistance to wear is certainly determined by the presence of carbides but also by the metallic matrix in which they are present. The best resistance to wear in alloys with a martensitic base is therefore inferred that the alligation of expensive alloy elements such as V, Mo, Ni, W, etc., that increase the hardenability of the material is essential. However, it is important to underline that the presence of residual austenite following a hardening treatment often makes the material unsuitable to work under abrasive wear conditions.

However, as reported in several studies[65] on this topic and practical tests, with friction with an abrasive impact, it is a matrix that consists of $5-10\%$ of austenite is an advantage because it guarantees a certain viscosity to the cast iron. Metal matrices made of ferrite and perlite make white cast iron poorly to wear, so durability is much lower than martensitic matrix alloys. The cast irons, whose structure contains cementite type carbides, or the M_3C type, which is an unstable phase, have lower wear resistance coefficients than those with special carbides, such as M_7C_3, MC. Normally the higher the percentage of these carbides, the greater the resistance to wear. As already reported, the chrome is certainly one of the most relevant alloy elements and always present in the cast iron, however there are some issues to be taken into consideration.

Chromium prevents the conversion of perlite by cooling the casting. An increase in the number of carbides in the wear-resistant cast iron structure is therefore recommended only in hypereutectic cast irons. In hypereutectic cast irons, the fragile and loose primary carbides influence the matrix and contribute to the formation of micro-chips, which significantly increase component wear. Another element that contributes to the high durability of the parts is the presence of mixed carbides with iron and chromium, which are obtained only with a Cr content of more than 11%. With more complex alligations, for example adding Si, Al, V, Ni, Mo, W, everything can also be made of cast iron with a lower chromium content.

As reported by the scholar Voinov B.A. following studies based on the inter-

action between the main main microstructural constituents present with abrasive particles, he proposed a classification of white cast iron on the basis of abrasive wear resistance, according to which they are divided into four categories: minimum, high, high and maximum wear resistance. The pearlitic-cementitic cast iron has the lowest resistance to wear, while the high-alloy cast iron with martensitic or martensitic-austenitic matrix, uniformly distributed chrome, titanium, vanadium and other carbides and borides have the highest resistance to wear.

In the white cast iron the impact on wear resistance of the individual structural components is clearly observed: the loss of mass of the samples during abrasive wear decreases with the increase of the eutectic content and the size of the grain, reducing the volume of the cementite and its position as separate isolated areas, the optimal number of eutectics with a more subtle and uniform structure distribution in interdendritic spaces, presence of carbides or mixed carbides in the microstructure in the form of small inclusions. The studies [65] carried out so far on the alloying of the cast iron in order to obtain wear resistant with the addition of several elements show that to obtain a good result it is necessary that:

- the content of carbides which give a positive contribution is as high as possible;
- there are minimal deformations to prevent cracking and chipping of carbides;
- the dimensions of the base areas between the carbides are small enough to minimize the wear of the base, the exposure of carbides, their elimination and breakage.

Some studies [65] available on the use of bainitic cast irons, as wear-resistant, show that with a bainitic structure containing a part of residual austenite can allow good performance, however, in the process of making components, it is difficult to obtain such a structure, especially if the particular is large, since the heat treatment, which provides cooling in salts is quite complex. Under strongly abrasive conditions, a fragile fracture may occur, when the limit values for the microvolume loading speed or the impact energy of an abrasive particle are exceeded. In these situations, the size of the carbides and their orientation with respect to the wear surface are extremely important for determining the strength of the workpiece. It is also important to check the ratio between the chromium and carbon content, if an optimal ratio is not guaranteed, the formation not only of hypereutectic carbides M_7C_3, $M_{23}C_6$ with microhardness 12000÷15000 MPa, but also cementite type carbides (M_7C) being brittle and large, which causes a lowering of the resistance to wear and it is also that the capacity of the cast iron to withstand impact loads decreases and the alloy hardenability is reduced. Therefore, as some literature sources report, a high resistance to abrasive wear with impacts is assured if:

- contains the maximum quantity of high hardness carbides such as M_7C_3 and MC;
- M_7C_3 carbides are oriented perpendicular to the wear surface;
- the carbide particles are fine and homogeneously distributed in the matrix, possibly martensitic with a fraction of austenite of optimal austenite.

1.7 High temperature resistant cast irons with high wear resistance

Metals are materials that often work in conditions where temperatures are high, or in any case in the presence of heat, so in order to maintain their high performance they must have high resistance to heat, or a high capacity to resist the heat oxidation and corrosion in the presence of gas at high temperatures. Corrosion during exposure of metal to the atmosphere is a spontaneous chemical process, whose driving force is the thermodynamic instability of the metallic state. Therefore, during the corrosive process, it oxidizes by passing to a thermodynamically more stable state. Heat resistant alloys are intended for the production of work pieces operating under generally limited loads and at temperatures above 550°C. According to GOST 7769-82, heat resistant cast irons should increase the mass due to oxidation not higher than 0.5 g/mh and therefore equal to 0.2% at a working temperature of 150 h. The cast iron alloyed with aluminum, silicon, chromium and nickel have a greater resistance to heat, these elements are in fact the ion of dense iron oxides, spinels and even their own oxides on the cast iron surface, increasing the resistance to corrosion. Furthermore, they ensure the stability of the structure during the temperature increase. The GOST 7769-82 standard indicates the following cast irons as resistant to temperature: The cast iron with a high content of corrosion resistant and heat resistant nickel also have a high resistance to heat, although their use as heat resistant is limited due to high price and nickel low availability.

Alloy	C	Si	Mn	Cr	P	S	MPa	MPa	HB
					Not more		Not less		Average
Low alloyed									
CH1	3.0-3.8	1.5-2.5	1.0	0.4-1.0	0.3	0.12	170	350	247
CH2	3.0-3.8	2.0-3.0	1.0	1.0-2.0	0.3	0.12	150	310	247
CH3	3.0-3.8	2.8-3.8	1.0	2.0-3.0	0.3	0.12	150	310	263
High alloyed									
CH16	1.6-2.4	1.5-2.2	1.0	13.0-19.0	0.1	0.05	350	700	425
CH28	0.5-1.6	0.5-1.5	1.0	25.0-30.0	0.1	0.08	370	560	243
4H32	1.6-3.2	1.5-2.5	1.0	30.0-3.40	0.1	0.08	290	490	293

Table 1.3: High temperature resistant cast irons (a)

Alloy	Chemical composition,% C	Si	Cr	Al	MPa	HB	Metal resistance g/m^2	Growth	T (°C)
							0.2	0.4	800
CS5	2.5-3.3	4.5-6.0	0.5-1.1	0	150	140-294	10	0.5	900
							20	1.0	1000
							0.05	0.1	800
CS5SC	2.7-3.3	4.5-6.5	0.2	0.1-0.3	290	220-294	0.2	0.5	900
							1.0	0.7	1000

Table 1.4: High temperature resistant cast irons (b)

Alloy	Chemical composition,% C	Si	Cr	Al	Mn	P	S	Properties MPa	HB
						Not more			
1	3.0-3.8	2.0-3.0	0.4-1.0	0.6-1.5	0.5		0.03	390	276
2	1.8-2.4	4.5-6.0	0	5.5-7.0	0.8	0.3	0.12	120	268
3	2.5-3.0	1.5-3.0	1.5-3.0	5.0-9.0	1.0	0.3	0.12	120	263
4	1.6-2.5	1.0-2.0	0	19.0-25.0	0.8	0.2	0.03	290	303
5	1.0-2.0	>0.5	0	29.0-31.0	0.7	0.04	0.08	200	457

Table 1.5: High temperature resistant cast irons (c)

Two of the main characteristics of these cast irons are the single-phase austenitic structure that does not undergo phase transformations and the formation of a stable protective film on the surface that is able to self-repair quickly once damaged due to its passivating characteristics during wear at high temperatures.

An increase in the humidity present in the air causes an increase in the corrosion rate, while in the presence of sulfur compounds in the gaseous medium causes the occurrence of intergranular corrosion phenomena in the cast irons, especially at temperatures above 1000°C. If the gaseous medium is the product of combustion of a fuel, the corrosion increases considerably, and the greater the coefficient of the flow of air with which the fuel is burned Strong corrosivity was observed if a vanadium-containing fuel is used. The combustion of low-cost liquid fuels contaminated with vanadium, such as fuel oils, produces large amounts of ash containing vanadium oxide V_2O_5. The ash, attached to the metal, increases its oxidation rate by a factor ranging from one to ten. The vanadium oxide interacts with various oxides of iron, nickel and chromium, destroys the protective film, forming pores in it, through which the oxygen of the gaseous phase and the liquid

V_2O_5, which oxidize the metal, penetrate relatively easily. At temperatures above 150-300°C, the aggressiveness of the gaseous environment increases considerably and the corrosion rate increases considerably. For the cast irons, it is possible to observe that a critical temperature exists, beyond which the oxidation processes proceed with great speed. This is due to the formation of wustite at a certain temperature. The type of heating can also have a major influence on the heat resistance and high stability of the cast iron. In the worst conditions there will be jets exposed to alternating heating and cooling. The rapid alternation of heating and cooling favors the formation of cracks in the oxide film and leads to a significant reduction in its ability to protect the metal. Therefore, in those alloys where there are elements that increase the temperature of wustite formation there will be a favorable effect on heat resistance. Other factors: one of the factors affecting the heat resistance and corrosion resistance of cast iron is the jet cooling rate. The oxidation of samples taken from thicker jets is greater than those in which the section is reduced. This is due to the fact that in the central part, with slow cooling of the casting, the carbide precipitates become larger than the surface. From this it should be noted that the effect of the jet cooling rate on cast iron growth can be weakened by various deoxidation methods. For the degree of heat resistance of cast iron, the origin of the filler materials and the melting conditions are very significant. All this determines the content of gas in the iron and the quality of the carbides. Vacuum melting favors an improvement in the heat resistance of cast iron, as there is a reduction in the content of harmful impurities, such as sulfur and phosphorus, small carbides and a limited gas content. An increase in carbon monoxide content in the CO atmosphere significantly reduces the corrosion rate, however, with a large amount of CO in the gaseous medium, carburizing of the alloy surface may occur, which is an increase in the carbon content, which will a decrease in the protective properties of the oxide film.

Chapter 2

METHODS OF RESEARCH, EQUIPMENT AND MATERIALS

2.1 Work strategy

The following chapter presents the strategy, the methodologies and the working equipment that have been used during the research activity on white cast irons and which were support for obtaining the results. As explained in the introduction and in chapter 1, the interest of this work is related to the development and to improvement of white cast irons, which are typically for the production of components, such as molds, mills for grinding,pumps, etc., which are used in industry and which typically work in very heavy conditions. The first part of the research was dedicated to the analysis of the effect of the alloyed elements on the two properties of interest for the material and building of the mathematical model necessary to be able to predict the properties given a certain content of the elements and therefore a certain composition of the alloy. To do this, the samples of known composition were made by melting operations in the laboratory and therefore the necessary equipment, raw materials and calculations are described and listed. The samples were initially characterized, the necessary technologies are then reported, and then hardness and the coefficient of wear resistance were measured on them, are reported instrumentation, procedures and the calculation methods. In this chapter the theories necessary for the construction and validation of the mathematical model and the one related to the optimization of the composition able to maximize the properties are also presented.

Then, having to take into consideration the economic aspects, to find the alloy that is the best compromise between operating performance and costs, the theory

relating to the calculation of costs and to the Material Selection is also presented.

There is, put in support of those who reads, a introductory flowchart to better understand the research path and the strategy.

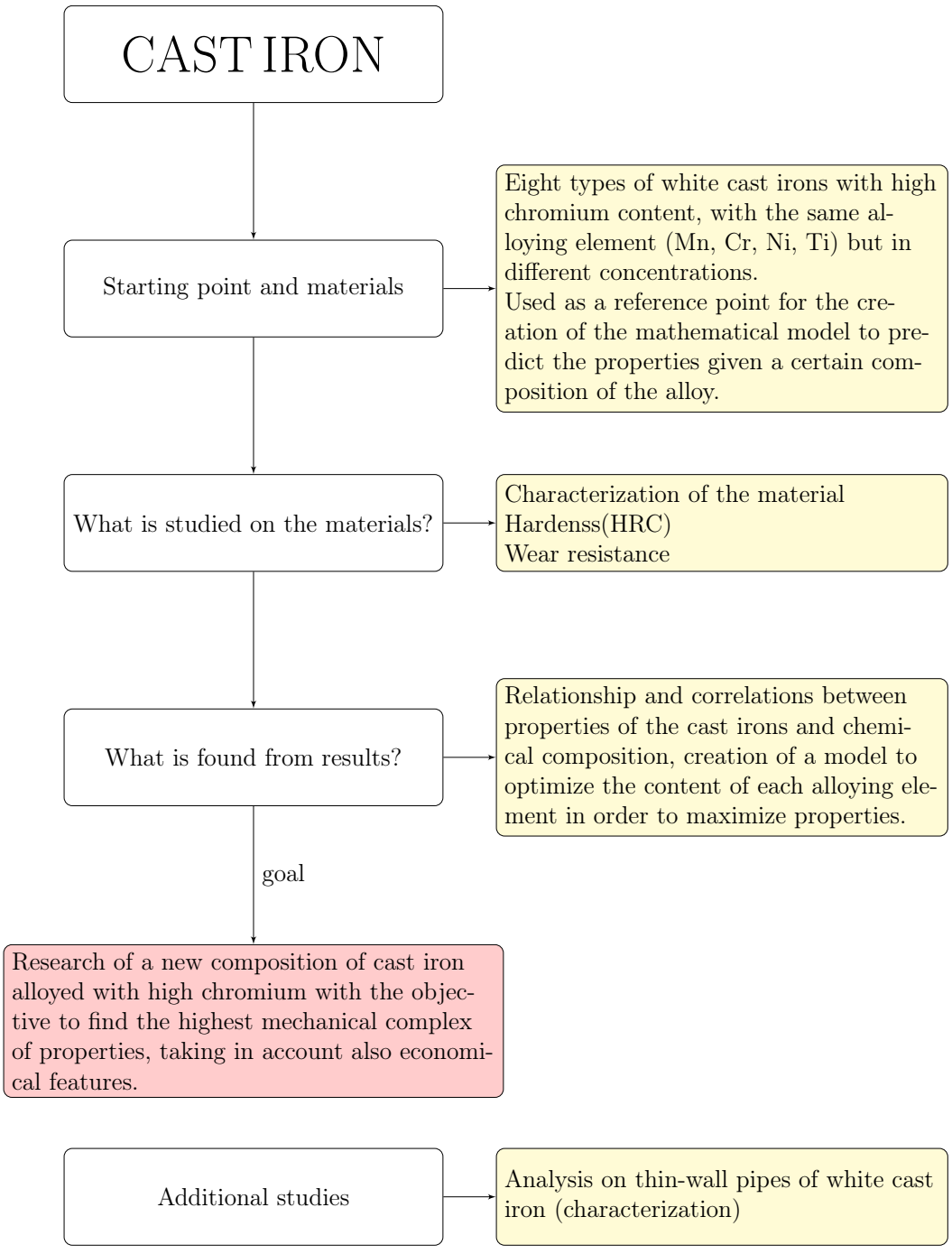

2.2 Melting of the experienced alloys

2.2.1 Equipment for the melting and casting of metal alloys

Experimental alloys were obtained to study structure and properties in the IST-006 induction furnace with refractory lining.

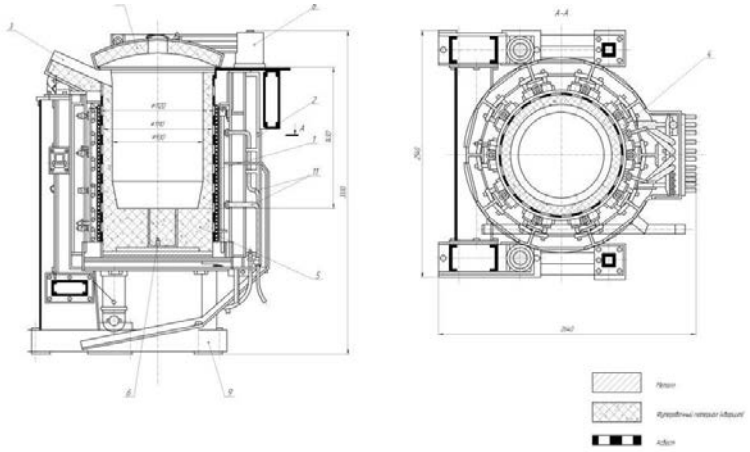

Figure 2.1: IST-006 induction furnace

Furnace capacity (t)	Power(kW)	Nominal current frequency (kHz)	Voltage (V)	Melting speed (t/h)
0.06	100	2.4	3×380	0.13

Table 2.1: Furnace properties

2.2.2 Ferroalloys

The ferroalloys used during the melting operations for the production of the samples were:

- Cast iron
  - P1, GOST 4832-80;
- Steel scrap:
  - 1A steel scrap, GOST 2787-86;

  - S255;
  - Iron armco.

- Ferrotitanium:
  - FeTi 32, GOST 4761-80;
  - Ti-CP.

- Ferrochromium:
  - FeA850 GOST 4757-91;
  - Carburized ferrochromium FCH260.

- Ferromanganese:
  - FeMn 70, GOST 4755-80;
  - Ferro-silicon-manganese FSN260.

- Metallic nikel;

As a deoxidizer used aluminum brand A 95 (GOST 11070-74). After melting, the molten metal was deoxidized in a crucible and poured in the sand-clay forms (FGD). Determination of the concentration of chemical elements in the melted samples carried out in the MMK laboratories.

Iron scrap	Fe (%)	C (%)	Si (%)	Mn (%)	P (%)	S (%)
P1	Balance	4.0-4.6	0.3	0.3	0.2	0.002
	Balance	3.0	1.2	-	-	-

Table 2.2: Chemical composition of iron scrap

Steel scrap	Fe (%)	C (%)	Si (%)	Mn (%)	P (%)	S (%)
1A	Balance	0.15	0.3	0.6	0.02	0.05
S255	Balance	0.2	0.6	1.6	0.075	0.05

Table 2.3: Chemical composition of steel scrap

Steel scrap	Fe (%)	C (%)	Mn (%)	P (%)	S (%)	N (%)	Cu (%)	Co (%)	Sn (%)
Iron armco	Balance	0.02	0.13	0.01	0.009	0.006	0.004	0.0025	0.0075

Table 2.4: Chemical composition of armco iron

Ferroalloy	Ti (%)	Al (%)	Si (%)	C (%)	P (%)	S (%)	Cu (%)	V (%)	Mo (%)	Zr (%)	Sn (%)
FeTi32	28.0÷37.0	8.0	4.0	0.12	0.04	0.03	0.4	0.8	0.4	0.2	0.01
Ti CP	99.12	-	0.001	-	-	-	0.02	0.038	0.148	0.009	-

Table 2.5: Chemical composition of ferrotitanium

Ferroalloy	Fe (%)	Cr (%)	C (%)	Si (%)	P (%)	S
FeA850	Balance	5.0.	8.5	2.0	0.03	0.05
FCH260	Balance	69.3	6.72	0.72	0.016	0.05

Table 2.6: Chemical composition of ferrochromium

Ferroalloy	Fe (%)	Mn (%)	C (%)	Si (%)	P (%)	S
FeMn70	Balance	65.0÷75.0	7.0	6.0	0.30÷0.70	0.02
FSN260	Balance	66.85	1.42	16.45	0.27	0.02

Table 2.7: Chemical composition of ferromanganese

2.3 Charge calculation

To prepare the samples it is necessary to combine certain quantities of raw materials, which in the cases under examination are reported in the section 2.2. To identify these quantities it is necessary to build and solve a system of equations;

the equations that are involved in these systems are the mass balances for the constituent elements of the alloys and a boundary condition. In the following section the steps in order to build a mass balance system are explained in general terms. First of all, however, it is necessary to define some quantities, so it is assumed that:

- FeX_i is the percentage of a certain ferroalloy necessary to be introduced in the batch;
- Y_i is the percentage of a certain type of scrap (steel and cast iron);
- M_i indicates the percentage of an element in the metallic state;
- x_{ij} represents the percentage mass fraction of the element j in the i-raw material;
- f_j is the loss fraction of the element j due to the oxidation that occurs during the melting operation;
- C_j the final content to be obtained in the alloy expressed in percentage;
- and n, m, p are the number of ferroalloys, scrap or pure metal available kinds.

A mass balance has the following generic form:

$$[C_j] = (1 - f_j)\left\{\sum_{i=1}^{n} [FeX_i]x_{ij} + \sum_{i=1}^{m} [Y_i]x_{ij} + \sum_{i=1}^{p} [M_i]x_{ij}\right\} \tag{2.1}$$

and this must be created for all the elements in the alloy. The boundary condition to be introduced is related to the fact that the sum of the percentages of raw the materials, that it is necessary to introduce and which constitute the charge, is equal to 100%.

$$\sum_{i=1}^{n} [FeX_i] + \sum_{i=1}^{m} [Y_i] + \sum_{i=1}^{p} [M_i] = 100 \tag{2.2}$$

So the final system that must be built to determine the composition of the charge is:

$$\begin{cases} [C_j] = (1 - f_j)\left\{\sum_{i=1}^{n} [FeX_i]x_{ij} + \sum_{i=1}^{m} [Y_i]x_{ij} + \sum_{i=1}^{p} [M_i]x_{ij}\right\} \\ \\ \sum_{i=1}^{n} [FeX_i] + \sum_{i=1}^{m} [Y_i] + \sum_{i=1}^{p} [M_i] = 100 \end{cases} \tag{2.3}$$

It is necessary to consider the loss coefficient due to oxidation, f_j, despite the melting operation of raw materials does not provide an oxidation phase, which is a typical operation of the BOF or EAF processes, in fact, no oxygen is blown into the crucible, but the atmosphere is not controlled or inert and a part of the elements interacts with oxygen, being oxidized. The oxidized elements go into slag and do not appear in the metal. The system of equation that is resolved returns the percentages of the raw materials of which the charge must be composed, after having fixed the quantity of material to be realized it will be possible to easily ascend to the actual mass in kg or g. In this thesis will be presented in detail only the calculations of the charge for the samples with the innovative compositions found thanks to the built models.

2.4 Investigations on the composition of the material with OES analysis

To determine the composition of the samples we used the technique of Optical Emission Spectrometry (O.E.S.) through the SPECTROMAXx instrument. This technique allows to obtain atomic spectra through which information is obtained on the elements that compose the material. This type of technique has as starting point the excitation of the samples through different techniques in order to extract the atoms present and study them in the form of free atoms, then proceed with a vaporization of a part of the sample. The part of the sample that evaporates is the one that contributes to the signal and the final response. Among the excitation techniques of the sample there is the one that involves the use of electric discharges, in particular of the direct current electric arc or the spark. In the case of instruments which provide excitation through the electric arc, an arc is triggered between two electrodes, one of which is usually the sample holder; a direct current source is used which is connected to the electrodes and there is a variable resistance which allows to regulate the power. When the electric arc is used the tensions are low and they are around 100 V so there is a thermal excitation, since it reaches only a few thousand degrees Kelvin (K) and this is useful for determining the elements present in traces. The second mode is precisely that of the high voltage spark ($10 \div 50$kV) which is generally produced between two electrodes, one of which in this case is the sample to be analyzed while the second is a counter-electrode, with normed characteristics. By using high voltage sparks, it is possible to reach much higher temperatures, of the order of 10000 K which allow greater excitation and the signal is on average more stable. In the case of the instrument used in the research this is the technology used. It is also possible to use low voltage discharges of the order of 10^3V. After having excited the material through

one of these techniques, what is obtained are electromagnetic radiations whose wavelengths are characteristic of the elements that are present in the sample. At this point, these radiations must be separated and analyzed using a spectrometer. The separation of the various radiations is carried out through the dispersion lattice which is one of the most important components of the spectrometer. The lattice in fact interferes with the radiations, which are characterized by different wavelengths, thus giving rise to a phenomenon of refraction. Other fundamental components of the spectrometer are the slit (which allows to have a spectrum in which each line corresponds to a specific wavelength and therefore to a specific element) and an image formation system consisting of lenses and / or a mirror concave on which the dispersion lattice is often obtained. The radiations are collected by a system of detectors, there are phototubes that convert the radiation into an electrical signal that is proportional to the characteristics of the same and based on this it is to generate an output spectrum. In this way, after appropriate calibration of the instrument, it is possible to identify which instruments are present in alloy and their quantities. The instrument was provided by the MMK company and the analysis with this instrument were performed in its laboratory.

Figure 2.2: SPECTROMAXx

2.5 Metallographic investigation tools and techniques

First the sample surface have been smoothed to obtain a mirror polished surface, without irregularities, minimum deformation and without scratches and corrosion residues. In order to smooth the surface of the samples, different abrasive papers have been used with a gradual grain size (320, 500, 800, 1200 grit) and two different diamond suspensions for final polishing (6 µm and 1 µm).

MIM-6, Neofot-21, METAM-LV31, EPIKVANT optical microscope have been used, also with the Thixomet PRO and ImageJ and have been made quantitative and qualitative analysis, using magnification in the order of 100x÷1000x, on samples before and after etching with special solution.

The etchant which has been used for the etching of the sample was a solution consisting in 25mg copper sulfate ($CuSO_4$) with 100 ml of hydrochloric acid (HCl) and 100 ml of water (H_2O) typically used for such studies on cast iron, according to the norm GOST 5639−82. The exposure time to the etching solution was about 3 seconds, after this time each sample has been cleaned with water and ethanol and dried using a stream of warm air. After the treatment the micro-structure has been studied and following the rules imposed by the norm GOST 8233−56 . To highlights the constituents and particulatity of the microstructure another etchant has been used: the Murakami etchant. In the case of ferrous alloys, these image analysis software allowed possible to carry out investigations related edges of the grains, to evaluate the size of the grains based on their number and their area. Through this tool it is also possible to conduct a study on non-metallic inclusions and on any secondary phases present in the sample. For non-metallic inclusions it is possible to evaluate volume, volume fraction and position. In the presence of dendrites it is also possible to evaluate their size. In order to carry out the investigation on inclusions and to be able to evaluate their composition, a scanning electron microscope (SEM) has been also used.

2.5.1 Dispersion analysis

The dispersion analysis concerns the investigation of samples following the observation of the samples under a microscope, where a dendritic structure is highlighted. It starts with the measurement, carried out through the analysis software of the aforementioned images, of the length of the primary axis of the dendrites, of the lateral arms of the dendrites and of the spacing between these (SDAS: secondary dendrite arm spacing). After completing this step we proceed with the calculation of the dispersion through the following formula:

$$dispersion = \frac{1}{SDAS} \tag{2.4}$$

2.6 Hardness measurement on the sample

2.6.1 HRC hardness

The Rockwell hardness (HRC) of the samples has been measured using the instrument Ernst AT 130D , in accordance with GOST 9013−59 , the determination

of the hardness has been performed using a diamond cone with an angle at the apex of 120° and a load of 1457 N. The indenter has been pressed into the sample thanks to the action of two load applied in sequence: a preliminary one and a general one. The residual penetration of the tip is measured after the removal of the general load. The test have been performed four times for each sample.

Figure 2.3: Hardness tester

2.6.1.1 Data analysis

Four measurement of the HRC hardness have been carried out on each sample, at the end the test the average hardness has been calculated with the formula 2.5 :

$$HRC_a = \frac{\sum_{i=1}^{4} Measure\ i}{4} \tag{2.5}$$

Where HRC_a stands for the average hardness.

2.6.2 Vickers microhardness

During the experiment, Vickers micro-hardness measurements have been carried out on some of the studied samples. The test have been carried out on a Leitz microdurometer using a weight of 500g (4.903N) and for each sample were carried out three measurements.

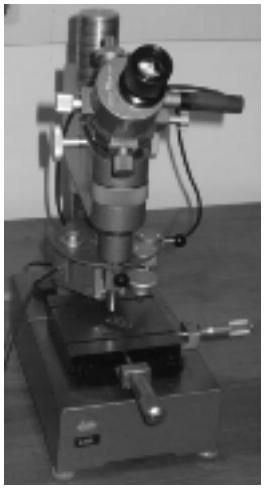

Figure 2.4: Microdurometer

2.6.2.1 Data analysis

Three measurement of the Vickers hardness have been carried out on each sample, at the end the test the average hardness has been calculated with the formula 2.6:

$$VK_a = \frac{\sum_{i=1}^{3} Measure\, i}{4} \tag{2.6}$$

Where VK_a stands for the average hardness.

2.7 Determination of the wear resistance of alloys

During the research experience tests for the evaluation of the wear resistance have been carried out following precise Russian norms, as GOST 23.208−79, whose title is *"Method of testing materials for abrasion resistance in friction against rigid abrasive particles"*. This is the standard which is usually applied to metals and metallic coatings. In the image 2.5 is represented the configuration of the testing machine.

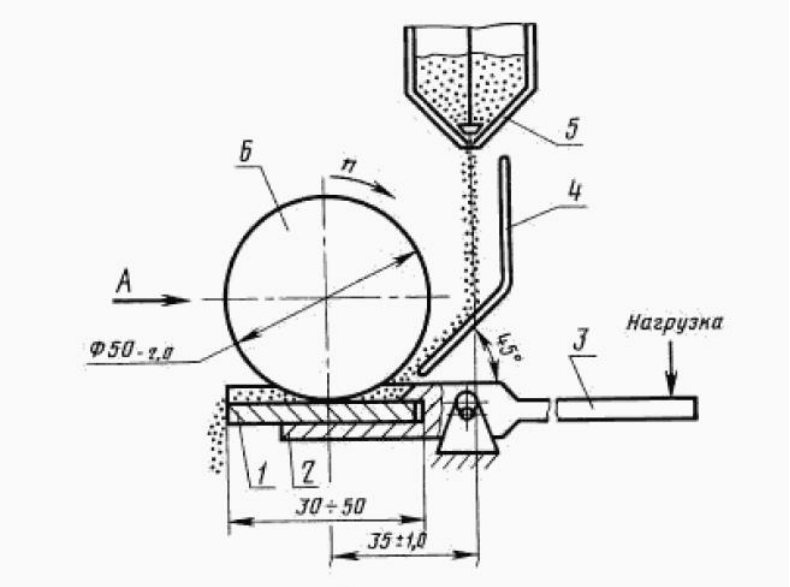

Figure 2.5: Schematic representation of the wear resistance tester (lateral view)

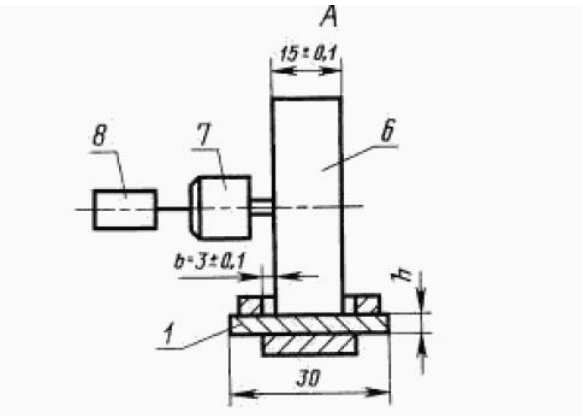

Figure 2.6: Schematic representation of the wear resistance tester (frontal view)

1. Sample;
2. Sample holder;
3. Shaft which allows the rotation of the system;
4. Guide for abrasive material;
5. Abrasive powder tank and opportune nozzle;

6. Rotating element made of rubber;

7. Turns counter.

Figure 2.7: Real representation of the wear test

The rubber roller which has been used during these experiments has been characterized diameter of 48÷50mm, a width of 15±0.1mm. The hardness of the rubber was in the range 78 ÷ 85 units, according to GOST 263−75 , the relative residual elongation from 15% ± 20% according to the norm GOST 270−75. The guide for the abrasive particle was inclined, the angle was 45° ± 2°, the gaps between the walls of the sample holder and the rotating element was about 3.0 ± 0.1 mm. The tested samples have been in form of plates with dimensions 35x10x10 mm, each sample has been clamped with a force and a force of 44.1±0.25 N has been applied by a rubber roller which could rotate at a speed of 60±2 rpm. The roller, during its rotation, moves the abrasive particles, coming from the thank through a nozzle and that flows on the guide, on the surface of the sample which is worn. The abrasive material was made of electrocorund granularity with 16-P according to GOST 3647−80 with a relative humidity content not higher than 0.15%.

Type of abrasive	Al_2O_3 (%)	Fe_2O_3 (%)	TiO_2 (%)	CaO (%)
Electrocorundum	93÷94	0.5÷0.7	1.8	0.8÷1.1

Table 2.8: Chemical composition of the abrasive powder

Each sample have been treated three times, as asked by the norm to do stastical considerations, and in each treatment the number of revolution completed by the

rotating element was 1800. The weight of the samples has been measured after each test with a balance made by the company ACCULAB, the model is ATL 224 , the maximum mass that can be measured is 220 g and it has accuracy of ± 0.0001 g.

Figure 2.8: Acculab balance

It has been necessary to use a reference samples, because the reference norm asks to make comparisons with the studied samples for the evaluation the wear resistance of the materials. The standard sample was made of steel 45 according to GOST 1050−88 in the annealed condition, and with Vickers hardness of of 190-200 HV. The reference has bees subjected to the same test of the other investigated samples.

Sample	Fe (%)	C (%)	Mn (%)	Si (%)	Cr (%)
Reference	Balance	0.45÷0.50	0.50÷0.80	0.17÷0.37	0.25

Table 2.9: Chemical composition of the Standard Sample

2.7.1 Data analysis

In order to obtain the resistance to wear of the material after carrying out the tests it has been necessary to perform some calculations. To describe them it necessary to start defining some quantities, therefore it is assumed that:

- m_1 (g) represents the initial mass of the sample;

- m_2 (g) is the mass after the first wear test;
- m_3 (g) is the mass after the second treatment;
- m_4 (g) is the final mass after the third treatment.

and from these it is possible to define:

$$\Delta_{m_i} = m_i - m_{i+1} \text{ (g)} \tag{2.7}$$

where $i \in \{1, 2, 3\}$. Then it is possible to introduce the following quantities:

- $\Delta_{m_1} = m_1 - m_2$ (g)
- $\Delta_{m_2} = m_2 - m_3$ (g)
- $\Delta_{m_3} = m_3 - m_4$ (g)

and these quantities represent the mass loss after each wear treatment to which a sample is subjected. At this point it possible to define the average mass loss:

$$\Delta_{m_a} = \frac{\sum_{i=1}^{3} \Delta_{m_i}}{3} \tag{2.8}$$

Now all the important quantities are fixed and described and in order to determine the coefficient of wear resistance K_i the norm prescribes to use the following formula 2.9:

$$K_i = \frac{\Delta_{m_a r} \times \rho_r \times N_r}{\Delta_{m_a s} \times \rho_s \times N_s} \tag{2.9}$$

In this formula:

- $\Delta_{m_a r}$ stands for the average mass loss of the reference sample;
- $\rho_r$indicates the density of the reference sample;
- N_r is the number of the completed round by the roller during the test for the reference sample;
- $\Delta_{m_a s}$ stands for the average mass loss of a studied sample;
- ρ_s indicates the density of the studied samples;
- N_s is the number of the completed round by the roller during the test for the studied samples.

This formula could be simplified assuming that the densities of the samples, standard sample and the studied samples, are the same and also the number of completed round was the same for all the samples. Therefore the formula becomes only the ratio between the average loss of the standard and a studied sample:

$$K_i = \frac{\Delta_{m_a r}}{\Delta_{m_a s}} \tag{2.10}$$

Therefore the coefficient of wear resistance has been calculated in this way.

2.8 Statistic and Design of experiment under optimal conditions

The most important objectives of the experiments, that has been prosecuted during the research, was to find the relationships between chemical composition of the alloy and the performance of the material and its properties, in order to find a new composition of a cast iron able to maximize them. The link between the chemical composition of the material and or the hardness of the material or its resistance to wear have been researched; this link was found managing experimental data and building a linear model; this model has been used to predict the performance of the material and to understand which composition maximizes that performance. Moreover it was necessary to verify also the goodness of the expressions carried out through a statistic analysis, since there is a strong influence of the methods of execution of the experiment. To accomplish this, tools of Design of Experiment (DOE) were used.

The design of an experiment and the construction of a linear model, in this type of research, are related to the theory of *the two-level factor variation.*

First of all is necessary to define some concepts: a factor is an involved variable, on which depend what is studied (a property) and the levels of a factor are simply the values that this factor can assume or the limits of a range of values. In general fixing the number of level for each factor, if the number of factors is known, it is possible to find out which are all possible combinations of a factor's levels and to understand immediately the number of experiments that are necessary to be carried out. In the case of a system with a number of levels equal to 2 the formula to calculate the number of experiments is simple and is:

$$N = 2^k \tag{2.11}$$

where:

- N is the number of experiments;

- 2 is the number of levels relative to each factor;
- k is the number of factors.

In general, an experiment in which various combinations of factor levels are performed is called a complete factorial experiment, therefore, if there is a number k of factors and the number of levels of each of the factors is two, then the experiment is defined as a complete factorial experiment of type 2^k. From this point a number of level is always considered.

Moreover, the coded values of the factors (the levels) that are normally used in the experiment planning are +1 and -1 and usually, to simplify the system, the units are omitted. In other words the values of the two levels are replaced with +1 and -1 for questions of homogeneity; in the case of calculation, however, it will then be necessary to make a conversion to the real values.

It is possible to describe the experiment in the form of a table, in this case each line of the system corresponds to a different experiment, while the columns are related to a specific factor. Each cell of the table contains +1 or -1, depending on the combination. These particular tables are called *the experiment planning matrices*. The columns of a planning matrix are called column vectors while each row is a row type vector.

If the experiment is characterized by only two factors it is evident that it is not difficult to write all the combinations of levels, therefore if $k = 2$ the matrix is:

Experiments	x_1	x_2	y_i
1	-1	-1	y_1
2	+1	-1	y_2
3	-1	+1	y_3
4	+1	+1	y_4

Table 2.10: Matrix for two factors

Where:

- x_1 and x_2 are the factors;
- y_i is the value of the measure.

When there are only two factors in the system, the combinations of the various factor levels are easy to find but when the number of factors increases then the matrix construction becomes complex and specific methods are used.

Neglecting of the number of factors that characterize a matrix, it has properties that are common to all the others, so there are some characteristics that are not a function of the number of factors. Furthermore they determine the quality of the model and allow to obtain a model with optimal properties.

Two properties follow directly from the construction of the matrix. The first of them is the symmetry with respect to the center. The second property, the so-called *condition of normalization* consists in the fact that the sum of the squares of the elements of each column is equal to the number of experiments (N). This simply because the factor values in the matrix are set to +1 and -1. The third property concerns the fact that the sum of the column vector components of the matrix is zero, this indicates that the matrix is orthogonal. The last property is called rotability, all the points in the planning matrix are chosen so that the accuracy of the values of the prediction is the same in every direction.

Now it is necessary to see how to build the linear law which is one of the objectives, because it is fundamental to relate in this case the quantity of a certain alloying element, that in this specific case are the factors, and the hardness or wear resistance, or both together. The linear model in general is:

$$Y = \sum_{j=0}^{k} b_j x_j \tag{2.12}$$

where:

- Y in the investigated property;
- x_j is the factor;
- j indicates the number of the factor, it is column index;
- k is the total number of factors;
- b_j are the coefficient that can be determined with equations 2.13

$$b_j = \frac{\sum_{i=1}^{N} x_{ij} y_i}{N} \tag{2.13}$$

  and $j \in \{0, 1, ..., k\}$;

- in particular b_o is the average value of the measurements y_i:

$$b_o = \frac{\sum_{i=1}^{N} y_i}{N} \tag{2.14}$$

  It is like having a column vector x_0 where all the components are "+1", but that is generally omitted in the matrix.

- The accuracy and reliability of the b_j coefficients depend on the characteristics of the tested sample and must undergo a statistical verification.

The coefficients b_j related to the factors indicate the strength of influence: the larger the numerical value of the coefficient, the greater the effect of the factor. When the coefficient is positive, the quantity studied increases when a factor increases, while if the sign is negative, then the quantity decreases.

When an experiment is designed, in the first phase normally who studies try to obtain a linear model. However, sometimes in this not the right way. In the case in which the best model is not linear it is important to also count the possible interactions between factors that are described in through the multiplications among them. The interactions are more numerous as the number of factors is high. It is possible to calculate them through the following formula:

$$C_k^m = \frac{k!}{m!(K-m)!} \tag{2.15}$$

In particularly complex situations, terms in which the coefficient with an exponent two may also be introduced.

A complete factorial experiment has a great redundancy of experiments. It would be a good idea to reduce the number by neglecting information that is not very significant when building linear models. At the same time, it must be must ensured that the planning matrix does not lose its characteristics. The rule found can be described as follows: to reduce the number of experiments, a new factor must be assigned to the array vector of the matrix relative to an interaction, which can be neglected. Therefore the value of the new factor in the experimental conditions is determined by the value of this column. A new matrix is created with a number of experiments compared to those normally expected with that number of factors. With this matrix a new tool is used and is called replication. The theory concerning the replicas is very extensive and is not presented in the work, it is analyzed only a particular case that will come back later in the thesis. The case that is studied is that of a system with five factors, in this case a replica is used, which is called 1/4 and the experiment can be described as follows:

$$N = 2^{5-2} = 8 \tag{2.16}$$

The number of experiments is considerably lower than expected and in this case the factors x_4 and x_5 contain interactions between two or more factors. The system thus becomes simpler and more manageable. The matrix is:

Sample	x_1	x_2	x_3	x_4	x_5
1	-1	-1	-1	+1	-1
2	+1	-1	-1	-1	+1
3	-1	+1	-1	-1	+1
4	+1	+1	-1	+1	-1
5	-1	-1	+1	+1	+1
6	+1	-1	+1	-1	-1
7	-1	+1	+1	-1	-1
8	+1	+1	+1	+1	+1

Table 2.11: 2^{5-2}

This matrix is the starting point for the construction of the model with this number of factor. The procedure then to get the model is the same.

At this point, after the brief explanation regarding the construction of the linear model, it is necessary to see how it is possible to validate the model and verify the quality of the experiment. The first thing to pay attention to is the reproducibility of the experiment, in practice it is necessary that the repeatability of the measured values is verified. It is necessary to control if practical experiment have been carried out in a correct way. When performing a series of experiments in parallel, one must start from the calculation of the average value for each of the series, then it is necessary to calculate the variance. In order to calculate the average value of a series of measurement it is necessary to use the typical formula 2.17:

$$\bar{x} = \frac{\sum_{i=1}^{m} x_i}{m} \tag{2.17}$$

It is important to specify that in this case the average of the values will refer to the measured quantities, hardness HRC and coefficient of wear resistance K_i. To calculate the variance is necessary the expression 2.18:

$$\sigma_i^2 = \frac{\sum_{i=1}^{m}(x_i - \bar{x})^2}{m} \tag{2.18}$$

Once these two results are known, the reproducibility of the experiment can be calculated and the Cochran criterion is used to do this. This criterion imposes the respect of the following disequation 2.19:

$$G_P \leq G_T(\alpha, f_N, f_i) \tag{2.19}$$

where G_P is:

$$G_P = \frac{\sigma_{imax}^2}{\sum_{i=1}^{m} \sigma_i^2} \tag{2.20}$$

In this case:

- σ^2_{imax} is the maximum variance between those in the series;

- σ^2_i the sum of variances in the system.

Instead G_T is a tabulated parameter in table 2.12 and it is obtained by combining some parameters that are α, N, n and f_i. The meaning of each parameters is:

- α is the probability of trust, it can assume several values (0.001, 0.005, 0.01,0.05 etc.) but is generally accepted equal to 0.05. In this experience α=0.05 is used;

- N represents the number of tests that take place in parallel. In other word it is the number of row in the matrix.

- n is the number of measures to which a sample is subjected for each series ;

- f_i is the number of degrees of freedom.

Moreover there is the following relationship between f_i ed n:

$$f_i = n - 1 \tag{2.21}$$

The table that is necessary to use for the calculation is table 2.12.

m	$q = n - 1$									
	1	2	3	4	5	6	8	10	16	36
2	0.99	0.97	0.93	0.90	0.87	0.85	0.81	0.78	0.73	0.66
3	0.97	0.93	0.79	0.74	0.70	0.76	0.63	0.60	0.54	0.47
4	0.90	0.76	0.68	0.62	0.59	0.56	0.51	0.48	0.43	0.36
5	0.84	0.68	0.60	0.54	0.50	0.48	0.44	0.41	0.36	0.26
6	0.78	0.61	0.53	0.48	0.44	0.42	0.38	0.35	0.31	0.25
7	0.72	0.56	0.48	0.43	0.39	0.37	0.34	0.31	0.27	0.23
8	0.68	0.51	0.43	0.39	0.36	0.33	0.30	0.28	0.24	0.20
9	0.64	0.47	0.40	0.35	0.33	0.30	0.28	0.25	0.22	0.18
10	0.60	0.44	0.37	0.33	0.30	0.28	0.25	0.23	0.20	0.16
12	0.57	0.39	0.32	0.29	0.26	0.24	0.22	0.20	0.17	0.14
15	0.47	0.33	0.27	0.24	0.22	0.20	0.18	0.17	0.14	0.11
20	0.39	0.27	0.22	0.19	0.17	0.16	0.14	0.13	0.11	0.08
24	0.34	0.29	0.19	0.16	0.15	0.14	0.12	0.11	0.09	0.07
30	0.29	0.20	0.16	0.14	0.12	0.11	0.10	0.09	0.07	0.06
40	0.24	0.16	0.12	0.10	0.09	0.08	0.07	0.07	0.06	0.04
60	0.017	0.11	0.08	0.07	0.06	0.06	0.05	0.05	0.04	0.02
120	0.09	0.06	0.04	0.04	0.03	0.03	0.02	0.02	0.02	0.01

Table 2.12: Value of G_T

When all the quantities have been calculated and are available, it is verified that the inequality is respected. Once the Cochran criterion is validated it is possible to state that in the experiment there are no evident errors and that there is homogeneity in the variances. In other case is better to repeat experiments. After this a second analysis is performed, which involves the Student's T distribution and criterion. The criterion needs that a disequation is respected, which is:

$$T_P = \frac{b_j}{\sigma_{bj}} \geq T_T(\alpha, f_y) \tag{2.22}$$

where:

- b_j refers to the the numerical value of the coefficient;
- σ_{bj} is the standard deviation of the regression coefficient. It can be calculated with formula 2.23

$$\sigma_{bj} = \sqrt{\frac{\sigma_y^2}{Nn}} \tag{2.23}$$

In this formula:

- σ_y^2 variance of reproducibility of the experiment;
- N is the number of experiences in the matrix;
- n is the number of parallel experiences. It is possible to calculate σ_y^2 with the following formula:

$$\sigma_y^2 = \frac{\sum_{i=1}^{N} \sigma_y^2}{N} \tag{2.24}$$

The value of f_y can be calculated knowing the structure of the experiments as:

$$f_y = N(n-1) \tag{2.25}$$

In table 2.13 is possible to find the value of T_T

f_y	probability of trust						
	0.200	0.100	0.050	0.025	0.010	0.005	0.001
1	3.078	6.314	12.076	25.452	63.657	127.320	-
2	1.886	2.920	4.4303	6.205	9.925	14.089	31.598
3	1.638	2.353	3.182	4.176	5.841	7.453	12.941
4	1.533	2.132	2.776	3.495	4.604	5.598	8.610
5	1.476	2.015	2.571	3.163	4.032	4.773	6.859
6	1.440	1.943	2.447	2.969	3.707	4.317	5.959
7	1.415	1.895	2.365	2.841	3.499	4.029	5.405
8	1.397	1.860	2.306	2.752	3.355	3.832	5.401
9	1.383	1.833	2.262	2.685	3.250	3.690	4.871
10	1.372	1.812	2.228	2.634	3.169	3.851	4.857
11	1.363	1.796	2.201	2.593	3.106	3.497	4.437
12	1.356	1.782	2.179	2.560	3.055	3.428	4.318
13	1.350	1.771	2.160	2.533	3.012	3.372	4.221
14	1.345	1.761	2.145	2.510	2.977	3.325	4.140
15	1.341	1.753	2.131	2.490	2.947	3.286	4.073
16	1.337	1.746	2.120	2.473	2.921	3.252	4.015
17	1.333	1.740	2.110	2.125	2.878	3.222	3.965
18	1.330	1.734	2.101	2.445	2.878	3.197	3.922
19	1.328	1.729	2.093	2.433	2.861	3.174	3.883
20	1.325	1.725	2.086	2.423	2.845	3.153	3.850

Table 2.13: Value of T_T

All the members of the regression equation, in which the coefficients satisfy the condition related to the student's T test, are maintained in the model, while

those that do not satisfy the disequation are instead removed. However, it should be kept in mind that each of the coefficients may be insignificant due to an erroneously varied range of variation. Therefore, the statistical importance of individual factor should be discussed from the technological point of view. In other words, this second statistical tool makes it possible to understand which factors are really important for the model and which makes sense to consider because it is able to strongly influence the studied quantity. At the end the correctness of the mathematical model is verified using also the Fisher criterion and the relative distribution F. Similarly to the previous criteria, this criterion is described by a disequation that must be satisfied, it is presentend in equation 2.26

$$F_P = \frac{\sigma_{ad}^2}{\sigma_y^2} \leq F_T(\alpha, f_{ad}, f_y) \tag{2.26}$$

In this equation:

- σ_{ad}^2 is the variance of the adequacy of the model

$$\sigma_{ad}^2 = \frac{n}{N-d} \sum_{i=1}^{N} (\bar{y} - \hat{y}) \tag{2.27}$$

- d is the number of members in the model that passed the previous test;
- $\bar{y}$ is the average value in every experience;
- $\hat{y}$ is the estimated value with the regression equation obtained for each experiment. It is calculated as:

$$\hat{y} = Y = b_o + \sum_{j=1}^{k} b_j x_j \tag{2.28}$$

  and j is the index of the factor which respects the Student's T criterion, so that survives in the.

- to thm f_{ad} is the number of the degrees of freedom, it can be calculated in the following way:

$$f_{ad} = N - d \tag{2.29}$$

- f_y has the same meaning that it has in the previous test.

In the following table it is possible to find the value of F_T:

f_y	f_{ad} ($\alpha = 0.05$)								
	1	2	3	4	5	6	7	8	9
1	161	200	216	225	230	234	237	239	242
2	18.51	19.0	19.16	19.25	19.30	19.33	19.36	19.37	19.38
3	1.13	9.55	9.28	9.12	9.01	8.94	8.88	8.84	8.81
4	7.71	6.94	6.59	6.39	6.26	6.16	6.09	6.04	6.00
5	6.61	5.79	5.41	5.19	5.05	4.95	4.88	4.82	4.78
6	5.99	5.14	4.76	4.53	4.39	4.28	4.21	4.15	4.10
7	5.59	4.74	4.35	4.12	3.97	3.87	3.79	3.73	3.68
8	5.32	4.46	4.07	3.84	3.69	3.58	3.50	3.44	3.39
9	5.12	4.26	3.86	3.63	3.48	3.37	3.29	3.23	3.18
10	4.96	4.10	3.71	3.48	3.33	3.22	3.14	3.07	3.02
11	4.84	3.98	3.59	3.35	3.20	3.09	3.01	2.95	2.90
12	4.75	3.88	3.49	3.25	3.11	3.00	2.92	2.85	2.80
13	4.67	3.80	3.41	3.18	3.02	2.92	2.84	2.77	2.72
14	4.60	3.74	3.34	3.11	2.96	2.85	2.77	2.70	2.65
15	4.54	3.68	3.29	3.06	2.90	2.79	2.70	2.64	2.59
16	4.49	3.63	3.24	3.01	2.85	2.74	2.66	2.59	2.54
17	4.45	3.59	3.20	2.96	2.81	2.70	2.62	2.55	2.50
18	4.38	3.55	3.16	2.93	2.70	2.66	2.58	2.51	2.46

Table 2.14: Value of F_T

If the disequation is satisfied, the mathematical model is adequate. In case the model is inadequate, it is necessary to use a more complex form of the mathematical model (second order plan, etc.), or, if possible, conduct the experiment again with a smaller range of factor variations. Once the model is validated, trend curves are constructed to identify the effect of each factor on the measured quantity and are being investigated from a mathematical and engineering point of view.

The model obtained at the end of this analysis is the instrument that will be used later to solve optimization problems.

2.9 Methods of optimization of the chemical composition of metals

After the creation of the model that it has been necessary to correlate the properties of interest to the factors, in the specific case of hardness work and wear resistance coefficient with the concentration of the alloy elements, the model have been used to optimize the composition.

There are several ways to optimize the composition with a model available, such as the Simplex Optimization Method or the Steep Ascent Method. In this research work the second method has been used, which is described in the subsection 2.9.1.

2.9.1 Steep ascent method

The first thing to do is to establish the composition interval in which the composition must be optimized and set a response threshold value to be reached. Then it is necessary to set variation intervals for each variable, in other words it is necessary to indicate the change in the content of each element which leads to a significant change in the response, in this case HRC hardness or wear resistance coefficient K_i. For each element a quantity Δx_i is then defined, where the index $i \in \{C, Mn, Cr, Ni, Ti\}$. To implement a steep gradient climb, let's define the base a new variable:

$$b_i \Delta x_i. \tag{2.30}$$

multiplying the coefficient b_i by the value of the variation interval Δx_i. Once the values of this new variable have been calculated, it is necessary to identify which is the maximum value in absolute value: the factor associated to it will be the base when a steep ascent is implemented. For this it is necessary to choose a step δ_i that depends on the composition interval in which the composition is to be optimized. In other words, since this is an iterative method, it is necessary to fix a hypothetical iteration number that will be made and divide the composition interval for this element and divide it by the number of iterations. Now other variables must be calculated:

$$\lambda = \frac{(\Delta x_i \times b_i)_{max}}{\delta_i} \tag{2.31}$$

At this point it is possible to calculate the other variation steps for the other element:

$$\delta_i = \frac{(\Delta x_j \times b_j)}{\lambda} \tag{2.32}$$

where pedex j is related to the other element in the system. After calculating all the variables necessary for the system, it is necessary to start with the iterations,

which are also called mental experiments. The very first step of iteration consists in evaluating through the model the value of the quantity for the starting composition. Subsequently, the quantities δ_i are added to the concentration values of the various elements and the response is recalculated.The experiment is repeated until the desired threshold is reached without leaving the composition intervals. All this must be done only after making a conversion of the concentrations of the elements: when the mathematical model of optimization was obtained the values of the factors were not corresponding to the true values of concentrations but for convenience are always assumed as values +1 and -1. What does this mean? It means that the range of compositions in which the model works is for each element -1÷1, so it is necessary to convert the real concentrations into the -1÷1 interval. If the value of the output value stops growing, then it starts systematically decrease, among all the experiences made is chosen the one that gave the best result and its conditions are considered the main factor level in a next series of experiments. So everything the procedure described is repeated for a new experimental center. It is advisable to accept values smaller than the intervals of variation.

2.10 Material selection

In general, when one has to select a suitable material for the realization of a certain component to be used in a given context, it is important to first identify the physics of the problem, identify the laws that govern it, identify which is the contribution that gives the material to the performance and therefore define the properties involved. Once this has been done, a pre-selection must be carried out using various strategies, such as those proposed by Ashby, so as to isolate a certain number of candidates from the overall set of all materials. Once a limited set of candidate materials has been identified, it is possible to proceed with the selection. A selection strategy that can be used is Farag's theory which involves the construction of a Z function of penalties or performance relative depending on the case. This is the one that has been used to find the best compromise between properties of the alloy during the work.

In general, the form of the Z function is:

$$Z = \sum_{i=1}^{N} \pi_i D_{ni} \tag{2.33}$$

Where:

- Z is the value of the performance or penalty function;
- π_i are the weight factors;

- while D_{ni} are the properties of interest for the normalized problem.

To make the selection it is necessary to calculate the function Z for each material of the set and then compare the values obtained. The winning material will be the one with the lowest value of Z if a penalty function is constructed, on the contrary with a performance function the highest value wins. The weight factors contained in the expression must always respect the following condition:

$$\sum_{i=1}^{N} \pi_i = 1 \tag{2.34}$$

It is therefore deduced that the factors always reside in the interval $0<\pi_i<1$ and that they must be dimensionless. From this it also derives that the properties must necessarily be dimensionless, the only way to respect this is to normalize them. This then explains why the normalized properties are used and also the relative adjective in the function name. The normalization of properties provides very precise rules that vary according to the trend of the property itself, different calculations are performed depending on whether the property should be maximized or minimized and also on the fact that the function is a penalty or a performance.

If it is used a penalty function and:

$$D_{ni} = \frac{D}{D_{max}} \tag{2.35}$$

if the property must be minimized;

$$D_{ni} = \frac{D_{min}}{D} \tag{2.36}$$

if a property must be maximized.

If it is used a performance function and :

$$D_{ni} = \frac{D}{D_{max}} \tag{2.37}$$

if the property must be maximized;

$$D_{ni} = \frac{D_{min}}{D} \tag{2.38}$$

if a property must be minimized. The calculation of weight factors follows the theory of Digital Logic Enhanced: the first thing to do is to define a scale of importance of properties, which obviously depends on the demands of the problem and the context; then compare the properties in pairs by assigning a score with the following rules:

1. 1 point to both properties if they are of equal importance
2. if one is more important than the other 2 points to the most important and 1 to the less;
3. if one is much more important than the other 3 points to the most important and 1 to the less;

Then for each property the scores obtained in each comparison are added together and the total score is calculated. Dividing the score obtained by each property for the assembly allows to obtain the weight factor. At this point you can calculate all the required quantities and find the value of the Z function for each of the materials The economic evaluations can be carried out in two ways: the first possibility is to treat the cost index, or the cost per unit of volume specific to a problem like all other properties and then insert it into the Z function from the beginning or if it is necessary to emphasize a lot the economic aspect then it is better to work with the figures of merit, but in this case it is necessary a performance function.

$$FM = \frac{Z}{C_v} = \frac{Z}{\rho C_m} \tag{2.39}$$

where:

- C_v is the cost per unit volume;
- C_m is the price per unit mass.

The material with the highest figure of merit is the winning material.

Chapter 3

ANALYSIS ON WEAR RESISTANT CAST IRONS FUNCTIONAL TO THE CONSTRUCTION OF THE MODELS

In this chapter it is described how the initial specimens have been obtained for the realization of the model, the results of the characterization and the tests of hardness and resistance to wear and the calculations made for the construction of the mathematical model. First of all it is necessary to define which alloy elements have been taken into consideration, these have been manganese, chrome, obviously since this work is about high-chromium white cast irons, nickel, and titanium. The second step is to define the concentration range for each of the elements studied which have been the typicals, which can be found in practice: C=[1.9÷2.5]%, Mn=[3.5÷5.0], Cr=[18.0÷19.0]%, Ni=[0.4÷1.0]% and Ti=[0.2÷0.6]%. The starting samples were produced in number and with a known fixed composition following the factorial experiments theory presented in chapter 2 in the 2.8 section: assuming that carbon, manganese, nickel, chromium and titanium are the five factors and that the levels (-1 and +1) are the lower and upper limit of the range of studied composition it turns out that the matrix of the experiment is but following:

Sample	C		Mn		Cr		Ni		Ti	
	X_1	(%)	X_2	(%)	X_3	(%)	X_4	(%)	X_5	(%)
1	-1	1.9	-1	3.5	-1	15	+1	1	-1	0.2
2	+1	2.5	-1	3.5	-1	15	-1	0.4	+1	0.6
3	-1	1.9	+1	5	-1	15	-1	0.4	+1	0.6
4	+1	2.5	+1	5	-1	15	+1	1	-1	0.2
5	-1	1.9	-1	3.5	+1	19	+1	1	+1	0.6
6	+1	2.5	-1	3.5	+1	19	-1	0.4	-1	0.2
7	-1	1.9	+1	5	+1	19	-1	0.4	-1	0.2
8	+1	2.5	+1	5	+1	19	+1	1	+1	0.6
Average	2.2		4.25		17		0.7		0.4	

Table 3.1: Matrix of the experiment

Therefore the starting samples with a known composition to be studied have the following theoretical composition presented in the table 3.2:

Sample	Fe (%)	C (%)	Mn (%)	Cr (%)	Ni (%)	Ti (%)
1	balance	1.9	3.5	15.0	1.0	0.2
2	balance	2.5	3.5	15.0	0.4	0.6
3	balance	1.9	5.0	15.0	0.4	0.6
4	balance	2.5	5.0	15.0	1.0	0.2
5	balance	1.9	3.5	19.0	1.0	0.6
6	balance	2.5	3.5	19.0	0.4	0.2
7	balance	1.9	5.0	19.0	0.4	0.2
8	balance	2.5	5.0	19.0	1.0	0.6

Table 3.2: Theoretical chemical composition of the Standard Samples

3.1 Real composition of cast irons

After having carried out the calculations of the charge and the melting of the raw materials following what indicated in the chapter 2 at the section 2.3 the real composition of the obtained samples was measured. The cast iron composition was studied through the OES analysis which was described in the previous chapter in

the 2.4 section. The samples were cast and cooled in molds on the ground, ensuring a cooling rate c_{r1}=9 °C/ sec.

Sample	Fe (%)	C (%)	Mn (%)	Cr (%)	Ni (%)	Ti (%)	Si (%)	Cu (%)
1	balance	2.12	3.88	16.43	0.99	0.12	0.08	0.03
2	balance	2.41	4.02	14.12	0.25	0.49	0.12	0.12
3	balance	1.72	6.31	17.01	0.65	0.59	0.15	0.08
4	balance	2.86	5.69	15.39	1.21	0.20	0.15	0.20
5	balance	2.20	3.05	22.93	1.03	0.71	0.04	0.01
6	balance	2.55	3.77	18.99	0.44	0.29	0.02	0.01
7	balance	1.68	7.98	21.56	0.45	0.49	0.20	0.16
8	balance	2.98	5.67	24.01	1.012	0.97	0.18	0.01

Table 3.3: Real chemical composition of the Standard Samples

It is possible to underline how the expected compositions and the real ones are partly different due to some factors such as the oxidation of the elements during melting and the real composition of the ferroalloys used. However, it is possible to consider acceptable deviations and in line with what is expected.

3.2 Results of the metallurgical characterization of cast iron

3.2.1 Micrographs

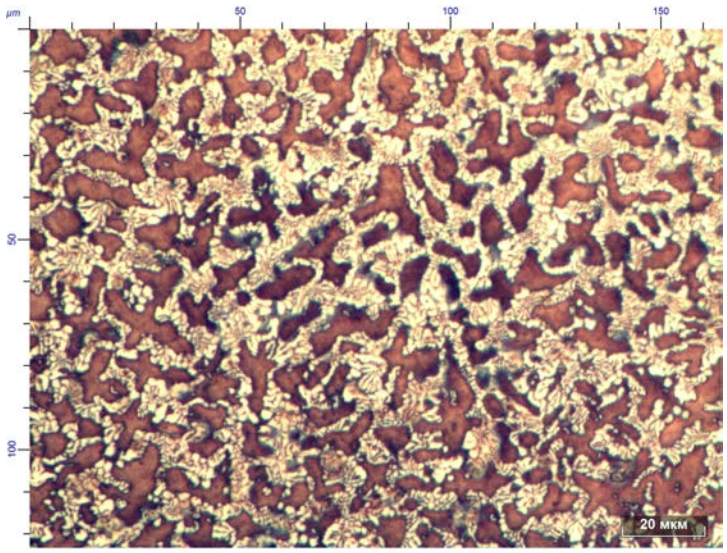

Figure 3.1: Microstructure sample 1 500x

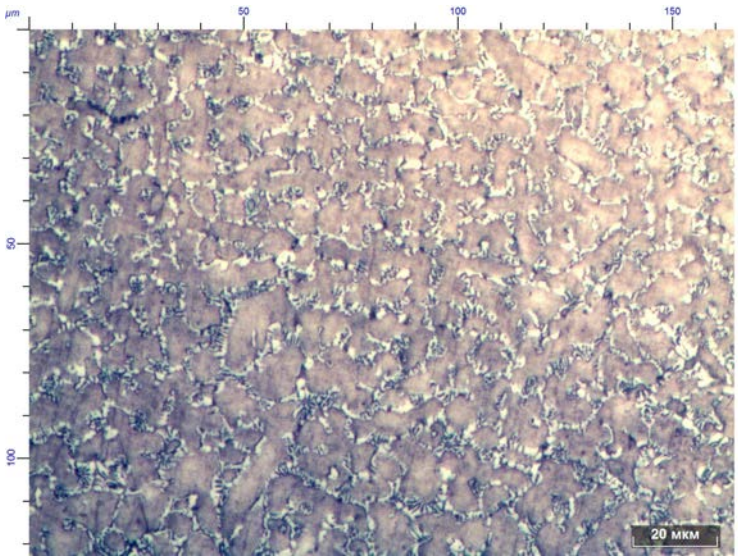

Figure 3.2: Microstructure sample 2 500x

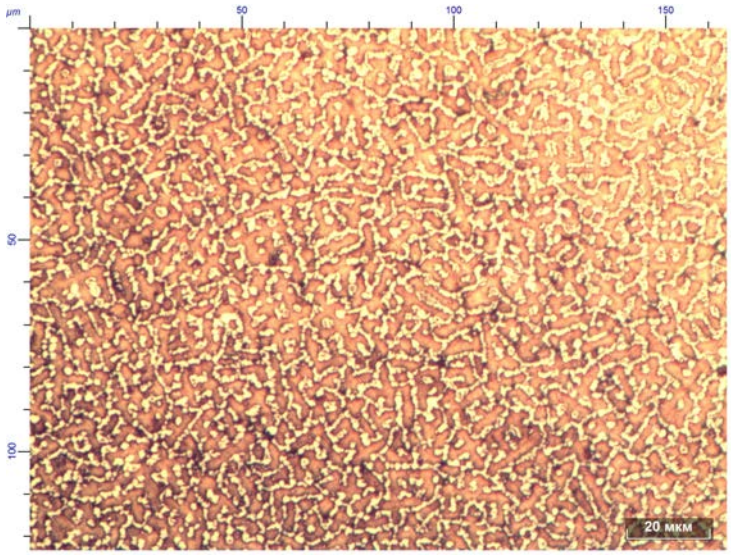

Figure 3.3: Microstructure sample 3 500x

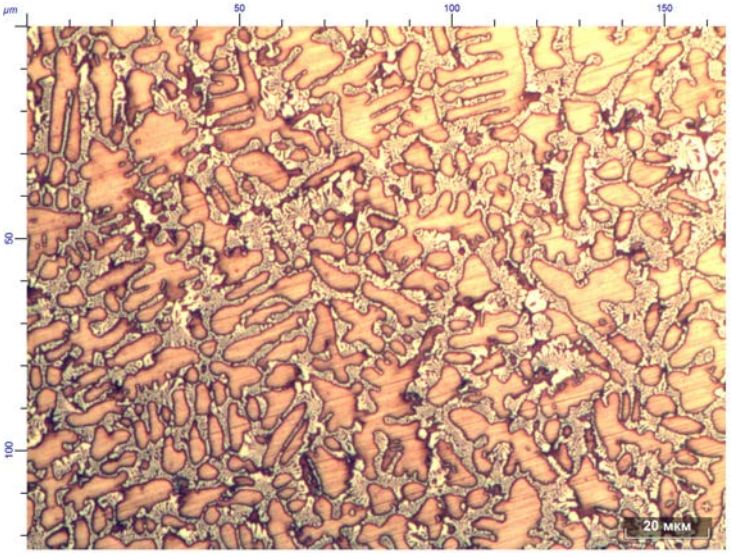

Figure 3.4: Microstructure sample 4 500x

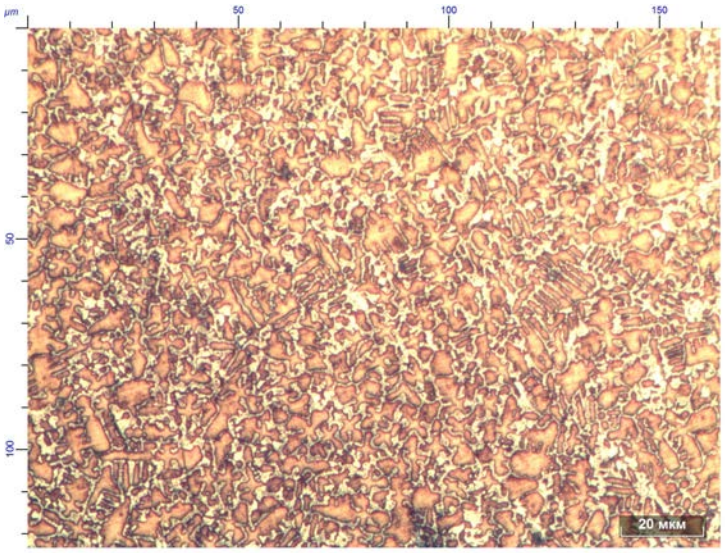

Figure 3.5: Microstructure sample 5 500x

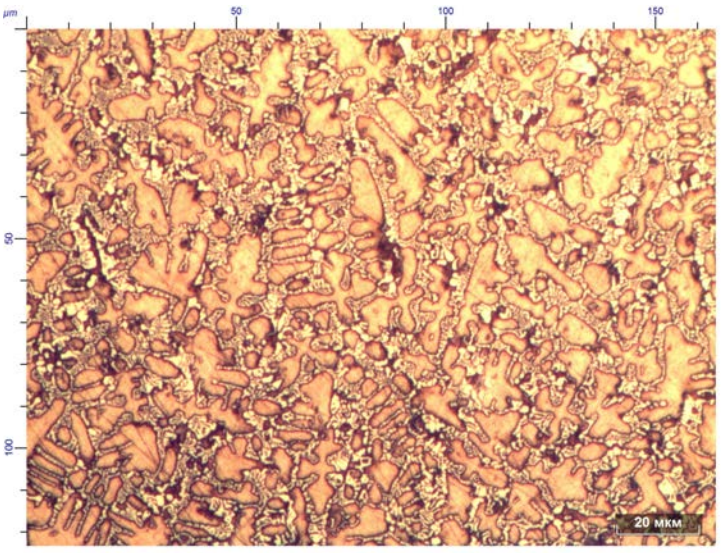

Figure 3.6: Microstructure sample 6 500x

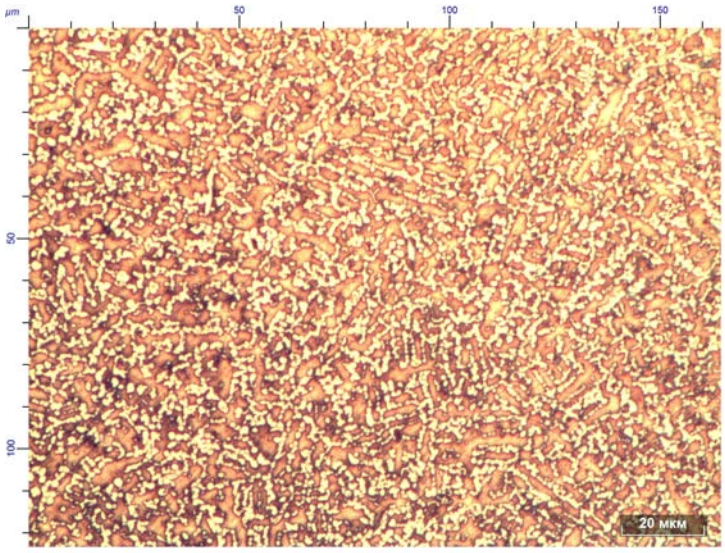

Figure 3.7: Microstructure sample 7 500x

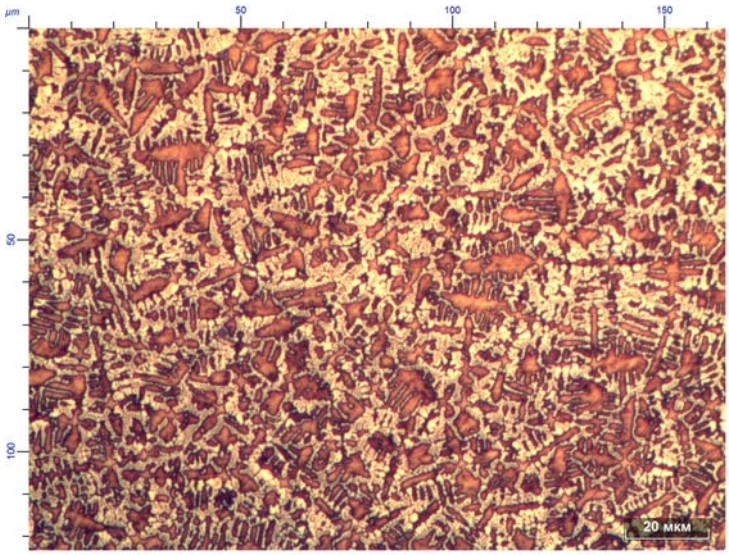

Figure 3.8: Microstructure sample 8 500x

3.2.1.1 Comment and considerations

In this subsection are described the microstructures of each sample:

- Graphite is not present thanks to a high content of chromium and manganese, contents of silicon and carbon lower than in the gray cast irons, in fact these are hypoeutectic alloy. The presence of chromium allows, in fact, to obtain a

white cast iron even without cooling the metal at extremely high speed. The presence of chromium and manganese allows also the presence of austenite.

- It has been established with metallographic analyzes that cast iron samples consist of hypoeutectic alloys. There austenite dendrites and there are eutectic carbides, like M_3C, M_7C_3 or $(M)_{23}C_6$ (like $(Fe,Cr)_{23}C_6$).
- In general it is possible to observe that in samples having a high content of chromium there is a thicker layer of carbides (with white colour) compared to those in which the content is lower.
- It is possible to find the titanium carbides, which have a green color.
- Sample 1: From the metallographic image it is possible to observe the presence of dendrites of austenites surrounded by iron and chromium carbides. In some points of the metal matrix it is possible to observe the presence of titanium carbides with a rounded and small size.
- Sample 2: The sample is characterized by a lower content of chromium, respect to sample 1 and as consequence lower quantity of carbides. There is a thin layer which surrounds the austenites's dendrites.
- Sample 3: The microstructure presents dendrites oriented randomly in the sample and with lateral arms of limited lengths. The grains are surrounded by a thin layer of well evident iron and chrome carbides.
- Sample 4: From the micrograph it is possible to see the appearance of a coarse grain and mainly oriented in one direction.
- Sample 5: This sample has a coarse grain, austenite dendrites constituting the metal matrix and a low content of iron, chromium and titanium carbides.
- Sample 6: The sample has a very high content of carbides both of chromium and of titanium and of the dendrites whose side arms are of limited size.
- Sample 7: The sample has large amounts of carbides as the previous one, and this is understandable in both cases since the chromium content is high respect to the other samples. They are homogeneously distributed, they are often small and with round shape and the grain is fine.
- Sample 8: This specimen, like the previous samples, is characterized by the presence of dendrites of austenite. They are oriented randomly and with lateral arms of variable length and surrounded by iron and chromium carbides. This sample present very high content of carbides as expected, looking to the real concentration of chromium.

3.2.2 Quantitative analysis

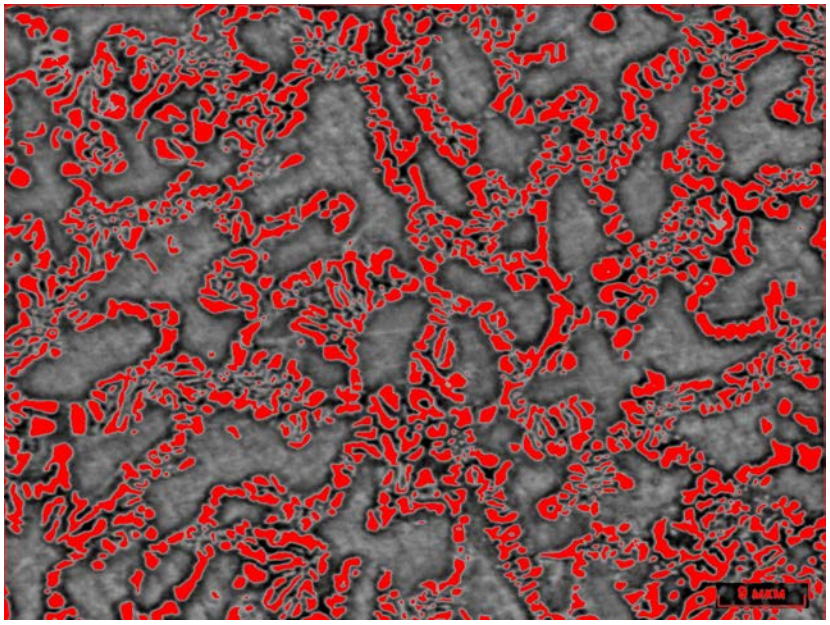

Figure 3.9: Quantitative analysis of the sample number 1

.

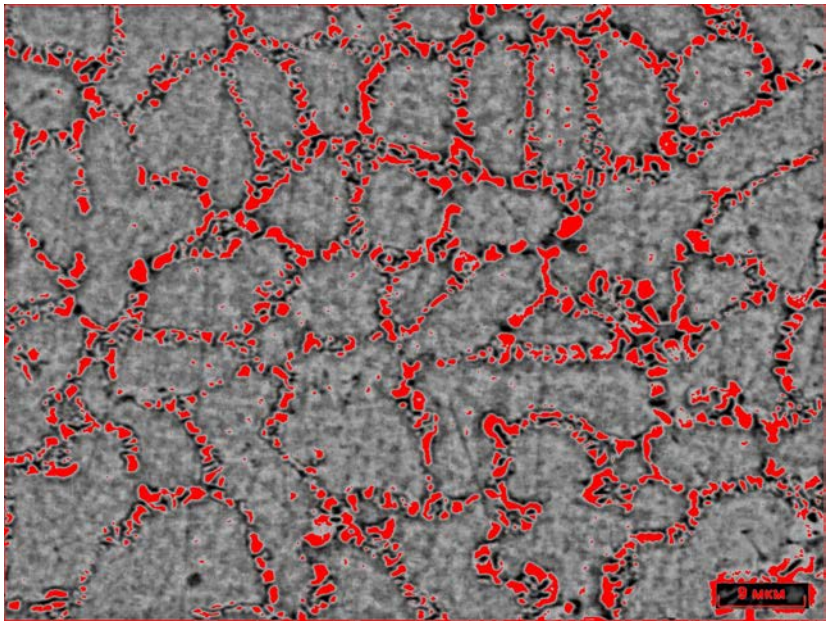

Figure 3.10: Quantitative analysis of the sample number 2

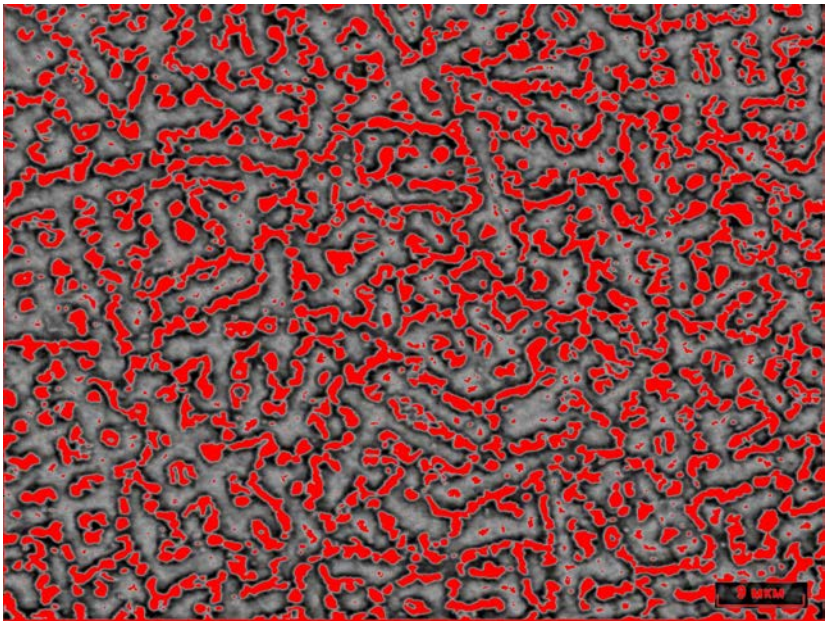

Figure 3.11: Quantitative analysis of the sample number 3

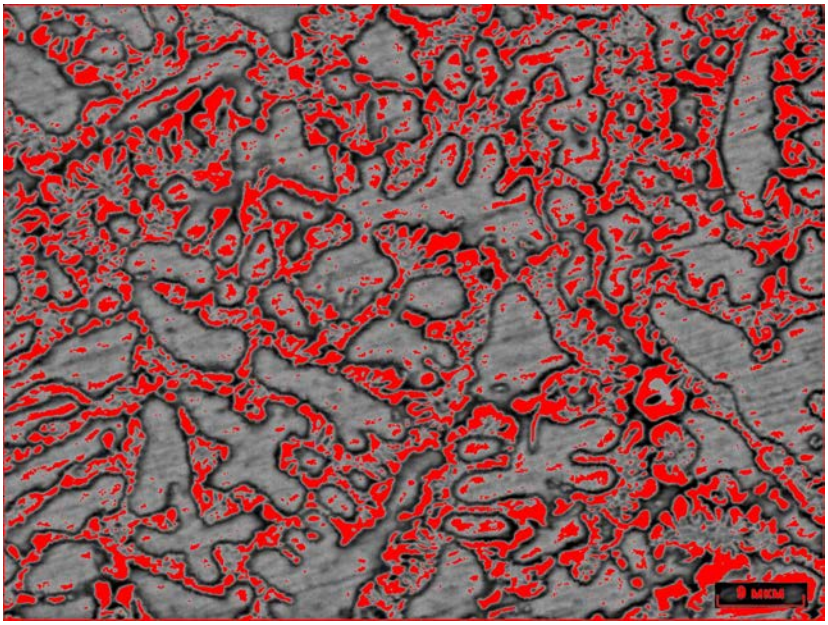

Figure 3.12: Quantitative analysis of the sample number 4

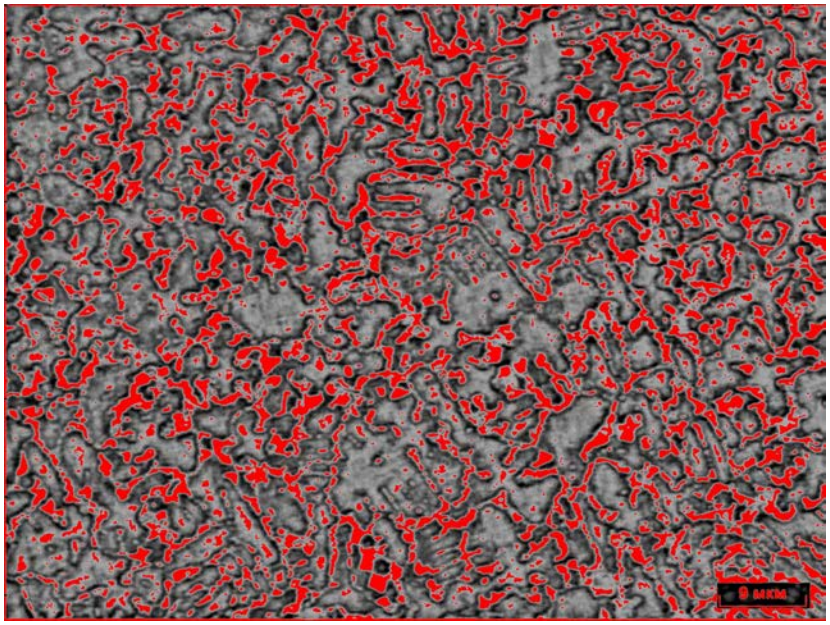

Figure 3.13: Quantitative analysis of the sample number 5

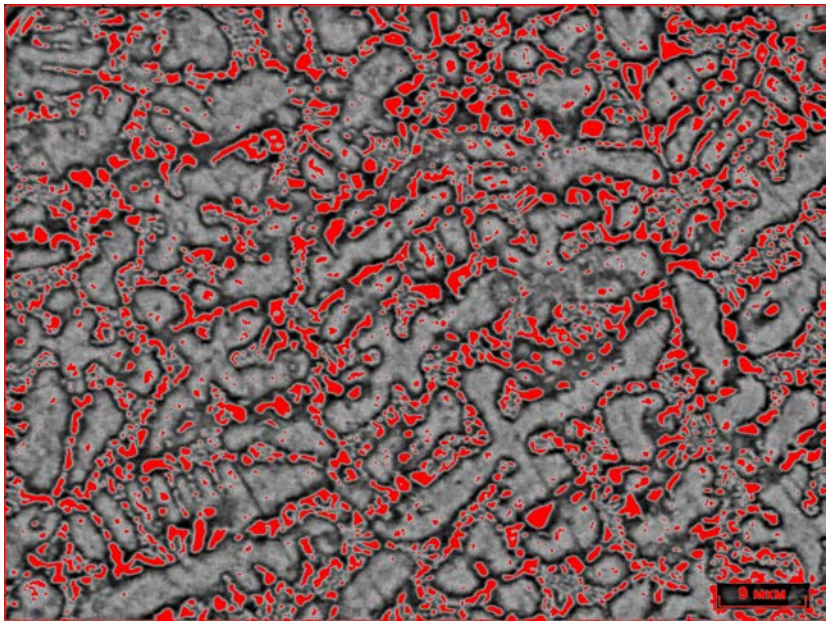

Figure 3.14: Quantitative analysis of the sample number 6

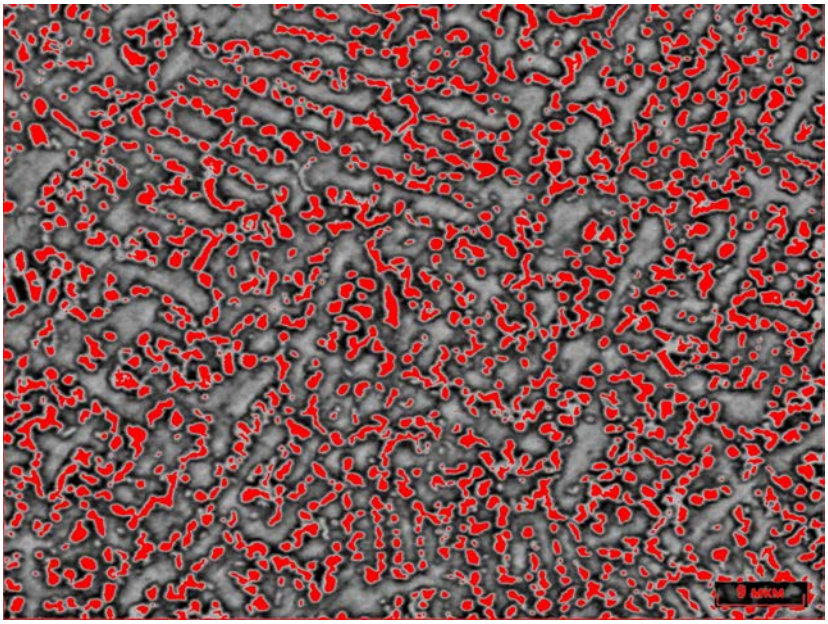

Figure 3.15: Quantitative analysis of the sample number 7

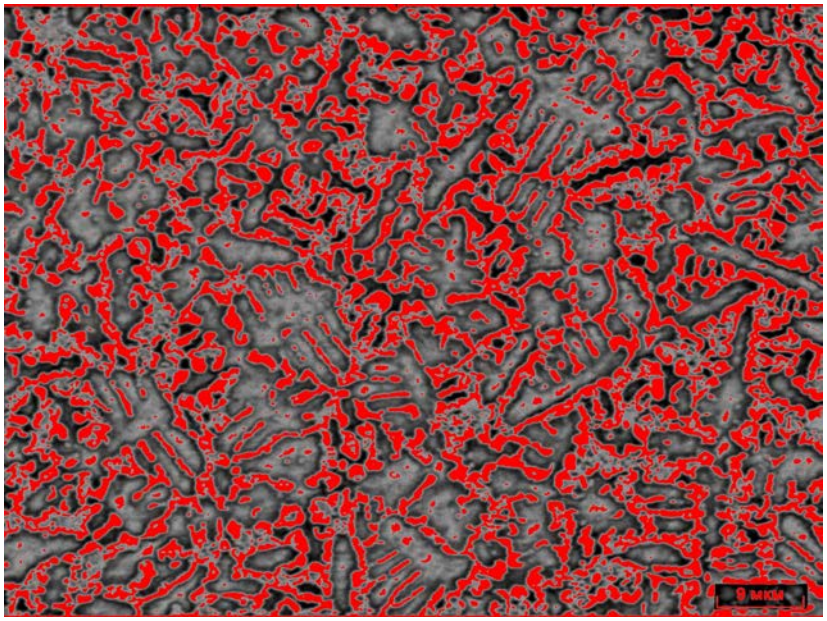

Figure 3.16: Quantitative analysis of the sample number 8

Sample	Carbide phase (%)	Metal matrix (%)
1	21.01	78.99
2	10.10	89.90
3	24.85	75.15
4	20.80	79.20
5	13.98	86.02
6	13.14	86.86
7	21.27	78.73
8	27.10	72.90

Table 3.4: Phase quantity evaluation

3.2.2.1 Comment and considerations

From the analysis with the microscope and from the use of the image analysis software it is possible to observe that in general the content of the metallic matrix exceeds, in percentage, the phase constituted by the carbides. It is possible to observe that the samples with a higher carbon and chromium concentration are characterized by a higher carbide content.

3.2.2.2 Dispersion analysis

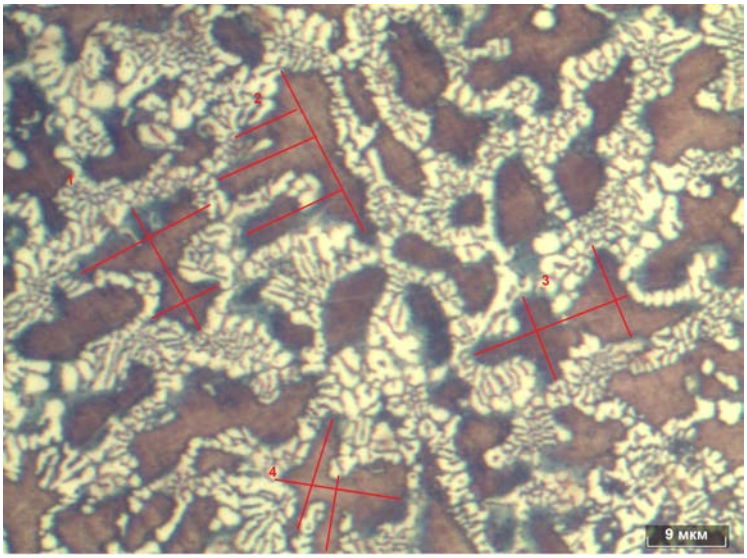

Figure 3.17: Dendrites' analysis of the sample number 1

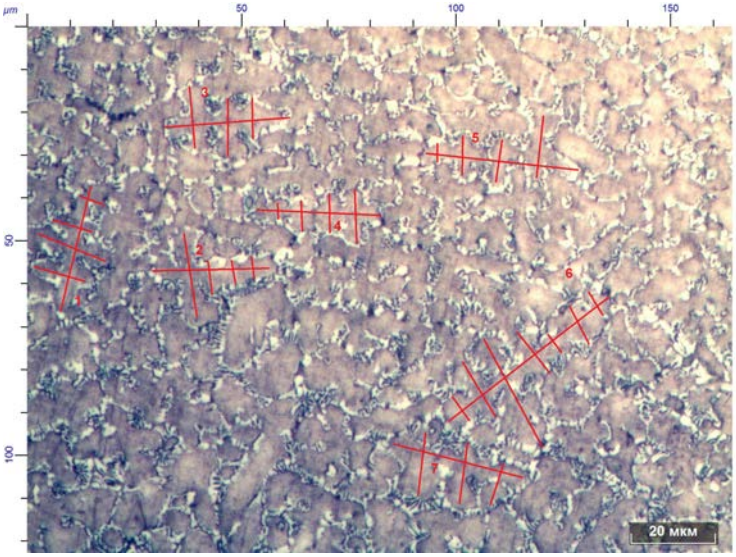

Figure 3.18: Dendrites' analysis of the sample number 2

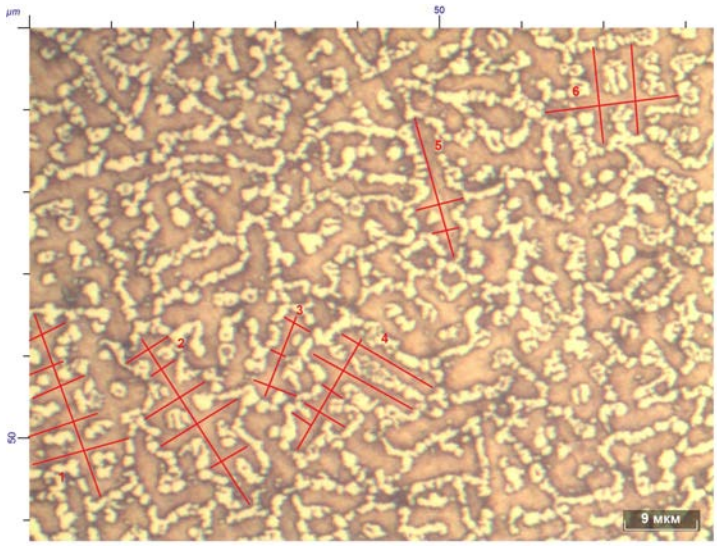

Figure 3.19: Dendrites' analysis of the sample number 3

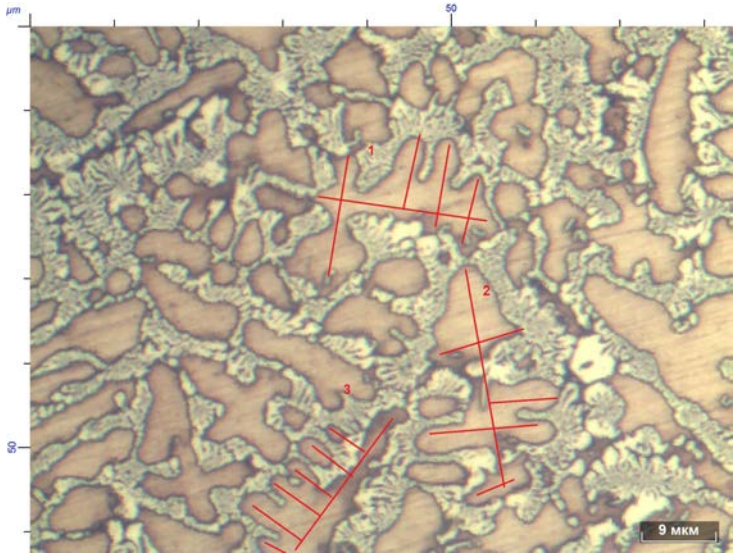

Figure 3.20: Dendrites' analysis of the sample number 4

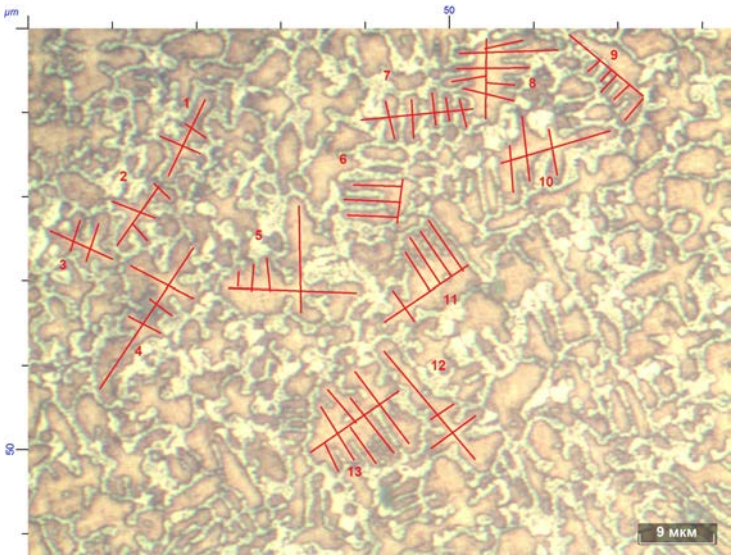

Figure 3.21: Dendrites' analysis of the sample number 5

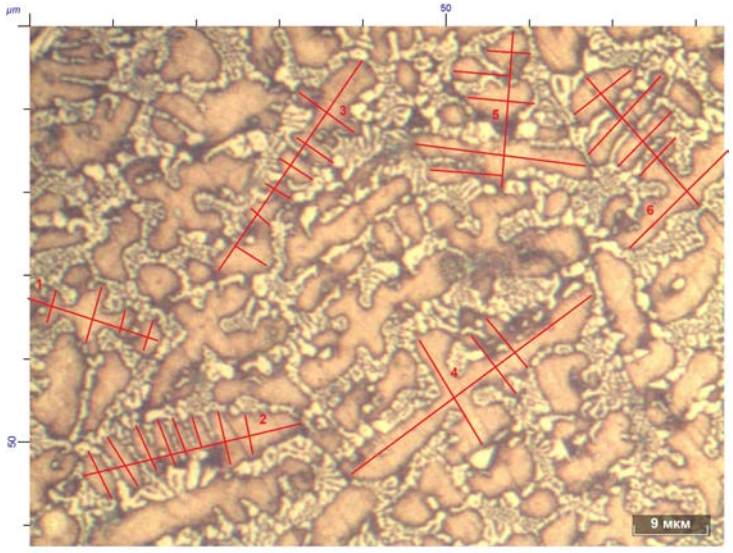

Figure 3.22: Dendrites' analysis of the sample number 6

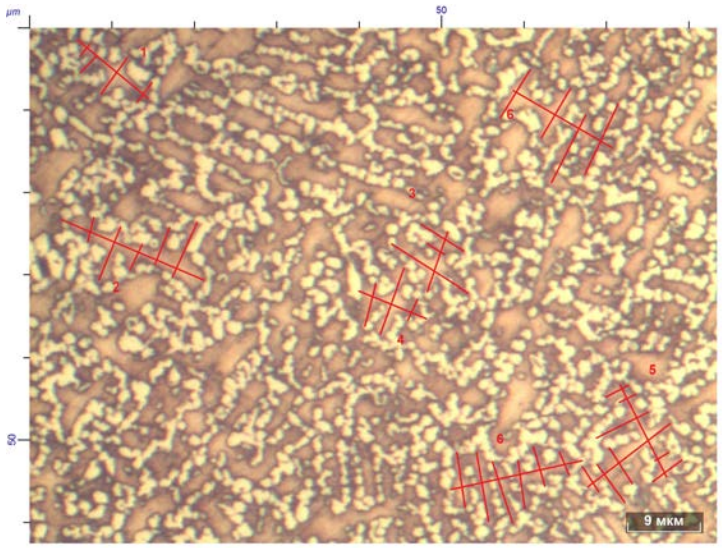

Figure 3.23: Dendrites' analysis of the sample number 7

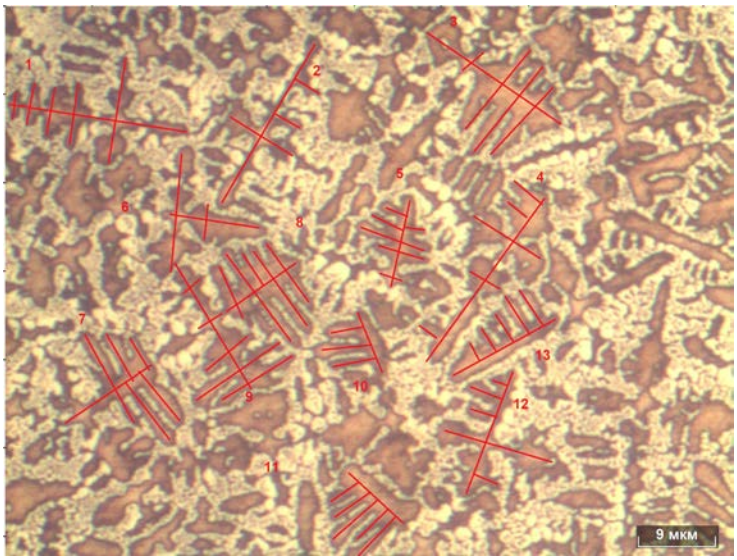

Figure 3.24: Dendrites' analysis of the sample number 8

Sample	Average dendrite first axe length (µm)	Average secondary arm length (µm)	SDAS (µm)	Dispersion (µm⁻1)
1	18.06	5.93	5.13	0.19
2	32.99	5.35	6.80	0.15
3	18.28	3.75	3.83	0.26
4	23.35	6.44	4.39	0.23
5	13.28	3.68	2.16	0.46
6	25.59	4.70	3.61	0.28
7	12.63	2.86	2.83	0.35
8	15.36	4.36	2.58	0.39

Table 3.5: Dispersion investigations

3.3 Hardness test on Cast irons

The tests have been performed exactly following what have been presented in section 2.6 and they gave the following results:

Sample	Measure 1	Measure 2	Measure 3	Measure 4	Average value HRC_a
1	43.0	42.3	41.3	42.6	42.3
2	45.1	44.7	45.0	45.8	45.2
3	44.1	44.7	45.0	45.5	44.8
4	46.1	45.7	45.7	45.7	46.2
5	47.6	45.1	46.9	48.1	46.3
6	51.4	49.9	50,0	50.4	50.4
7	52.9	55.2	54.0	52.8	53.7
8	46.5	48.6	45.2	47.4	46.9

Table 3.6: Hardness test results (HRC)

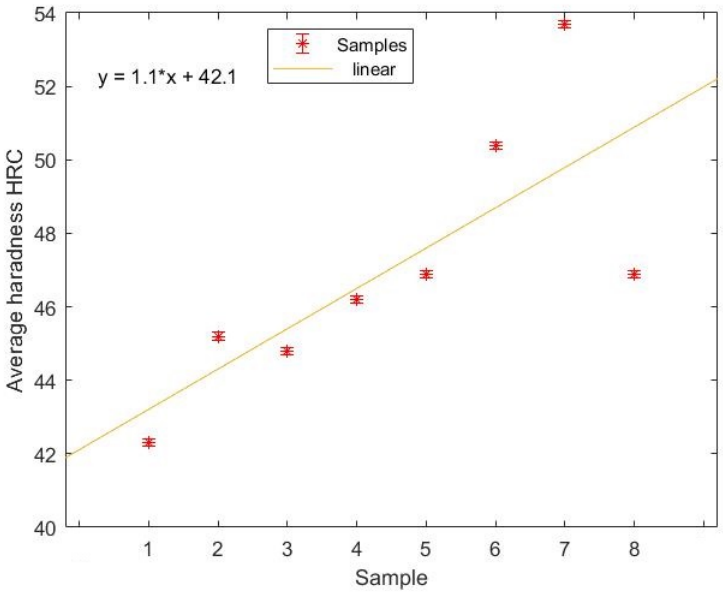

Figure 3.25: Average hardness (HRC) of the samples

3.3.1 Comments and considerations

Results are presented with only one significant digit after the decimals separator because the instrument is able to give only one digit. Average sample hardness is in the range of 42÷54 HRC units. From the comparison between the metal composition and the hardness values found it is possible to deduce that a higher chromium content leads to higher value of the hardness. In this case there is also a chance to observe a strong concordance between the results obtained in practice and the expected values looking at the theoretical and real compositions. The real value of the content of the alloy elements justify the hardness values and the expected values. Samples with higher hardness are also those that present in the metallographic images in fact a higher content of carbides immersed in the metal matrix, with the finest grain and with little preferential orientation. Sample number 7 has the highest average hardness HRC compared to the other cast iron samples analyzed. On the other hand, sample number 1 has the lowest value. The high hardness values of samples 6 and 7 can be explained by the fact that there is a high content of chromium which form the carbides, with small and rounded shape and uniformly distributed and thanks to the fine grain.

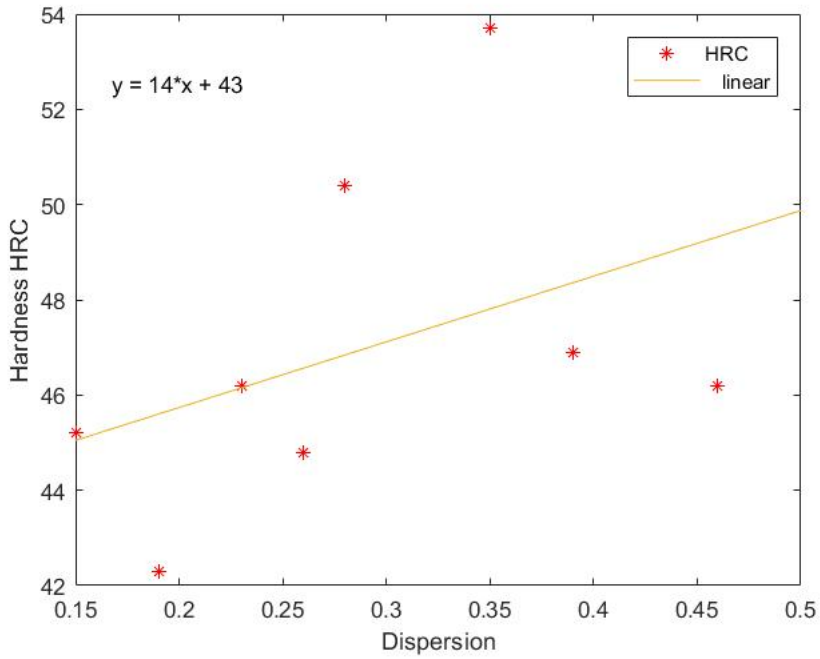

Figure 3.26: Relationship between dispersion and HRC

Despite some deviations, the graph shows that an increase in hardness is linked to ithe increase dispersion.

3.3.2 Design of experiments and creation of the mathematical model

The starting point of the statistical analysis has been the evaluation of the effect of the alloy elements present in the cast irons on hardness (HRC). As said before there have been five investigated elements, which constituted the composition of the starting alloys, they are carbon (C), manganese (Mn), chromium (Cr), nickel (Ni) and finally titanium (Ti). The factors that have composed the system have been five, one for each element, therefore the design of experiment has been related to the fractional experiment with replication of the type 2^{5-2}, which is presented in the previous chapter. The two levels are the extremes of the concentration ranges.

The design matrix has been therefore the following:

Sample	C		Mn		Cr		Ni		Ti	
	X_1	(%)	X_2	(%)	X_3	(%)	X_4	(%)	X_5	(%)
1	-1	1.9	-1	3.5	-1	15	+1	1	-1	0.2
2	+1	2.5	-1	3.5	-1	15	-1	0.4	+1	0.6
3	-1	1.9	+1	5	-1	15	-1	0.4	+1	0.6
4	+1	2.5	+1	5	-1	15	+1	1	-1	0.2
5	-1	1.9	-1	3.5	+1	19	+1	1	+1	0.6
6	+1	2.5	-1	3.5	+1	19	-1	0.4	-1	0.2
7	-1	1.9	+1	5	+1	19	-1	0.4	-1	0.2
8	+1	2.5	+1	5	+1	19	+1	1	+1	0.6
Average	2.2		4.25		17		0.7		0.4	

Table 3.7: Coefficients for statistical consideration

The linear model, that has been intended to be built and validated through the following steps, is something like:

$$Y = HRC = b_o + b_1[C] + b_2[Mn] + b_3[Cr] + b_4[Ni] + b_5[Ti] \tag{3.1}$$

where [C], [Mn], [Cr], [Ni] and [Ti] represent the concentration of each element.

First of all the calculation of the coefficients have been performed:

$$b_0 = \frac{42.3 + 45.2 + 44.8 + 46.2 + 46.9 + 50.4 + 53.7 + 46.9}{8} = 47.056 \tag{3.2}$$

$$b_1 = \frac{-42.3 + 45.2 - 44.8 + 46.2 - 46.9 + 50.3 - 53.7 + 46.9}{8} = 0.456 \tag{3.3}$$

$$b_2 = \frac{-42.3 - 45.2 + 44.8 + 46.2 - 46.9 - 50.3 + 53.7 + 46.9}{8} = 0.856 \tag{3.4}$$

$$b_3 = \frac{-42.3 - 45.2 - 44.8 - 46.2 + 46.9 + 50.3 + 53.7 + 46.9}{8} = 2.444 \tag{3.5}$$

$$b_4 = \frac{42.3 - 45.2 - 44.8 + 46.2 + 46.9 - 50.3 - 53.7 + 46.9}{8} = -1.475 \tag{3.6}$$

$$b_5 = \frac{-42.3 + 45.2 + 44.8 - 46.2 + 46.9 - 5.3 - 53.7 + 46.9}{8} = -1.100 \tag{3.7}$$

Name of the coeffcients	Value
b_0	47.056
b_1	0.113
b_2	0.856
b_3	2.444
b_4	-1.475
b_5	-1.100

Table 3.8: Coeffcients

After the practical measure of the the hardness it has been necessary to make some considerations from the statistical point of view, to reason about the repeatability of the experiments and verify it. In this case eight series of experiments have been carried out in parallel, each with four measurements, and thanks to this information it have been possible to evaluate the parameters of interest for the statistics.

N	n	f_i	G_T
8	4	3	0.43

Table 3.9: Cochran's parameter

$H\bar{R}C$	σ_i^2	σ_{imax}^2	$\sum_{i=1}^{m} \sigma_i^2$	G_P
42.3	0.527	2.063	7.105	0.29
45.2	0.217			
44.8	0.343			
46.2	0.503			
46.9	1.725			
50.4	0.470			
53.7	1.263			
46.9	2.063			

Table 3.10: Cochran's parameter

$$\boxed{0.29 \leq 0.43} \tag{3.8}$$

The disequation is respected this shows the repeatability of the experiments that have been carried out. After that, a second analysis has been performed, this involved the Student's T distribution. Using equation presented in section 2.8 it was possible to find the necessary parameter for the test.

σ_y^2	σ_{bj}	f_y	T_T
0.888	0.167	24	2.064

Table 3.11: Student's T parameter

Factor	T_P
T_{P1}	258.459
T_{P2}	0.675
T_{P3}	5.140
T_{P4}	14.669
T_{P5}	8.854
T_{P6}	6.603

Table 3.12: Value of T_P

At this point it has been necessary to check if the disequations was respected and what were the factors that had to be maintained within the model:

$$\boxed{282.459 \geq 2.064} \tag{3.9}$$

$$\boxed{0.675 \ngeq 2.064} \tag{3.10}$$

$$\boxed{5.140 \geq 2.064} \tag{3.11}$$

$$\boxed{14.669 \geq 2.064} \tag{3.12}$$

$$\boxed{8.854 \geq 2.064} \tag{3.13}$$

$$\boxed{6.603 \geq 2.064} \tag{3.14}$$

Not all coefficients satisfy the Student T criterion and therefore only five of them have been stored in the model and the coefficient related to carbon have been deleted. The next phase has involved analysis the Fisher criterion to validate the correctness of the model. All the parameters were explained in 2.8.

n	N	d	f_{ad}	f_y
4	8	5	3	24

Table 3.13: Fisher's parameter

Series of experiment	$\hat{y} = H\hat{R}C$
1	43.4
2	44.1
3	45.8
4	45.1
5	46.1
6	51.2
7	52.9
8	47.8

Table 3.14: Fisher's calculation

σ^2_{ad}	F_P
0	0

Table 3.15: Fisher's final calculation

From table 2.14: F_T=3.24

$$0 = F_P \leq F_T = 3.24 \tag{3.15}$$

The disequation, which represents the criterion of Fisher, is respected and this indicates the correctness and validity of the model used up to now. The model that has been built, validated and that have been used after is:

$$Y = HRC = 47.06 + 2.44[Cr] + 0.856[Mn] - 1.100[Ti] - 1.475[Ni] \tag{3.16}$$

The order of the coefficients with which the model is presented is linked to the fact that the elements are ordered according to their ability to influence the property, in particular a descending order has been chosen.

Now the calculation of the coefficients and the validation of the model allow to make some considerations.

Comment and Considerations

- In the model there is not the term related to the carbon because the factor was excluded after Student's T test. The fact that carbon does not appear in the model is very strange because it is known that it is among the elements that most influence the mechanical properties of cast iron.However, this could be due to the fact that the range of composition variation in which it is working is very small and there is also an error component. Another reason that could explain why carbon is not so influential and therefore not present in the model could be linked to the specimen production parameters. The metal after its melting in the induction furnace is poured, from the ceramic crucible, into special molds where it solidifies, the cooling rate is considered high and this would lead to an inhibition of the effect of carbon on the hardness of the metal.

- The coefficients linked to the manganese and chromium content are positive, therefore in this case an increase in their content should allow an increase in the value of HRC. It is necessary to pay great attention to the chromium since it is the main regulating element of the hardness of the alloys as it is responsible for a significant increase in the hardness of the matrix and involves a large increase in the presence of the reinforcement phases.

- On the contrary, nickel and titanium are associated with negative coefficients, this should mean that an addition in alloy of their content leads to a reduction in the coefficient.

- What is deduced from the construction of the model is in agreement with the experimental data collected and with the considerations deriving from the characterization.

At this point what was done was to build curves of dependence that allow us to highlight the effect of the individual factors on the studied material and its properties. Thanks to these influence curves it have been possible, therefore, to reach the main objective of the research work, ie the identification of an optimal cast iron composition that is able to maximize the mechanical properties of the material while reducing the cost. In this specific case, in fact, the factors represent the various elements in the alloy, so thanks to the analysis it has been possible to understand how each of them contributes to the value of the property, HRC hardness, and therefore what must be the quantity necessary to maximize them.

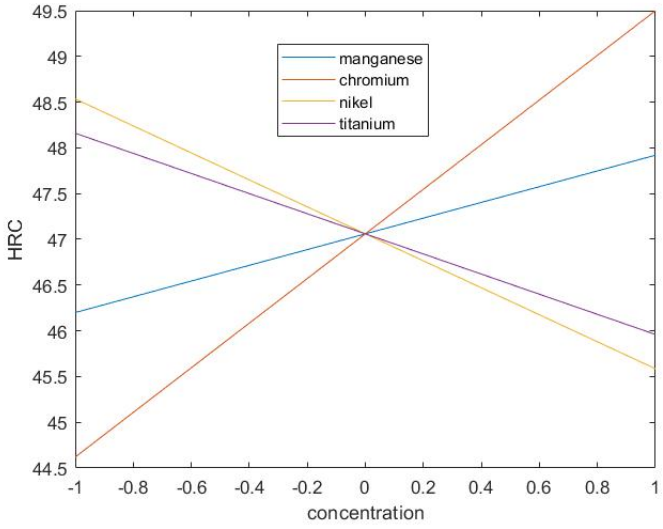

Figure 3.27: Effect of the elements

It is evident that chromium is the element that most affects the value of the hardness of the material, in fact the line associated with it has the highest and most positive slope. An increase in the chromium content in the alloy is able to increase and, more rapidly than other elements, the hardness value. Manganese has a minor effect but nevertheless contributes to the increase of the hardness, instead nickel and titanium lead to a reduction.

A practical validation of the built model has been carried out comparing the practical values obtained with the measures and values predicted by the model.

Sample	Practical value of HRC	Theoretical value of HRC	|Differences|
1	42.3	43.4	1.2
2	45.2	44.1	1.0
3	44.8	45.9	1.1
4	46.2	45.1	1.8
5	46.9	46.0	0.9
6	50.4	51.2	0.8
7	53.7	52.9	0.8
8	46.9	47.7	0.9

Table 3.16: Verification of experimental data

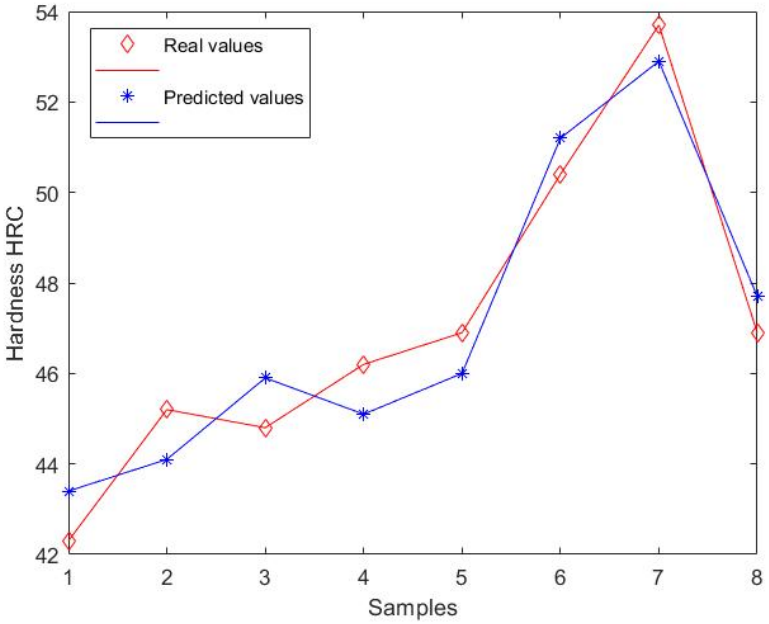

Figure 3.28: Fitting capacity of the model

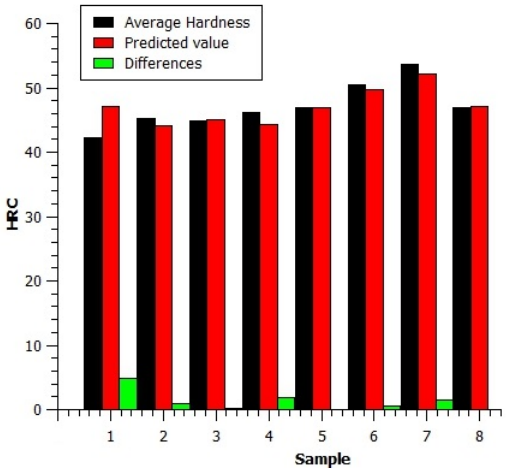

Figure 3.29: Fitting capacity of the model

It is noted that the model fits well the experimental data so much that for some samples, such as the numbers 5, 6, 7 and 8 is less than unity. In other cases, the value falls within the range of measured values to find the average value, except for the first sample and the difference is between one and two units. Although carbon

is not present in the model, it can still be seen that this is able to accurately predict the properties of the material, although as mentioned before the absence from the model may appear strange.

3.4 Wear resistance of the Cast irons

The wear test carried on the sample have been the same as are described in the section 2.7.
What have been found during these test is presented in the following pages with tables and graphs.

Sample	m_1 (g)	m_2 (g)	m_3 (g)	m_4 (g)
1	40.6636	40.5699	40.4381	40.3473
2	37.4050	37.2960	37.1944	37.0871
3	36.2146	36.0921	35.9777	35.8696
4	35.8942	37.7529	35.6260	35.5267
5	41.3893	41.2660	41.1087	40.9669
6	40.5010	10.4362	40.3871	40.3190
7	38.414	38.3502	38.292	38.2328
8	37.6422	37.5807	37.5131	34.4411

Table 3.17: Sample mass after each treatment

In this table there are the values of the mass loss of each sample after each wear treatment with abrasive powder after 1800 revolutions.

Sample	Δ_{m_1} (g)	Δ_{m_2} (g)	Δ_{m_3} (g)	Average value Δ_{m_as} (g)
1	0.0937	0.1318	0.0908	0.1054
2	0.1090	0.1016	0.1073	0.1060
3	0.1225	0.1144	0.1081	0.1150
4	0.1413	0.1269	0.0993	0.1225
5	0.1233	0.1573	0.1418	0.1408
6	0.0648	0.0491	0.0681	0.0607
7	0.0638	0.0573	0.0601	0.0604
8	0.0615	0.0676	0.0720	0.0670

Table 3.18: Mass difference of the samples between two treatments

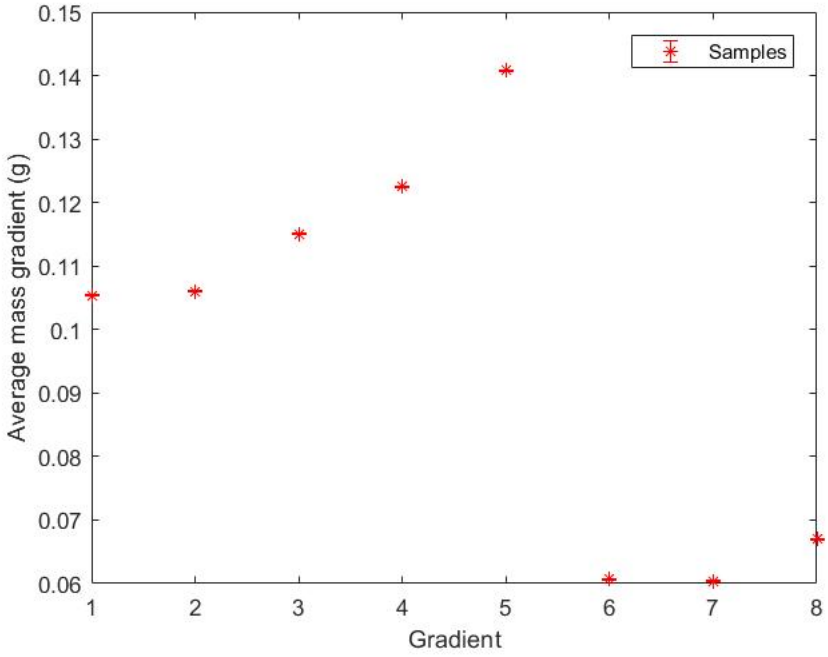

Figure 3.30: Average mass loss for the samples

Results related to the standard sample:

Sample	m_1 (g)	m_2 (g)	m_3 (g)	m_4 (g)
Reference	71.7566	71.6065	71.4486	71.3504

Table 3.19: Mass of the reference after each treatment

Sample	Δ_{m_1} (g)	Δ_{m_2} (g)	Δ_{m_3} (g)	Average value Δ_{m_ar} (g)
Reference	0.1501	0.1579	0.0982	0.1354

Table 3.20: Mass difference of the samples between two treatments

Using again the formula 2.10 it was possible to calculate the values of the Coefficient for wear resistance which are reported in the table 3.21.

Sample	K_{i1}	K_{i2}	K_{i3}	$\bar{K}_i$	Difference with standard (%)
1	1.44	1.03	1.49	1.32	32.12
2	1.24	1.33	1.26	1.28	27.89
3	1.11	1.18	1.25	1.18	18.05
4	0.95	1.07	1.36	1.13	12.96
5	1.10	0.86	0.95	0.97	-2.87
6	2.09	2.76	1.99	2.28	127.85
7	2.12	2.36	2.25	2.25	124.61
8	2.20	2.00	1.88	2.03	102.84

Table 3.21: Results of the calculations

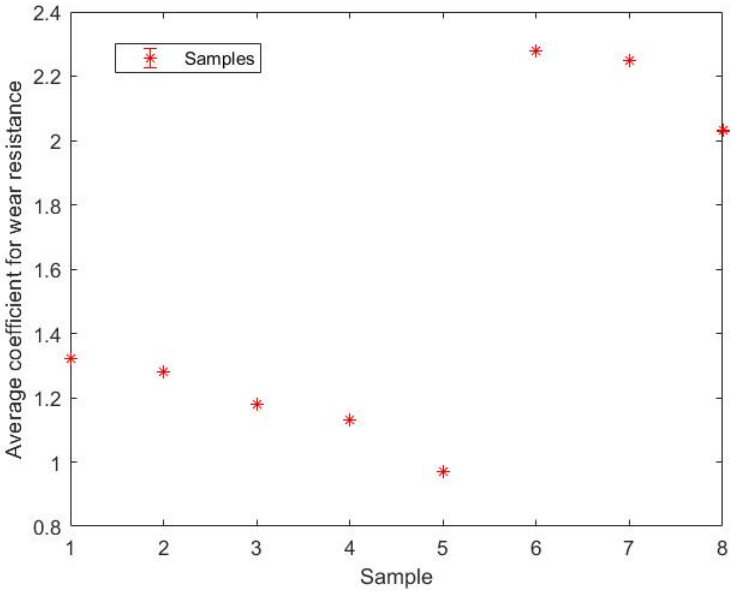

Figure 3.31: K_i values

3.4.1 Comment and considerations

The experiments have been characterized by some difficulties and irregularities that occurred: again the flow of the abrasive powder was not always regular and sometimes it was interrupted, probably due to the dust packing in the nozzle, forcing test stops several times. During the experiment it was necessary to replace the rolling element in the wear test machine because it was excessively

worn and non-compliant. What happened was that the abrasive powder did not come into contact properly with the sample surface due to the irregularity of the wheel thickness. All this caused the presence of improper abrasion marks on the surface of the material. Observed this, the specimens that had been tested were smoothed, their surface was made flat and uniform and then tested using a new rotating element. As with hardness, it is observed that the values of wear resistance coefficients agree with the actual composition of the sample. It is possible to observe that one sample, number 5 is less performing respect to the standard sample, it may be related to some problems during the experiment or during the preparation of the material, in particular during the melting of the cast iron or during the measurement of wear resistance. Sample 6 results as the best in term of wear resistance, in fact it has the highest coefficient K_i and the major difference respect to the standard sample. Sample number 6 has the highest value of the average wear resistance coefficient and this could also be an expected result being the second sample as hardness values. The sample number 7 instead that was highlighted in the hardness measurements, as it is harder than the others, is characterized by a value of K_i practically equal to that of sample 6, so it is very performing. Also this result was expected, given the previous measurements. The sample number 1 which was characterized by having the lowest hardness, however, does not show the lowest resistance to wear. The results that have been obtained agree that with what has been obtained from metallographic investigations.

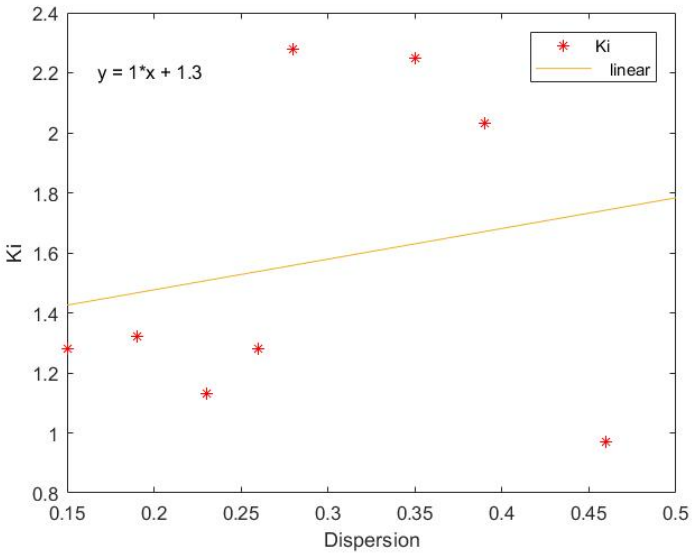

Figure 3.32: Relationship between dispersion and K_i

3.4.2 Surface analysis

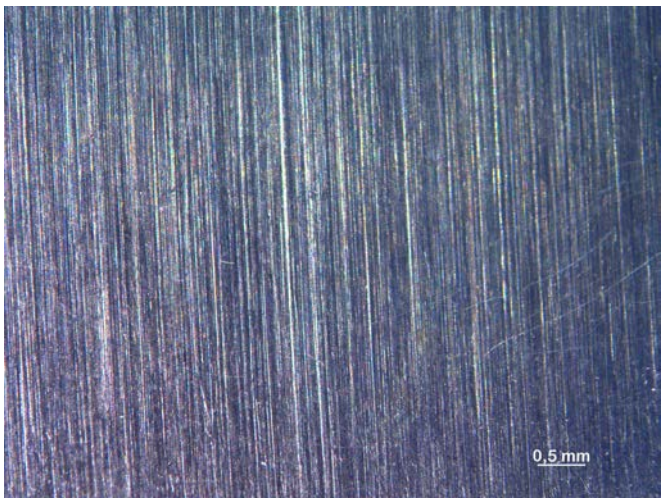

Figure 3.33: Worn surface

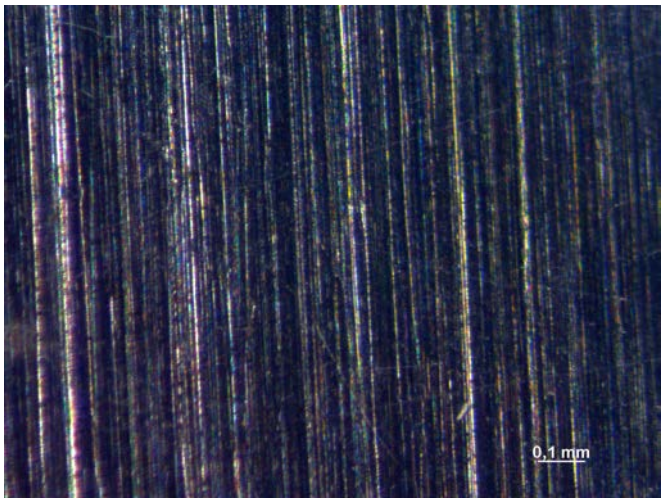

Figure 3.34: Worn surface

On the surface of the material there is no evidence of abrasive powder particles, this is an indication that there has not been adhesion between the powder particles and the metal and therefore the process is an abrasive and non-adhesive wear.

3.4.3 Design of experiment and creation of the mathematical model

At this point the same statistical analysis has been carried out analogous to the one carried out for the hardness, following the same steps and calculations.

Sample	C		Mn		Cr		Ni		Ti	
	X_1	(%)	X_2	(%)	X_3	(%)	X_4	(%)	X_5	(%)
1	-1	1.9	-1	3.5	-1	15	+1	1	-1	0.2
2	+1	2.5	-1	3.5	-1	15	-1	0.4	+1	0.6
3	-1	1.9	+1	5	-1	15	-1	0.4	+1	0.6
4	+1	2.5	+1	5	-1	15	+1	1	-1	0.2
5	-1	1.9	-1	3.5	+1	19	+1	1	+1	0.6
6	+1	2.5	-1	3.5	+1	19	-1	0.4	-1	0.2
7	-1	1.9	+1	5	+1	19	-1	0.4	-1	0.2
8	+1	2.5	+1	5	+1	19	+1	1	+1	0.6
Average	2.2		4.25		17		0.7		0.4	

Table 3.22: Coefficients for statistical consideration

As happended for HRC hardness the linear model that has been intended to be built and validated through the following steps is like:

$$Y = K_i = b_o + b_1[C] + b_2[Mn] + b_3[Cr] + b_4[Ni] + b_5[Ti] \tag{3.17}$$

First of all the calculation of the coefficients have been performed:

$$b_0 = \frac{1.32 + 1.28 + 1.18 + 1.13 + 0.97 + 2.28 + 2.25 + 2.03}{8} = 1.55 \tag{3.18}$$

$$b_1 = \frac{-1.32 + 1.28 - 1.18 + 1.13 - 0.97 + 2.28 - 2.25 + 2.03}{8} = 0.12 \tag{3.19}$$

$$b_2 = \frac{-1.32 - 1.28 + 1.18 + 1.13 - 0.97 - 2.28 + 2.25 + 2.03}{8} = 0.09 \tag{3.20}$$

$$b_3 = \frac{-1.32 - 1.28 - 1.18 - 1.13 + 0.97 + 2.28 + 2.25 + 2.03}{8} = 0.33 \tag{3.21}$$

$$b_4 = \frac{1.28 - 1.28 - 0.89 + 1.11 + 0.96 - 2.23 - 2.24 + 2.02}{8} = -0.19 \tag{3.22}$$

$$b_5 = \frac{-1.28 + 1.28 + 0.89 - 1.11 + 0.96 - 2.23 - 2.24 + 2.02}{8} = -0.19 \tag{3.23}$$

Name of the coefficients	Value
b_0	1.55
b_1	0.12
b_2	0.09
b_3	0.32
b_4	-0.19
b_5	-0.19

Table 3.23: Coefficients

As regards the repeatability analysis of the experiments has been performed: in this case eight series of experiments have been carried out in parallel, for each series three measurements, therefore at this point it was possible to define the parameters necessary to be used in the Cochran criterion. The parameters are presented in the following table:

N	n	f_i	G_T
8	3	2	0.51

Table 3.24: Cochran's parameter

K_i	σ_i^2	σ_{imax}^2	$\sum_{i=1}^{m} \sigma_i^2$	G_P
1.32	0.0653	0.1748	0.3468	0.50
1.28	0.0022			
1.18	0.0054			
1.13	0.0440			
0.97	0.0143			
2.28	0.1748			
2.25	0.0145			
2.03	0.0263			

Table 3.25: Cochran's parameter

$$\boxed{0.50 \leq 0.51} \tag{3.24}$$

As it is possible to note that the disequation is respected, this confirms the repeatability of the experiments that have been carried out. After that a second analysis has been performed, which involves the Student's T distribution. Using equation presented in section 2.8 it has been possible to find the necessary parameters for the test.

σ_y^2	σ_{bj}	f_y	T_T
0.043354	0.042502	16	2.120

Table 3.26: Student's T parameter

Note: T_T have been chosen with an accuracy of 95% (α=0.05)

Factor	T_P
T_{P1}	36.57
T_{P2}	2.93
T_{P3}	2.16
T_{P4}	7.70
T_{P5}	4.51
T_{P6}	4.46

Table 3.27: Value of T_P

At this point it has been necessary to check if the disequations were respected and what were the factors that had to be maintained within the model:

$$\boxed{36.57 \geq 2.120} \tag{3.25}$$

$$\boxed{2.93 \geq 2.120} \tag{3.26}$$

$$\boxed{2.16 \geq 2.120} \tag{3.27}$$

$$\boxed{7.70 \geq 2.120} \tag{3.28}$$

$$\boxed{4.51 \geq 2.120} \tag{3.29}$$

$$\boxed{4.46 \geq 2.120} \tag{3.30}$$

All the six coefficients satisfied the Student T criterion and therefore all of them were stored in the model. The next phase involved analysis with the Fisher criterion to validate the correctness of the model. All the parameter are explained in 2.8.

n	N	d	f_{ad}	f_y
4	8	6	2	16

Table 3.28: Fisher's parameter

Using the equation 2.28:

Series of experiment	$\hat{y} = \hat{K}_i$
1	1.10
2	1.35
3	1.11
4	1.10
5	1.62
6	2.26
7	2.14
8	1.62

Table 3.29: Fisher's calculation

σ^2_{ad}	F_P
0.12	2.08

Table 3.30: Fisher's final calculation

From table 2.14: F_T=3.24

$$2.08 = F_P \leq F_T = 3.24 \tag{3.31}$$

The disequation, which represents the criterion of Fisher, is respected and this indicates the correctness and validity of the model used up to now. The model that has been built, validated and that have been used after is:

$$Y = K_i = 1.55 + 0.33[Cr] + 0.12[C] + 0.09[Mn] - 0.19[Ni] - 0.19[Ti] \tag{3.32}$$

The calculation of the coefficients and the validation of the model allows to make some considerations.

Comment and Consideration

- The coefficient linked to the carbon is positive, therefore in this case an increase in the content should allow an increase in the value of K_i. The same happens for manganese and chromium.

- On the contrary, nickel and titanium are associated with negative coefficients, this should mean that an addition in alloy of their content leads to a reduction in the coefficient.

- What is deduced from the construction of the model is in agreement with the experimental data collected and with the considerations deriving from the characterization.

At this point what have been done was the construction of curves of dependence that allow to highlight the effect of the individual factors on the studied material and its properties. Thanks to these influence curves it have been possible, therefore, to reach the main objective of the research work, ie the identification of an optimal cast iron composition that is able to maximize the mechanical properties of the material while reducing the cost. In this specific case, in fact, the factors represent the various elements in the alloy, so thanks to the analysis it has been possible to understand how each of them contributes to the value of the property, coefficient for wear resistance, and therefore what must be the quantity necessary to maximize them.

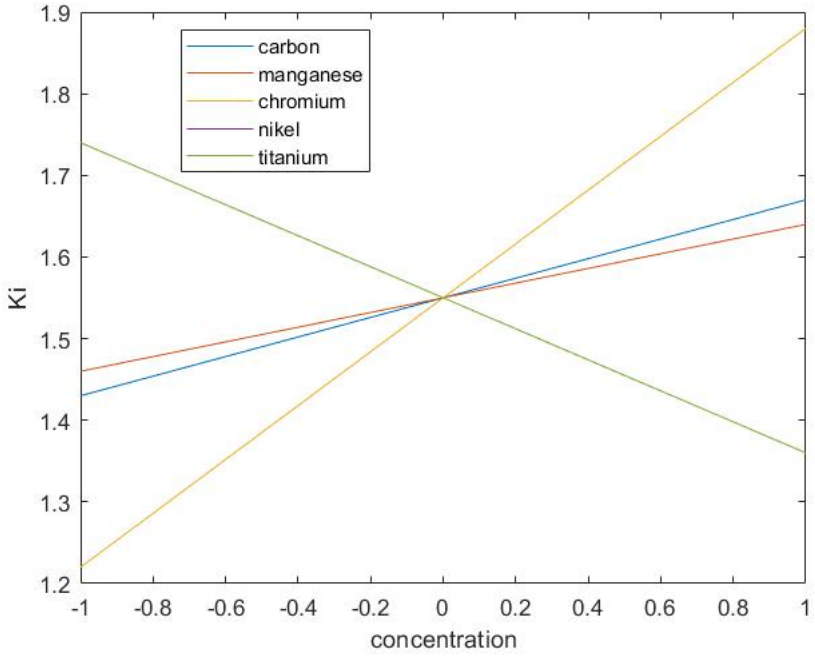

Figure 3.35: Effect of the elements

For this graph the same considerations made for the case of HRC hardness can be maintained.

A practical validation of the built model has been carried out comparing the practical values obtained with the measures and values predicted by the model.

Sample	Theoretical value of K_i	Practical value of K_i	|Differences|
1	1.01	1.32	0.31
2	1.25	1.28	0.03
3	1.19	1.18	0.01
4	1.43	1.13	0.30
5	1.29	0.97	0.32
6	2.29	2.28	0.01
7	2.23	2.25	0.02
8	1.71	2.03	0.32

Table 3.31: Fitting capacity of the model

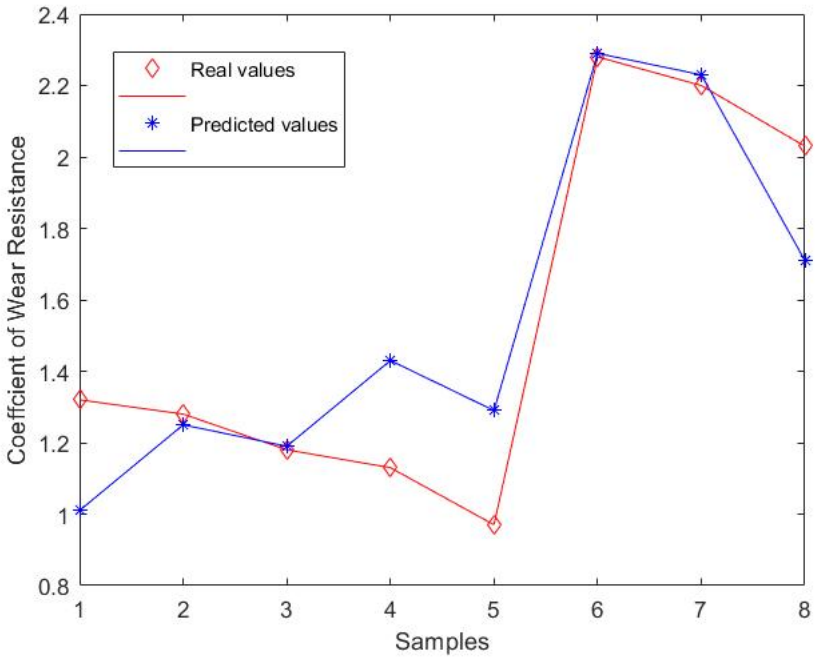

Figure 3.36: Fitting capacity of the model

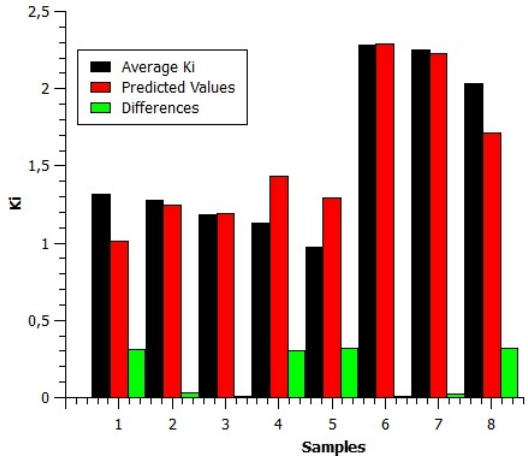

Figure 3.37: Fitting capacity of the model

The model in first approximation seems to fit the experimental data, for samples 2, 3, 6, 7 the values predicted by the model and those measured the difference is minimal. For the other samples there are no significant differences between the values.

Chapter 4

DEVELOPMENT OF A NEW CAST IRON COMPOSITION

After an in-depth statistical and practical analysis, two mathematical models were obtained and validated. A first comparison was made with the first experimental values obtained which showed that the models produced are able to correctly predict the experimental data. At this point it was possible to proceed with the application of the models to calculate the optimal composition that is able to optimize/maximize the HRC hardness and the Wear resistance, expressed through the coefficient of wear resistance K_i. In order to find the desired compositions the Steep Ascent Method, which has been previously described in correspondence of the section 2.9.1, has been used.

In the following pages are presented all the steps and calculations that have been necessary to obtain the compositions.

4.1 Optimization of the composition to maximize hardness

The first thing that is required for the method is to define a composition range to explore for each alloying element. As ranges of concentration have been chosen the ranges set at the beginning of the work, which are typical of the practice and are also those for which the method is valid. In fact, the mathematical model that is possible to build through this method is valid only in the prefixed ranges and could not be applied outside it.

Sample	Fe (%)	C (%)	Mn (%)	Cr (%)	Ni (%)	Ti (%)
1	balance	1.9	3.5	15.0	1.0	0.2
2	balance	2.5	3.5	15.0	0.4	0.6
3	balance	1.9	5.0	15.0	0.4	0.6
4	balance	2.5	5.0	15.0	1.0	0.2
5	balance	1.9	3.5	19.0	1.0	0.6
6	balance	2.5	3.5	19.0	0.4	0.2
7	balance	1.9	5.0	19.0	0.4	0.2
8	balance	2.5	5.0	19.0	1.0	0.6

Table 4.1: Chemical composition of the starting samples

so:

Intervals of the composition
1.9≤ C≤2.5
3.5≤Mn≤5
15≤Cr≤19
0.4≤Ni≤1
0.2≤Ti≤0.6

Table 4.2: Explored intervals

In the new compositions the concentration of each element must be inside this interval because the model works only in these intervals. In the second step has been necessary to fix the change in composition that is considered significant for each element. The following values have been fixed:

Element	Δx_i	Value (%)
C	Δx_C	0.2
Mn	Δx_{Mn}	0.1
Cr	Δx_{Cr}	0.5
Ni	Δx_{Ni}	0.1
Ti	Δx_{Ti}	0.05

Table 4.3: Variation step of the composition

To implement a steep gradient climb, as sad in theoretic part, it has been necessary to define these new variables:

$$X_C = \Delta x_C \times b_1 = 0.023 \tag{4.1}$$

$$X_{Mn} = \Delta x_{Mn} \times b_2 = 0.257 \tag{4.2}$$

$$X_{Cr} = \Delta x_{Cr} \times b_3 = 1.222 \tag{4.3}$$

$$X_{Ni} = \Delta x_{Ni} \times b_4 = -0.148 \tag{4.4}$$

$$X_{Ti} = \Delta x_{Ti} \times b_5 = -0.006 \tag{4.5}$$

Element	$\Delta x_i \times b_i$	$(\Delta x_i \times b_i)_{max}$
C	0.023	
Mn	0.257	
Cr	1.222	1.222
Ni	-0.148	
Ti	-0.006	

Table 4.4: $\Delta x_i \times b_i$

It is possible to see that the product $\Delta x_{Cr} \times b_{Cr}$ has the highest absolute value therefore, the variable x $_{Cr}$ has been the base when the steep climb has been implemented. The choice of the step value of the main level is linked to the variation of the chromium content in the cast iron: the lower limit is 15% and the upper limit is 19%, it has been assumed that the number of mental experiments and iterations does not exceed the number of the performed experiments, and therefore that no more than eight iterations are needed to reach the maximum admissible chromium value. So in order to reach 19% in eight iterations the step had to be δ_{Cr}=0.5%.

At this point it was possible to define the following variables, λ and the step for the other elements:

$$\lambda = \frac{\Delta x_i \times b_i}{\delta_{Cr}} = \frac{1.222}{0.5} = 2.444 \tag{4.6}$$

$$\delta_C = \frac{\Delta x_C \times b_C}{\lambda} = 0.009 \tag{4.7}$$

$$\delta_{Mn} = \frac{\Delta x_{Mn} \times b_{Mn}}{\lambda} = 0.105 \tag{4.8}$$

$$\delta_{Ni} = \frac{\Delta x_{Ni} \times b_{Ni}}{\lambda} = -0.060 \tag{4.9}$$

$$\delta_{Ti} = \frac{\Delta x_{Ti} \times b_{Ti}}{\lambda} = -0.002 \tag{4.10}$$

After that it has been necessary a composition x_{i0} as a starting point with the iterations, the one that has been chosen is:

Element	Concentration (%)
C	2.00
Mn	3.70
Cr	15.50
Ni	0.90
Ti	0.50

Table 4.5: Starting composition x_{i0}

Continuing, the last thing that has been necessary to perform were the iteration and mental experiment. All the iterations carried out are presented in the table 4.6 on the next page.

Properties of the problem	Factors X_1 (C)	X_2 (Mn)	X_3 (Cr)	X_4 (Ni)	X_5 (Ti)	
x_{i0}	2	3.7	15.5	0.9	0.5	
Δx_i	0.1	0.1	0.5	0.1	0.005	
x_{i-}	1.9	3.6	15	0.8	0.45	
x_i^+	2.1	3.8	16	1	0.55	
Number of the experiment	Factors X_1 (C)	X_2 (Mn)	X_3 (Cr)	X_4 (Ni)	X_5 (Ti)	HRC
1	-1	-1	-1	+1	-1	42.3
2	+1	-1	-1	-1	+1	45.2
3	-1	+1	-1	-1	+1	44.9
4	+1	+1	-1	+1	-1	46.2
5	-1	-1	+1	+1	+1	46.9
6	+1	-1	+1	-1	-1	50.4
7	-1	+1	+1	-1	-1	53.4
8	+1	+1	+1	+1	+1	46.9
b_i	0.11	0.86	2.44	-1.48	-1.10	
$\Delta x_i \times b_i$	0.023	0.257	1.222	-0.148	-0.006	
$(\Delta x_i \times b_i)_{max}$			1.222			
λ			2.444			
δ_i	0.009	0.105	0.500	-0.060	-0.002	
Number of iteration	Factors C (%)	Mn (%)	Cr (%)	Ni (%)	Ti (%)	HRC
1	2.01	3.81	16.00	0.84	0.50	41.8
2	2.02	3.91	16.50	0.78	0.50	42.0
3	2.03	4.02	17.00	0.72	0.49	42.2
4	2.04	4.12	17.50	0.66	0.49	46.7
5	2.05	4.23	18.00	0.60	0.49	46.9
6	2.06	4.33	18.50	0.54	0.49	50.4
7	2.07	4.44	19.00	0.48	0.48	50.6
Opt. interval	2.05÷2.07	4.23÷4.44	18.0÷19.0	0.48÷0.60	0.48÷0.49	

Table 4.6: Iterations

The first four compositions that have been found through iterations at this point will be considered as theoretical experiments. The compositions number 5, 6, 7 instead are the reference compositions for the following tests, which consist in consists of a further verification of this model. The composition interval that results from the optimization process for each of the elements is as follows: [C]=2.05÷2.07, [Mn]=4.23÷4.44, [Cr]=18.0÷19.0, [Ni]=0.48÷0.60 and [Ti]=0.48÷0.49. Carbon evolution has been included to highlight its behaviour even if it is not included in the model but only in the composition, it is not considered in the predicted value. It is important also to observe that its variation is very low between two subsequent iterations.

4.2 Optimization of the composition to maximize wear resistance

The procedure used to optimize the composition is identical to that used in the previous case with the HRC hardness. First, the range of concentrations to be explored has been defined, similar to the previous one because the same considerations, previously made, remain valid.

Sample	Fe (%)	C (%)	Mn (%)	Cr (%)	Ni (%)	Ti (%)
1	balance	1.9	3.5	15.0	1.0	0.2
2	balance	2.5	3.5	15.0	0.4	0.6
3	balance	1.9	5.0	15.0	0.4	0.6
4	balance	2.5	5.0	15.0	1.0	0.2
5	balance	1.9	3.5	19.0	1.0	0.6
6	balance	2.5	3.5	19.0	0.4	0.2
7	balance	1.9	5.0	19.0	0.4	0.2
8	balance	2.5	5.0	19.0	1.0	0.6

Table 4.7: Chemical composition of the Samples

so:

Intervals of the composition
1.9≤ C≤2.5
3.5≤Mn≤5
15≤Cr≤19
0.4≤Ni≤1
0.2≤Ti≤0.6

Table 4.8: Interval

In the new composition the concentration of each element must be inside this interval because the model works only in these intervals. In the second step has been fixed the change in composition that was considered significant for each element. The following values have been decided:

Element	Δx_i	Value (%)
C	Δx_C	0.2
Mn	Δx_{Mn}	0.1
Cr	Δx_{Cr}	0.5
Ni	Δx_{Ni}	0.1
Ti	Δx_{Ti}	0.05

Table 4.9: Variation step of the composition

To implement a steep gradient climb, as sad in theoretic part, it has been necessary to define these new variables:

$$X_C = \Delta x_C \times b_1 = 0.012 \tag{4.11}$$

$$X_{Mn} = \Delta x_{Mn} \times b_2 = 0.009 \tag{4.12}$$

$$X_{Cr} = \Delta x_{Cr} \times b_3 = 0.163 \tag{4.13}$$

$$X_{Ni} = \Delta x_{Ni} \times b_4 = -0.019 \tag{4.14}$$

$$X_{Ti} = \Delta x_{Ti} \times b_5 = -0.001 \tag{4.15}$$

Element	$\Delta x_i \times b_i$	$(\Delta x_i \times b_i)_{max}$
C	0.012	
Mn	0.009	
Cr	0.163	0.163375
Ni	-0.019	
Ti	-0.001	

Table 4.10: $\Delta x_i \times b_i$

It is possible to see that the product $\Delta x_{Cr} \times b_{Cr}$ has the highest absolute value therefore, the variable x $_{Cr}$ has been the base when the steep climb has been implemented. The choice of the step value of the main level is linked to the variation of the chromium content in the cast iron: the lower limit is 15% and the upper limit is 19%, it has been assumed that the number of mental experiments and iterations does not exceed the number of the performed experiments, and therefore that no more than eight iterations are needed to reach the maximum admissible chromium value. So in order to reach 19% in eight iterations the step had to be δ_{Cr}=0.5%.

At this point it was possible to define the following variables, λ and the step for the other elements:

$$\lambda = \frac{\Delta x_{Cr} \times b_{Cr}}{\delta_{Cr}} = \frac{0.163}{0.5} = 0.327 \tag{4.16}$$

$$\delta_C = \frac{\Delta x_C \times b_C}{\lambda} = \frac{0.163}{0.327} = 0.038 \tag{4.17}$$

$$\delta_{Mn} = \frac{\Delta x_{Mn} \times b_{Mn}}{\lambda} = \frac{0.009}{0.327} = 0.028 \tag{4.18}$$

$$\delta_{Ni} = \frac{\Delta x_{Ni} \times b_{Ni}}{\lambda} = \frac{-0.019}{0.327} = -0.059 \tag{4.19}$$

$$\delta_{Ti} = \frac{\Delta x_{Ti} \times b_{Ti}}{\lambda} = \frac{-0.001}{0.327} = -0.003 \tag{4.20}$$

After that it was necessary a composition x_{i0} as a starting point with the iterations, the one that was chosen is:

Element	Concentration (%)
C	2.00
Mn	3.70
Cr	15.50
Ni	0.90
Ti	0.50

Table 4.11: Starting composition x_{i0}

Continuing, the last things that has been necessary to perform were the iteration and mental experiment. All the iterations carried out are presented in the table 4.12 on the next page.

Properties of the problem			Factors			
	X_1 (C)	X_2 (Mn)	X_3 (Cr)	X_4 (Ni)	X_5 (Ti)	
x_{i0}	2	3.7	15.5	0.9	0.5	
Δx_i	0.1	0.1	0.5	0.1	0.005	
x_{i-}	1.9	3.6	15	0.8	0.45	
x_i^+	2.1	3.8	16	1	0.55	
Number of the experiment	X_1 (C)	X_2 (Mn)	Factors X_3 (Cr)	X_4 (Ni)	X_5 (Ti)	K_i
1	-1	-1	-1	+1	-1	1.32
2	+1	-1	-1	-1	+1	1.28
3	-1	+1	-1	-1	+1	1.18
4	+1	+1	-1	+1	-1	1.13
5	-1	-1	+1	+1	+1	0.97
6	+1	-1	+1	-1	-1	2.28
7	-1	+1	+1	-1	-1	2.25
8	+1	+1	+1	+1	+1	2.03
b_i	0.12	0.09	0.33	-0.19	-0.19	
$\Delta x_i \times b_i$	0.012	0.009	0.163	-0.019	-0.001	
$(\Delta x_i \times b_i)_{max}$			0.163			
λ			0.327			
δ_i	0.038	0.028	0.500	-0.059	-0.003	
Number of iteration	C (%)	Mn (%)	Factors Cr (%)	Ni (%)	Ti (%)	K_i
1	2.04	3.73	16.00	0.84	0.50	0.73
2	2.08	3.76	16.50	0.78	0.49	0.75
3	2.11	3.78	17.00	0.72	0.49	0.78
4	2.15	3.81	17.50	0.67	0.49	1.38
5	2.19	3.84	18.00	0.61	0.49	1.40
6	2.23	3.87	18.50	0.55	0.48	1.88
7	2.27	3.90	19.00	0.49	0.48	1.91
Opt. interval	2.2÷2.3	3.8÷3.9	18.0÷19.0	0.5÷0.6	0.48÷0.49	

Table 4.12: Iterations

The first four compositions that have been found through iterations at this point will be considered as theoretical experiments. The compositions number 5, 6, 7 instead are the reference compositions for the following tests, which consist in consists of a further verification of this model. The composition interval that results from the optimization process for each of the elements is as follows: [C]=2.20÷2.30, [Mn]=3.8÷3.9, [Cr]=18.0÷19.0, [Ni]= 0.50÷0.60 and [Ti]=0.48÷0.49.

4.3 Summary

Composition[1]	Fe (%)	C (%)	Mn (%)	Cr (%)	Ni (%)	Ti (%)
5-H	balance	2.05	4.23	18.00	0.60	0.49
6-H	balance	2.06	4.33	18.50	0.54	0.49
7-H	balance	2.07	4.44	19.00	0.48	0.48
5-W	balance	2.19	3.84	18.00	0.61	0.49
6-W	balance	2.23	3.87	18.50	0.55	0.48
7-W	balance	2.27	3.90	19.00	0.49	0.48

Table 4.13: Optimized compositions

Alloying element	K_i	HRC	Optimum content of the alloying elements HRC (%)	K_i(%)
Carbon	-	↑	2.05÷2.07	2.10÷2.30
Manganese	↑	↑	4.23÷4.44	3.80÷3.90
Chromium	↑	↑	18.00÷19.00	18.00÷19.00
Nickel	↓	↓	0.50÷0.60	0.50÷0.60
Titanium	↓	↓	0.48÷0.49	0.48÷0.49

Table 4.14: Effect of the alloying element and Optimized composition ranges

[1]W:model for wear; H:model for hardness; the designation of the alloys is kept below in all parts

Chapter 5

ANALYSIS OF THE NEW CAST IRON COMPOSITIONS OBTAINED FROM MODELS

In this chapter the alloys obtained through the method for the optimization of the chemical composition in the previous chapter are studied, theoretical values and compositions come from that calculations. First the alloys obtained with the model for wear resistance and then those for hardness were studied.

5.1 Cast irons and properties of cast irons from Wear optimization

5.1.1 Compositions from wear optimization

Composition	Fe (%)	C (%)	Mn (%)	Cr (%)	Ni (%)	Ti (%)
5-W	balance	2.19	3.84	18.00	0.61	0.49
6-W	balance	2.23	3.87	18.50	0.55	0.48
7-W	balance	2.27	3.90	19.00	0.49	0.48

Table 5.1: Investigated composition

Sample	Theoretical value of K_i	Theoretical value of HRC
5-W	1.40	48.7
6-W	1.88	48.9
7-W	1.91	49.1

Table 5.2: Theoretical value of the properties

5.1.2 Samples' preparation

In this section are presented the calculations carried out for the determination of the charge for the preparation of the cast iron samples, which have been necessary to test the mathematical model that have been built in the previous sections, to optimize the chemical composition. The ferroalloys used were those presented in the chapter 2 to the section 2.2, in particular:

- P1, GOST 4832-80;
- 1A steel scrap, GOST 2787-86;
- FeTi 32, GOST 4761-80;
- FeA850 GOST 4757-91;
- FeMn 70, GOST 4755-80;
- Metallic nikel;

The ferroalloys iron and steel scrap used came from the MMK metallurgical plant placed in Magnitogorsk. The difference between the optimized theoretical composition and thereal one is due to some elements such as silicon, phosphorus and sulfur which derive from the ferroalloys used in the charge. But how have they been obtained? In the following pages there are the systems containing the mass balances and the boundary condition that must be respected.

$$\begin{cases} (1-\frac{8}{100})[Fe-Cr]\frac{65}{100} = 18.00 \\ [Ni]\frac{99.9}{100} = 0.61 \\ (1-\frac{10}{100})\left\{[Fe-Mn]\frac{70}{100} + [SS]\frac{0.6}{100} + [PI]\frac{0.3}{100}\right\} = 3.84 \\ (1-\frac{50}{100})[Fe-Ti]\frac{32}{100} = 0.49 \\ (1-\frac{35}{100})\left\{[Fe-Cr]\frac{8.5}{100} + [Fe-Mn]\frac{7}{100} + \right. \\ \left.[Fe-Ti]\frac{0.12}{100} + [SS]\frac{0.15}{100} + [PI]\frac{4.3}{100}\right\} = 2.19 \\ [Fe-Cr] + [Ni] + [Fe-Mn] + [Fe-Ti] + [SS] + [PI] = 100 \end{cases} \tag{5.1}$$

$$\begin{cases} (1-\frac{8}{100})[Fe-Cr]\frac{65}{100} = 18.5 \\ [Ni]\frac{99.9}{100} = 0.55 \\ (1-\frac{10}{100})\left\{[Fe-Mn]\frac{70}{100} + [SS]\frac{0.6}{100} + [PI]\frac{0.3}{100}\right\} = 3.87 \\ (1-\frac{50}{100})[Fe-Ti]\frac{32}{100} = 0.48 \\ (1-\frac{35}{100})\left\{[Fe-Cr]\frac{8.5}{100} + [Fe-Mn]\frac{7}{100} + \right. \\ \left.[Fe-Ti]\frac{0.12}{100} + [SS]\frac{0.15}{100} + [PI]\frac{4.3}{100}\right\} = 2.23 \\ [Fe-Cr] + [Ni] + [Fe-Mn] + [Fe-Ti] + [SS] + [PI] = 100 \end{cases} \tag{5.2}$$

$$
\begin{cases}
(1-\frac{8}{100})[Fe-Cr]\frac{65}{100}=19.00 \\
[Ni]\frac{99.9}{100}=0.49 \\
(1-\frac{10}{100})\left\{[Fe-Mn]\frac{70}{100}+[SS]\frac{0.6}{100}+[PI]\frac{0.3}{100}\right\}=3.90 \\
(1-\frac{50}{100})[Fe-Ti]\frac{32}{100}=0.49 \\
(1-\frac{35}{100})\left\{[Fe-Cr]\frac{8.5}{100}+[Fe-Mn]\frac{7}{100}+\right. \\
\left.[Fe-Ti]\frac{0.12}{100}+[SS]\frac{0.15}{100}+[PI]\frac{4.3}{100}\right\}=2.27 \\
[Fe-Cr]+[Ni]+[Fe-Mn]+[Fe-Ti]+[SS]+[PI]=100
\end{cases}
\tag{5.3}
$$

Type of ferroalloy	Used amount (%)	Used amount (g)
Ferrochromium [Fe-Cr]	30.10	301.00
Metallic Nickel [Ni]	0.61	6.10
Ferromanganese [Fe-Mn]	5.59	55.90
Ferrotitanium [Fe-Ti]	3.06	3.06
Steel Scrap [SS]	52.80	528.00
Pig Iron [Pi]	7.84	78.40
Element	Loss due to oxidation of the elements (%)	
C	35.00	
Mn	10.00	
Cr	8.00	
Ni	0.00	
Ti	50.00	
Si	50.00	
P	25.00	
S	45.00	
Element	Final mass of each elements (g)	
Fe	balance	
C	21.90	
Mn	38.40	
Cr	180.00	
Ni	6.10	
Ti	4.90	
Si	4.70	
P	0.60	
S	0.20	
Element	Final Concentration (%)	
Fe	balance	
C	2.19	
Mn	3.84	
Cr	18.00	
Ni	0.61	
Ti	0.49	
Si	0.47	
P	0.06	
S	0.02	

The following tables show the results related to the production of 1 kg of material

Table 5.3: Charge of sample 5-W

Type of ferroalloy	Used amount (%)	Used amount (g)
Ferrochromium [Fe-Cr]	30.94	309.40
Metallic Nickel [Ni]	0.55	5.50
Ferromanganese [Fe-Mn]	5.63	56.30
Ferrotitanium [Fe-Ti]	3.00	30.00
Steel Scrap [SS]	52.33	523.30
Pig Iron [Pi]	7.56	75.50
Element	Loss due to oxidation of the elements (%)	
C	35.00	
Mn	10.00	
Cr	8.00	
Ni	0.00	
Ti	50.00	
Si	50.00	
P	25.00	
S	45.00	
Element	Final mass of each elements (g)	
Fe	balance	
C	22.30	
Mn	38.70	
Cr	185.00	
Ni	5.50	
Ti	6.10	
Si	4.70	
P	0.60	
S	0.20	
Element	Final Concentration (%)	
Fe	balance	
C	2.23	
Mn	3.87	
Cr	18.50	
Ni	0.55	
Ti	0.48	
Si	0.47	
P	0.06	
S	0.02	

The following tables show the results related to the production of 1 kg of material

Table 5.4: Charge of sample 6-W

Type of ferroalloy	Used amount (%)	Used amount (g)
Ferrochromium [Fe-Cr]	31.77	317.70
Metallic Nickel [Ni]	0.49	4.90
Ferromanganese [Fe-Mn]	5.72	57.52
Ferrotitanium [Fe-Ti]	3.00	30.00
Steel Scrap [SS]	51.74	517.40
Pig Iron [Pi]	7.28	72.80
Element	Loss due to oxidation of the elements (%)	
C	35.00	
Mn	10.00	
Cr	8.00	
Ni	0.00	
Ti	50.00	
Si	50.00	
P	25.00	
S	45.00	
Element	Final mass of each elements (g)	
Fe	balance	
C	22.70	
Mn	39.00	
Cr	190.00	
Ni	4.90	
Ti	4.80	
Si	4.80	
P	0.60	
S	0.20	
Element	Final Concentration (%)	
Fe	balance	
C	2.27	
Mn	3.90	
Cr	19.00	
Ni	0.49	
Ti	0.48	
Si	0.48	
P	0.06	
S	0.02	

The following tables show the results related to the production of 1 kg of material

Table 5.5: Charge of sample 7-W

Note: In the final calculation there are also silicon, phosphorus and sulfur contents, which are not present in the built model, but which are important for the cast iron having a major impact on the properties of the material. They come from the raw materials used for the production of the alloys.

5.1.3 Results of metallurgical characterization of new cast irons

5.1.3.1 Effective cast irons compositions

Sample	Fe (%)	C (%)	Mn (%)	Cr (%)	Ni (%)	Ti (%)	Si (%)	P (%)	S (%)
5-W	balance	2.25	4.05	16.41	0.72	0.04	1.23	0.05	0.01
6-W	balance	2.35	4.97	17.09	0.66	0.14	0.85	0.05	0.02
7-W	balance	2.56	5.58	17.54	1.08	0.20	1.00	0.06	0.02

Table 5.6: Real chemical composition of the alloys

Comments and considerations

The real composition of the samples obtained was measured through the quantometer at the Zanardi Fonderie company in Minerbe (VR). It is possible to observe a difference between the actual and expected composition that could be linked to the calibration of the instrument and therefore should be considered indicative. However, the increases/decreases in the elements are as expected.

Sample	Solidification cooling rate (c_{r1}=°C/ sec)
1÷8	9

Table 5.7: Cooling Rate

5.1.3.2 Micrographs

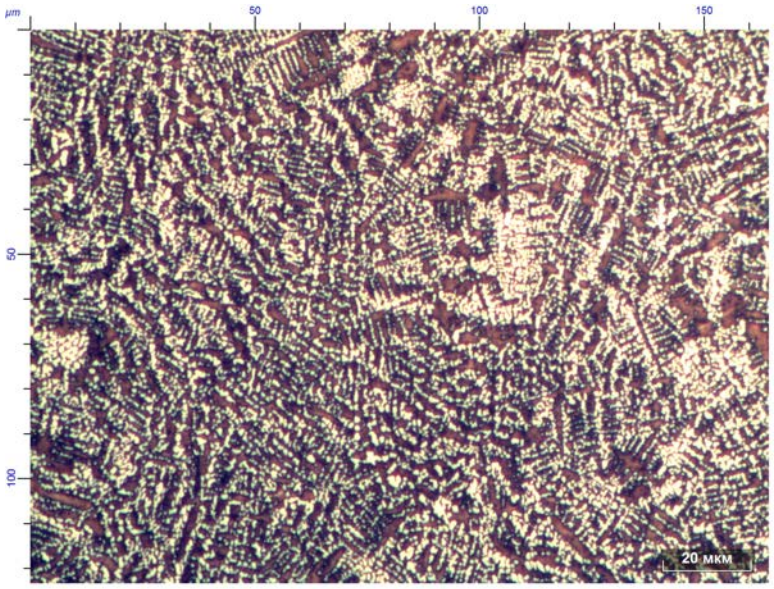

Figure 5.1: Microstructure sample 5-W 500x new

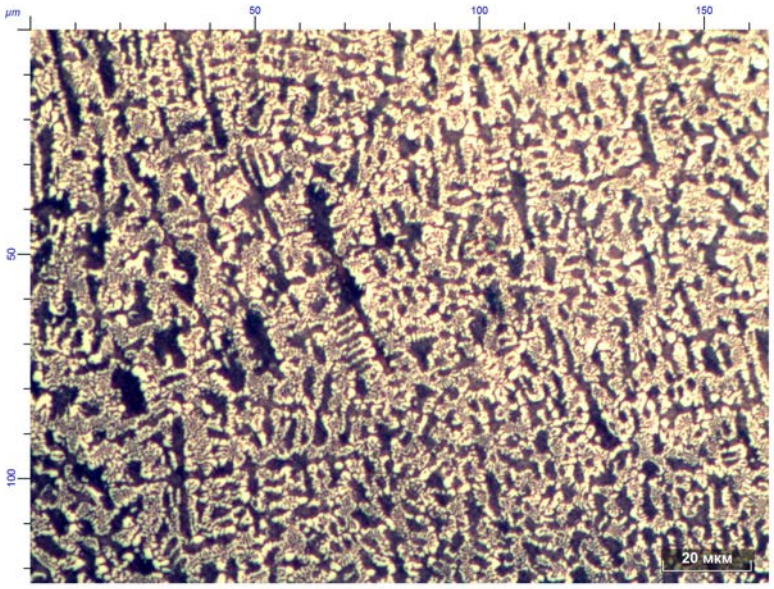

Figure 5.2: Microstructure sample 6-W 500x new

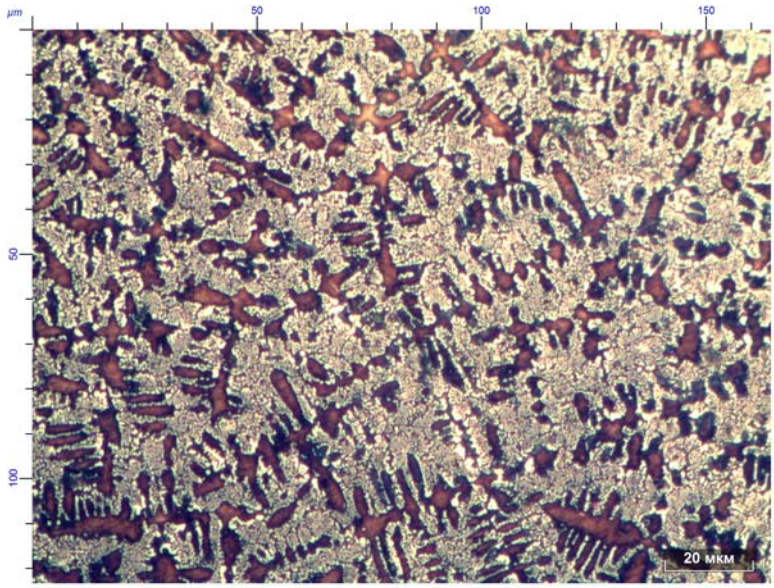

Figure 5.3: Microstructure sample 7-W 500x new

Comments and considerations

- Samples: It is possible to observe that all three samples have a microstructure with austenite dendrites and in all cases the metal matrix is surrounded by carbides. As expected, there is no presence of graphite in the material due to high quantity of chromium and high cooling rate during the production of the material.

- Sample 5-W: In this case it is observed a lower quantity of carbides compared to the other samples and there are a lot of randomly oriented dendrites.

- Sample 6-W: It is possible to note that the percentage of carbides is very high compared to that of sample number 5, in particular there is a high content of austenitic eutectic carbides of the type M_3C and M_7C_3.

- Sample 7-W: The micrograph shows a large presence of iron, chromium and titanium carbides. The orientation of the dendrites, whose arms are of reduced length, are oriented randomly allowing to hypothesize that the material is isotropic. Titanium carbides are well visible in the image thanks to the green color allows to distinguish them from the others. The sample 7-W also highlights other elements: moving from the outside of the sample and going towards the core it is possible to observe the presence of the small equiaxial grains which are determined by the initial high cooling rate in the ingot forming an outer skin. After that, columnar grains and dendrites

are encountered, and this is caused by the decrease in cooling rate which is decreasing. The orientation of dendrites is determined by the flow of heat during cooling.

5.1.3.3 Quantitative analysis

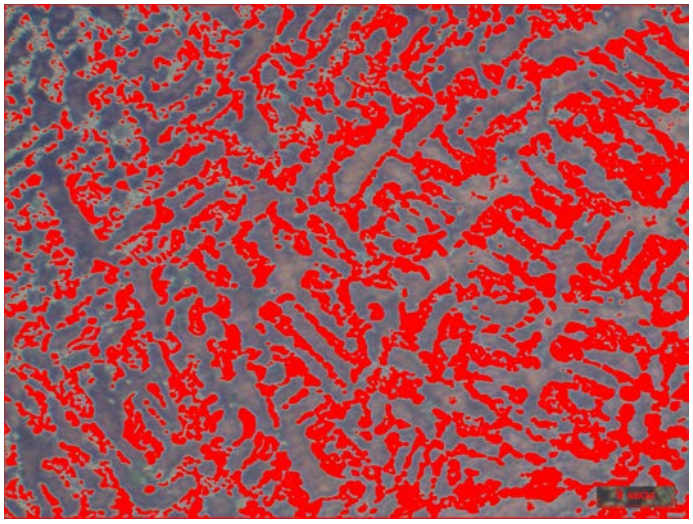

Figure 5.4: Quantitative analysis of the new sample number 5-W

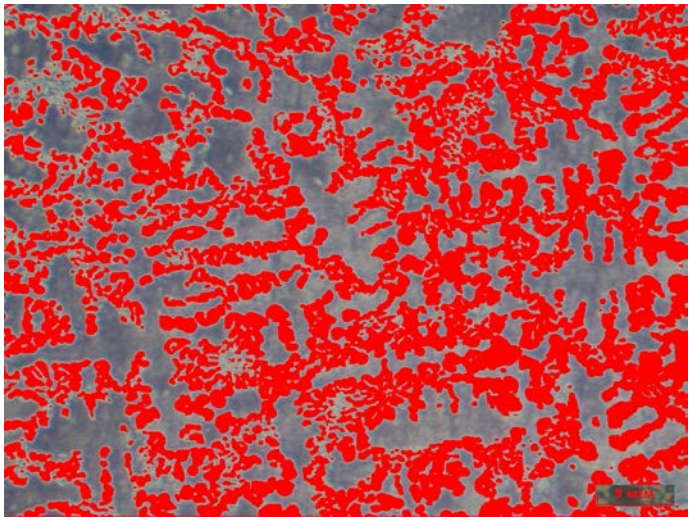

Figure 5.5: Quantitative analysis of the new sample number 6-W

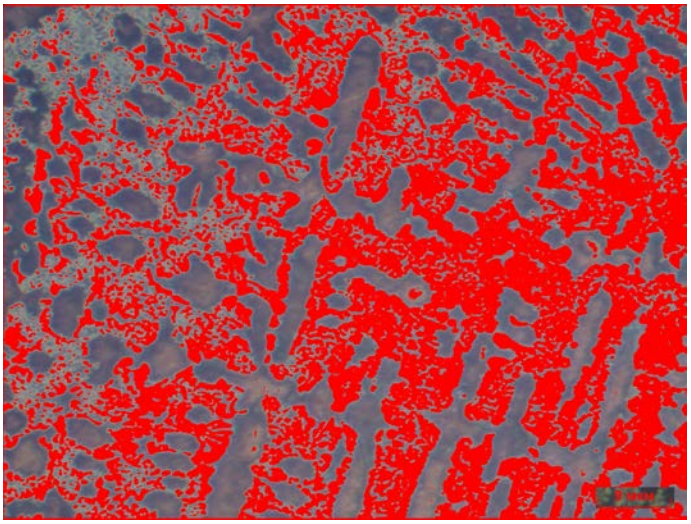

Figure 5.6: Quantitative analysis of the new sample number 7-W

Sample	Carbide phase (%)	Metal matrix (%)
5-W	39.59	60.41
6-W	45.88	54.12
7-W	50.36	49.64

Table 5.8: Phase quantity evaluation

Comments and considerations

It is possible to observe that as the chromium content increases in the samples, the percentage of carbides increases, in fact the sample number 7 which has 19% of chromium is characterized by the maximum percentage. This is in agreement with what has already been observed before.

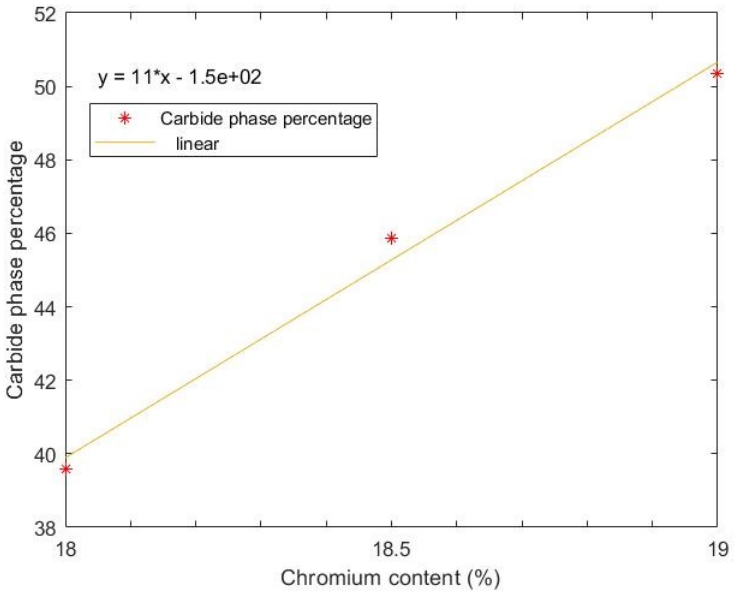

Figure 5.7: Relationship between the chromium content and the quantity of carbide phase

5.1.3.4 Dispersion analysis

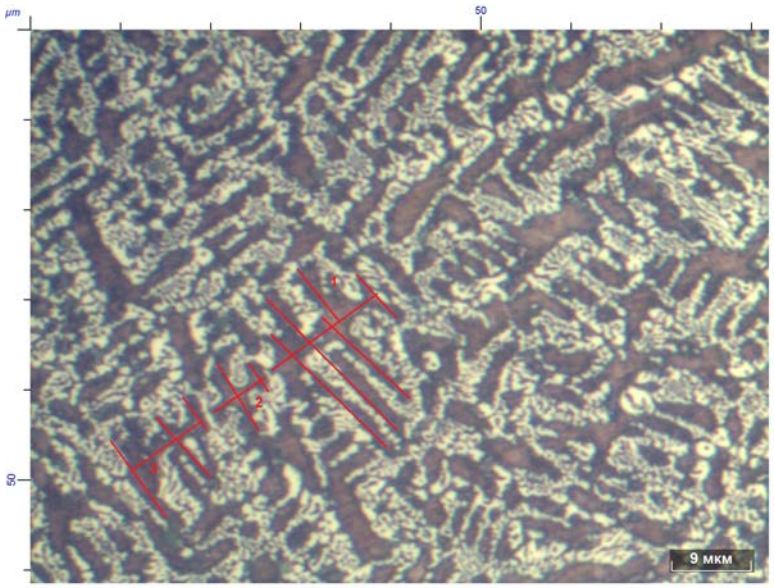

Figure 5.8: Dendrites' analysis of the sample number 5-W

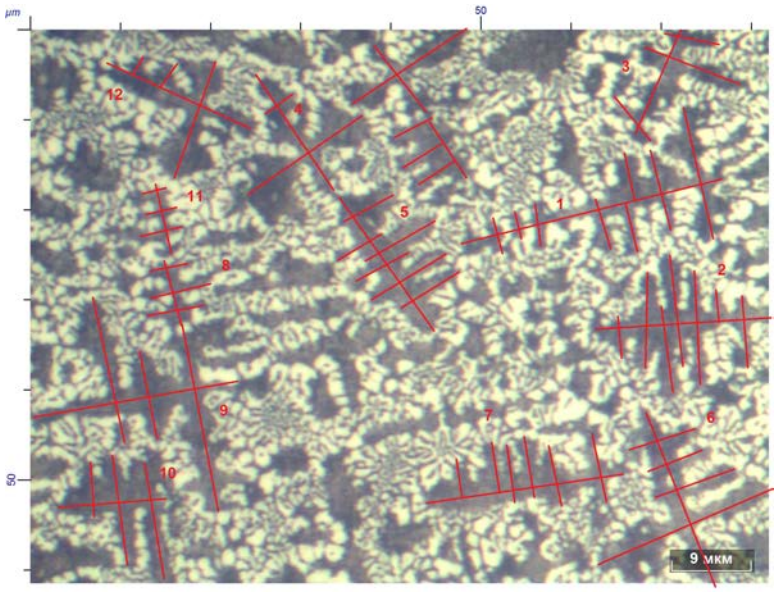

Figure 5.9: Dendrites' analysis of the sample number 6-W

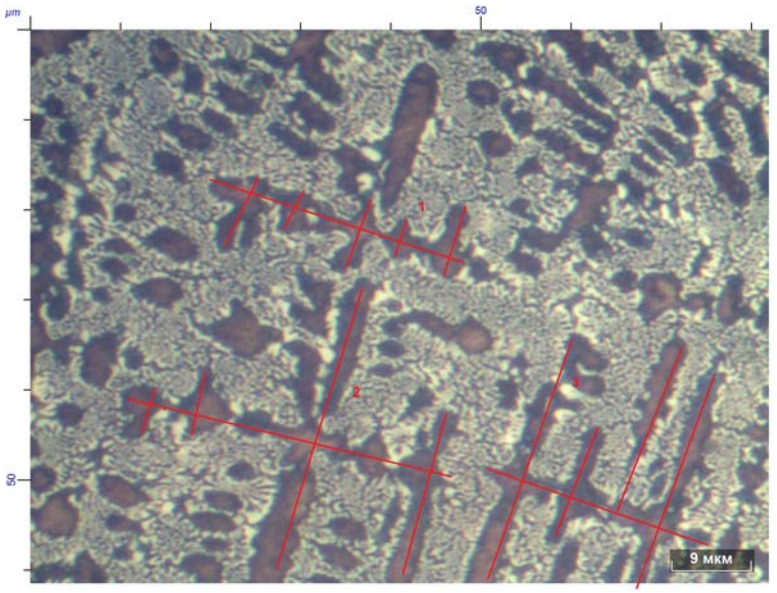

Figure 5.10: Dendrites' analysis of the sample number 7-W

Sample	Average dendrite first axe length (µm)	Average secondary arm length µm	SDAS (µm)	Dispersion (µm⁻1)
5-W	10.41	5.18	3.48	0.28
6-W	16.61	4.42	3.08	0.33
7-W	32.42	7.37	7.18	0.14

Table 5.9: Dispersion investigations

It is observed that sample number 7 has the lowest dispersion and the dendrites of greater dimensions compared to the other samples.

5.1.4 Hardness test on new cast irons

In order to have a greater certainty regarding the validity of the mathematical models, the hardness of the samples obtained thanks to the model for wear resistance has been studied. As was done for the eight initial samples, the hardness has been measured according to what described in chapter 2 in the subsection 2.6.1 and then the values have been compared with those predicted using the model constructed using the appropriate composition values.

Sample	Measure 1	Measure 2	Measure 3	Measure 4	Average value HRC_a
5-W	50.4	51.1	50.46	51.5	50.9
6-W	50.3	48.4	49.40	48.5	49.2
7-W	50.0	47.8	49.90	48.1	49.0

Table 5.10: Hardness test results (HRC) on samples coming from Wear model

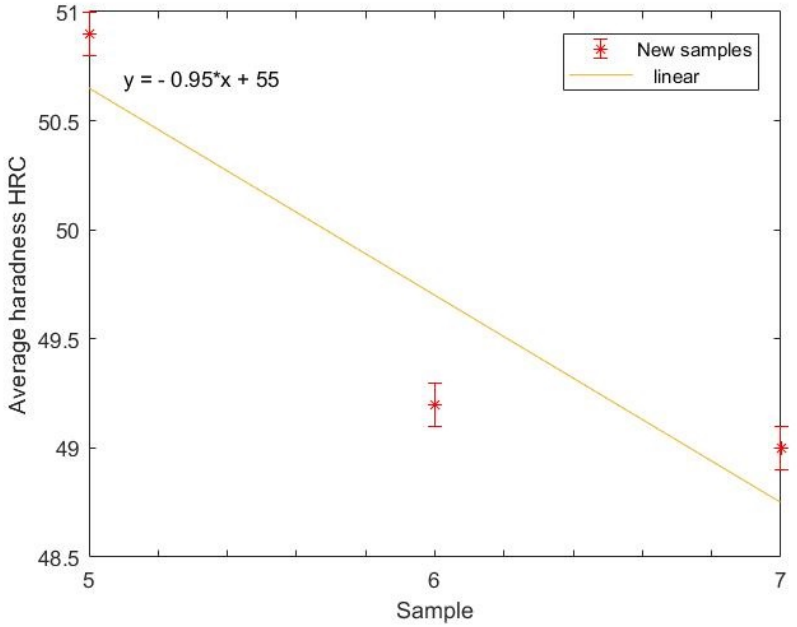

Figure 5.11: Average Hardness (HRC) of the new samples

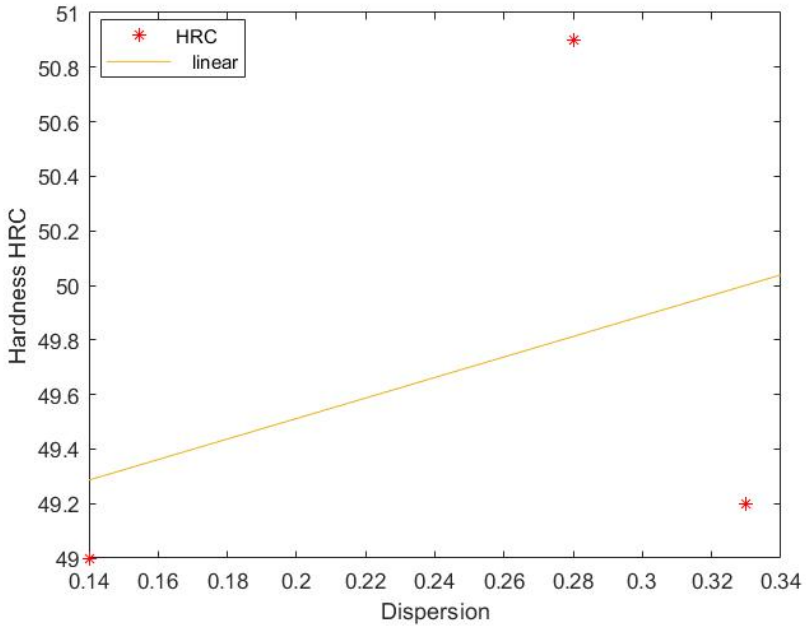

Figure 5.12: Relationship between dispersion and HRC

Sample	Practical Value of HRC	Difference between theoretical and practical value (%)
5-W	50.9	4.52
6-W	49.2	0.61
7-W	49.0	0.2

Table 5.11: Comparison between practice and theory on samples coming from Wear model

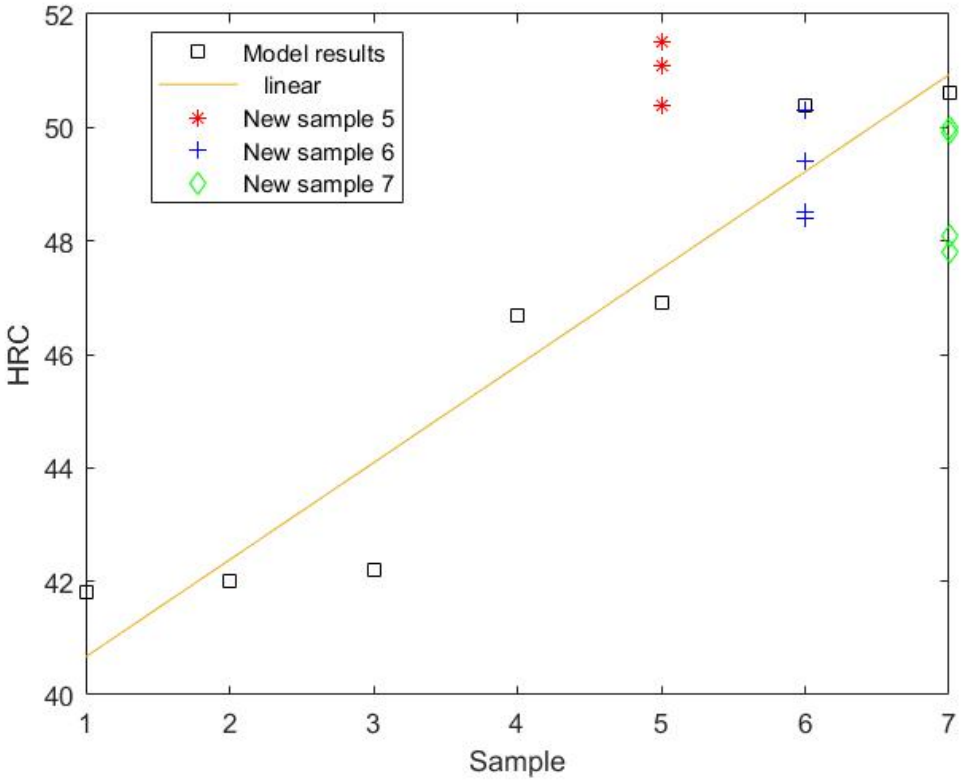

Figure 5.13: Difference between real and Theoretical values of HRC on sample from Wear model

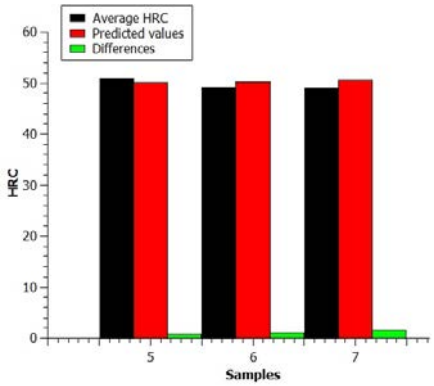

Figure 5.14: Difference between real and Theoretical values of HRC on sample from Wear model

5.1.5 Comment and considerations

The HRC hardness values measured in the three samples are very close to each other, perhaps underlining the fact that the difference in the content of the alloy elements maybe is not such as to make appreciable significant differences. The values are very similar to those found in samples of similar compositions studied in the first part of the work for the construction of the mathematical model and therefore in line with the expected. It is necessary, at the end, to consider an error component linked to the experiment. It is possible to observe that the performances offered by the cast iron are very close to those offered by the cast iron on the market, however, with a lower content of very expensive alloy elements such as vanadium and niobium. Furthermore, it must be taken into account that very high hardness is reached with niobium and vanadium but the wear resistance for hardness values of 60 HRC is low.

5.1.6 Wear test on new cast irons

Sample	m_1 (g)	m_2 (g)	m_3 (g)	m_4 (g)
5-W	37.0683	36.9958	36.9118	36.8463
6-W	37.7295	37.6598	37.5870	37.5132
7-W	35.7878	35.7147	35.6481	35.5846

Table 5.12: New sample's mass after each treatment (from Wear model)

Sample	Δ_{m_1} (g)	Δ_{m_2} (g)	Δ_{m_3} (g)	Average value Δ_{m_as} (g)
5-W	0.0725	0.0760	0.0725	0.0737
6-W	0.0697	0.0708	0.0738	0.0721
7-W	0.0728	0.0669	0.0635	0.0677

Table 5.13: Mass difference of the new samples from Wear model between two treatments

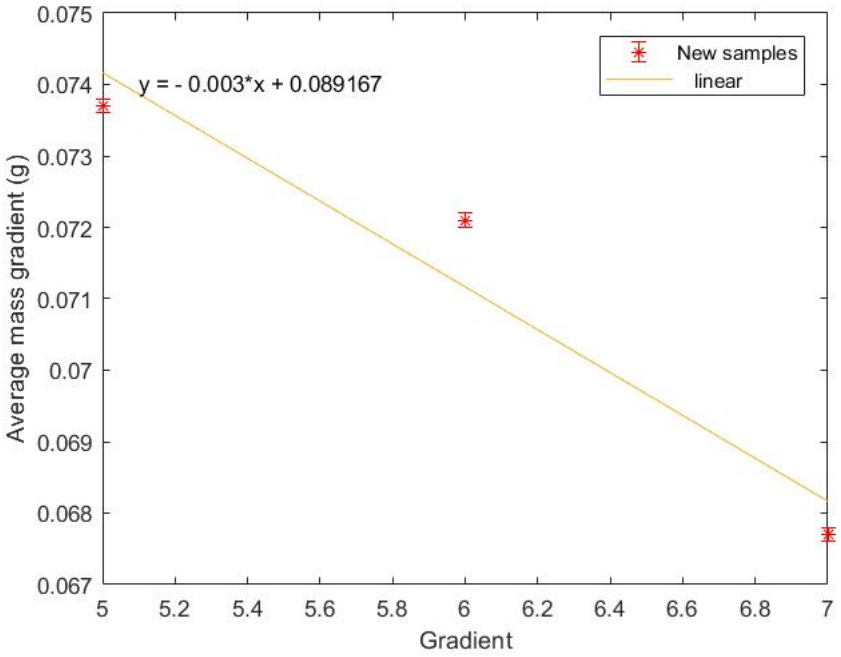

Figure 5.15: Average mass loss for the new samples

Results related to the standard sample:

Sample	m_1 (g)	m_2 (g)	m_3 (g)	m_4 (g)
Reference	71.7566	71.6065	71.4486	71.3504

Table 5.14: Mass of the reference after each treatment

Sample	Δ_{m_1} (g)	Δ_{m_2} (g)	Δ_{m_3} (g)	Average value Δ_{m_ar} (g)
Reference	0.1501	0.1579	0.0982	0.1354

Table 5.15: Mass difference of the standard sample between two treatments

Using the formula 2.10 it was possible to calculate the values of the coefficient for wear resistance which are reported in the table 5.16.

Sample	K_{i1}	K_{i2}	K_{i3}	$\bar{K_i}$	Difference with standard (%)
5-W	1.87	1.78	1.87	1.84	83.89
6-W	1.94	1.86	1.82	1.88	87.90
7-W	1.87	2.02	2.13	2.01	100.53

Table 5.16: Results of the calculations from wear model samples

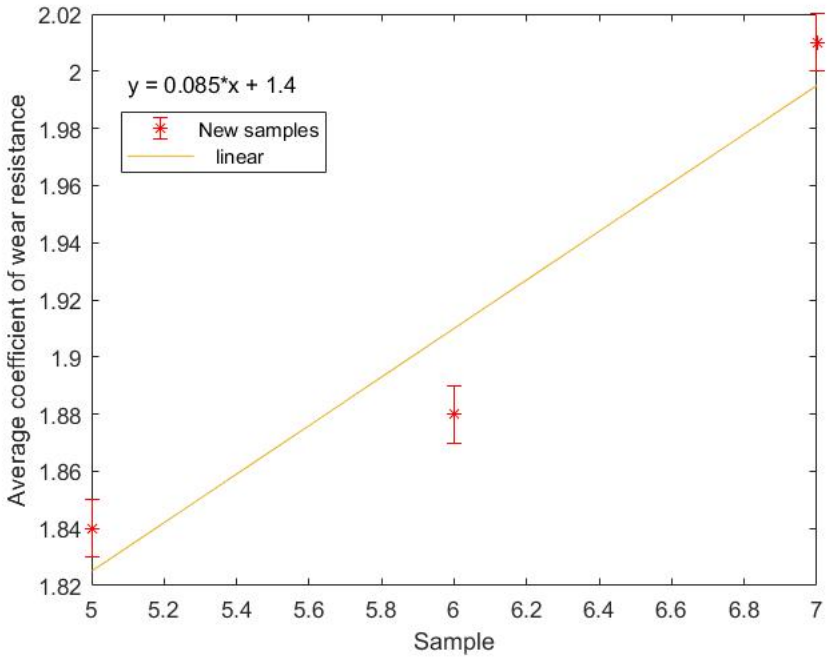

Figure 5.16: K_i values for the new samples from Wear model

Sample	Practical Value of K_i	Difference between theoretical and practical value (%)
5-W	1.84	37.86
6-W	1.88	0.00
7-W	2.01	4.99

Table 5.17: Comparison between practice and theory on sample from Wear model

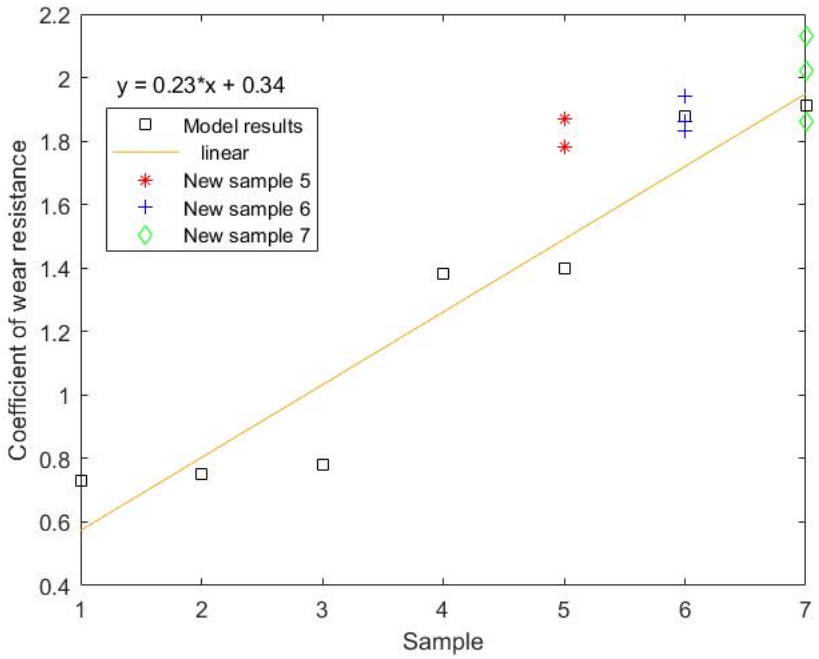

Figure 5.17: Difference between real and theoretical values of K_i from Wear model

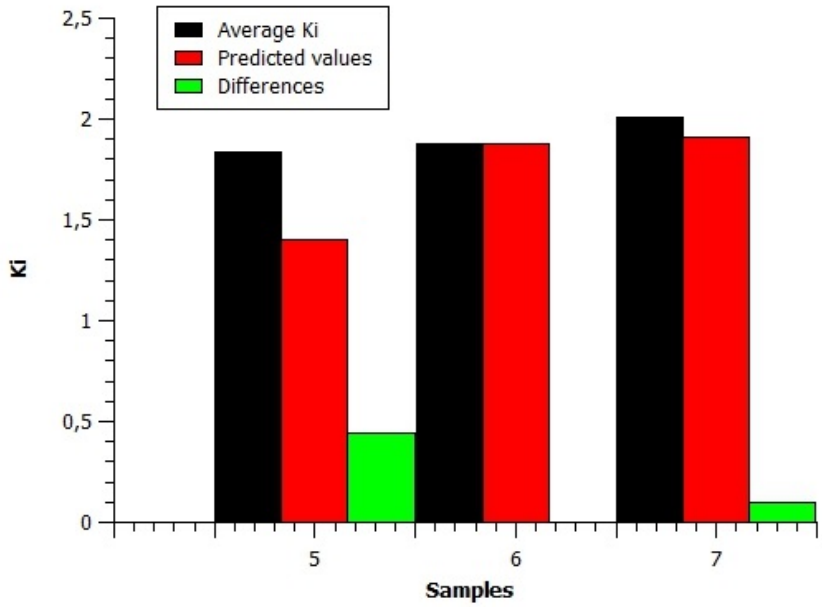

Figure 5.18: Difference between real and theoretical values of K_i from Wear model

Comments and considerations

Samples from Wear Resistance Model:

It is observed that the values obtained with the model are not exactly equal to experimental values, in particular they are lower, especially in the case of samples 5-W and 7-W. Moreover in the case of sample 7-W the values differ only by 5%, finally, in the case of sample 6-W, the difference between the average and the predicted coefficients coincides. The model predicts that values of the wear resistance coefficients for the three samples that differ significantly, while the experimental data were close to each other, perhaps because from a practical point of view these differences in the contents of the alloy elements are not significant and able to highlight big differences. What is important is that it is possible to observe a growth as predicted by the model to increase the content of alloy elements such as carbon, manganese and chromium and to decrease nickel and titanium. As it happened for the hardness there is the influence of the unwanted alloy elements or non metallic inclusions and the error component in the production of the samples and in the execution of the experiment. It is also important to consider the fact that the composition did not coincide exactly with that obtained with the model obtained, since in the ferro-alloys there are unwanted alloy elements such as phosphorus and sulfur which could alter the real properties of the metal, that are not included in the model, but that are certainly harmful for the metal and the

performances. However, the fact that the value of the wear resistance coefficient measured is higher than that foreseen by the model can be considered positive. The values of wear resistance coefficient found are to be considered very high for these alloys, which makes them competitive with those on the market.

5.1.6.1 Surface analysis

In order to understand whether the phenomenon of wear that occurs during the test with the abrasive, necessary for the evaluation of the wear resistance of the material, is abrasive or adhesive, an analysis of the worn surface has been carried out through stereo microscope.

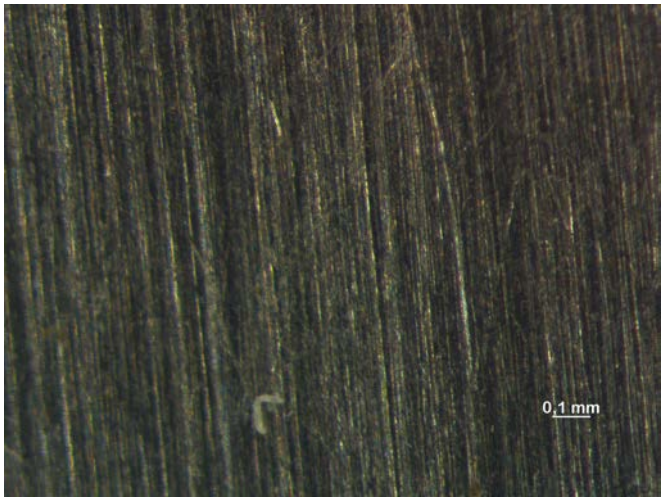

Figure 5.19: Sample 5-W

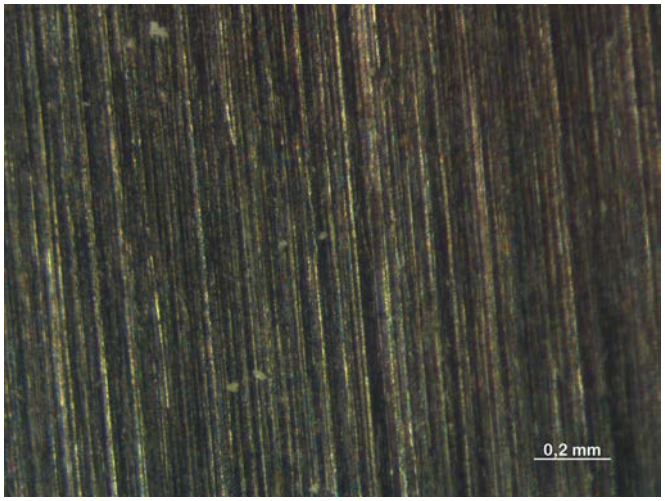

Figure 5.20: Sample 6-W

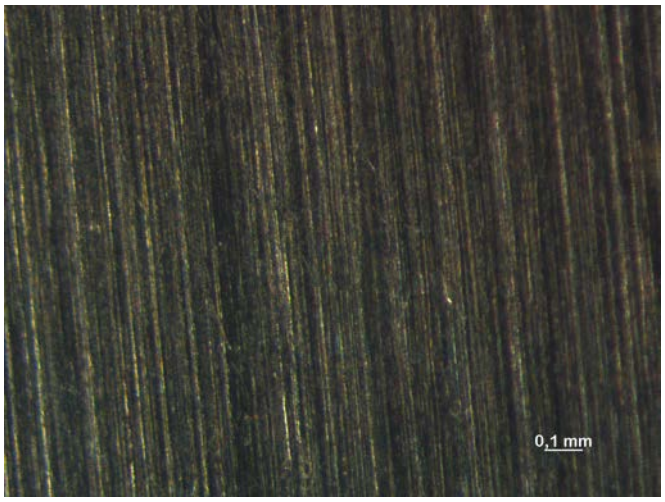

Figure 5.21: Sample 7-W

On the surface of the material there is no evidence of abrasive powder particles, this is an indication that there is no adhesion between the powder particles and the metal and therefore the process is an abrasive and non-adhesive wear.

5.2 Cast irons from hardness HRC model

5.2.1 Compositions and properties of cast irons from HRC optimization

Composition	Fe (%)	C (%)	Mn (%)	Cr (%)	Ni (%)	Ti (%)
5-H	balance	2.05	4.23	18.00	0.60	0.49
6-H	balance	2.06	4.33	18.50	0.54	0.49
7-H	balance	2.07	4.44	19.00	0.48	0.48

Table 5.18: Investigated composition

Sample	Theoretical value of K_i	Theoretical value of HRC
5-H	1.41	46.9
6-H	1.68	50.4
7-H	1.71	50.6

Table 5.19: Theoretical value of the properties

The theoretical values were calculated using the two models built in the previous chapter.

5.2.2 Samples' preparation

In this section are presented the calculations carried out for the determination of the charge for the preparation of the cast iron samples, which were necessary to test the mathematical model that had been built in the previous sections, to optimize the chemical composition. The ferroalloys and the scraps used were those presented in the chapter 2 to the section 2.2, in particular:

- Cast iron scrap;
- S255;
- Ti-CP;

- FCH260;

- FSN260;

- Metallic nickel.

The ferroalloys, iron and steel scrap used come from the DUEDI SRL company and Pometon SPA company.

The difference between the optimized theoretical composition and the real one is due to some elements such as silicon, phosphorus and sulfur which derive from the ferroalloys used in the charge. But how were they obtained? In the following pages there are the systems containing the mass balances and the boundary condition that must be respected.

$$\begin{cases} (1-\frac{8}{100})[Fe-Cr]\frac{69.3}{100} = 18.00 \\ [Ni]\frac{99.9}{100} = 0.60 \\ (1-\frac{10}{100})\left\{[Fe-Si-Mn]\frac{66.9}{100} + [SS]\frac{1.6}{100}\right\} = 4.23 \\ (1-\frac{50}{100})[Ti-CP]\frac{99.1}{100} = 0.49 \\ (1-\frac{35}{100})\left\{[Fe-Cr]\frac{6.72}{100} + [Fe-Si-Mn]\frac{1.4}{100} + \right. \\ \left.[SS]\frac{0.2}{100} + [PI]\frac{3}{100}\right\} = 2.05 \\ [Fe-Cr] + [Ni] + [Fe-Mn] + [Ti-CP] + [SS] + [PI] = 100 \end{cases} \tag{5.4}$$

$$\begin{cases} (1-\frac{8}{100})[Fe-Cr]\frac{69.3}{100} = 18.50 \\ [Ni]\frac{99.9}{100} = 0.54 \\ (1-\frac{10}{100})\left\{[Fe-Si-Mn]\frac{66.9}{100} + [SS]\frac{1.6}{100}\right\} = 4.33 \\ (1-\frac{50}{100})[Ti-CP]\frac{99.1}{100} = 0.49 \\ (1-\frac{35}{100})\left\{[Fe-Cr]\frac{6.72}{100} + [Fe-Si-Mn]\frac{1.4}{100} + \right. \\ \left.[SS]\frac{}{100} + [PI]\frac{3}{100}\right\} = 2.06 \\ [Fe-Cr] + [Ni] + [Fe-Si-Mn] + [Ti-CP] + [SS] + [PI] = 100 \end{cases} \tag{5.5}$$

$$\begin{cases} (1-\frac{8}{100})[Fe-Cr]\frac{69.3}{100} = 19.00 \\ [Ni]\frac{99.9}{100} = 0.48 \\ (1-\frac{10}{100})\left\{[Fe-Si-Mn]\frac{66.9}{100} + [SS]\frac{1.6}{100} + [PI]\frac{}{100}\right\} = 4.44 \\ (1-\frac{50}{100})[Ti-CP]\frac{99.1}{100} = 0.48 \\ (1-\frac{35}{100})\left\{[Fe-Cr]\frac{}{100} + [Fe-Si-Mn]\frac{1.4}{100} + \right. \\ \left.[SS]\frac{6.72}{100} + [PI]\frac{3}{100}\right\} = 2.07 \\ [Fe-Cr] + [Ni] + [Fe-Si-Mn] + [Ti-CP] + [SS] + [PI] = 100 \end{cases} \tag{5.6}$$

Type of ferroalloy	Used amount (%)	Used amount (g)
Ferrochromium [Fe-Cr]	28.23	28.23
Metallic Nickel [Ni]	0.60	0.60
Ferromanganese [Fe-Si-Mn]	6.22	6.22
Ferrotitanium [Ti-CP]	0.99	0.99
Steel Scrap [SS]	26.96	26.96
Pig Iron [Pi]	37.00	37.00
Element	Loss due to oxidation of the elements (%)	
C	35.00	
Mn	10.00	
Cr	8.00	
Ni	0.00	
Ti	50.00	
Si	50.00	
P	25.00	
S	45.00	
Element	Final mass of each elements (g)	
Fe	balance	
C	2.05	
Mn	4.23	
Cr	18.00	
Ni	0.60	
Ti	0.48	
Si	0.49	
P	0.03	
S	0.02	
Element	Final Concentration (%)	
Fe	balance	
C	2.05	
Mn	4.23	
Cr	18.00	
Ni	0.60	
Ti	0.49	
Si	0.49	
P	0.03	
S	0.02	

The following tables show the results related to the production of 100 g of material

Table 5.20: Charge of sample 5-H

Type of ferroalloy	Used amount (%)	Used amount (g)
Ferrochromium [Fe-Cr]	29.01	29.01
Metallic Nickel [Ni]	0.54	0.54
Ferromanganese [Fe-Si-Mn]	6.40	6.40
Ferrotitanium [Ti-CP]	0.99	0.99
Steel Scrap [SS]	27.06	27.06
Pig Iron [Pi]	36.00	36.00
Element	Loss due to oxidation of the elements (%)	
C	35.00	
Mn	10.00	
Cr	8.00	
Ni	0.00	
Ti	50.00	
Si	50.00	
P	25.00	
S	45.00	
Element	Final mass of each elements (g)	
C	2.06	
Mn	4.33	
Cr	18.50	
Ni	0.554	
Ti	0.49	
Si	0.50	
P	0.09	
S	0.02	
Element	Final Concentration (%)	
Fe	balance	
C	2.070	
Mn	4.33	
Cr	18.50	
Ni	0.54	
Ti	0.49	
Si	0.50	
P	0.09	
S	0.02	

The following tables show the results related to the production of 100 g of material

Table 5.21: Charge of sample 6-H

Type of ferroalloy	Used amount (%)	Used amount (g)
Ferrochromium [Fe-Cr]	29.80	29.80
Metallic Nickel [Ni]	0.48	0.48
Ferromanganese [Fe-Si-Mn]	6.57	6.57
Ferrotitanium [Ti-CP]	0.97	0.97
Steel Scrap [SS]	27.18	27.18
Pig Iron [Pi]	35.00	35.00
Element	Loss due to oxidation of the elements (%)	
C	35.00	
Mn	10.00	
Cr	8.00	
Ni	0.00	
Ti	50.00	
Si	50.00	
P	25.00	
S	45.00	
Element	Final mass of each elements (g)	
Fe	balance	
C	2.08	
Mn	4.44	
Cr	19.00	
Ni	0.48	
Ti	0.48	
Si	0.51	
P	0.09	
S	0.02	
Element	Final Concentration (%)	
Fe	balance	
C	2.50	
Mn	4.44	
Cr	19.00	
Ni	0.48	
Ti	0.48	
Si	0.51	
P	0.09	
S	0.02	

The following tables show the results related to the production of 100 g of material

Table 5.22: Charge of sample 7-H

In the final calculation there are also the silicon, phosphorus and sulfur contents, which are not present in the built model, but which are important for the cast iron having a major impact on the properties of the material.

For the compositions 5 and 6 two samples were produced, which were cast in different molds, one in ceramic material and the other in sand-resin. The samples cast in the latter type of molds are shown in the tables with an asterisk (*).

5.2.3 Results of metallurgical characterization of new cast irons

5.2.3.1 Real cast irons compositions

Composition	Fe (%)	C (%)	Mn (%)	Cr (%)	Ni (%)	Ti (%)
5-H 5-H*	48.01	-	3.50	25.00	0.10	0.36
6-H 6-H*	66.69	-	4.56	22.30	0.10	0.43
7-H	68.37	-	3.12	22.50	0.10	0.29

Table 5.23: Investigated composition

Comments and considerations

Carbon was not detected because the samples were examined through EDS analysis. It is possible to observe differences between the expected compositions and the real ones due to some problems during metal melting and sample preparation.

5.2.3.2 Micrographs

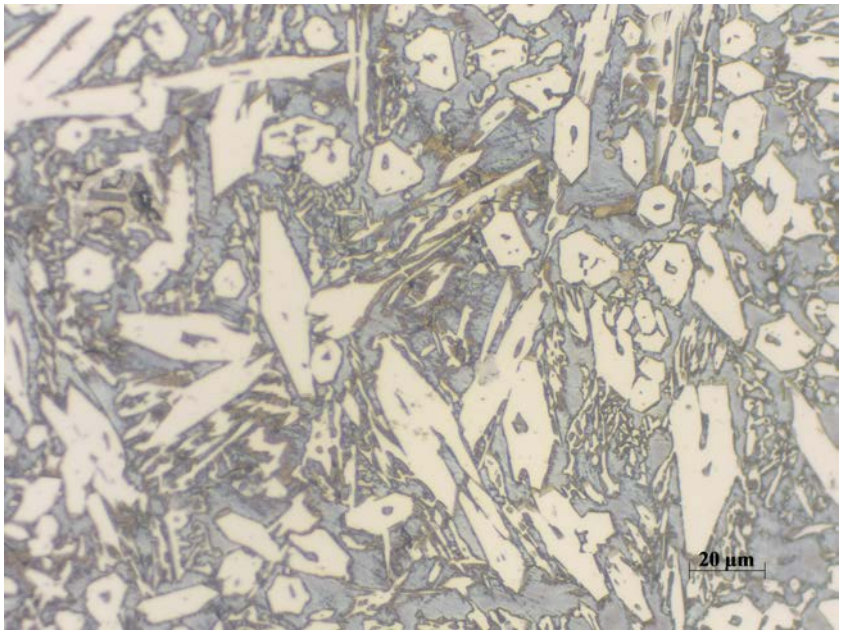

Figure 5.22: Microstructure sample 5-H 500x cast in ceramic mold

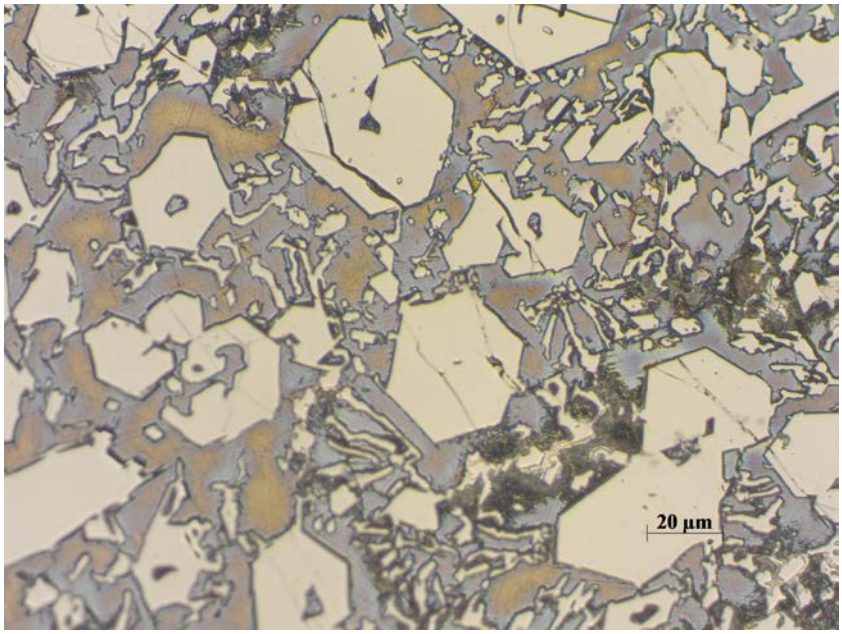

Figure 5.23: Microstructure sample 5-H 500x cast in sand-resin mold

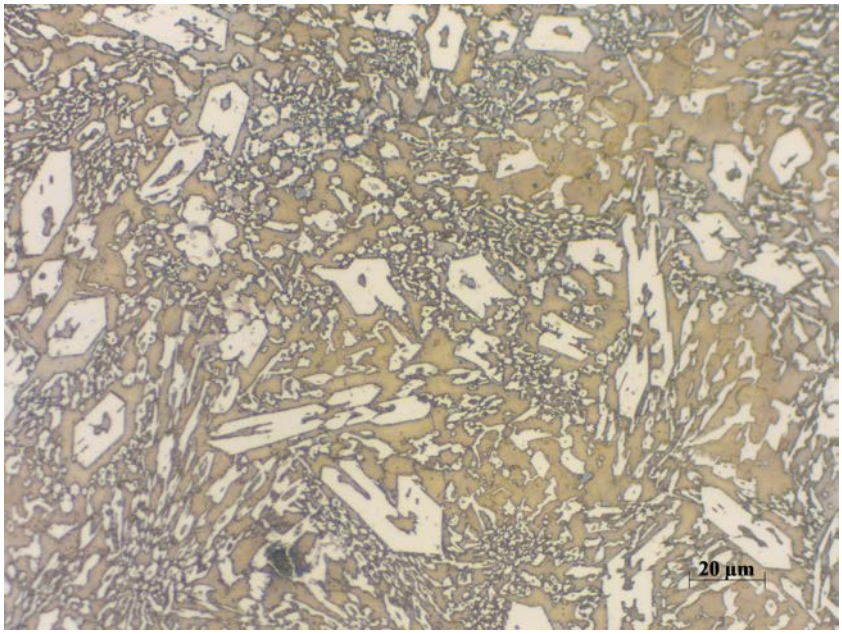

Figure 5.24: Microstructure sample 6-H 500x cast in ceramic mold

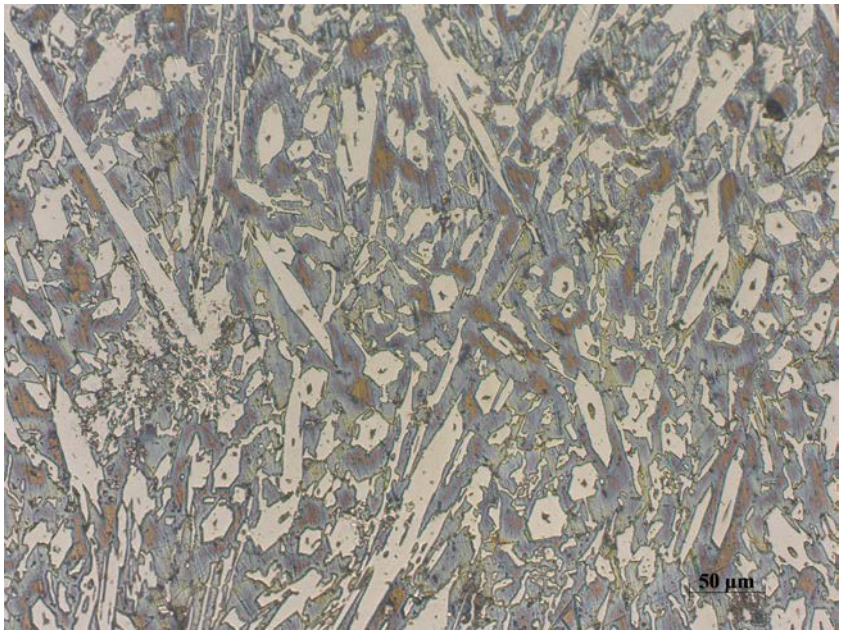

Figure 5.25: Microstructure sample 6-H 200x cast in sand-resin mold

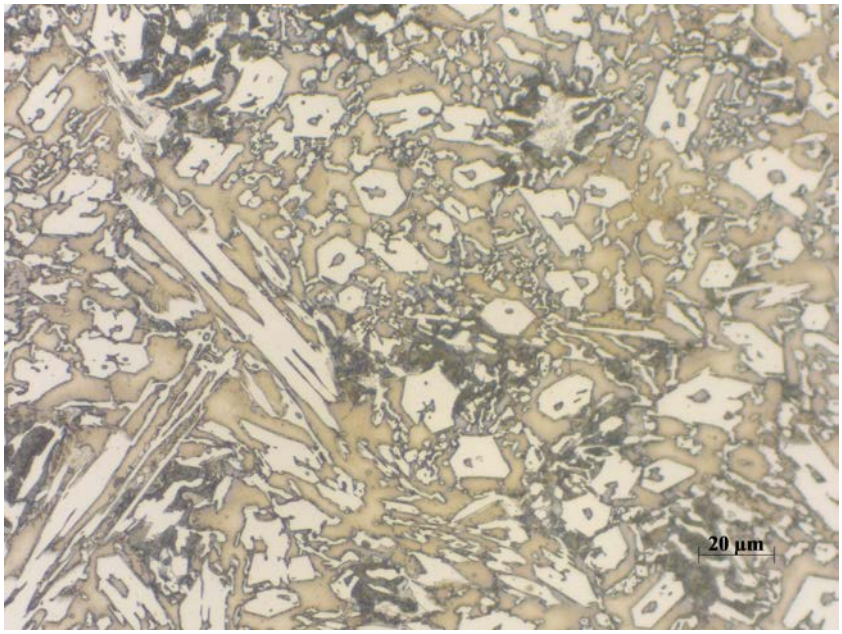

Figure 5.26: Microstructure sample 7-H 500x cast in ceramic mold

Comments and considerations

The microstructure of the produced samples appears different compared to that obtained after the casting of the other samples, in fact there is no presence of austenite dendrites and interdendritic carbides. The carbides in this case are very small and in the form of polygons (hexagons), very small and homogeneously distributed over the whole section of the samples. It is also possible to find the presence of carbides in the form of lamellas. Ledeburite is also found in the specimens. The different microstructure of the solidified material could be due to the different conditions and environment of solidification during the melting of the raw materials used. The samples in fact were not cast in sand like all the previous ones but in molds of ceramic or sand-resin material. No differences are observed between the microstructures of solidified samples in molds of ceramic material and those of the samples cast in sand-resin molds.

5.2.4 Quantitative analysis

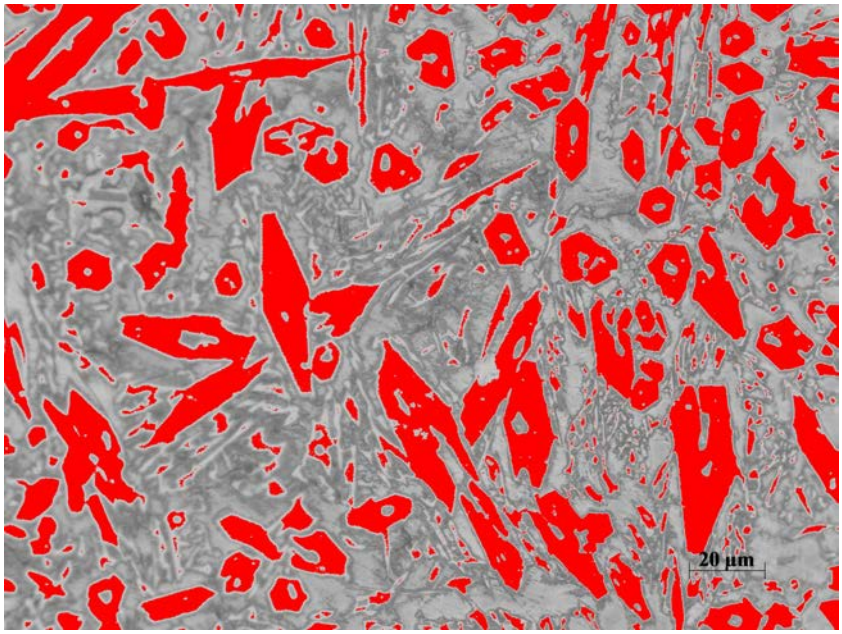

Figure 5.27: Quantitative analysis of the sample number 5-H cast in ceramic mold

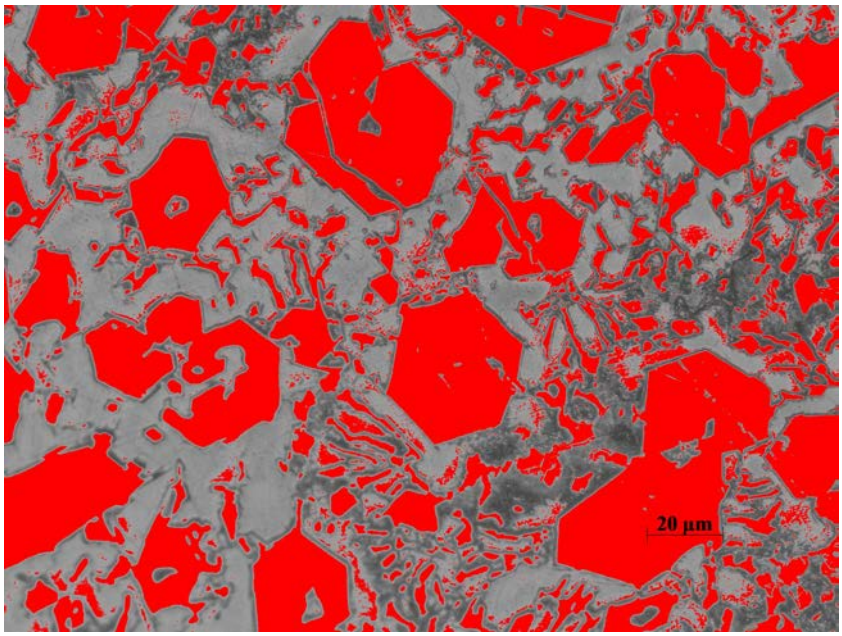

Figure 5.28: Quantitative analysis of the sample number 5-H cast in sand-resin mold

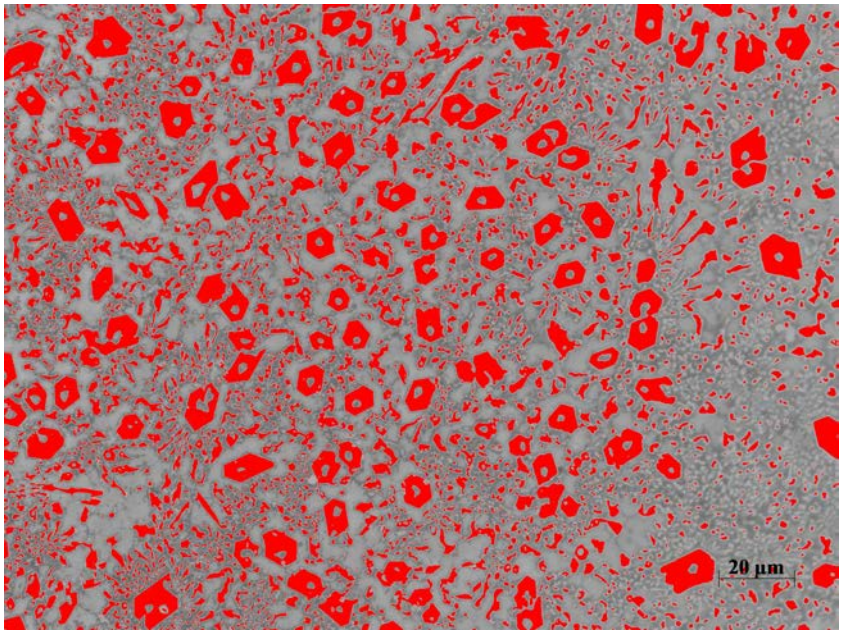

Figure 5.29: Quantitative analysis of the sample number 6-H cast in ceramic mold

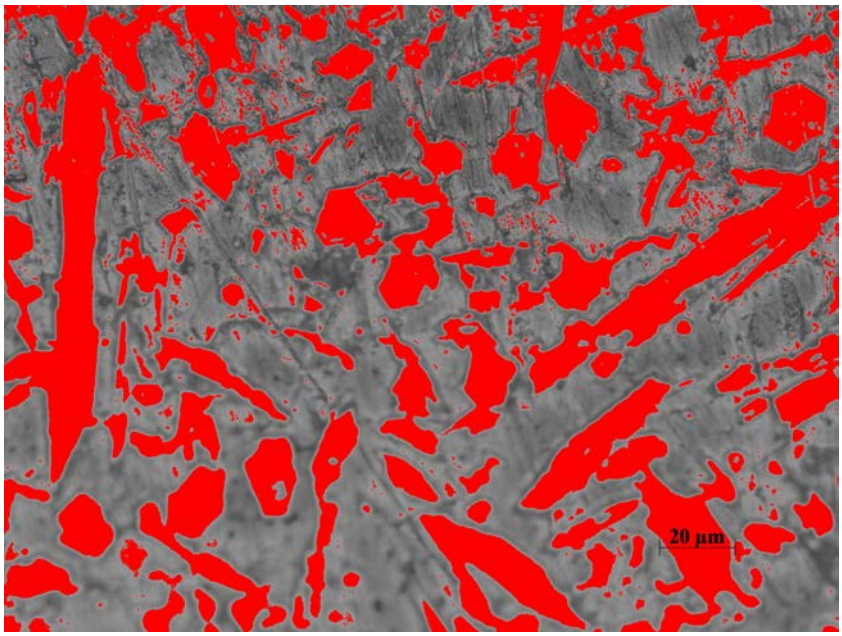

Figure 5.30: Quantitative analysis of the sample number 6-H cast in sand-resin mold

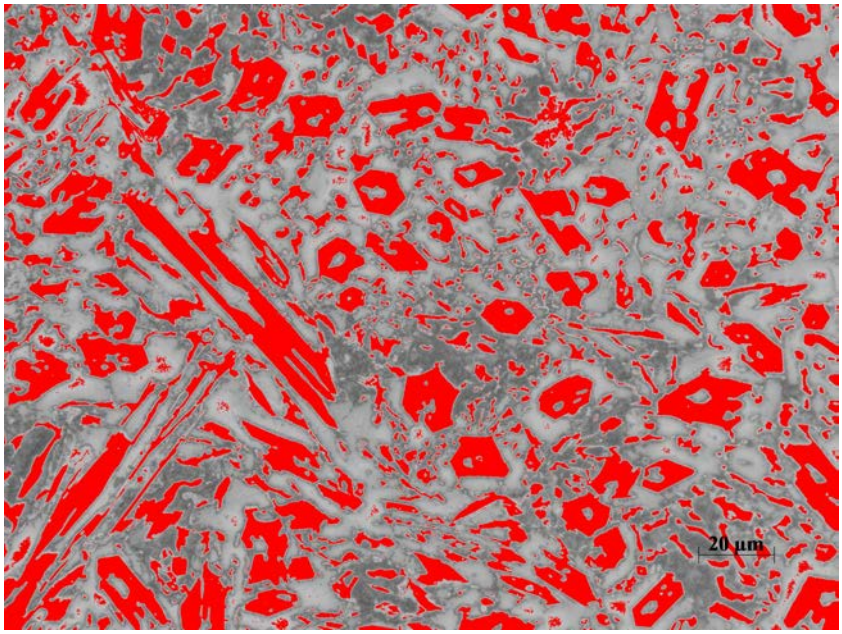

Figure 5.31: Quantitative analysis of the sample number 7-H cast in ceramic mold

Sample	Carbide phase (%)	Metal matrix (%)
5-H	27.17	72.83
5-H*	43.82	56.18
6-H	24.32	75.68
6-H*	34.91	65.19
7-H	29.51	70.49

* Indicates that the sample were cast in the sand-resin mold

Table 5.24: Phase quantity evaluation

Larger carbide particles are observed in the samples cooled in sand-resin molds.

5.2.5 Hardness test on new cast irons

Sample	Measure 1	Measure 2	Measure 3	Measure 4	Average value HRC_a
5-H	53.6	58.0	58.3	58.7	57.2
5-H*	50.3	46.1	51.6	53.1	50.3
6-H	55.2	55.9	57.9	59.7	57.2
6-H*	53.0	42.4	50.9	51.0	49.8
7-H	54.6	60.6	59.6	59.4	58.6

Table 5.25: Hardness test results (HRC) on samples coming from HRC model

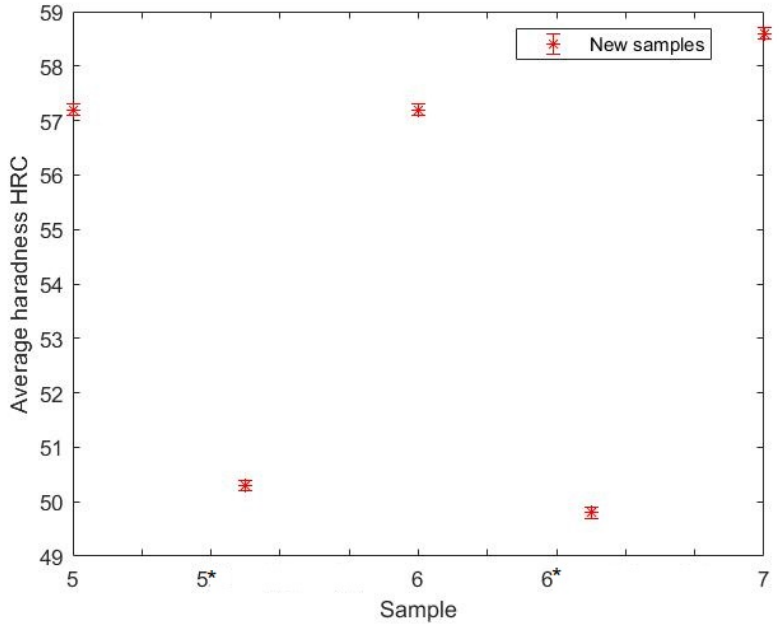

Figure 5.32: Average HRC of the new samples coming from the HRC model

Sample	Practical Value of HRC	Difference between theoretical and practical value (%)
5-H	57.2	19.46
5-H*	50.3	4.14
6-H	57.2	13.50
6-H*	49.8	1.19
7-H	58.6	15.81

Table 5.26: Comparison between practice and theory on samples coming from HRC model

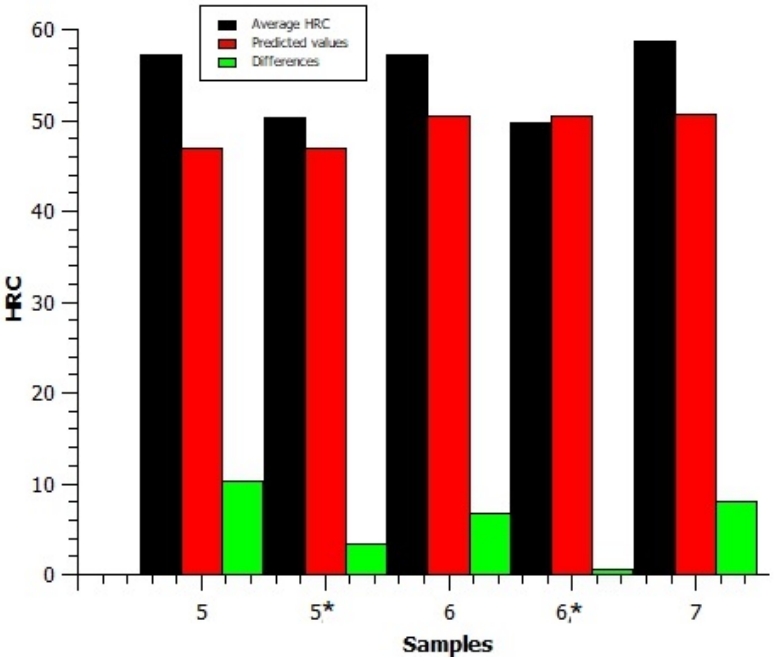

Figure 5.33: Difference between real and Theoretical values of HRC on sample from HRC model

Samples from HRC Hardness Model:
Obviously the samples have different properties from those expected initially given the composition and the different solidification conditions and in particular they are higher. In addition to the composition it could be due to how the samples were poured, since there is a significant difference between the properties of the samples cast in a ceramic mold and those cast in sand-resin, which have lower properties.

The expected results of the model for these compositions have therefore been compared with the measured results and there are small but acceptable differences.. The results must be taken with caution because the chrome exceeds the range in which the model was built and the cooling system are different.

Sample	Theoretical Value of HRC	Practical Value of HRC	Difference between values (%)
5-H	55.9	57.2	2.32
6-H	55.8	57.2	2.51
7-H	55.4	58.6	2.88

Table 5.27: Comparison between predicted value and the real

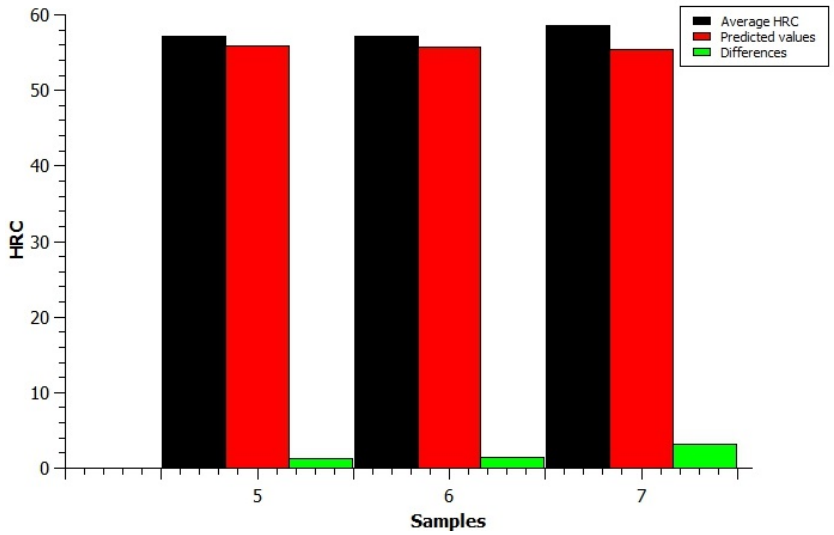

Figure 5.34: Comparison between real and Theoretical values

5.3 Economical considerations

The cost of the alloys obtained has been evaluated taking into account the price of the raw materials used, neglecting the energetic resources necessary to obtain the alloys. Only the starting cast irons, used for building the models, and those obtained from the model for wear resistance were considered, since they are the only ones of which all the data were available. The study of wear resistance on

the cast irons obtained from the hardness model was not possible, because of the absence of the instrument and the problems occurred.

Ferroalloy	Price ($/kg)
Cast iron P1	0.13
1A steel scrap	0.22
Iron armco	2.13
Ferrotitanium FeTi 32	1.93
Ferrochromium FeA850	1.71
Ferromanganese FeMn 70	1.13
Metallic nickel	13.06

Table 5.28: Cost of raw materials

Ferroalloy	Price of the alloy ($/kg)	Density (kg/m^3)	Cost per unit volume ($/m^3)
5-W	0.842	7.8	1.080×10^{-4}
6-W	0.848	7.8	1.088×10^{-4}
7-W	0.854	7.8	1.095×10^{-4}
A	0.777	7.8	9.967×10^{-5}
B	0.728	7.8	9.335×10^{-5}
C	0.773	7.8	9.912×10^{-5}
D	0.836	7.8	1.072×10^{-4}
E	0.933	7.8	1.196×10^{-4}
F	0.798	7.8	1.023×10^{-4}
G	0.834	7.8	1.096×10^{-4}
H	0.944	7.8	1.210×10^{-4}
Maximum	0.854		1.210×10^{-4}

Table 5.29: Cost of the alloy

5.3.1 Material selection

The identification of different white cast irons that differ in terms of composition, cost, hardness and wear resistance coefficients opened the door to material selection reasoning. The materials studied are cast iron typically used for components such as pumps, molds that must guarantee a high resistance to wear,

hardness, limited costs, so there are three properties, two of which must be maximized and a third that must be minimized. Since there were a number of properties to be maximized in this problem, higher than that of the quantities to be minimized, it was better to construct a performance function. In addition, the costs were processed using the cost per unit of volume and were included in the function Z without using the figures of merit. The overall performance in this case was:

$$Z_i = \pi_{iHRC} HRC_n + \pi_{iK_i} K_{in} + \pi_{iC_v} C_{vn} \tag{5.7}$$

Here the compositions of the materials, investigated, as an example of a material selection during the research, are presented. However, only the initial starting alloys for the construction of the model and those produced thanks to the wear resistance model have been studied. It was not possible to measure the wear resistance coefficient for alloys obtained from the hardness model due to lack of equipment. The eight initial alloys were renamed in this section using letters to distinguish them from those obtained with the mathematical model.

Composition	Fe (%)	C (%)	Mn (%)	Cr (%)	Ni (%)	Ti (%)
5-W	balance	2.19	3.84	18.00	0.61	0.49
6-W	balance	2.23	3.87	18.50	0.55	0.48
7-W	balance	2.27	3.90	19.00	0.49	0.48
A	balance	1.90	3.50	15.00	1.00	0.20
B	balance	2.50	3.50	15.00	0.40	0.60
C	balance	1.90	5.00	15.00	0.40	0.60
D	balance	2.50	5.00	15.00	1.00	0.20
E	balance	1.90	3.50	19.00	1.00	0.60
F	balance	2.50	3.50	19.00	0.40	0.20
G	balance	1.90	5.00	19.00	0.40	0.20
H	balance	2.50	5.00	19.00	1.00	0.60

Table 5.30: Investigated composition

In the following table are summarized the properties of the investigated alloys:

Name of the material	Properties		
	HRC	K_i	C_v
5-W	50.9	1.84	1.080×10^{-4}
6-W	49.2	1.88	1.088×10^{-4}
7-W	49.0	2.01	1.095×10^{-4}
A	42.3	1.32	9.967×10^{-5}
B	45.2	1.28	9.335×10^{-5}
C	44.9	1.18	9.912×10^{-5}
D	46.2	1.13	1.072×10^{-4}
E	46.9	0.97	1.196×10^{-4}
F	50.4	2.28	1.023×10^{-4}
G	53.7	2.25	1.069×10^{-4}
H	46.9	2.03	1.210×10^{-4}

Table 5.31: Materials subject to material selection

This last properties' table presents the normalized properties and the reference values for each properties:

Sample	HRC_{max}	K_{imax}	C_{vmin}	HRC_n	K_{in}	C_{vn}
5-W				0.948	0.846	0.864
6-W				0.9161	0.824	0.858
7-W				0.912	0.882	0.853
A				0.788	0.579	0.937
B				0.842	0.561	1
C	53.7	2.28	9.335×10^{-5}	0.836	0.518	0.942
D				0.860	0.496	0.871
E				0.873	0.425	0.780
F				0.938	1	0.913
G				1	0.986	0.873
H				0.873	0.890	0.772

Table 5.32: Normalization of the properties

With the following tables and equations the material selection is performed, evaluating the behaviour of the properties, the relationships between each properties and the calculations of the weight factors and the performance functions.

Properties	Behaviuor
K_i	must be mazimized (↑)
HRC	must be mazimized (↑)
C_v	must be minimized (↓)

Table 5.33: Trend of the properties

Relationship between properties
Wear resistance > HRC
Wear reesistance > Cost per unit volume
HRC > Cost per unit volume

Table 5.34: Relationship between properties

Properties	1^{st} round		2^{nd} round
K_i	2	3	
HRC	1		2
C_v		1	1

Table 5.35: Comparison between properties

Properties	Individual score	Total score	Weight factor (π_i)
K_i	5	10	π_{Ki}=0.5
HRC	3		π_i=0.3
C_v	2		π_{Cv}=0.2
			Sum=1

Table 5.36: Weight factor

$$Z_{5-W} = 0.3HRC_n + 0.5K_{in} + 0.2C_{vn} = 0.880 \tag{5.8}$$

$$Z_{6-W} = 0.3HRC_n + 0.5K_{in} + 0.2C_{vn} = 1.147 \quad (5.9)$$

$$Z_{7-W} = 0.3HRC_n + 0.5K_{in} + 0.2C_{vn} = 1.194 \quad (5.10)$$

$$Z_A = 0.3HRC_n + 0.5K_{in} + 0.2C_{vn} = 0.916 \quad (5.11)$$

$$Z_B = 0.3HRC_n + 0.5K_{in} + 0.2C_{vn} = 0.930 \quad (5.12)$$

$$Z_C = 0.3HRC_n + 0.5K_{in} + 0.2C_{vn} = 0.879 \quad (5.13)$$

$$Z_D = 0.3HRC_n + 0.5K_{in} + 0.2C_{vn} = 0.854 \quad (5.14)$$

$$Z_E = 0.3HRC_n + 0.5K_{in} + 0.2C_{vn} = 0.780 \quad (5.15)$$

$$Z_F = 0.3HRC_n + 0.5K_{in} + 0.2C_{vn} = 1.314 \quad (5.16)$$

$$Z_G = 0.3HRC_n + 0.5K_{in} + 0.2C_{vn} = 1.313 \quad (5.17)$$

$$Z_H = 0.3HRC_n + 0.5K_{in} + 0.2C_{vn} = 1.173 \quad (5.18)$$

Material	Overall penalty function Z
5-W	0.880
6-W	1.147
7-W	1.194
A	0.916
B	0.930
C	0.879
D	0.854
E	0.780
F	1.314
G	1.313
H	1.173

Table 5.37: Results

5.3.2 Comments and considerations

The analysis indicates as best materials the alloys 7, F, G, as they represent the best compromise between high wear resistance, high hardness and low cost.

Chapter 6

ADDITIONAL STUDIES: INVESTIGATION OF THE EFFECT OF COOLING RATE ON THE CRYSTAL STRUCTURE OF THIN-WALL TUBES OF WHITE CAST IRON WITH NEW COMPOSITION

Currently in Russia, thanks to the presence of large sites belonging to the steel industry, such as the one located in the city that hosts the university in which this period of research was carried out, many studies are related to the field of metallurgy in order to improve manufacturing technologies and product characteristics. Among the issues that are being addressed there is the one connected to the manufacturing of metal pipes, with high mechanical performance and without joints, such as welding cords, which constitute the weak point under mechanical load. One of the methods that is being developed regards the use of organic glass tubes as molds in which, through a vacuum pump, the glass is cast and in which the metal solidifies. The use of these techniques is necessary to guarantee high solidification speeds, which in turn should guarantee equiaxed crystalline grain of reduced dimensions, resulting in high mechanical resistance properties and performance during operation, according to the Hall-Petch law:

$$\sigma_y = \sigma_0 + \frac{k_y}{\sqrt{d}} \tag{6.1}$$

σ_y is the Peierls stress, σ_0 is the yield stress, k_y is a materials constant and d is the diameter of the grains.

During this research, as a second part of the work, an analysis was carried out on this technique by analyzing the pipes made in the foundry laboratory of the MGTU university. Under a vacuum, liquid cast iron was injected into the tube, the cooling rate of the metal was about 50 °C/ sec. At the end of the cooling of the iron, the glass tube was broken, and a hollow sample was obtained from the inside with a clean surface. The cavity inside the tube is the result of metal shrinkage. During the experiment, it was possible to obtain hollow products of 12-15 mm with a wall thickness varying from 2 to 3 mm.

(a) Tubes used as dies (b) Cast iron tubes

Figure 6.1: Additional studied material

6.1 Investigation on cast iron tubes solidified under extremely high cooling rate

6.1.1 Composition of new cast irons

Because of the conformation of the samples it was not possible to perform an analysis at the quantometer, therefore only a semi-quantitative SEM analysis was performed (EDS). The instrument made it possible to detect the presence of chromium, manganese, titanium as in the materials previously studied, as well as a consistent presence of aluminum. However, it was not possible to quantify the elements precisely, especially carbon. Following there are some spectra that describe the composition obtained with the SEM analysis, not all the spectra are present due to the equality of some of them.

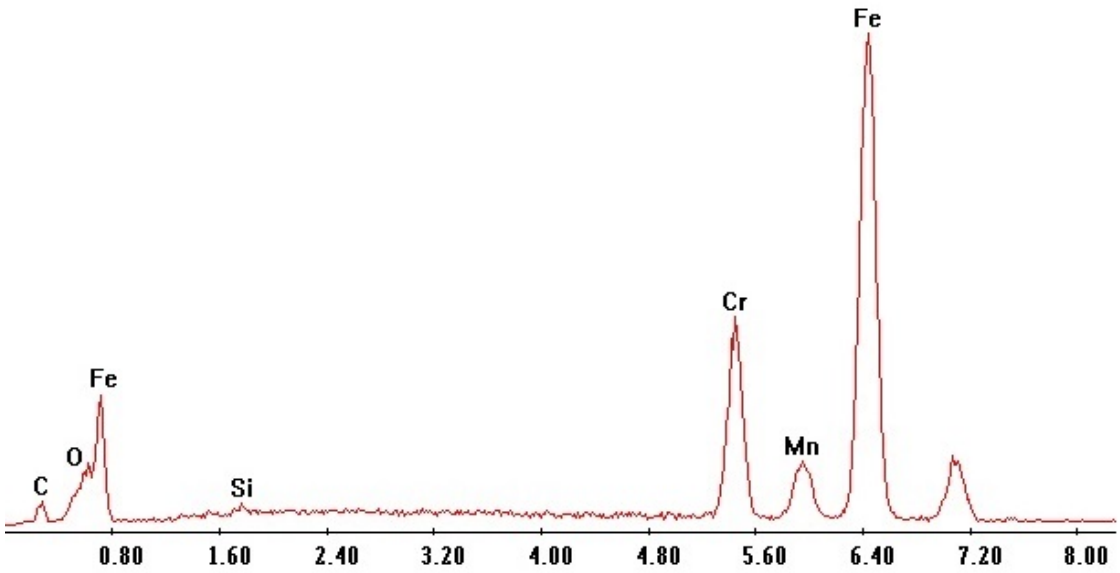

Figure 6.2: Semiquantitative analysis of the composition with SEM (Sample 3)

The spectrum also highlights the presence of traces of oxygen.

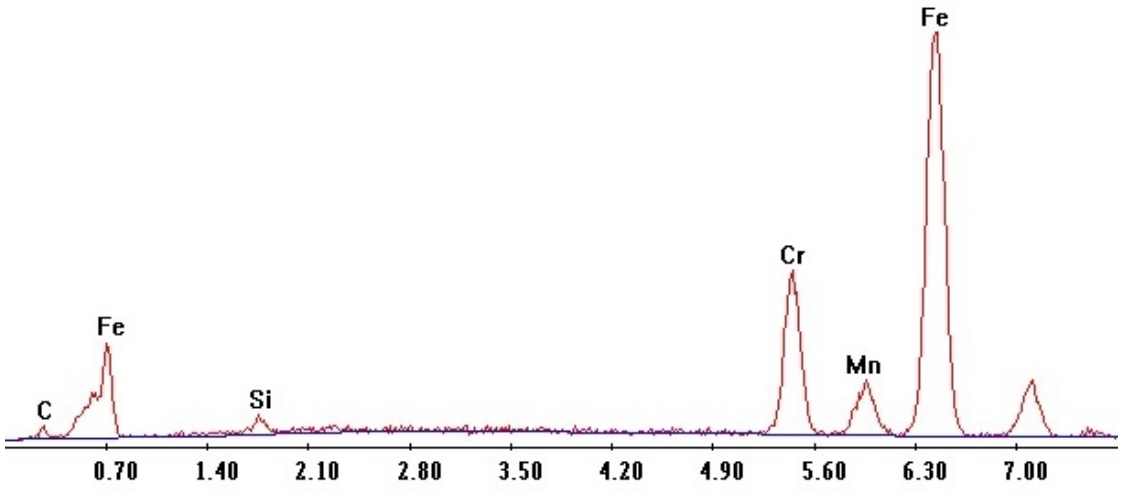

Figure 6.3: Semiquantitative analysis of the composition with SEM (Sample 5)

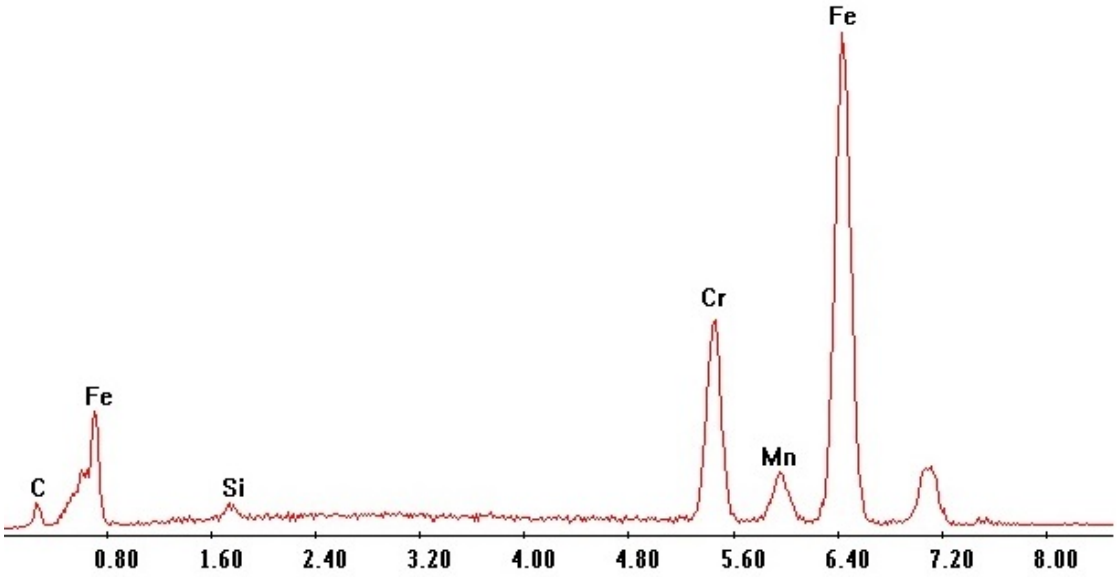

Figure 6.4: Semiquantitative analysis of the composition with SEM (Sample 6)

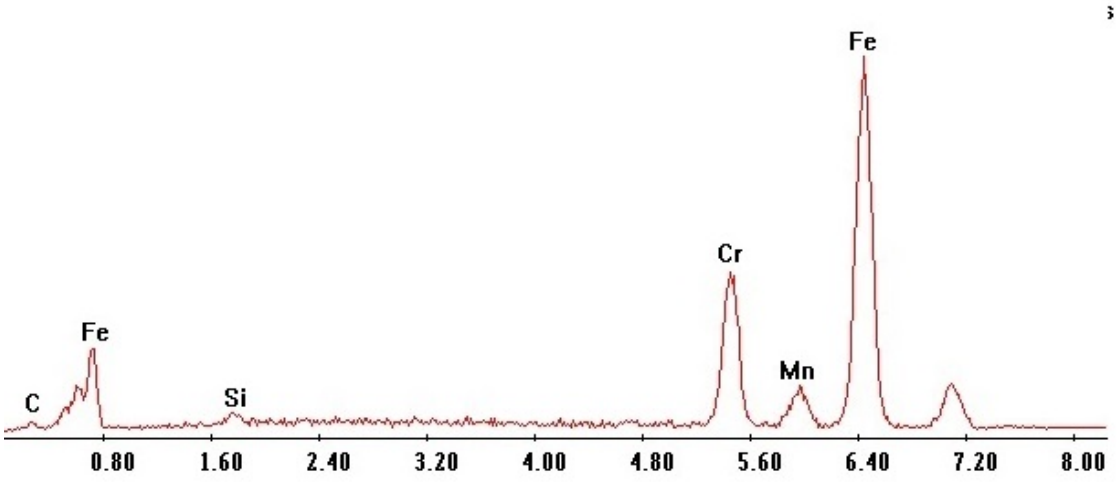

Figure 6.5: Semiquantitative analysis of the composition with SEM (Sample 7)

6.1.2 Results of metallurgical characterization of cast irons

6.1.2.1 Micrographs

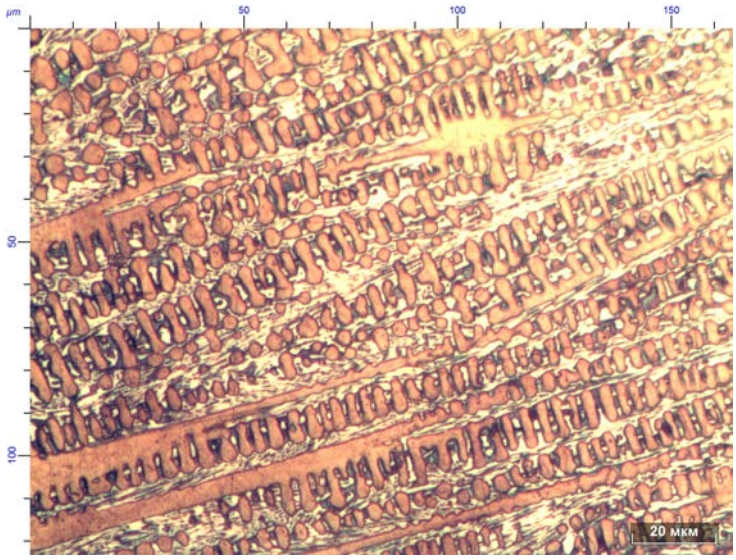

Figure 6.6: Microstructure sample 2-T 500x cooled at high rate

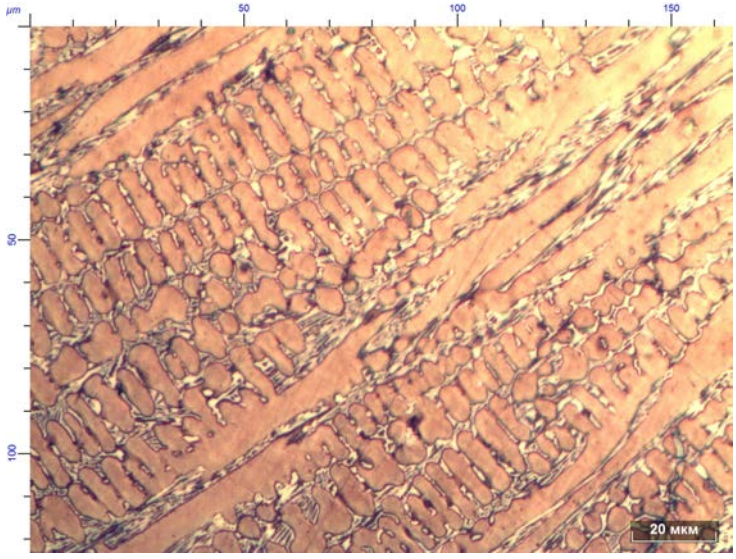

Figure 6.7: Microstructure sample 3-T 500x cooled at high rate

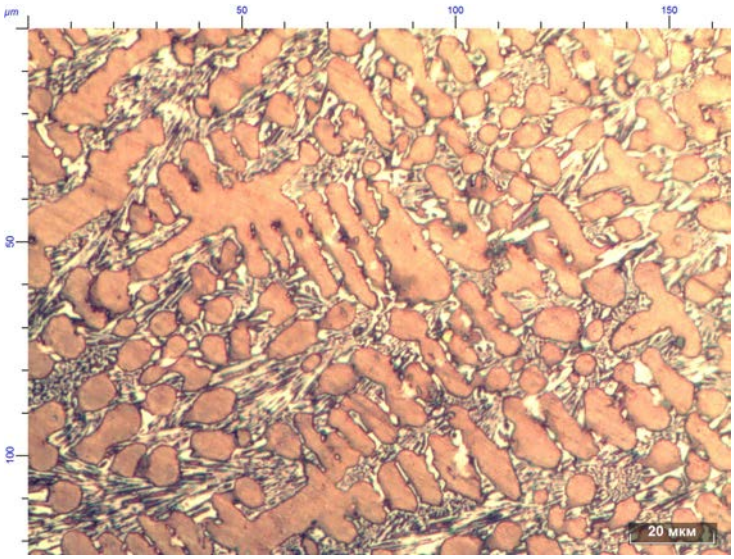

Figure 6.8: Microstructure sample 3-T 500x cooled at high rate

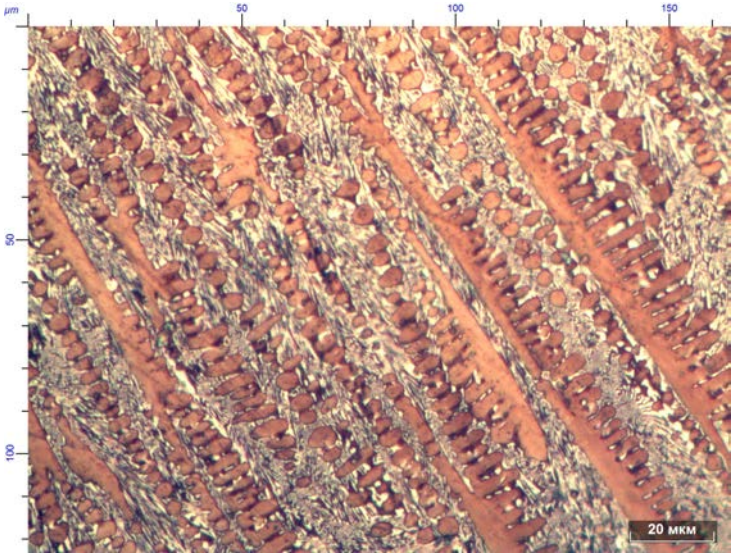

Figure 6.9: Microstructure sample 3-T 500x cooled at high rate

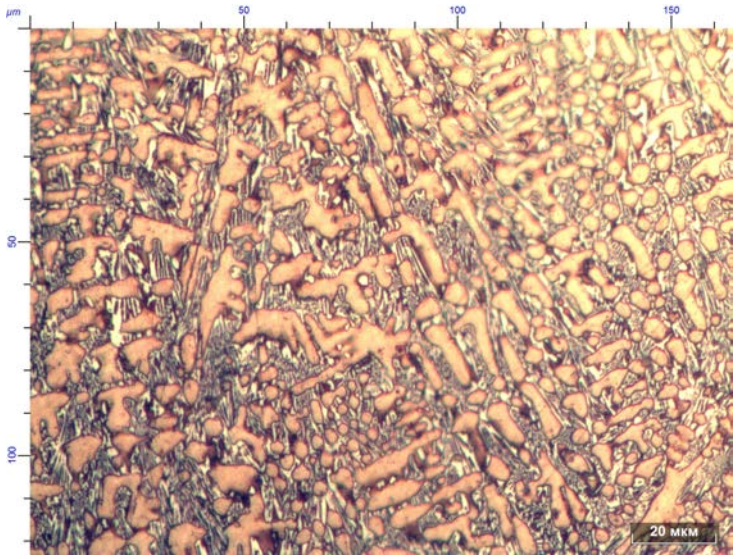

Figure 6.10: Microstructure sample 3-T 500x cooled at high rate

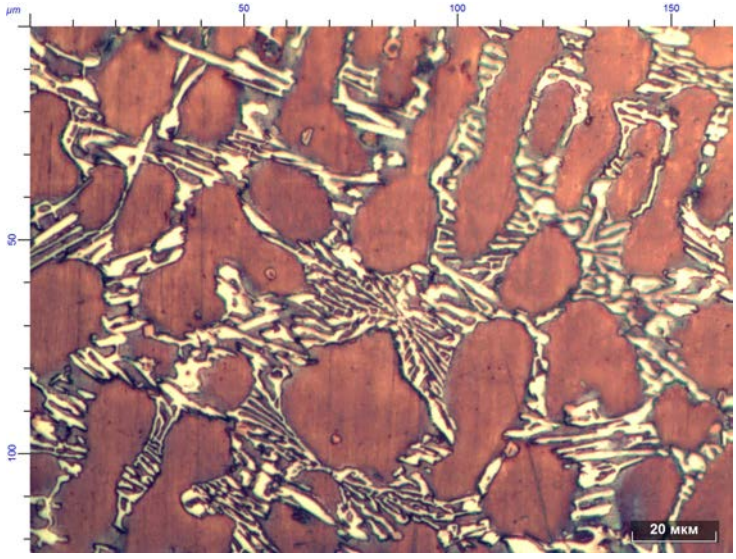

Figure 6.11: Microstructure sample 5-T 500x cooled at high rate

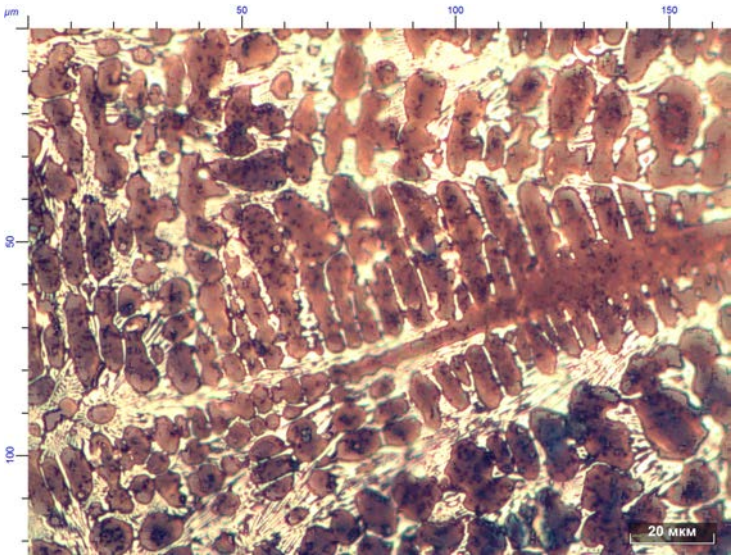

Figure 6.12: Microstructure sample 6-T 500x cooled at high rate

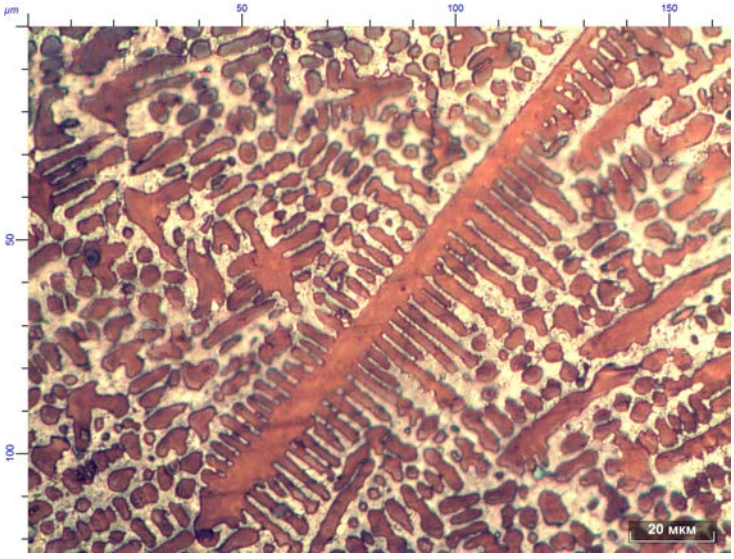

Figure 6.13: Microstructure sample 7-T 500x cooled at high rate

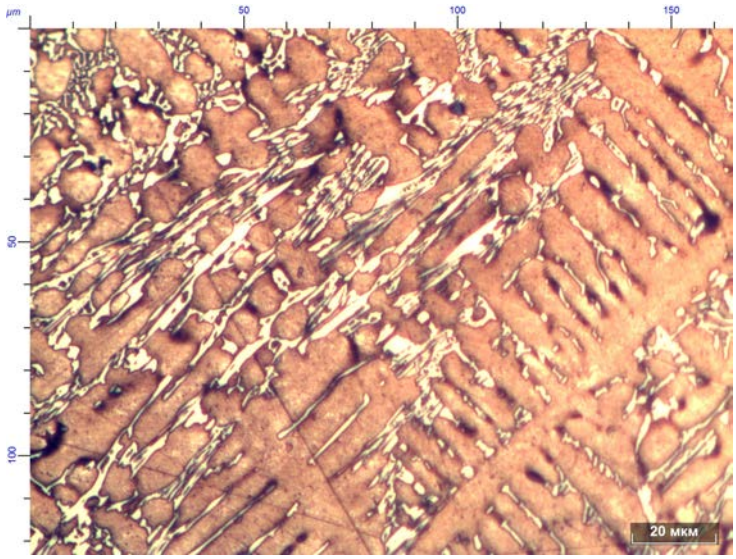

Figure 6.14: Microstructure sample 8-T 500x cooled at high rate

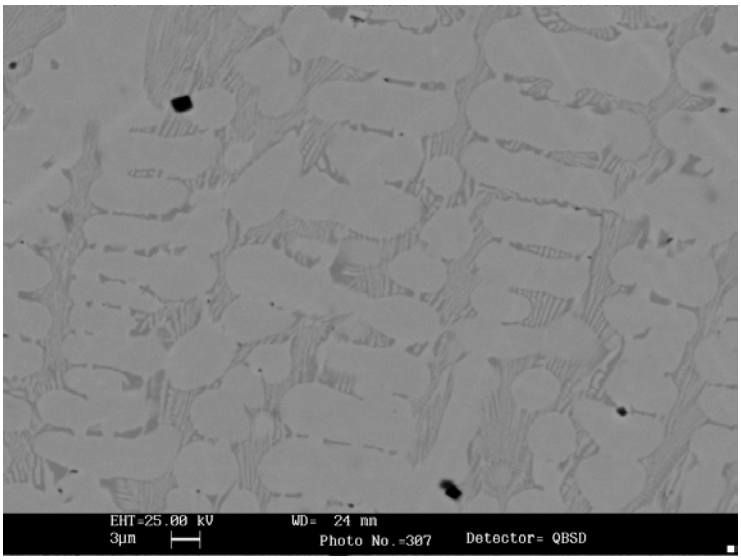

Figure 6.15: Microstructure obtained with SEM (3)

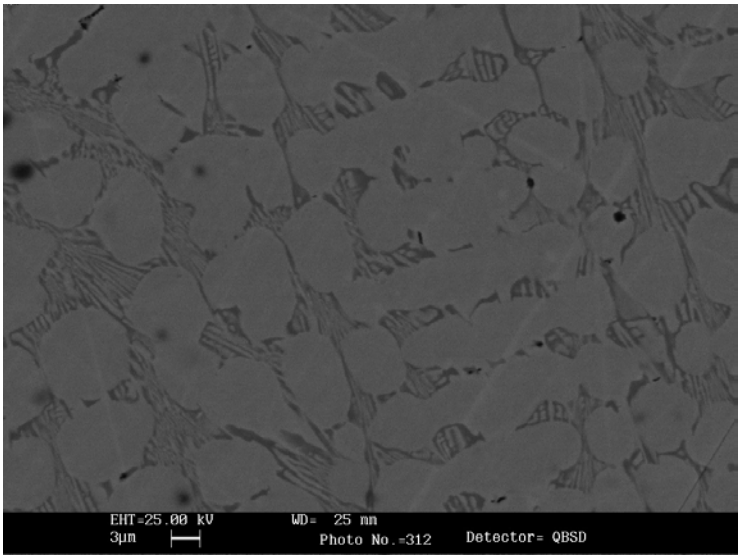

Figure 6.16: Microstructure obtained with SEM (6)

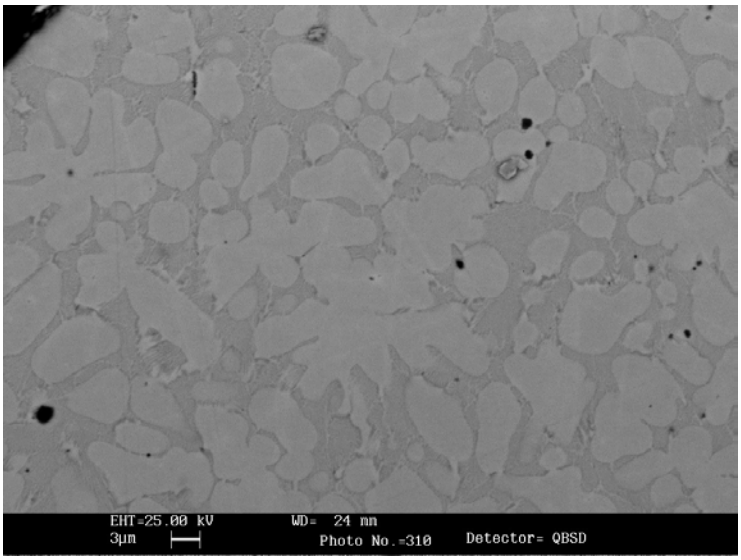

Figure 6.17: Microstructure obtained with SEM (7)

Comments and considerations

The theory that is used to explain the process of solidification of metals is that of nucleation and growth, according to what the theory asserts a high rate of cooling favors the nucleation process compared to that of growth and therefore what is expected is that the metal that constitutes the tubes both characterized by a small-sized crystalline grain and equiaxed. However, what is highlighted

by the metallography is that there are a lot of dendrites, a symptom of a non-homogeneous heat flow in your directions. The presence of the dendrites could be associated to the system in which the material is cast and solidified, in fact it could be due to the non-homogeneity of thermal conductivity between the walls of the glass tube and the air present internally along the tube axes, or anisotropy in the properties of glass. Moreover, there are dendrites with a very long main axes which indicates a heat flow in cooling strongly oriented in one direction. There is an evident presence of eutectic carbides and in some samples, like number 6-T, 7-T it is also possible to observe the presence of titanium carbides thanks to the green color and the rounded shape. In the samples 2-T and 6-T there is a strong orientation of the dendrites in a preferential direction, this could also indicate a significant anisotropy in the mechanical properties of the material, which most probably are poor. The observation of some samples with the SEM allows to identify the presence of a lot of non-metallic inclusions and particles within the metal matrix that may be the cause of poor mechanical properties. The preparation of the samples in order to perform the analysis under the microscope has allowed to observe that the material is extremely fragile and non-deformable, since minimal stresses and impacts have caused the breaking of the material. It was possible to point out also that solidification technique does not guarantee uniform thickness over the entire length of the tube.

6.1.2.2 Quantitative analysis

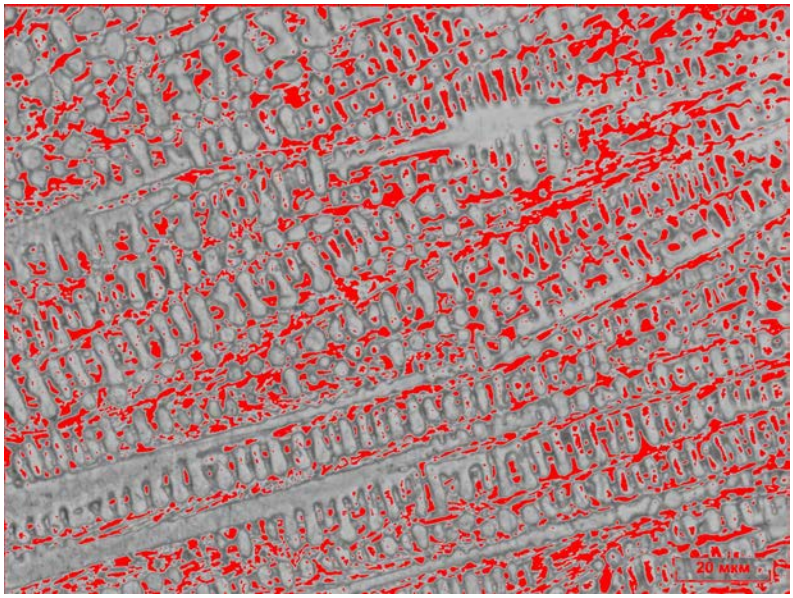

Figure 6.18: Quantitative analysis on sample 2-T

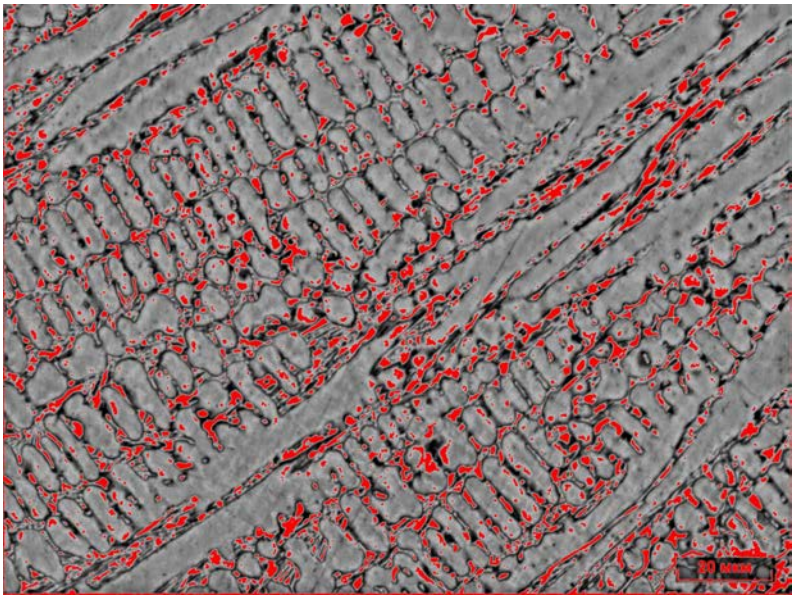

Figure 6.19: Quantitative analysis on sample 3-T

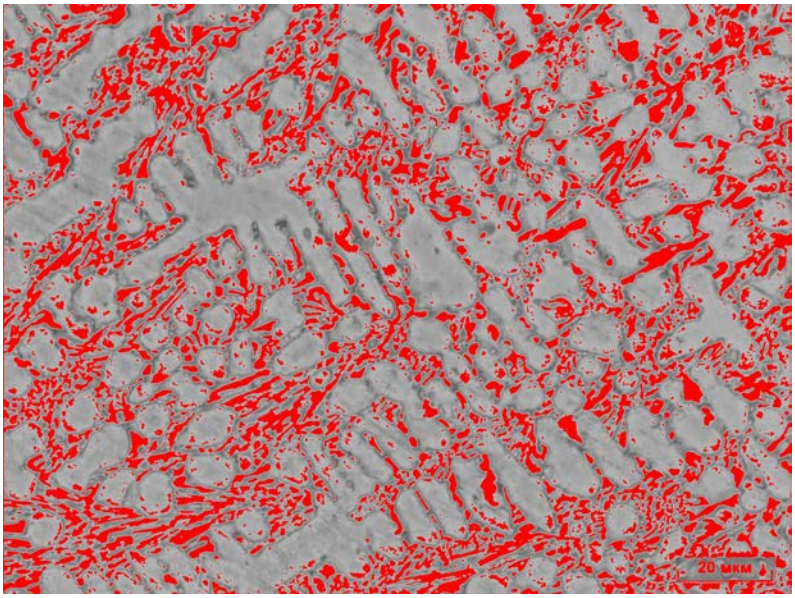

Figure 6.20: Quantitative analysis on sample 3-1T

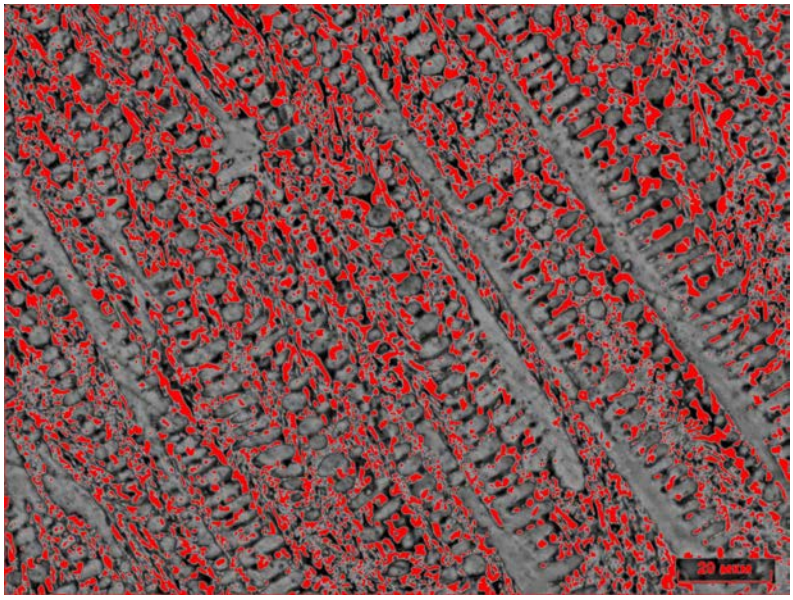

Figure 6.21: Quantitative analysis on sample 3-2T

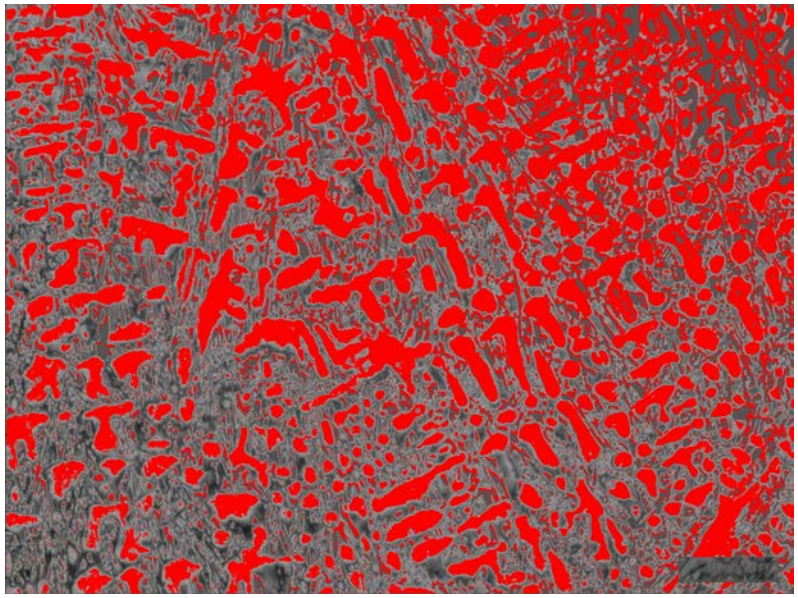

Figure 6.22: Quantitative analysis on sample 3-3T

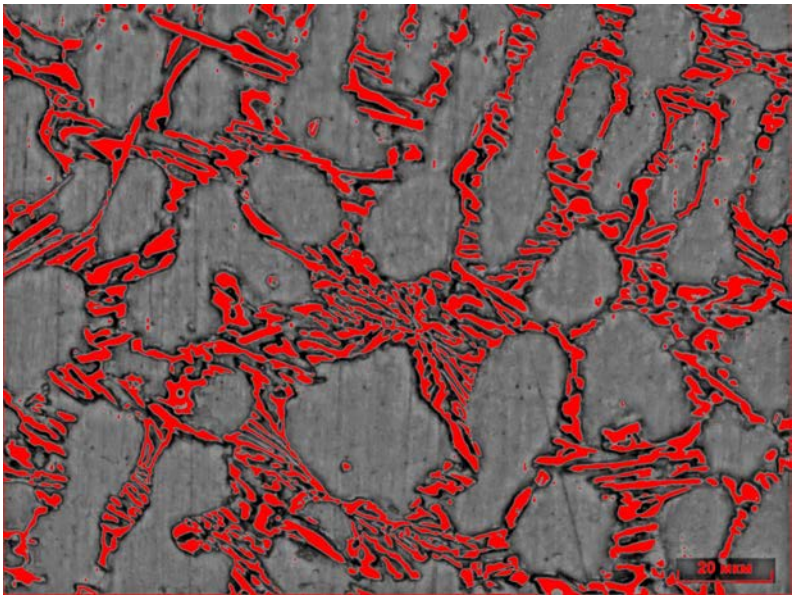

Figure 6.23: Quantitative analysis on sample 5-T

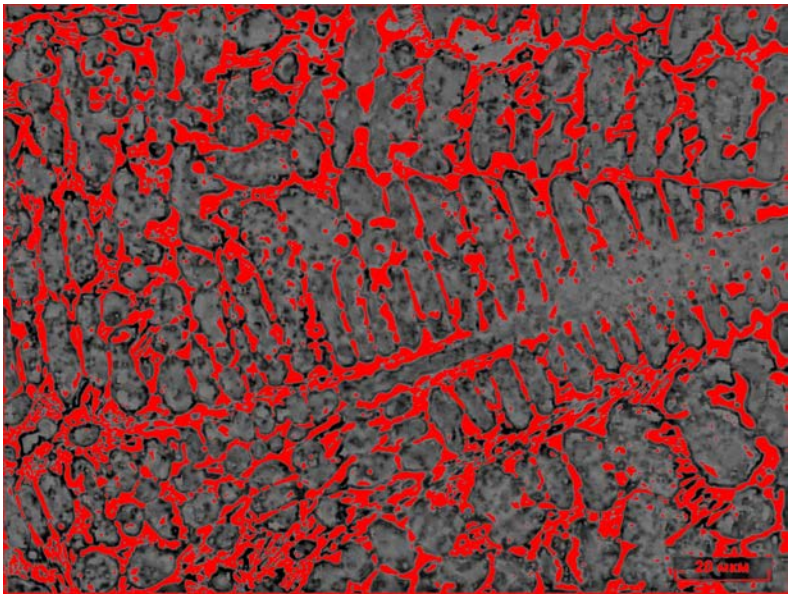

Figure 6.24: Quantitative analysis on sample 6-T

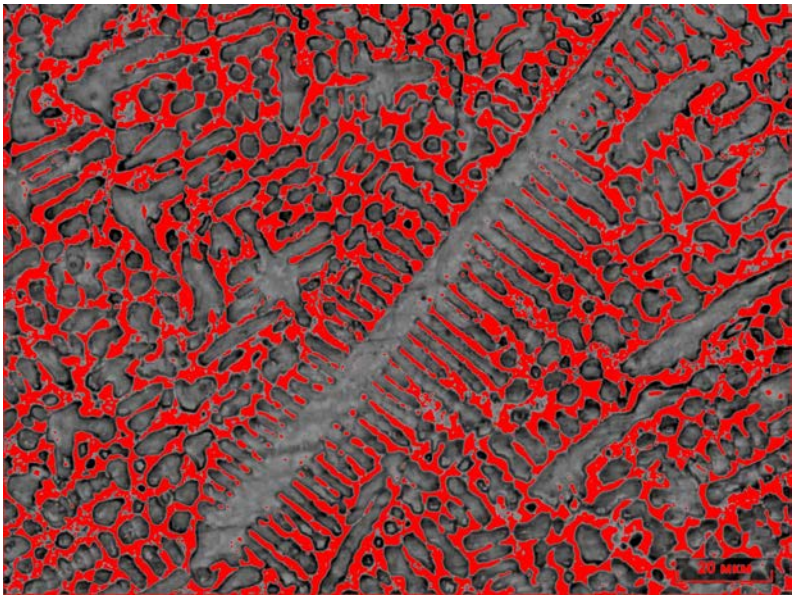

Figure 6.25: Quantitative analysis on sample 7-T

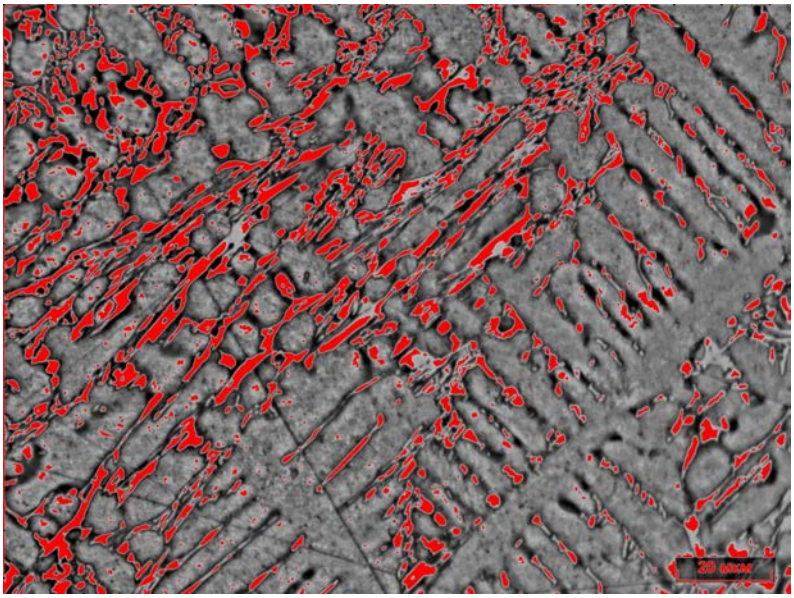

Figure 6.26: Quantitative analysis on sample 8-T

Sample	Secondary phase (%)	Metal matrix (%)
2-T	18.34	81.66
3-T	40.29	59.76
3-1T	22.74	77.36
3-2T	18.26	81.74
3-3T	8.73	91.27
5-T	16.08	83.92
6-T	24.47	75.53
7-T	27.24	72.76
8-T	11.17	88.83

Table 6.1: Phase quantity

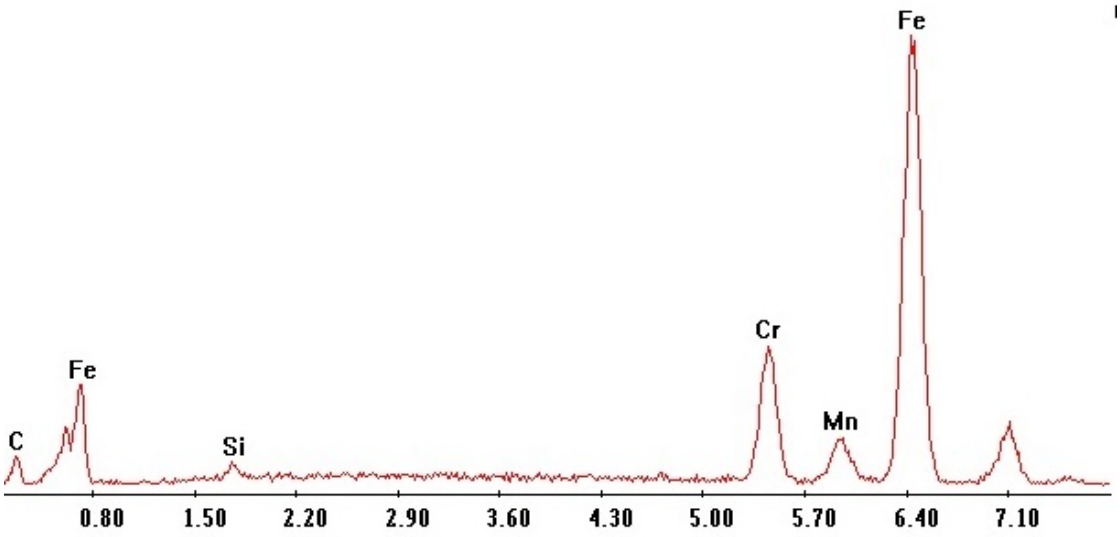

Figure 6.27: Metallic phase composition (Semiquantitative analysis with SEM)

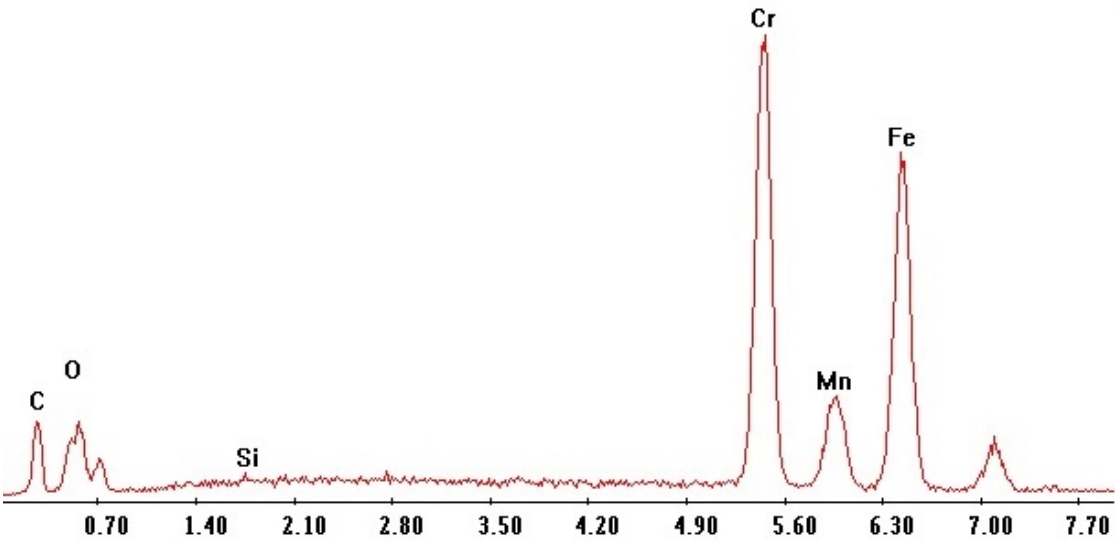

Figure 6.28: Example of secondary phase composition (Semiquantitative analysis with SEM)

6.1.2.3 Dispersion analysis

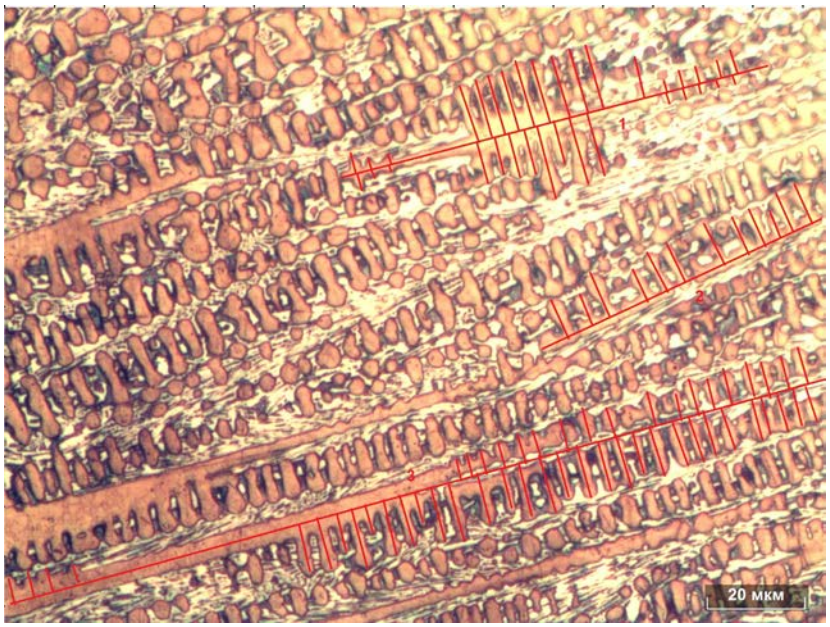

Figure 6.29: Quantitative analysis of the sample 2-T

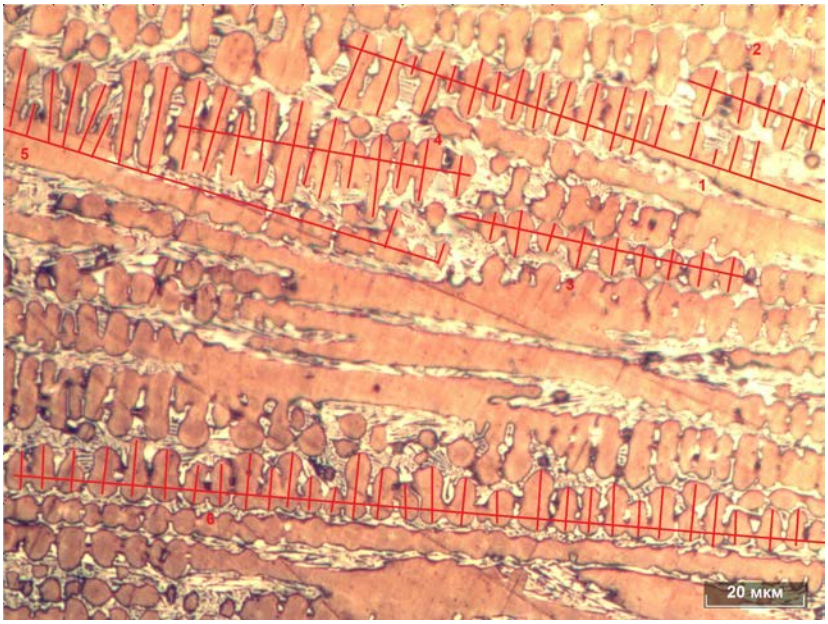

Figure 6.30: Quantitative analysis of the sample 3-T

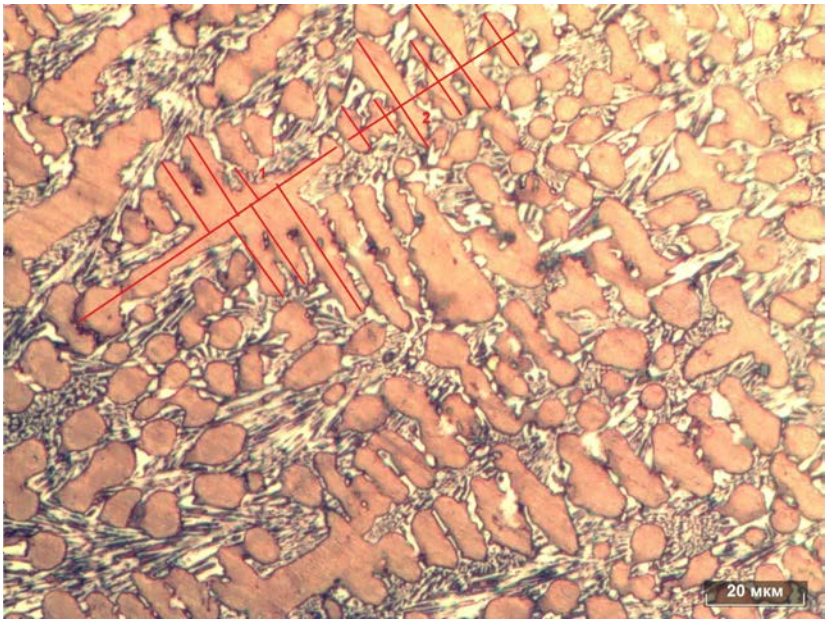

Figure 6.31: Quantitative analysis of the sample 3-1T

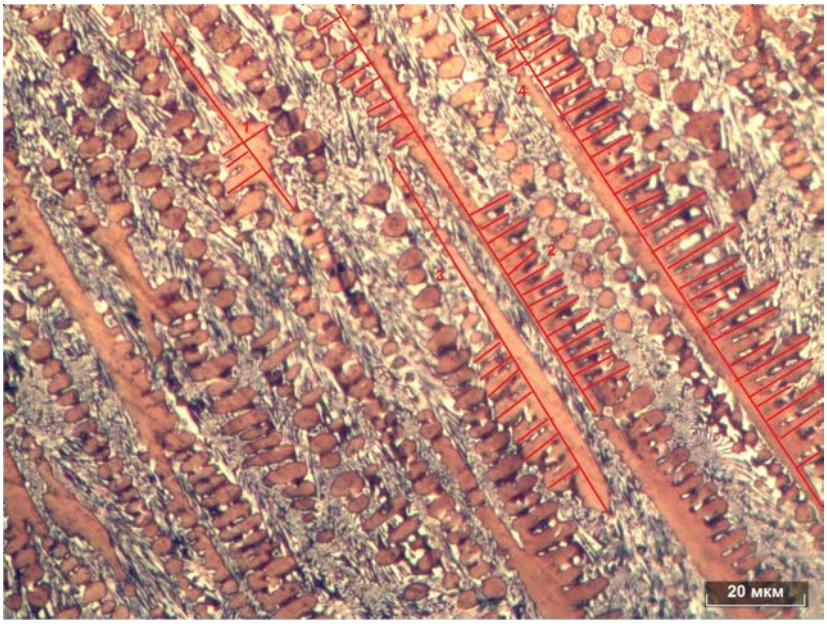

Figure 6.32: Quantitative analysis of the sample 3-2T

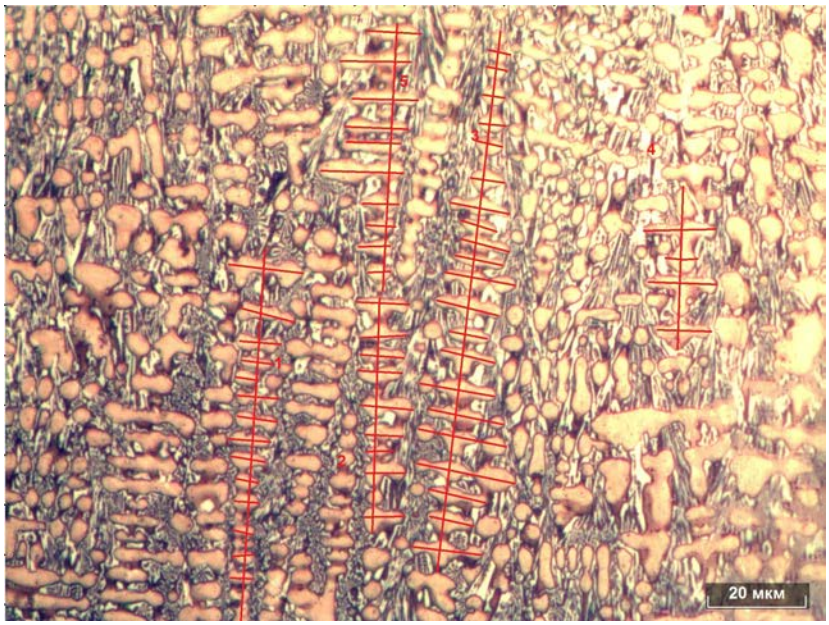

Figure 6.33: Quantitative analysis of the sample 3-3T

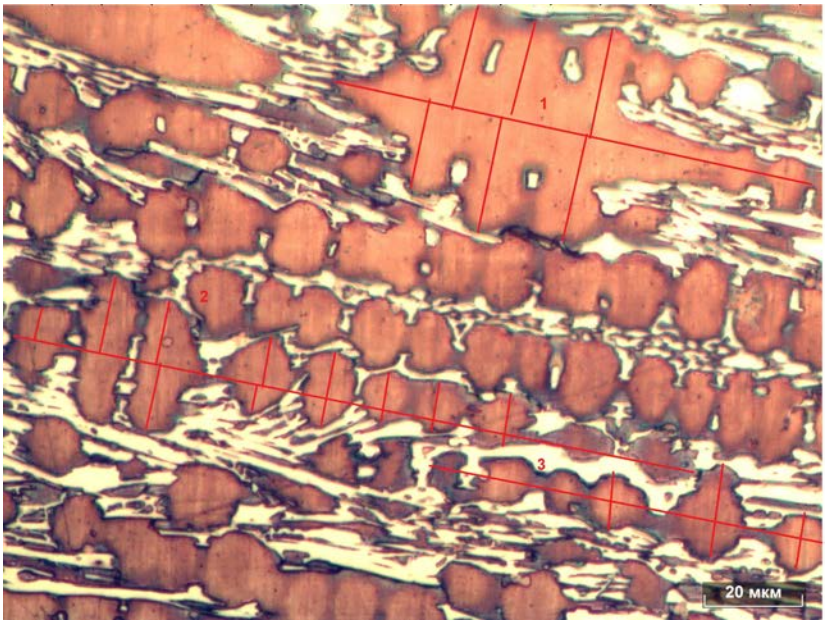

Figure 6.34: Quantitative analysis of the sample 5-T

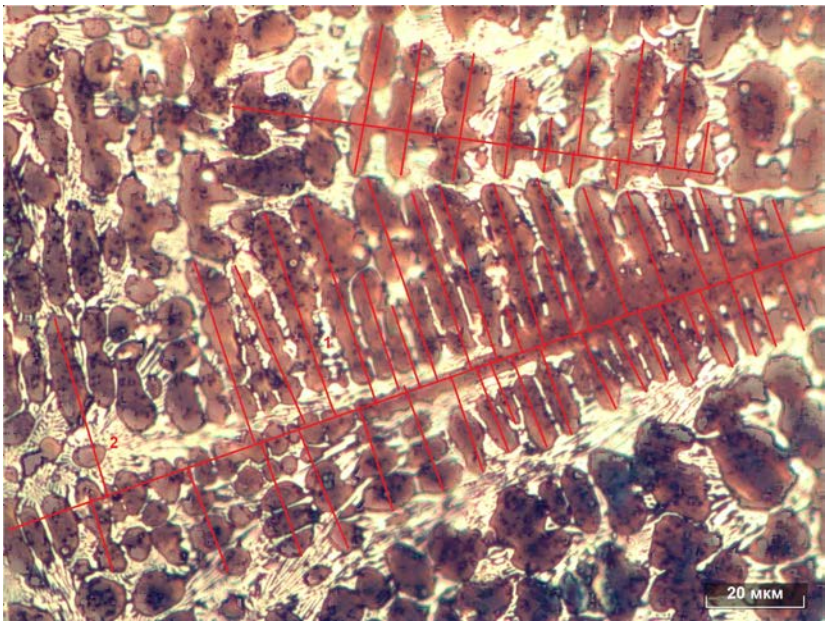

Figure 6.35: Quantitative analysis of the sample 6-T

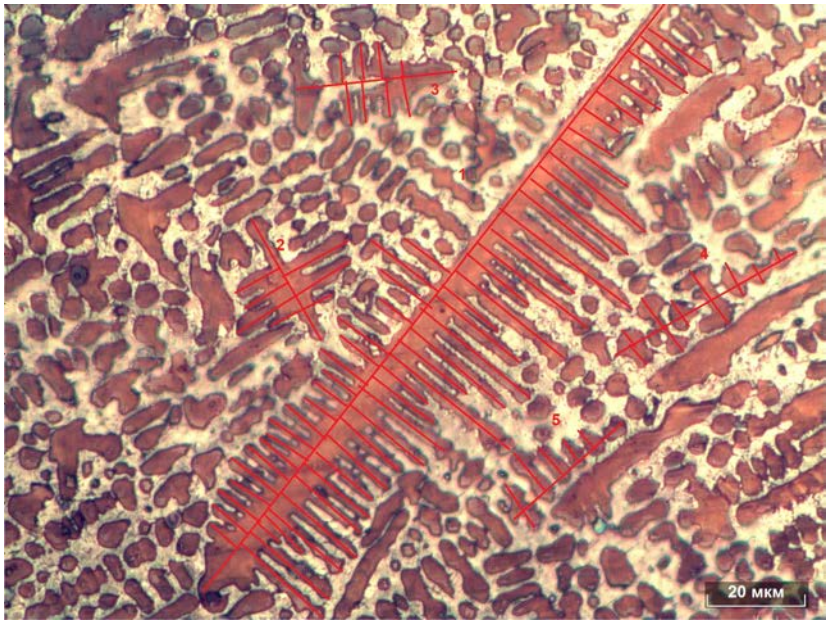

Figure 6.36: Quantitative analysis of the sample 6-T

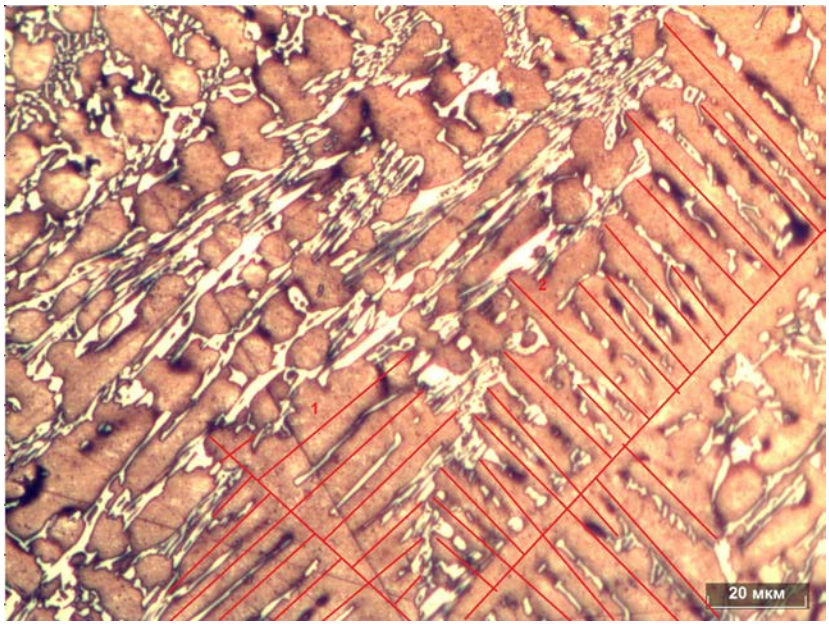

Figure 6.37: Quantitative analysis of the sample 6-T

Sample	Average dendrite first axe length (µm)	Average secondary arm length (µm)	SDAS (µm)	Dispersion (µm^{-}1)
2-T	108.53	7.72	3.88	0.26
3-T	51.58	12.04	5.12	0.20
3-1T	87.37	9.12	4.29	0.23
3-2T	64.41	4.74	5.34	0.19
3-3T	86.48	6.10	6.12	0.16
5-T	107.66	9.54	13.05	0.08
6-T	138.88	21.04	5.29	0.19
7-T	57.40	12.71	3.72	0.27
8-T	83.02	25.94	5.79	0.17

Table 6.2: Dispersion investigations

6.1.2.4 Difference with the other samples

Comments and considerations

The dendrites also have an average length of the axes greater than the samples studied previously, which have solidified with a cooling rate of an order of magnitude of less, for which a dendritic structure is expected. Compared to the samples studied previously, the average length of the dentrites is five to ten times higher, while the length of the lateral arms and the distance between them is of the same order of magnitude and the values are similar. The presence of large and strongly oriented columnar grains, in accordance with the direction of heat flow, is in theory an indication of poor mechanical properties.

6.1.2.5 Inclusions analysis

As said before, from the study under the optical microscopes and the SEM of the samples it has been possible to observe the presence of numerous non-metallic inclusions, of considerable size and often very close one to each other. The results of the measurements are shown in the following tables and in the appendix A at the end of the thesis.

Sample	Average content of inclusions(V_V,%)	Average dimensions of inclusions (µm^2)	Average length of inclusions (µm)
2-T	0.40	1.87	1.25
3-T	0.39	2.35	1.317
3-1T	0.42	6.14	2.30
3-2T	0.624	2.22	1.29
3-3T	0.509	1.62	1.012
5-T	0.65	2.35	1.20
6-T	0.26	1.85	1.19
7-T	2.07	3.30	1.55
8-T	0.83	2.06	1.28

Table 6.3: Inclusions properties

Figure 6.38: Inclusions observed with SEM microscope (sample 3-T)

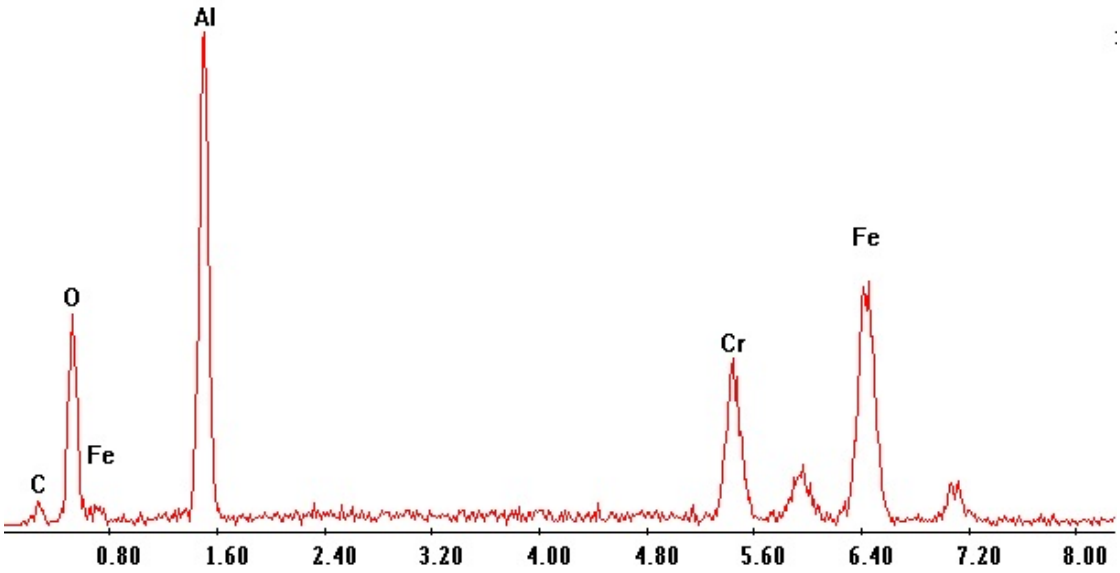

Figure 6.39: Inclusions observed with SEM microscope (sample 3-T)

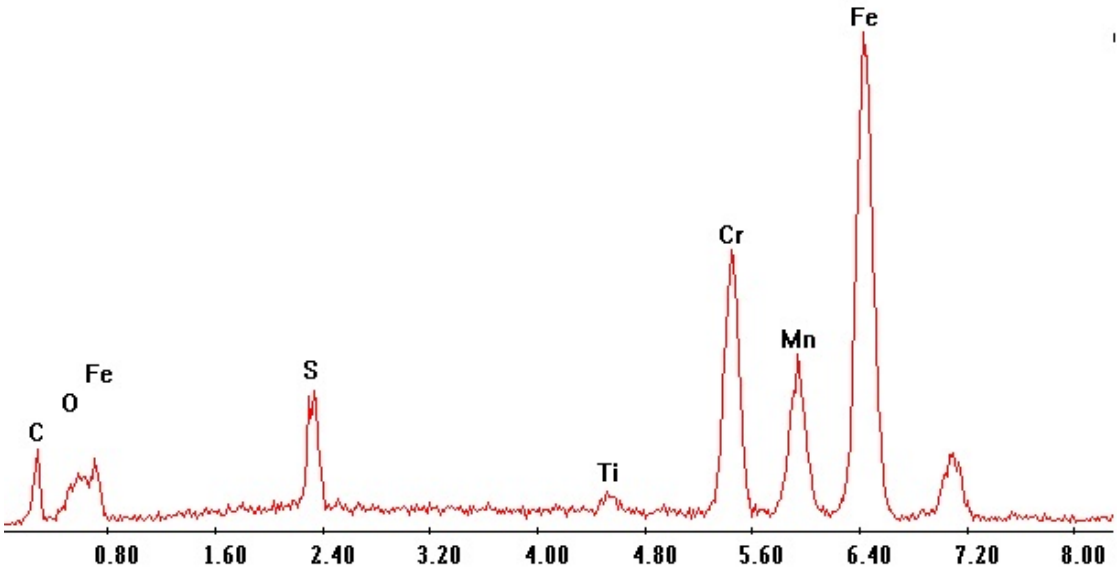

Figure 6.40: Inclusions observed with SEM microscope (sample 3-T)

The inclusions that have been identified through the SEM microscope analysis are of different types and have different compositions: in fact there are inclusions

of aluminum oxide Al_2O_3 and manganese sulfide Mn_2S. The aluminum inclusions can derive from the oxidation of the aluminum present in the alloy and from the slagging agent.

Figure 6.41: Inclusions observed with SEM microscope (sample 5-T)

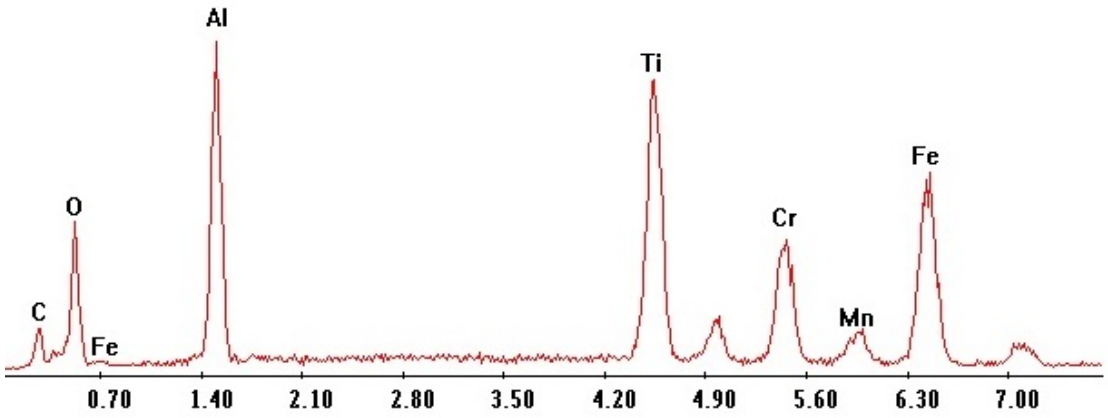

Figure 6.42: Inclusions composition (sample 5-T)

This image shows the presence of titanium carbide (TiC) (black part) and aluminum oxide (gray).

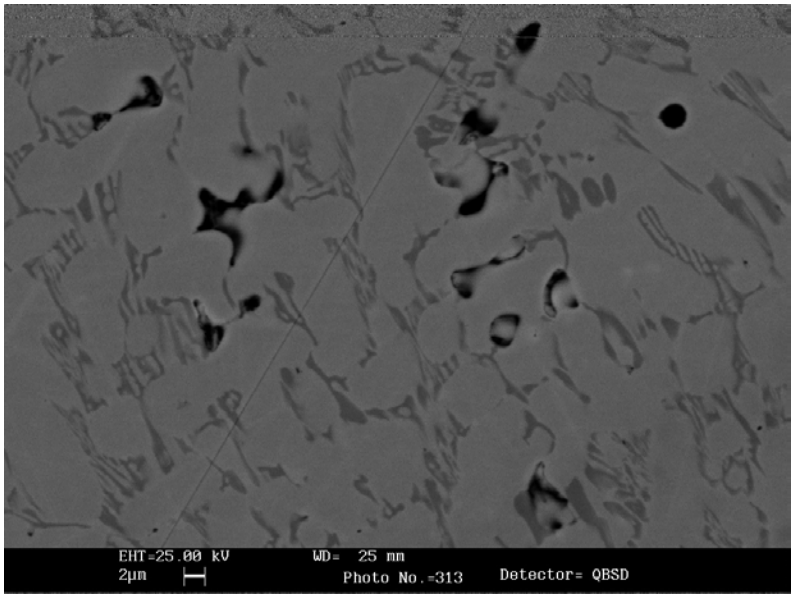

Figure 6.43: Inclusions compositions (sample 6-T)

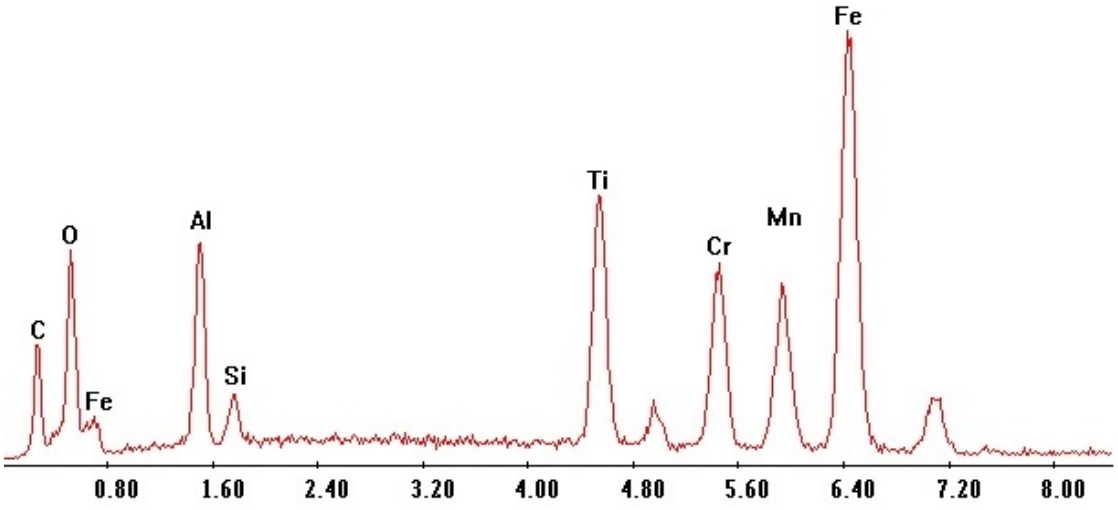

Figure 6.44: Inclusions compositions (sample 6-T)

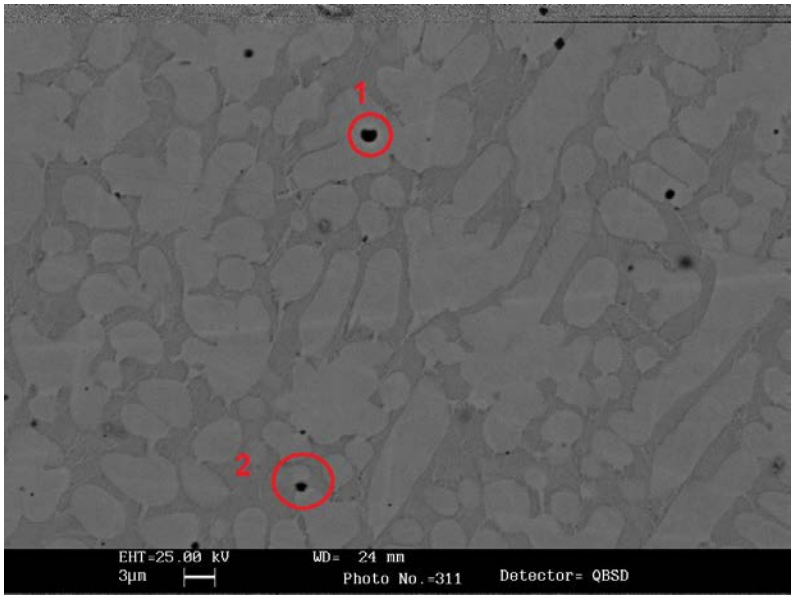

Figure 6.45: Inclusions observed with SEM microscope (sample 7-T)

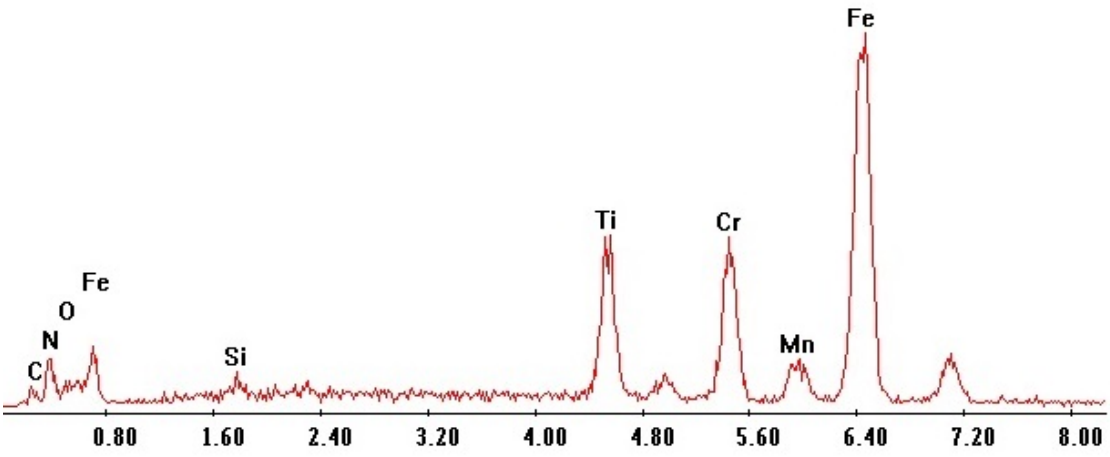

Figure 6.46: Upper inclusion compositions (sample 7-T)

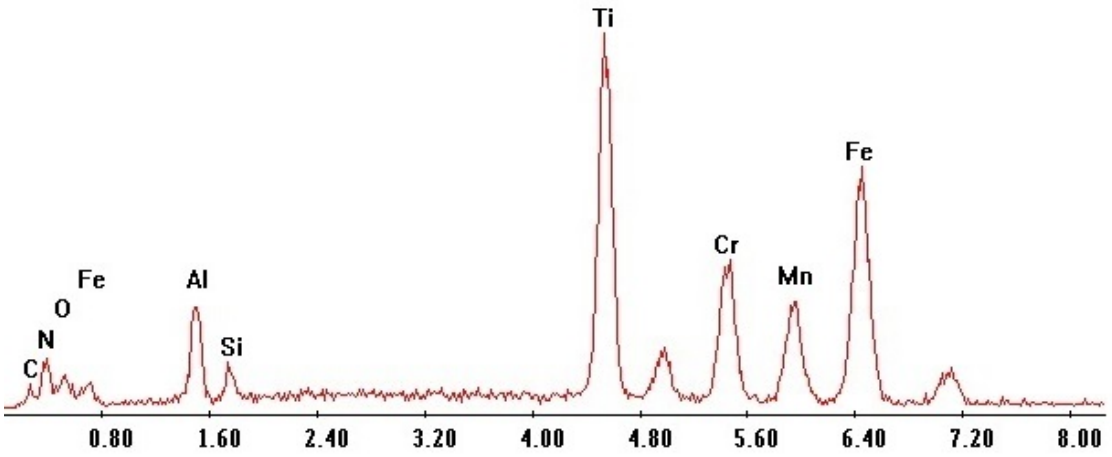

Figure 6.47: Lower inclusion compositions (sample 7-T)

Comments and considerations

The significant presence of inclusions together with the dendritic structure highlighted above indicates that the material may not have the expected mechanical characteristics, since these elements cause degradation of the metal and its performances. Furthermore it is necessary to control the atmosphere during the casting process to reduce the problem.

Only the singularities identified in the various samples have been reported.

6.1.3 Hardness test on cast iron cooled at high cooling rate

Sample	Microhardness Vickers (HV)			
	Measure 1	Measure 2	Measure 3	VK_a
2-T	511	492	448	484
3-T	513	490	479	494
5-T	458	429	458	448
6-T	526	466	490	494
7-T	492	468	526	495
8-T	580	610	580	590

Table 6.4: Hardness test results (HV)

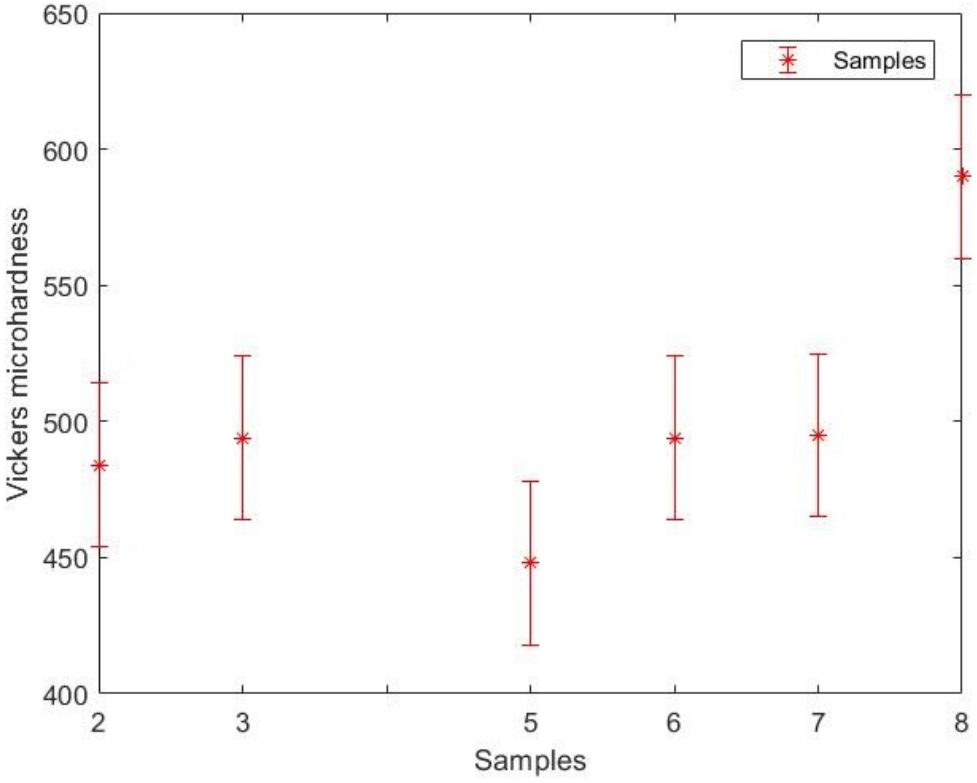

Figure 6.48: Average hardness (HV) of the samples

Chapter 7

CONCLUSIONS

During this thesis a study was carried out on white cast iron with high chromium content, which are materials are used for the the production of molds, mill pumps and grinding mills. This components, while working, are subjected to high wear, therefore it is necessary that these cast irons have a high value of the wear resistance coefficient (K_i) and hardness (HRC). The goal of this work is to try to improve these materials, using as a method of material improvement the alloying with elements able to raise the two properties and finding their best content in the material in order to guarantee high performance and maximize these two properties. The alloying elements used were manganese, chromium, nickel and titanium, in the following ranges: C[%]=[1.90÷2.50], Mn[%]=[3.50÷5.00], Cr[%]=[15.00÷19.00], Ni[%]=[0.40÷1.00] and Ti[%]=[0.20÷0.60]. These elements are typical in white cast iron and the ranges are typically used in practice. In order to find the best combination of alloying elements was built a mathematical models using the experimental data. The starting point was a set of white cast irons with a known composition, with pre-established content of the various alloy elements, thanks to the experimental theory. This theory establishes the number of starting samples and the content of each element. After melting operations, necessary to have the samples, these were characterized to see their microstructure, after hardness and coefficient of resistance to abrasive wear have been measured. All the samples have a metal matrix of austenite (dendrites) surrounded by chromium and titanium carbides. The values of hardness are in the range HRC=[42÷54] and for the coefficient the interval of values is K_i=[0.97÷2.26].

The data obtained through the measurements were elaborated in order to obtain mathematical models that allow to highlight the influence of the various alloy elements on the properties based on their content in the material and to predict the properties given a certain combination of the elements in the previous ranges.

The process of model's building consisted in the following phases: the experimental data collected were first subjected to statistical repeatability analysis,

through the Cochran test, to evaluate the quality of the measurements of the results of the tests carried out. Through the theory of factorial experiments and linear regression, the two mathematical models were constructed, verified with the Student's and F's T test by Fisher, and are shown below:

$$HRC = 47.06 + 2.44[Cr] + 0.86[Mn] - 1.10[Ti] - 1.48[Ni] \tag{7.1}$$

$$K_i = 1.55 + 0.33[Cr] + 0.12[C] + 0.09[Mn] - 0.19[Ni] - 0.19[Ti] \tag{7.2}$$

The model concerning the hardness of the material shows how chromium and manganese are able to increase the hardness of the material as their content increases, in particular the chromium being a strong element forming carbides. Chromium is also able to prevent the formation of graphite in the microstructure and favors the presence of austenite. In this model does not appear a term that indicates the effect of carbon on hardness, although it is the main alloying element able to influence the characteristics of ferrous alloys. Carbon is not included in the model because it does not survives when the Student T criterion is applied. This result could be linked to the high cooling rates during the production phase of the samples studied during the research. Most probably the high cooling rate inhibits the effect of this element, as occurred in several previous studies carried out on this topic at the university. Another reason may be related to too narrow range sizes. In the case of the wear resistance coefficient model it is once again possible to observe that manganese and chromium give a positive contribution while nickel and titanium are a negative contribution. Unlike what happened previously, carbon is able to influence, with a positive contribution, resistance to wear. Investigations were also conducted on cast irons to find correlations between the composition, properties and microstructure of the material itself. It was noted that as the chromium content increases, there is a progressive increase in the carbide content of the material and that the samples that have a smaller or smaller size of the crystalline grain and the extent of the dendrites are the ones that have the most high mechanical level property. The models were subjected to a preliminary check with regard to the first eight products and experimental data: in both cases it was observed that the models provide concordant values with those measured. Once this was carried out, with the models, that were built, were found the chemical compositions able to maximize the two properties through the Steep Ascent method; from each model have been obtained three compositions that present the best performances. The samples were produced, by melting operations, to proceed

to another verification of the model by performing the same tests carried out for the initial test samples.

The samples obtained with the wear resistance model provide performances comply with the model as regards the value of K_i and as regards their hardness, the difference between experimental data and data expected with the model appears minimal. This shows how the models agree with the experimental data and are able to effectively predict values of the properties of the materials. For these samples the value of the hardness of HRC that was measured also agrees with that found through the model built to predict the hardness, this further signals the goodness of the built model. The samples show a microstructure reach in chromium and titanium carbides and dendrites of austenite, equal to that of the initial samples; it was highlighted that as the chromium and carbon content increase, the carbide content increases and the size of the dendrites arms is also increasing and this is expected, accompanied by a progressive increase in the mechanical properties of the material. The samples obtained with the HRC model do not fully confirm the experimental results due to some problems during the fusion, however taking into account all the results it is observed that the model is able to fit the experimental data well. The different preparation conditions of the samples allowed to obtain a different microstructure respect to the other samples, without dendrites, with the presence of ledeburite, chromium and titanium carbides with polygonal or lamellar shape.

From the results obtained it is possible to conclude that the optimal composition intervals are:

- Optimized interval for HRC:
  - C [%]=[2.05÷2.07]
  - Mn[%]=[4.23÷4.44]
  - Cr[%]=[18.00÷19.00]
  - Ni[%]=[0.48÷0.60]
  - Ti[%]=[0.48÷0.49]
- Optimized interval for Wear:
  - C [%]=[2.19÷2.27]
  - Mn[%]=[3.84÷3.90]
  - Cr[%]=[18÷19]
  - Ni[%]=[0.49÷0.61]
  - Ti[%]=[0.48÷0.49]

Considering all the data obtained, considerations were made regarding the theme of the selection of materials, also taking into consideration the economic aspects, assessing which overall is the best material as compromise of cost and properties. The best resultant combination is the 7-W alloy obtained through the wear resistance model together with the starting G and H alloys. In conclusion, the investigated alloys show positive performances, in line with the previsions of the built model and also with respect to the alloys already present on the market.

At the end of this analysis additional studies were carried out concerning white cast iron with a high content of chromium but with the presence of further elements with respect to the previous ones, such as aluminum. The cast irons studied in this second part present a further difference compared to those initially studied: the cooling speed in the casting phase was extremely high, obtained thanks to the solidification in glass tubes, with the help of vacuum. The samples of these cast irons were first characterized with the use of the optical and SEM to observe the microstructure. The microstructure shows something unexpected, in fact the photos show the presence of dendrites. Dendrites are not something to be expected because the cooling rate in the sample production phase would have led to small-sized equiaxed grains. Observation with an optical and electronic microscope made it possible to highlight the presence of numerous inclusions that were analyzed from the point of view of quantity, size, distribution and chemical composition. On the samples the microhardness on the thickness of the sample was also evaluated, it is very high (>400 HV) to confirm the high fragility and minimum ductility of the material obtained through this method of forming. The extreme fragility of the material has already been highlighted in the preparation phase of the samples: the application of loads and the attempt to cut the material to incorporate the samples into resin have led to the fragile breakage of the material. This tube forming technique also did not allow to obtain tubes with a constant thickness over the entire length of the tube. It will also be necessary to study the effect of the operative parameters and find a suitable set-up in order to have material with better microstructural and macroscopic characteristics.

Appendix A

REPORT OF INCLUSIONS ANALYSIS

REPORT
According to the results of the study sample number 2-T

Sample information:

- The number of measured fields of view: 3
- Field Area: 13 mm^2
- Total measured area: 0.38 mm^2
- Microscope magnification: 200
- Calibration: 0.200338 µm
- The analysis was carried out taking into account border inclusions.

Measured values for each type of inclusions (sulphides and oxides) or each type of particles constituting the structure

value measured	Nonmetallic inclusions average value	standard deviation	confidence interval (95%)	relative accuracy (%)
Volume fraction,V_V ,%	0.40	0.23	0.26	65
Number, N_A, 1 /mm^2	2059	778	898	43
Number of intersections N_l,1 /mm	2.63	1.20	1.39	52
Length,l,µm	1.25	0.22	0.25	20
Area, A,µm^2	1.87	0.63	0.73	38
Average interparticle distance,µm	447	235	271	60
Average diameter of Feret,µm	1.32	0.26	0.30	22
Max. Feret diameter,µm	1.56	0.31	0.36	23

Table 1.1: Inclusions analysis of sample 2-T

Maximum size of inclusions:

Nonmetallic inclusions	
Area,µm^2	45
Length,µm	9.62
Maximum diameter,µm	10.6

Table 1.2: Maximum size of inclusions of sample 2-T

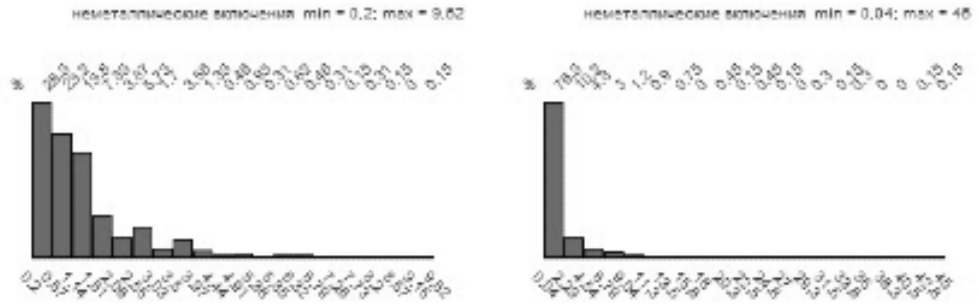

(a) (b)

Figure 1.1: Inclusions distributions of sample 2-T

REPORT

According to the results of the study sample number 3-T

Sample information:

- The number of measured fields of view: 3
- Field Area: 13 mm^2
- Total measured area: 0.38 mm^2
- Microscope magnification: 200
- Calibration: 0.200338 µm
- The analysis was carried out taking into account border inclusions.

Measured values for each type of inclusions (sulphides and oxides) or each type of particles constituting the structure

value measured	Nonmetallic inclusions average value	standard deviation	confidence interval (95%)	relative accuracy (%)
Volume fraction,V_V ,%	0.39	0.13	0.15	39
Number, N_A, 1 /mm^2	1724	793	9168	53
Number of intersections N_l,1 /mm	2.22	0.85	0.98	44
Length,l,µm	1.317	0.097	0.112	8
Area, A,$µm^2$	2.35	0.27	0.31	13
Average interparticle distance,µm	493	181	209	42
Average diameter of Feret,µm	1.42	0.14	0.17	11
Max. Feret diameter,µm	1.68	0.17	0.19	11

Table 1.3: Inclusions analysis of sample 3-T

Maximum size of inclusions:

Nonmetallic inclusions	
Area,$µm^2$	12
Length,µm	13.6
Maximum diameter,µm	14.4

Table 1.4: Maximum size of inclusions of sample 3-T

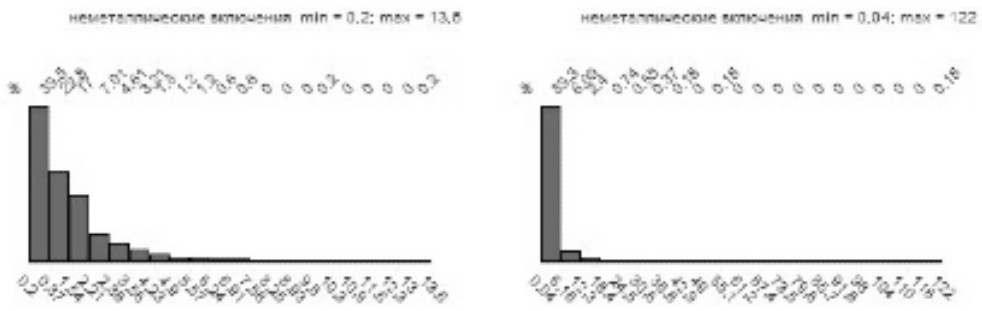

(a) (b)

Figure 1.2: Inclusions distributions of sample 3-T

REPORT

According to the results of the study sample number 3-1T

Sample information:

- The number of measured fields of view: 3
- Field Area: 0.5 mm^2
- Total measured area: 1.49 mm^2
- Microscope magnification: 100
- Calibration: 0.397711 µm
- The analysis was carried out taking into account border inclusions.

Measured values for each type of inclusions (sulphides and oxides) or each type of particles constituting the structure

value measured	Nonmetallic inclusions average value	standard deviation	confidence interval (95%)	relative accuracy (%)
Volume fraction,V_V ,%	0.42	0.036	0.042	9
Number, N_A, 1 /mm^2	708	195	225	3
Number of intersections N_l,1 /mm	1.60	0.29	0.33	31
Length,l,µm	2.30	0.25	0.28	12
Area, A,$µm^2$	6.14	1.16	1.034	21
Average interparticle distance,µm	635	113	131	20
Average diameter of Feret,µm	2.50	0.26	0.30	12
Max. Feret diameter,µm	2.94	0.31	0.36	12

Table 1.5: Inclusions analysis of sample 3-1T

Maximum size of inclusions:

Nonmetallic inclusions	
Area,$µm^2$	149
Length,µm	36.6
Maximum diameter,µm	36.6

Table 1.6: Maximum size of inclusions of sample 3-1T

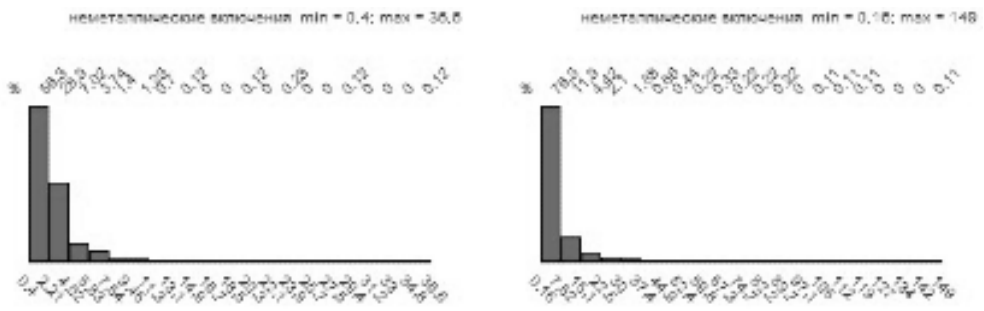

(a) (b)

Figure 1.3: Inclusions distributions of sample 3-1T

REPORT

According to the results of the study sample number 3-2T

Sample information:

- The number of measured fields of view: 3
- Field Area: 0.13 mm^2
- Total measured area: 0.37 mm^2
- Microscope magnification: 200
- Calibration: 0.200338 µm
- The analysis was carried out taking into account border inclusions.

Measured values for each type of inclusions (sulphides and oxides) or each type of particles constituting the structure

value measured	Nonmetallic inclusions average value	standard deviation	confidence interval (95%)	relative accuracy (%)
Volume fraction,V_V ,%	0.624	0.051	0.059	9
Number, N_A, 1 /mm^2	2826	301	348	12
Number of intersections N_l,1 /mm	3.63	0.14	0.16	12
Length,l,µm	1.29	0.11	0.13	10
Area, A,$µm^2$	2.22	0.25	0.29	13
Average interparticle distance,µm	273.7	10.6	12.3	4
Average diameter of Feret,µm	1.416	0.092	0.107	7
Max. Feret diameter,µm	1.68	0.12	0.14	8

Table 1.7: Inclusions analysis of sample 3-2T

Maximum size of inclusions:

Nonmetallic inclusions	
Area,$µm^2$	67.7
Length,µm	10.8
Maximum diameter,µm	14

Table 1.8: Maximum size of inclusions of sample 3-2T

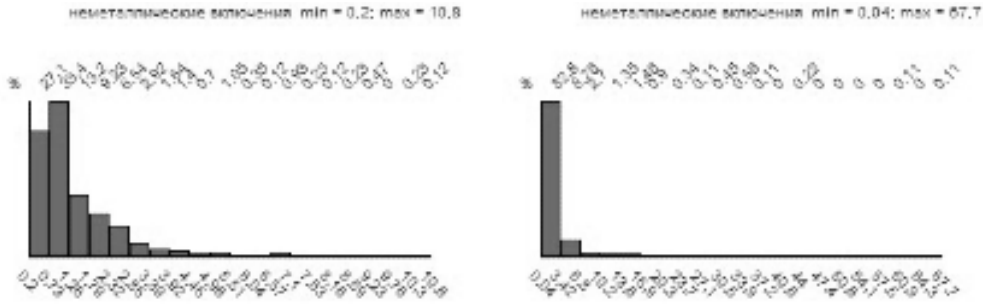

(a) (b)

Figure 1.4: Inclusions distributions of sample 3-2T

REPORT

According to the results of the study sample number 3-3T

Sample information:

- The number of measured fields of view: 3
- Field Area: 0.13 mm^2
- Total measured area: 0.38 mm^2
- Microscope magnification: 200
- Calibration: 0.200338 µm
- The analysis was carried out taking into account border inclusions.

Measured values for each type of inclusions (sulphides and oxides) or each type of particles constituting the structure

value measured	Nonmetallic inclusions average value	standard deviation	confidence interval (95%)	relative accuracy (%)
Volume fraction,V_V ,%	0.509	0.099	0.114	22
Number, N_A, 1 /mm^2	3218	526	608	18
Number of intersections N_l,1 /mm	3.23	0.36	0.42	12
Length,l,µm	1.012	0.097	0.112	11
Area, A,$µm^2$	1.62	0.49	1.56	34
Average interparticle distance,µm	310.4	35.2	40.7	13
Average diameter of Feret,µm	1.13	0.11	0.13	11
Max. Feret diameter,µm	1.32	0.14	0.16	11

Table 1.9: Inclusions analysis of sample 3-3T

Maximum size of inclusions:

Nonmetallic inclusions	
Area,$µm^2$	163
Length,µm	13.8
Maximum diameter,µm	418.8

Table 1.10: Maximum size of inclusions of sample 3-3T

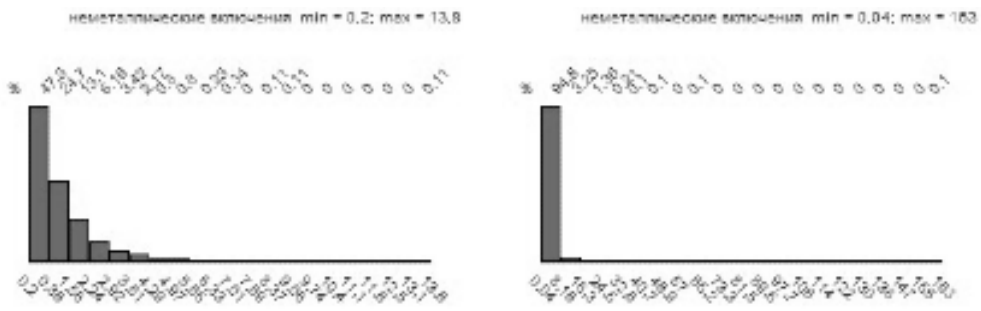

(a) (b)

Figure 1.5: Inclusions distributions of sample 3-3T

REPORT

According to the results of the study sample number 5-T

Sample information:

- The number of measured fields of view: 3
- Field Area: 0.13 mm^2
- Total measured area: 0.38 mm^2
- Microscope magnification: 200
- Calibration: 0.200338 µm
- The analysis was carried out taking into account border inclusions.

Measured values for each type of inclusions (sulphides and oxides) or each type of particles constituting the structure

value measured	Nonmetallic inclusions average value	standard deviation	confidence interval (95%)	relative accuracy (%)
Volume fraction,V_V ,%	0.65	0.24	0.28	43
Number, N_A, 1 /mm^2	2756	781	902	32
Number of intersections N_l,1 /mm	3.33	1.25	1.44	43
Length,l,µm	1.20	0.19	0.22	17
Area, A,$µm^2$	2.35	0.46	0.53	22
Average interparticle distance,µm	328	121	40	42
Average diameter of Feret,µm	1.34	0.19	0.21	15
Max. Feret diameter,µm	1.61	0.21	0.15	15

Table 1.11: Inclusions analysis of sample 5-T

Maximum size of inclusions:

Nonmetallic inclusions	
Area,$µm^2$	108
Length,µm	17.6
Maximum diameter,µm	18.5

Table 1.12: Maximum size of inclusions of sample 5-T

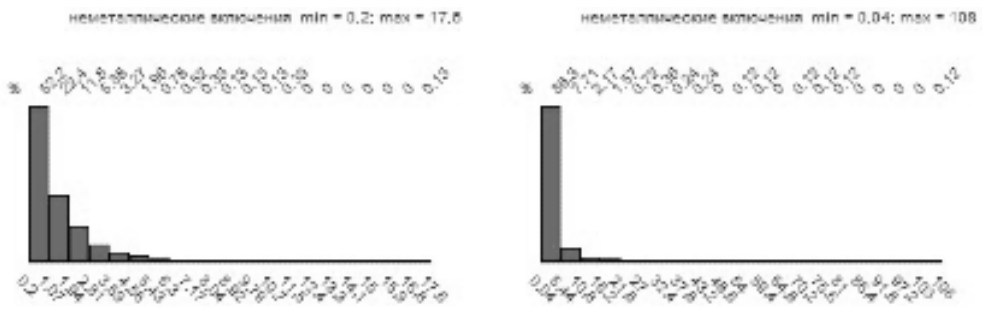

(a) (b)

Figure 1.6: Inclusions distributions of sample 5-T

REPORT

According to the results of the study sample number 6-T

Sample information:

- The number of measured fields of view: 3
- Field Area: 0.13 mm^2
- Total measured area: 0.38 mm^2
- Microscope magnification: 200
- Calibration: 0.200338 µm
- The analysis was carried out taking into account border inclusions.

Measured values for each type of inclusions (sulphides and oxides) or each type of particles constituting the structure

value measured	Nonmetallic inclusions average value	standard deviation	confidence interval (95%)	relative accuracy (%)
Volume fraction,V_V ,%	0.26	0.21	0.25	96
Number, N_A, 1 /mm^2	1233	765	884	71
Number of intersections N_l,1 /mm	1.56	1.16	1.34	85
Length,l,µm	1.19	0.19	0.22	18
Area, A,$µm^2$	1.85	0.57	0.66	35
Average interparticle distance,µm	1036	886	1023	98
Average diameter of Feret,µm	1.28	0.17	0.20	15
Max. Feret diameter,µm	1.47	0.22	0.25	17

Table 1.13: Inclusions analysis of sample 6-T

Maximum size of inclusions:

Nonmetallic inclusions	
Area,$µm^2$	58.2
Length,µm	11.4
Maximum diameter,µm	18.1

Table 1.14: Maximum size of inclusions of sample 6-T

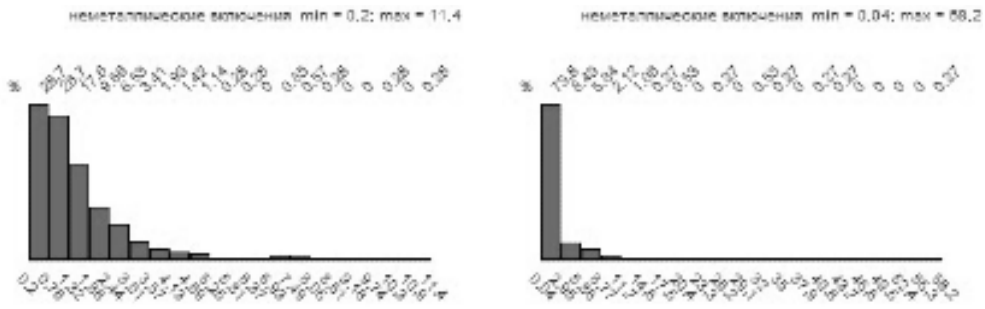

(a) (b)

Figure 1.7: Inclusions distributions of sample 6-T

REPORT

According to the results of the study sample number 7-T

Sample information:

- The number of measured fields of view: 3
- Field Area: 0.13 mm^2
- Total measured area: 0.38 mm^2
- Microscope magnification: 200
- Calibration: 0.200338 µm
- The analysis was carried out taking into account border inclusions.

Measured values for each type of inclusions (sulphides and oxides) or each type of particles constituting the structure

value measured	Nonmetallic inclusions average value	standard deviation	confidence interval (95%)	relative accuracy (%)
Volume fraction,V_V ,%	2.07	1.04	1.04	50
Number, N_A, 1 /mm^2	6209	2695	2695	43
Number of intersections N_l,1 /mm	9.92	5.34	5.34	53
Length,l,µm	1.55	0.23	0.23	14
Area, A,$µm^2$	3.30	0.57	0.57	17
Average interparticle distance,µm	124.5	65.1	65.1	52
Average diameter of Feret,µm	1.75	0.21	0.21	12
Max. Feret diameter,µm	2.12	0.27	0.27	12

Table 1.15: Inclusions analysis of sample 7-T

Maximum size of inclusions:

Nonmetallic inclusions	
Area,$µm^2$	120
Length,µm	66.1
Maximum diameter,µm	69.5

Table 1.16: Maximum size of inclusions of sample 7-T

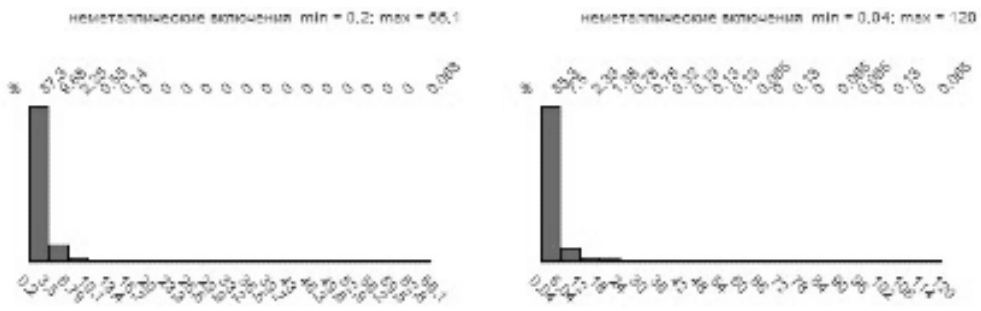

(a) (b)

Figure 1.8: Inclusions distributions of sample 7-T

REPORT

According to the results of the study sample number 8-T

Sample information:

- The number of measured fields of view: 3
- Field Area: 0.13 mm^2
- Total measured area: 0.38 mm^2
- Microscope magnification: 200
- Calibration: 0.200338 µm
- The analysis was carried out taking into account border inclusions.

Measured values for each type of inclusions (sulphides and oxides) or each type of particles constituting the structure

value measured	Nonmetallic inclusions average value	standard deviation	confidence interval (95%)	relative accuracy (%)
Volume fraction,V_V ,%	0.83	0.28	0.32	38
Number, N_A, 1 /mm^2	3961	1092	1261	31
Number of intersections N_l,1 /mm	5.17	1.93	2.23	43
Length,l,µm	1.28	0.13	0.15	11
Area, A,$µm^2$	2.06	0.13	0.15	7
Average interparticle distance,µm	208.7	68.7	79.3	38
Average diameter of Feret,µm	1.38	0.12	0.13	9
Max. Feret diameter,µm	1.66	0.13	0.15	8

Table 1.17: Inclusions analysis of sample 8-T

Maximum size of inclusions:

Nonmetallic inclusions	
Area,$µm^2$	126
Length,µm	15
Maximum diameter,µm	26.8

Table 1.18: Maximum size of inclusions of sample 8-T

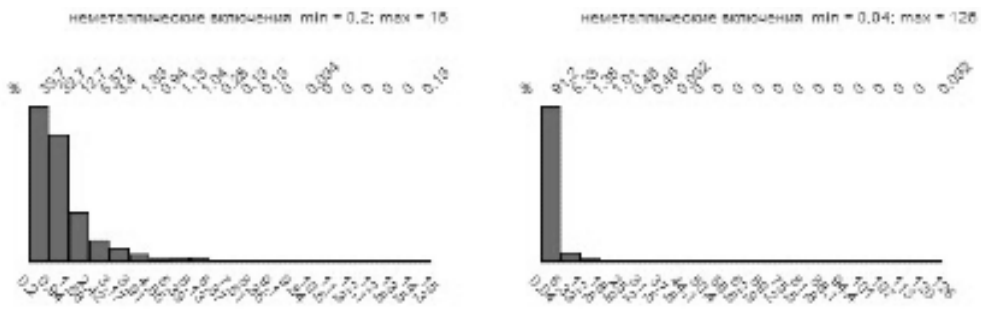

(a) (b)

Figure 1.9: Inclusions distributions of sample 8-T

Bibliography

[1] Arzamasov B.N.(1990),*Structural Materials: Reference Book*,Arzamasov B.N. Moskow, Mechanical Engineering. -688 p.

[2] Guryev A.M. (2005) *Theory and practice of producing a cast tool*,Guryev A.M., Kharaev Yu.P, Barnaul publishing house in AltSTU. -220 p.

[3] Poznyak L.A.(1980): *Die steel*,Poznyak L.A., Yu.M. Skrynchenko, SI. Tishaev SI. Moscow: Metallurgy. -244 p.

[4] Kolokoltsev V.M.(2007) *High-quality steel melting for shaped casting: a tutorial*.under. Ed. V.M. Kolokoltsev, Bakhmetev V.V., VdovinK.N.,Kozlov L.Ya.,Laptin V.V., Semin A.E. Magnitogorsk: MSTU. -268 p.

[5] Geller Yu.A. (1975): *Tool steels*, Geller Yu.A., 4th ed.Moscow: Metallurgy. -584 p.

[6] Kharaev Yu.P.(2004): *Structure and properties of the cast tool*,Kharaev Yu.P.. Barnaul: AltSTU. -143 p.

[7] Deordieva NT.(1964): *Stamp steel: composition, properties, thermal processing*.Deordieva NT.,Poznyak L.A. -M: Mechanical Engineering. -129 p.

[8] Trakhtenberg, B.F,(1968): *Some regularities of weakening and destruction of contact volumes of the tool during hot stamping*;Kenis M.S., Shubina MA.,Stamp steel.-No.-No 18, 37-54 p.

[9] Goldstein M.I., (1985): *Special Steel: A Textbook for Universities*,Gol'dstein M.I., GrachevSW., Wexler Yu.G.,Moscow: Metallurgy. -408 p.

[10] Storozhev M.V., (1967): *Forging and steel forging*; Ed. M.V. Hundred-rozhov. -M:Mechanical Engineering. -T.1.203.

[11] Velsky, E.I. (1975): *Persistence of forging stamps*Velsky, E.I, Minsk: Science and Technology. -239 p.

[12] Vorobyova G.A (2005): *Instrumental Materials: A Textbook for High Schools*,Vorobyova G.A ,Skladnova E.E., Leonov A.F., Erofeev V.K.St, Petersburg .: Polytechnics. -268 p.

[13] Trakhtenberg B.F (1968): *Influence of the thermal treatment regime on the resistance of thermomechanical fatigue of some die-cast steels and the tool's durability*,Trakhtenberg B.F, Ivanov A.I. et al. Stamp materials. No 18, -C.20-22.

[14] Shkatov A.P (1964): *Investigation of the structure and properties of some steels for hot-deforming dies*, *Stamp steel: a collection of articles*,Shkatov A.P,Zenchenko T.I, Moscow. No 9, -15-28 p.

[15] Shkatov, A.P. (1964):*Investigation of the structure and properties of some steels for hot-deforming dies*, Stamp steel: a collection of articles, Shakatov A.P., Zenchenko T.I., Moscow. No 9, 15-28p.

[16] Zhuravlev V.N. (1976): *Stamps for hot deformation, modes and ways of their manufacture*. Moscow.-55 p.

[17] Nikitin M.V. (2010): *Increase of wear resistance of structural steels due to metallurgical factors of production*Nikitin M.V, Maslyuk V.M., Laz'ko N.V.. Metallurg. No 1, -45-47 p.

[18] Kunilovsky V.V (1987): *Cast dies for hot volumetric deformation*,Kunilovsky V.V, Krutikov V.K. -L: Machine building. The Leningrad branch, -126 p.

[19] Storozhev M.V.(1968): *Forging and steel forging*.Ed. M.V. Hundred-rozhov. -M .: Mechanical Engineering. .-T.2. -449 p.

[20] Guryev A.M (1995): *Features of heat treatment of cast tool steels*,Guryev A.M, Kharaev Yu.P., Progressive technologies in machine-building: a collection of symposium materials, Rubtsovsk. -84-86 p.

[21] Guryev A.M, Voroshnin L.G. et al.: *Method of thermocycling of tool steels*.Patent No. 2078440, RF, cl. From 21 D 1/78 from 27.04.97.

[22] Guryev A.M., Okolovich G.A, Cheprasov D.P, Zemlyakov S.A.: *Method of thermocycling of tool steel*. The patent No. 2131469, the Russian Federation, With 21 D 1/78 10.06.99. Bul. No 16.

[23] Guryev A.M (2005): *Thermocyclic and chemical thermocyclic hardening of steels*,Guryev A.M, Voroshnin L.G., Kharaev Yu.P., Lygdenov B.D., Zemlyakov S.A., Gurieva O.A, Kolyadin A.A., Popova O.V., Polzunovsky Herald. No 2, -36-43 p.

[24] Guryev A.M.(2005): *Hardening of a cast high-speed steel by thermal cycling treatment*,Guryev A.M., Kharaev Yu.P., Guriev M.A., Modern science-intensive technologies. No 10 -79-81 p.

[25] Timoshpolsky, V.I.(2000): *Steel ingot*,Timoshpolsky, V.I, Samoilovich Yu.A.-Mn .: Belarus Navuka.-TH. 583 sec.

[26] Kolokoltsev, V.M. (1993): *Doping and modification of cast steels*. Kolokoltsev B.M., Magnitogorsk: MGMI. -80 p.

[27] Kondratyuk, C.E. (2003): *On the increase in the properties of cast steels*, Kondratyuk C.E.,Foundry. -39-41 p.

[28] Lubianoy D.A.,(2009): *Application of thermo-time treatment and non-stationary blowdown for refining iron-carbon melts at ZSMK*, Lubianoy D.a., The Week of Metal in Moscow. November 11-14, 2008 Sat. proceeding of conferences, -246-252 p.

[29] Bakhmetev V.V. (2006): *Increase in the properties of casting steels with extra-furnace calcium-magnesium ligatures with REM*, Bakhmetev V.V, Kolokoloktsev V.M., Miliyaev A.F.,Foundry production. No 11, -7-10 p.

[30] Belyanchikov L.N. (2008): *Modern trends in improving the quality of steel for cutting and metalworking tools. Sputtering formation of deposit ingots*,Belyanchikov L.N.,Electrometallurgy. No 8, -10-33 p.

[31] (1982) *Instrumental steels and their heat treatment: Per. with Hungarian*,Artinger I. Moscow: Metallurgy.-312 p.

[32] Kozlov L.Ya, (2003): *Manufacture of steel castings: a textbook for universities*. Ed. L.Ya. Kozlov / L.Ya. Kozlov, V.M. Kolokoltsov, K.N. Vdovin, E.B. Ten, LB Dolgopolova, A.A. Filippenkov. Moscow: MISIS.-352 p.

[33] Vdovin K.N. (2006): *Choice of melting aggregates and calculation of charge for smelting iron and steel: a textbook*. Magnitogorsk: MSTU.-121 p.

[34] Baum, B.A., (1987): *Increase of technological properties of metal products by the way of thermo-time treatment of melt*. B.A. Baum, G.V. Tyagunov, P.S. Popel, G.A. Khasin, L.V. Kovalenko Steel. No 10, -21 -24 p.

[35] Ponkratin E.N.(2009): *New heat-resistant steels for hot deforming stamps* / Ponkratin E.N, Lenartovich D.V., Steblov A.B., Steel. No 1-C., 77-80 P.

[36] Steblev A.B. (2009): *New steel for hot-deforming stamps*A.B. Steblev, D.V. Lenartovich, Ponkratin E.N., Metallurgist. No 2, -41-43 p.

[37] Babaskin Yu.Z.(2003): *Structural and special casting steels with carbonitride hardening* ,Babaskin Yu.Z., Shipitsyn S.Ya. et al.,Foundry. No 8, -32-38 p.

[38] Kremnev L.S.(2008): *Theory of alloying and the creation on its basis of heat-resistant tool steels and alloys* and Kremnev L.S.: *Metal Science and Thermal Processing of Metals*. No 11, -18-27 p.

[39] Pilyushenko V.L.(1987): *The influence of microalloying on the service characteristics of steel*, Pilyushenko V.L., Steel. No 10, -24 -26 p.

[40] Pilyushenko V.L.(1987): *Technological aspects of microalloying and modification of steel for mass use* Pilyushenko V.L., Vikhlevshchuk V.A., Leporskiy S.V., Steel. No 10, -35-39 p.

[41] Makarov D.N.(2008): *Mastering the smelting of complex alloy structural steel tool steels in a 100-ton electric furnace*,Makarov D.N., Antonov V.I. et al.,Steel. No 3, -44-45 p.

[42] Stetsenko, V.Yu.(2006): *Activation of the processes of modifying metals and alloys*, Stetsenko V.Yu., Marukovich E.I, Foundry.-No 11, -2-6 p.

[43] Shub L.G.(2006): *On the advisability of modifying*,Shub L.G., Ah-madeyev A.Yu., Metallurgy of machine building. No 5, -38-41 p.

[44] Panov A.G.(2006): *Role and place of modifying cast iron and melts from the point of view of heredity of alloys*, Panov A.G., Metallurgy of machine building. No.5-C.22-27 p.

[45] Dubrovsky SA,(2008): *A hypothesis of the cluster nature of heredity of raw materials in the metallugy of black alloys*,Dubrovky S.A., Shilpelnikov A.A., Rigorsky A.N., News of higher educational institutions of Chernozem region. No.1 (5), -89-96 p.

[46] Nikitin V.I.,(2014): *Development and application of the phenomenon of structural inheritance in aluminum alloys*. Nikitin KV. Nikitin, Journal of Siberian Federal University Engineering and Technologies. No 7, -424-427 p.

[47] Kovalenko: L.V.,(2003): *Application of external influences during solidification of ingots*,Kovalenko L.V., Panov-M A.G.: Metallurgy.-153 p.

[48] Savina L.G.,(2003): *Effect of high-temperature melt processing on the structure and properties of high-carbon alloys of iron: diss. to the soisk. uch. degree of Cand. tech. Sciences* Savina Lidia Gennadievna. - Ekaterinburg.-129 p.

[49] Baum, B.A.,(1984): *Liquid steel* / B.A. Baum, G.A. Khasin, G.V. Tyagunov, K.A. Klimenkov - Moscow: Metallurgy. -208 p.

[50] Raspopova G.A.,(1981): *Influence of the conditions of the thermo-time treatment of the melt on the structure formation of steel XI2 and P6M5: diss. to the soisk. uch. degree of Cand. tech. Sciences*, Raspopova G.A.,Sverdlovsk.-184 p.

[51] Baum B.A.,(1996): *Thermal treatment of liquid alloys and steel*, Baum B.A., Tyagunov G.V. et al.,Steel.No.6.-16-18 p.

[52] Panov A.G.,(2010): *Study of the formation of molten iron. Influence of heredity on the properties of castings from cfg.* Panov A.G., Konashkov V.V. et al. The Roaster of Russia. No 4, - 18-20 p.

[53] Kondratyuk, C.E.,(2008): *Heredity of the structure and properties of cast steel* CE. Kondratyuk,Foundry production. No 9, -6-10 p.

[54] Elansky, G.N.,(1995):*Structure and properties of metal melts*,G.N. Elansky, D.G. Elansky. - M: MGVMI, 2006. - 228 p.

[55] Nikitin, V.I. Heredity in cast alloys / V.I. Nikitin. - Samara: Samara State Technical University.-248p.

[56] Ri Hosen, (2001): *Theory of casting processes* Ri Hosen. - Khabarovsk: Khabar, state. tech. University.- 275 p.

[57] Skrebtsov, A.M.: *Influence of temperature and holding time of the melt with it on the quality of the solidified casting* Skrebtsov A.M., Ivanov G.A., Kuz'min Yu.D., Kachikov A.S.. Bulletin of the Azov State Technical University.-No 2.-140-144 p.

[58] Skrebtsov, A.M.: *Methods for determining the temperature of disordering of metal melt clusters in the development of thermo-time treatment regimes* A.M. Skrebtsov, Bulletin of the Azov State Technical University. No 14, - 140-144 p.

[59] Dubrovsky S.A.,(2007): *Cluster mechanism of heredity of charge materials* Dubrovsky S.A., Shipelnikov A.A., Rogotovsky A.N. LSTU Bulletin - LEGI. -Lipetsk: LSTU-LEGI. No 1 (15), -42-46 p.

[60] Ghosh A., Chattarjee A.(2008): *Ironmakin And Steelmaking: Theory and Practice*. Phi Learning Private limited, New Delhi.

[61] Vladimirovna M.I.(2004): *Selection and justification of the high temperature treatment mode of die cast steel in order to improve it. structures and properties*,Magnitogorsk State Technical University,G.I. Nosov.

[62] Wear resistance of Hadfield steel, alloyed with nitrided ferroalloys.

[63] Calliari I.(2017), notes for the course: *Characterization of materials*, University of Padova.

[64] Yuryevna M O.(2007): *Development of thermal treatment technology and investigation of its effect on the structure and properties of forged 150 HNM*

[65] Thesis work realized at Magnitogorsk Magnitogorsk State Technical University,G.I Nosov.

[66] Mashchenko A.F., Shchek A.V. (2003): *Charge calculation for melting duty steel*, Suevalova L.A., Ministry of Education of the Russian Federation State educational institution higher vocational education Khabarovsk State Technical University.

[67] Kazakov A. A., Pakhomova O. V., Kazakova E. I.(November 2012): *Study of the cast structure of industrial Ferrite-pearlite steel slab*, Development of metallurgy in Russia and Cis countries, "Black Metals".

Consulted websites

[68] http://www.cntd.ru/english.html

[69] https://www.researchgate.net/

[70] http://appmath.narod.ru

[71] https://nakal.all.biz/en/furnace-laboratory-pl-2012-5-g6044388

[72] https://nanovision.it

[73] https://thixomet.ru/

[74] http://www.ernsthardnesstesters.com

[75] http://ima.textildom-nn.ru/detskie/6d2f6b4a7bc6956ea542f23046c8654d.php

[76] https://elearning.unipd.it/dii

[77] http://scicenter.online

ACKNOWLEDGMENTS

Nel corso di questi anni di università e del periodo di lavoro che mi ha portato alla stesura di questa tesi di laurea, molte sono state le persone che, in un modo o nell'altro, mi hanno aiutato ad affrontare questo percorso, che ora si conclude.

La prima persona che ringrazio è il prof. Manuele Dabalà, relatore di questa tesi di laurea, il quale mi ha permesso di intraprendere l'esperienza di Erasmus a Magnitogorsk, i professori M.V. Potapova e M.G. Potapov per avermi permesso di svolgere attività di ricerca presso la loro università, seguito e aiutato passo dopo passo nella ricerca.

Ringrazio infinitamente e con tutto il cuore i miei genitori, mio fratello Alberto e Valentina per aver sempre creduto in me, per avermi sostenuto con tutte le loro energie nei momenti felici e in quelli più difficili, per avermi dato la possibilità di prendere parte a questa esperienza incredibile. Grazie perché se sono qui è soprattuto grazie a voi, mi avete sempre spronato e fatto che sì che non mollassi mai. A voi dedico tutte queste pagine e tutto il mio lavoro.

Ringrazio gli amici di sempre per tutti i momenti passati assieme, le esperienze vissute e tutti i ricordi che insieme abbiamo costruito e che porteremo sempre con noi. Un ringraziamento miei compagni di squadra di questi ultimi anni a Castione, compagni di mille battaglie, grazie per avermi insegnato il valore dell'amicizia, il concetto dell'essere squadra e per tutto il divertimento non manca mai.

Vorrei dire grazie alla Russia, per avermi fatto crescere, mettendomi davanti ostacoli e difficoltà, per essere stata la mia casa, per avermi fatto conoscere una storia, una cultura un modo di vivere nuovi e per avermi regalato amici. Ad Alexis, Aleksei e la sua famiglia che hanno contribuito e rendere i sei mesi in Russia speciali e indimenticabili, per avermi aiutato e per avermi fatto sentire a casa.

Infine concludo ringraziando tutte le persone che conosciuto o anche solo incontrato in questi anni, con i quali ho condiviso anche solo un momento perchè chi più chi meno e, nel bene o nel male, mi ha dato qualcosa che mi ha reso ciò che sono oggi.

Mattia